

Reinforced Concrete Subjected to Restraint Forces

Analytical and Non-Linear Finite Element Analysis

Master's Thesis in the International Master's Programme Structural Engineering

JOHAN NESSET

SIMON SKOGLUND

Department of Civil and Environmental Engineering

Division of Structural Engineering

Concrete Structures

CHALMERS UNIVERSITY OF TECHNOLOGY

Göteborg, Sweden 2007

Master's Thesis 2007:23

MASTER'S THESIS 2007:23

Reinforced Concrete Subjected to Restraint Forces

Analytical and Non-Linear Finite Element Analysis

Master's Thesis in the International Master's Programme Structural Engineering

JOHAN NESSET, SIMON SKOGLUND

Department of Civil and Environmental Engineering
Division of Structural Engineering
Concrete Structures

CHALMERS UNIVERSITY OF TECHNOLOGY

Göteborg, Sweden 2007

Reinforced Concrete Subjected to Restraint Forces
Analytical and Non-Linear Finite Element Analysis
Master's Thesis in the International Master's Programme Structural Engineering
JOHAN NESSET, SIMON SKOGLUND

© JOHAN NESSET, SIMON SKOGLUND, 2007

Master's Thesis 2007:23
Department of Civil and Environmental Engineering
Division of Structural Engineering
Concrete Structures
Chalmers University of Technology
SE-412 96 Göteborg
Sweden
Telephone: + 46 (0)31-772 1000

Cover:

Top: reinforced concrete prism subjected to restraint of intrinsic imposed deformation.
In between: figure of global response versus deformation. Bottom: mesh showing
cracked regions.

Chalmers Reproservice / Department of Civil and Environmental Engineering
Göteborg, Sweden 2007

Reinforced Concrete Subjected to Restraint Forces
Analytical and Non-Linear Finite Element Analysis
Master's Thesis in the International Master's Programme Structural Engineering
JOHAN NESSET, SIMON SKOGLUND
Department of Civil and Environmental Engineering
Division of Structural Engineering
Concrete Structures
Chalmers University of Technology

ABSTRACT

In this master's project, the behaviour of reinforced concrete subjected to restraint forces has been studied. In Sweden the design methods normally used are unsatisfactory in order to predict the cracking process of structures subjected to restraint forces. When predicting the number of cracks that will appear and also the crack widths, it is generally assumed that the cracking is caused by an external force instead of restraint of intrinsic imposed deformations. The aim of this project was to examine if an analytical method with cracks modelled as linear springs together with non-linear FE-analyses could give a basis for a more reliable design approach.

In order to find a reliable design approach it is of importance to study the theory which deals with the cracking process, the parameters which influence this and the models which are in use today. Problem when designing with respect to restraint forces and differences between Swedish and European standards should be presented.

Several parametric studies using both an analytical method and non-linear FE-analysis have been performed with different objectives in order to understand the cracking process under restraint.

It was found that the analytical method gave results that were comparable with the non-linear FE-analysis and both approaches also showed differences compared to the common design method based on the Swedish code. The number of cracks and also the crack widths gave a more reliable response when using the analytical method. The non-linear FE-analyses can in an even more accurate way describe the cracking process of restrained structures. The influence of varying parameters showed significant effects by means of the number of developed cracks and the crack widths.

Key words: Analytical method, bond, cracking process, non-linear FE-analyses, parametric study, restraint force, restraint stress, tension stiffening, thermal strain, transfer length.

Armerad betong utsatt för tvångskrafter
Analytisk och icke-linjär finita element analys
Examensarbete inom det internationella mastersprogrammet Structural Engineering
JOHAN NESSET, SIMON SKOGLUND
Institutionen för bygg- och miljöteknik
Avdelningen för Konstruktionsteknik
Betongbyggnad
Chalmers tekniska högskola

SAMMANFATTNING

I det här examensarbetet har beteendet av armerad betong utsatt för tvångskrafter studerats. Dagens dimensioneringsmetoder baseras generellt sett på svenska normer vilka inte är tillräckliga för att förutspå sprickprocessen hos konstruktioner utsatta för tvångskrafter. När dagens konstruktörer dimensionerar med hänsyn till antalet sprickor som kan uppstå samt spricköppningen, antar man normalt att sprickorna beror på en yttre dragpåkänning istället för en inre påtvingad töjning. Målet med det här arbetet är undersöka om en analytisk metod där sprickor är modellerade med hjälp av linjära fjädrar tillsammans med icke-linjära FE-analyser kan ge riktlinjer för en mer tillförlitlig dimensioneringsmetod.

För att hitta en tillförlitlig metod är det viktigt att studera teorin om sprickprocessen, parametrar som påverkar detta och hur modellerna används idag. Problem vid dimensionering med avseende på tvångskrafter och skillnader i svenska och europeiska standarder kommer också att presenteras.

Ett antal parameterstudier är utförda med hjälp av den analytiska metoden men också med hjälp av icke-linjära FE-analyser för att förstå parametrarnas inverkan.

Det visades att den analytiska metoden är relativt jämförbar med icke-linjära FE-analyserna samt att båda kan sägas ge skillnader jämfört med dagens dimensioneringsmetoder baserade på den svenska normen. Antalet sprickor och dess sprickbredd gav ett mer tillförlitligt beteende när den analytiska modellen användes. Den icke-linjära FE-modellen gav en ännu bredare förståelse för uppsprickningsprocessen av konstruktioner utsatta för tvång. Variation av studerade parametrar påvisade tydlig inverkan på antalet utvecklade sprickor samt sprickbredden.

Nyckelord: Analytisk metod, icke-linjära FE-analyser, parameterstudie, sprickprocess, springutbredning, tvångskraft, tvångsspänning, temperaturlast, ”tension stiffening”, vidhäftning, överföringssträcka.

Contents

ABSTRACT	I
SAMMANFATTNING	II
CONTENTS	III
PREFACE	VI
NOTATIONS	VII
1 INTRODUCTION	1
1.1 Problem description	1
1.2 Aim	1
1.3 Method	2
1.4 Limitations	2
1.5 Outline of the thesis	2
2 CRACKING PROCESS	3
2.1 Cracking stages	3
2.1.1 Uncracked stage	3
2.1.2 Crack formation	5
2.1.3 Stabilised cracking	7
2.2 Restraint	7
2.3 Restraint stresses	9
2.3.1 Thermal strain	9
2.3.2 Shrinkage strain	10
2.3.3 Creep	11
2.3.4 Creep and shrinkage according to Swedish code BBK 04	13
3 MATERIAL AND BOND BEHAVIOUR	15
3.1 Concrete	15
3.1.1 Modelling in FE-analysis	16
3.1.2 Modelling with analytical methods	17
3.2 Steel	18
3.3 Bond behaviour	18
3.4 Crack distribution	20
4 PARAMETERS INFLUENCING THE RISK OF CRACKING	23
4.1 Specimen and basic input parameters	23
4.2 Results	25
4.2.1 Influence of bar diameter	25
4.2.2 Influence of concrete cross section area	26

4.2.3	Influence of length	27
4.2.4	Influence of support conditions	28
4.3	Concluding remarks	29
5	THE CRACKING PROCESS STUDIED BY AN ANALYTICAL METHOD	31
5.1	Basic input parameters	31
5.2	Calculations	32
5.3	Result	33
5.3.1	Influence of bar diameter	33
5.3.2	Influence of concrete cross section area	35
5.3.3	Influence of reinforcement ratio	35
5.3.4	Influence of creep coefficient	37
5.3.5	Influence of length of specimen	38
5.4	Concluding remarks	38
6	FINITE ELEMENT ANALYSIS	39
6.1	Modelling approach	39
6.2	Input data	39
6.2.1	Geometry	39
6.2.2	Material models	40
6.2.3	Boundary conditions and loading	43
6.2.4	Mesh	44
6.2.5	Interface behaviour modelled by non-linear springs	44
6.3	Solution process	46
6.3.1	Classification with regard to type of analysis	46
6.3.2	Iteration method	47
6.3.3	Time step and tolerances	48
6.4	Verification	48
6.5	Performed analyses	50
6.6	Results	51
6.6.1	Introduction	51
6.6.2	Global response	51
6.6.3	Stress and strain development	59
7	COMPARISONS	63
7.1	External load and restraint forces	63
7.1.1	Number of cracks	63
7.1.2	Simple example using Swedish code BBK 04	64
7.2	Improved analytical model	66
7.3	Improved analytical and FE-model	68
8	CONCLUSIONS	74
8.1	General	74

8.2	Further investigations	74
9	REFERENCES	76
APPENDIX A	CALCULATION OF SHRINKAGE	79
APPENDIX B	CALCULATION OF CREEP	83
APPENDIX C	DIFFERENCES IN CODES REGARDING SHRINKAGE	87
APPENDIX D	DIFFERENCES IN CODES REGARDING CREEP	89
APPENDIX E	DIFFICULTIES AND APPROACHES IN FE-MODELLING	91
APPENDIX F	RESULTS FROM FE-ANALYSIS	97
APPENDIX G	CALCULATION OF CONCRETE STRESSES AND STIFFNESS DUE TO APPLIED ΔT	129
APPENDIX H	CALCULATION THE RESPONSE USING AN ANALYTICAL METHOD	133
APPENDIX I	COMPARISON OF CRACK WIDTH	141
APPENDIX J	DETERMINING THE NUMBER OF CRACKS	145
APPENDIX K	INPUT FILES FOR ADINA	149
APPENDIX L	NOTATION AND DETAILS FOR ANALYSES	156

Preface

In this master's project, improved analytical models and non-linear analyses have been used to investigate the behaviour of reinforced concrete subjected to restraint forces. The work has been carried out from September 2006 to February 2007. The project was carried out at the Division of Structural Engineering, Concrete Structures, Chalmers University of Technology, Sweden. The initiative to the project was taken by Ph.D. Morgan Johansson, design engineer at Reinertsen Sverige AB, where also the project was performed.

Professor Björn Engström and Morgan Johansson were supervisors and the former was also the examiner. We would like to thank all the staff at the office of Reinertsen Sverige AB in Göteborg for their hospitality and involvement. Also thanks to our opponents Daniel Ekström and Lars-Levi Kieri for their feedback and support during the work.

Göteborg February 2007

Johan Nasset and Simon Skoglund

Notations

Roman upper case letters

A	area
A_I	transformed area in state I
A_{II}	transformed area in state II
E	modulus of elasticity
E_{cm}	modulus of elasticity for concrete, mean value
$E_{cm,ef}$	effective modulus of elasticity for concrete, mean value, considering creep
E_{sm}	modulus of elasticity for steel, mean value
F	force
G_f	fracture energy
N	axial normal force
N_{cr}, N_I	cracking load
N_y	yielding load
R	restraint degree
S	stiffness of support
T	temperature

Roman lower case letters

b	width of beam/cross-section
d	effective height of cross-section
c	concrete cover
f_{cm}	concrete compressive strength, mean value
$f_{ctk0.05}$	lower characteristic value of concrete tensile strength
$f_{ctk0.95}$	upper characteristic value of concrete tensile strength
f_{ctm}	concrete tensile strength, mean value
f_k	characteristic value of material strength
f_d	design value of material strength
f_{yd}	yield strength for steel, design value
h	height of beam/cross-section
h_0	notional height
k	stiffness
k_h	size coefficient
l	length
l_{el}	element length
l_t	transfer length
$l_{t,max}$	transfer length, maximum value
s	slip
s_{rm}	crack spacing, mean value
$s_{r,min}$	crack spacing, minimum value
$s_{r,max}$	crack spacing, maximum value
t	time
u	displacement
w_k	crack width, characteristic value
w_m	crack width, mean value
w_u	crack opening when concrete stresses are zero in cracks

Greek lower case letters

α	modular ratio
α_{et}	modular ratio, taking creep in consideration
α_e	coefficient of thermal expansion
$\beta(f_{cm})$	factor which considers concrete strength
$\beta(t_0)$	factor which considers when the concrete was loaded
$\beta(t, t_0)$	time function of creep coefficient
β_{ds}	drying shrinkage time function
β_{RH}	ambient relative humidity factor
ε	strain
ε_c	concrete strain
ε_{ca}	concrete autogenous shrinkage strain
ε_{cd}	concrete drying shrinkage strain
ε_{cdi}	start value of concrete drying strain
$\varepsilon_{c,el}$	elastic concrete strain
ε_{ci}	initial concrete strain
ε_{cr}	concrete strain when crack occurs
ε_{cs}	concrete shrinkage strain
ε_{cT}	concrete thermal strain
ε_{cu}	ultimate concrete strain
ϕ	bar diameter
ϕ_{RH}	factor for relative humidity
$\varphi(t, t_0)$	creep coefficient
ζ	strength reduction factor
ξ	strain ratio
ρ	density
ρ_r	reinforcement ratio
σ	stress
σ_c	concrete stress
σ_{ci}	initial concrete stress
σ_s	steel stress
τ_b	bond stress
τ_{bm}	bond stress, mean value
τ_{max}	maximum bond stress
ν	poisson's ratio

1 Introduction

1.1 Problem description

When the temperature decreases or increases, concrete structures will have a need for deformation. Shrinkage of concrete is also a source of deformation which is related to the age of concrete. If a structure in any way is hindered to deform, restraint forces will appear. The prevented intrinsic deformation results in tensile stresses, which will result in cracking if the concrete tensile strength is reached.

Engineers today seem to have difficulties predicting the cracking behaviour of reinforced concrete due to restraint stresses. This might be a result of insufficient knowledge of how to use the codes and interpret them, but also lack of experience. Furthermore, Swedish codes have today unsatisfactory guidelines for prediction of cracks and estimation of crack widths due to restraint stresses.

Sections of reinforced concrete structures are considered as composite sections where the materials interact according to each material's characteristics. The combined response of concrete and reinforcing steel gives a preferable behaviour in structures. However this kind of composite can also result in problems such as restraint situations and cause unwanted cracks.

In the Ultimate Limit State (ULS), the crack formation is assumed to be fully developed. Cracks are natural for the structure if the high tensile capacity of steel is to be utilised. Without any cracks, the ordinary reinforcing steel has negligible influence on the load bearing capacity.

When cracks occur in concrete structures, the concrete cover by which the reinforcement once was protected is damaged. Open cracks are a highway for moisture and oxygen, which are two of the elements needed for a corrosion process. Corrosion of the reinforcement will result in decreased load bearing capacity of the structure, why crack control in the Serviceability Limit State (SLS) is required.

1.2 Aim

The main aim of this project was to study and visualise the cracking behaviour of reinforced concrete members subjected to restraint forces. Together with theory and hand calculations, a study will be made regarding crack propagation of reinforced concrete subjected to restraint forces. The cracking response should be studied both with analytical models and non-linear finite element analyses, hereafter denoted as FE-analyses. Further comparisons with design approaches in codes should be carried out.

1.3 Method

A theoretical base is needed in order to treat the given problem and its aim. Firstly, the theory regarding cracking of reinforced concrete element is studied. In addition, the restraint cracking process is treated by means of non-linear response of analytical models and FE-models. These are then verified with different geometries and parametric studies.

1.4 Limitations

The project should focus on theory and analysis of the cracking response under restraint forces in mature reinforced concrete elements. Mature concrete is defined as concrete with 28-days strength. All calculations have been carried out in the SLS and it is assumed that there are no initial stresses or strains acting on the elements. The theory behind cracking process is limited in this report and only deals with the basics.

The FE-analysis is mainly made on two different element sizes, one low and one high member. In order to study the influence of different parameters, input data are changed in the two different models.

1.5 Outline of the thesis

The first part of the project consists of Chapter 2 and Chapter 3 and gives the reader a brief background to the theory of the cracking process and the material response.

In order to start the analysis, Chapter 4 guides the reader through a parametric study with the intention to give a basic overview of the influence of different parameters regarding risk of cracking. Chapter 4 is followed by an analytical study on crack propagation in Chapter 5. This cracking process study is based on linear simplifications and it is a rather simple tool to use in order to describe the cracking process of reinforced concrete subjected to restraint forces.

Chapter 6 contains the FE-analysis using the commercial software ADINA. The material models and geometrical conditions are described, as well as results obtained in the analyses.

In Chapter 7 a comparison between the analytical method and the FE-model is carried out. Also to be found in Chapter 7, is a comparison between an approach using external load and the investigated methods.

Finally Chapter 8 contains conclusions that have been obtained from the work presented in this project. Also, in this chapter suggestions for further investigations are given.

2 Cracking process

To be able to understand the sometimes notable behaviour of cracking of reinforced concrete structures, it is important to understand some of the most pronounced theory of concrete. In this chapter the different cracking stages, the need for movement and different restraints are introduced. Also differences regarding external load acting on the concrete element and imposed end displacement is considered.

2.1 Cracking stages

2.1.1 Uncracked stage

One of the most fundamental and important relation in crack control is the probability condition of cracking. The concrete will most likely remain uncracked if the tensile stress is lower than the lower characteristic value, defined by the 5%-fractile, $f_{ctk0.05}$ of the tensile strength, f_{ctm} . The frequency curve is a result of natural scatter of the tensile strength after production, see Figure 2.1.

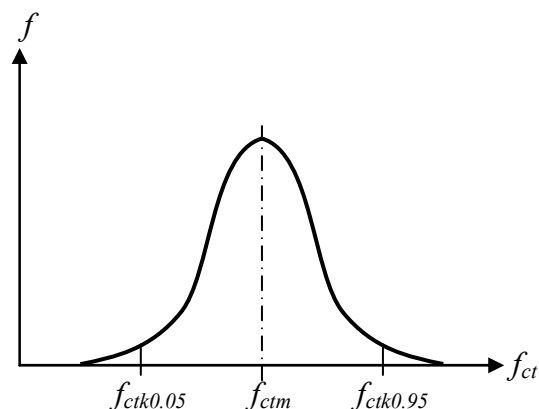


Figure 2.1 Frequency curve of tensile strength in concrete.

The frequency curve shows the relation between the mean, lower (5% fractile) and upper characteristic value (95% fractile) of the concrete tensile strength. For instance if the concrete stress is equal to $f_{ctk0.05}$, there is a probability of 5% that the concrete is cracked.

To be able to find the lower characteristic value of the tensile strength, the following relationships can be used according to Table 3.1, *Analytical relation*, in Eurocode 2, CEN (2004).

$$f_{ctm} = 0.30 \cdot (f_{ck})^{2/3} \quad \text{for } \leq C50/60 \quad (2.1)$$

$$f_{ctm} = 2.12 \cdot \ln\left(1 + \frac{f_{cm}}{10}\right) \quad \text{for } > C50/60 \quad (2.2)$$

$$f_{ctk0.05} = 0.7 \cdot f_{ctm} \quad (2.3)$$

Standard tests made by Jonasson et al. (1994) showed that long-term loading of a 0.7 m thick wall resulted in reduced tensile strength to 65 – 80 %. Therefore the following reduction of the tensile strength is recommended in case of sustained loading, see equation (2.4). However, a similar reduction is not needed according to Eurocode 2.

$$f_{ctk0.05,l} = 0.7 \cdot f_{ctk0.05} \quad (2.4)$$

While calculating, and also assuming that a section is uncracked, it is important to use corresponding parameters.

$$\sigma_c \leq f_{ctk0.05} \quad (2.5)$$

$$\sigma_c = E_{cm} \cdot \varepsilon_c = \frac{F}{A_I} \quad (2.6)$$

A transformed concrete section A_I is a weighed area which includes the influence of the reinforcement, see Figure 2.2.

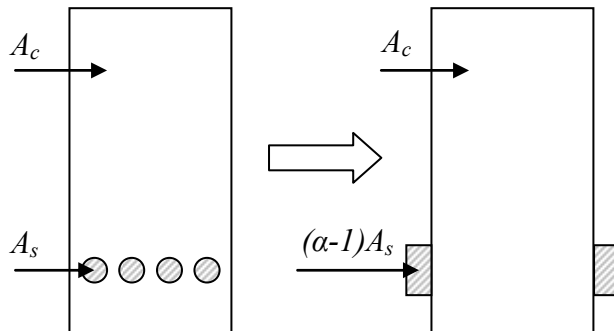


Figure 2.2 Illustration of a transformed concrete section A_I .

The transformed concrete area may be calculated according to equation (2.7).

$$A_I = A_c + (\alpha - 1)A_s \quad (2.7)$$

where $\alpha = E_{sm} / E_{cm}$

In case of long-term loading modifications of the parameters must be made as follows.

$$E_{cm,ef}(t, t_0) = \frac{E_{cm}}{1 + \varphi(t, t_0)} \quad (2.8)$$

where $\varphi(t, t_0)$ = creep coefficient at age t for load applied at age t_0 .

The transformed concrete section in case of long-term loading, is defined according to equation (2.9).

$$A_{l,ef} = A_c + (\alpha_{ef} - 1)A_s \quad (2.9)$$

$$\text{where } \alpha_{ef} = \frac{E_{sm}}{E_{cm}} (1 + \varphi(t, t_0))$$

2.1.2 Crack formation

Cracking of concrete is almost impossible to avoid in a loaded structure. Cracks will appear in concrete structures when the tensile stresses reach the tensile strength. Due to the limitations in this thesis, evaluations are only made in serviceability limit state

In the cracked state a stiffness contribution is formed due to the uncracked concrete between the transverse cracks. The total stiffness is found to be higher than the pure stiffness of a reinforcement bar in a cracked section. The stiffness contribution after cracking, referred to as the tension stiffening effect, see Figure 2.3, depends on the stresses between the reinforcement bar and the surrounding concrete. Note that the figure shows the mean value of the global strain.

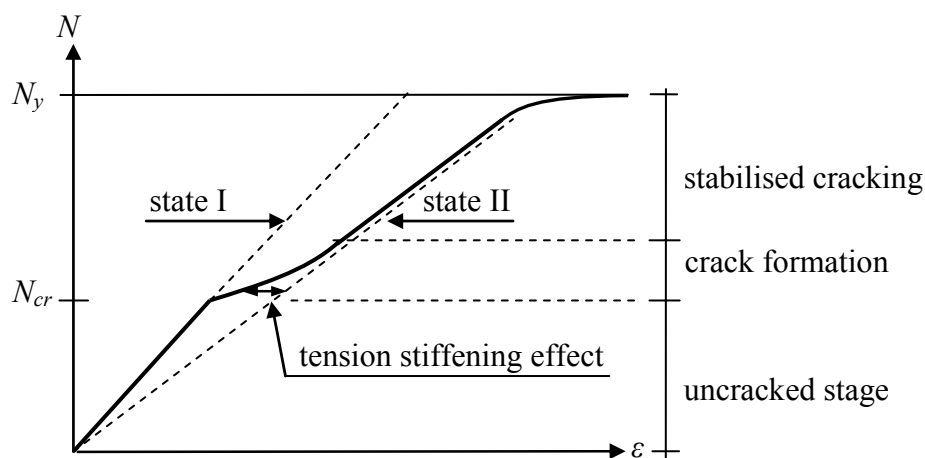


Figure 2.3 Global average response of concrete element at various cracking stages.

Tensile stresses can either be a result of external load acting on the concrete structure or due to restrained intrinsic deformations. Such deformation could be a result from thermal strain or drying shrinkage strain, as described in CEB Bulletin 235, CEB (1997).

According to CEB-FIP Model Code 90, CEB (1991), the first crack occurs when the load has reached N_{cr} defined in equation (2.10) and new cracks will appear under small load increase until the element is fully cracked or when the restraint forces decreases below the concrete tensile capacity.

$$N_{cr} = f_{ctm} [A_{ef} + (\alpha - 1)A_s] \quad (2.10)$$

where A_{ef} = effective concrete area according to Figure 2.4.

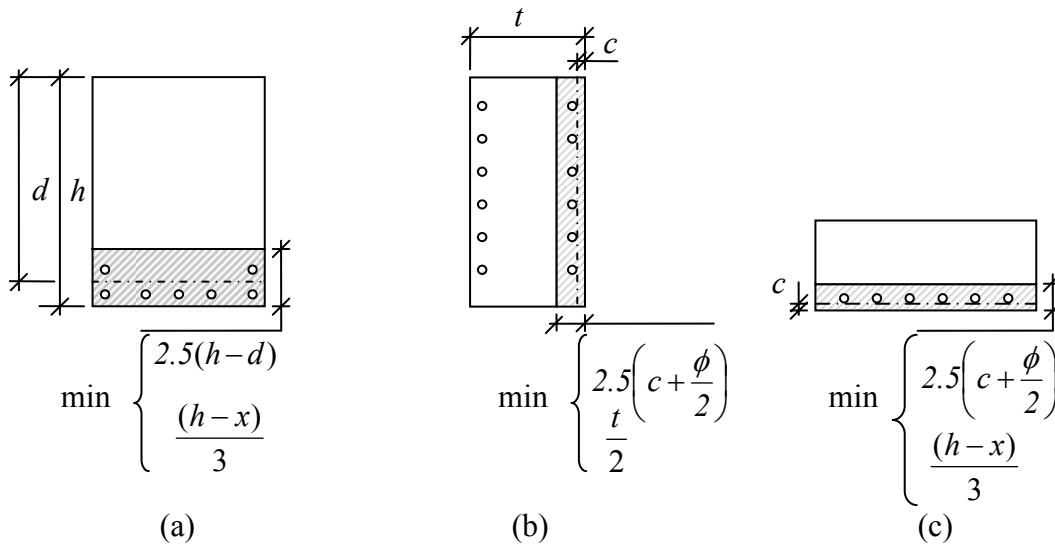


Figure 2.4 Effective concrete area for (a) an ordinary reinforced beam with no reinforcement in compressed section; (b) an infinite long wall; (c) a slab with bottom reinforcement in tension, according to CEB-FIP MC 90.

For a crack to be initiated in a thick wall, the surface region must be cracked. The surface region may be defined as the effective area shown in Figure 2.4. For a thin member, the surface region will always be defined as half of the thickness, as shown in Figure 2.4 (b).

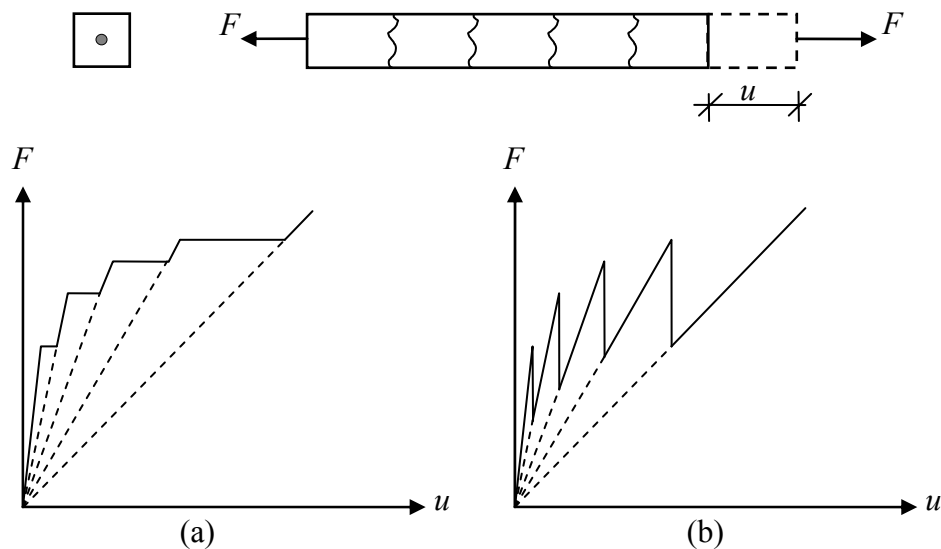


Figure 2.5 Reinforced concrete subjected to (a) axial force F ; (b) imposed end displacement u . Both diagrams show the same number of formed cracks.

When a reinforced concrete member is loaded in tension with a force F , the deformation will increase instantaneously for each crack that appears, without increased load. As shown in Figure 2.5 (a), the end displacement increases rapidly for the 4 cracks that are shown. When the loading is prescribed as an end displacement, the response is rather different, as shown in Figure 2.5 (b). As the cracks appear the force is reduced as a result of reduced overall stiffness. This will occur for all four cracks as long as the element remains in the *crack formation* stage, see Figure 2.3.

When a crack appears, the global stiffness is reduced. This is shown in both Figure 2.5 (a) and (b). The inclination of the dashed line shows how the stiffness decreases for each crack.

2.1.3 Stabilised cracking

In this stage (see Figure 2.3), no new cracks can appear. The width of the already existing cracks increases with small load increment, until the reinforcement reaches yielding. The reason for this is that the distance between two cracks is not long enough for transferring stresses between the reinforcement and the concrete. Hence, the concrete stress will not become high enough to cause cracking, see further in Sections 3.3 and 3.4.

2.2 Restraint

Deformation of a concrete member can be restrained due to a number of reasons. The most common are boundary conditions (external restraint), see Figure 2.6, and the interaction between concrete and reinforcement bars (internal restraint), see Figure 2.7.

The restraint degree is defined according to equation (2.11) - (2.13), Engström (2006).

$$\text{restraint degree} = \frac{\text{actual imposed strain}}{\text{imposed strain in case of full restraint}} \quad (2.11)$$

$$R = \frac{\varepsilon_c}{\varepsilon_{cT}} \quad (2.12)$$

$$R = \frac{\frac{\sigma_c}{E_c}}{\sigma_c \left(\frac{1}{E_c} + \frac{A_c}{S \cdot l} \right)} \quad (2.13)$$

where S = total stiffness of the supports $S=N/u$

N = normal force

u = total displacement of the supports

A_c = concrete area

l = length of element

In Figure 2.6 different external restraint situations are presented. The different types of support conditions and natural surroundings will restrain the elements. When a temperature load is applied restraint forces will appear. The following cases, in Figure 2.6 and Figure 2.7, have different restraint degree and can be calculated using equation (2.13).

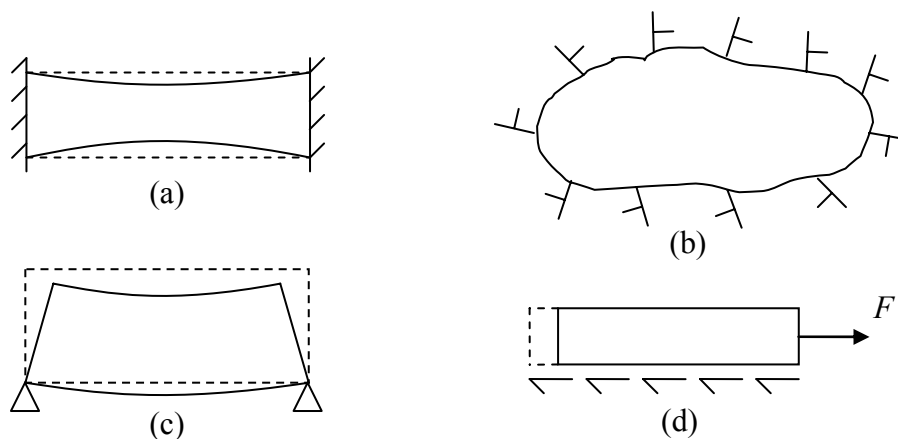


Figure 2.6 Examples of external restraint.

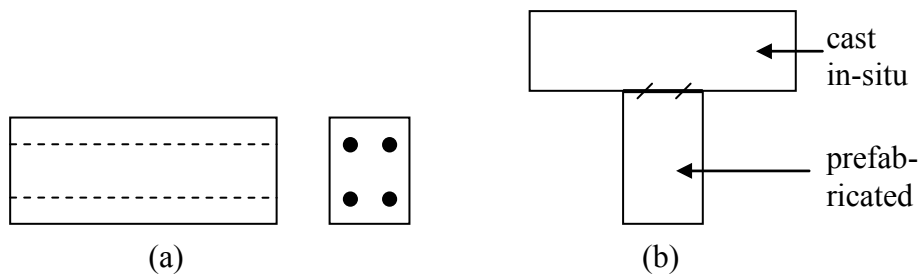


Figure 2.7 Examples of internal restraint.

Figure 2.7 shows examples of internal restraint situations due to steel bars and concrete (a) and new concrete cast in contact with mature concrete (b). Internal restraint occurs when different fibres in the section have different need for deformation. In the reinforced concrete section for example, the steel bars will restrain the concrete when the concrete shrinks. For the cast in-situ slab, the drying shrinkage can be prevented by the prefabricated concrete and in the end lead to tensile stresses. The restraint degree can in Figure 2.7 (a) be calculated according to equation (2.14), compared to external restraint, see equation (2.13), Engström (2006).

$$R = \frac{1}{1 + \frac{E_c}{E_s} \frac{A_{net}}{A_s}} \quad (2.14)$$

where $A_{net} = A_c - A_s$

2.3 Restraint stresses

There are different phenomena and actions that cause stresses and strains in concrete elements. Some strains are stress-dependent and some are stress-independent. Stress-dependent strains occur when elements are loaded so that stresses appear. The opposite is stress-independent strains, which occur without stresses, e.g. strain due to temperature variation. Stress dependent strains occur because of the prevented need for movements due to stress-independent strains.

2.3.1 Thermal strain

Temperature changes produce strains in structures due to the need for expansion or contraction. If this deformation is restrained, stresses will occur. Temperature changes ΔT , can be applied uniformly across the section or as a gradient, linear or non-linear, see Figure 2.8. The coefficient of thermal expansion for concrete and steel is

approximately the same¹: $\alpha_e = 10.5 \cdot 10^{-6} \text{ 1/K}$. In this thesis the effect of a uniform temperature distribution shown in Figure 2.8 (a), will be studied.

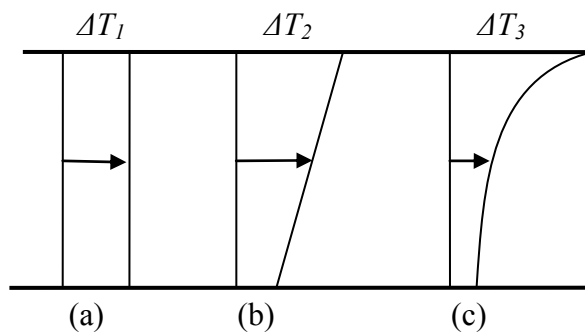


Figure 2.8 Schematic view of different temperature distributions over the height of a concrete member. These distributions can also be used for shrinkage strains.

According to Ghali and Favre (1994), the temperature distribution in a structure varies due to several variables, such as:

- geometry
- thermal conductivity
- absorptivity and convection coefficients
- latitude and altitude of the location
- season
- variations of temperature and wind speed

2.3.2 Shrinkage strain

Shrinkage of concrete starts already during casting, but the final value $\epsilon_{cs}(\infty)$ is reached after long time. Even though the final shrinkage strain is fairly small, 0.1 - 0.5‰, it may have large influence on the concrete stresses and the risk of cracking, Engström (2006). Note that shrinkage can be applied as linear or non-linear gradients over the height, as described for temperature in Figure 2.8.

¹ According to Eurocode 2 and BBK 04 the coefficient for thermal expansion is $10.0 \cdot 10^{-6} \text{ 1/K}$. By using $10.5 \cdot 10^{-6} \text{ 1/K}$ the thermal strain will be overestimated with 5%, resulting in the same response as 31.5°C when a temperature change of 30°C is used.

According to Eurocode 2, CEN (2004), the shrinkage strain, ε_{cs} can be determined from:

$$\varepsilon_{cs}(t) = \varepsilon_{cd}(t) + \varepsilon_{ca}(t) \quad (2.15)$$

where ε_{cd} and ε_{ca} are drying shrinkage strain and autogenous shrinkage strain of concrete.

Drying shrinkage depends on the transport of moisture inside the concrete, while autogenous shrinkage is a type of chemical shrinkage caused by the hydration process, Engström (2006). Both types develop with time.

In order to estimate the drying and autogenous shrinkage strain, the following equations can be used according to Eurocode 2.

$$\varepsilon_{cd}(t) = \beta_{ds}(t) \cdot \varepsilon_{cd}(\infty) \quad (2.16)$$

$$\varepsilon_{ca}(t) = 2.5(f_{ck} - 10) \cdot 10^{-6} \quad (2.17)$$

How to calculate each variable is not an aim in this thesis. Hence, it is described further in APPENDIX A and a comparison between Eurocode 2 and BBK 04 is made in APPENDIX C.

2.3.3 Creep

Concrete subjected to stress has a need for deformation. How these deformations occur is a matter of time and material properties. When a force is applied on a concrete element it will result in a stress dependent deformation, Figure 2.9. This stress dependent deformation can be divided into an immediate elastic deformation $\varepsilon_{c,el}$ and a creep deformation $\varphi(t, t_0) \cdot \varepsilon_{c,el}$. The creep deformation will increase with time, as the load is acting on the structure. However, after long time the creep is assumed to reach a final value.

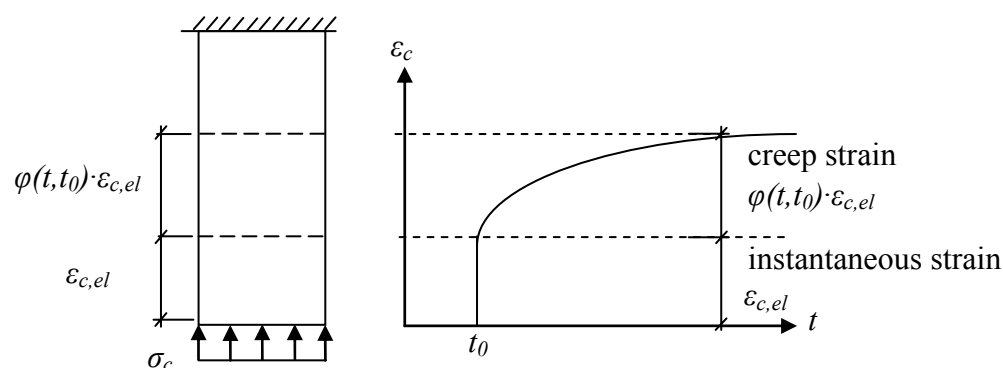


Figure 2.9 Stress dependant strain of concrete subjected to long-term loading with constant stress, based on Ghali and Favre (1994).

Figure 2.9 shows first the instantaneous strain $\varepsilon_{c,el}$ which appears at t_0 when the load is applied. The second branch illustrates the creep deformation that develops with time.

According to CEB (1997), the growth of creep strain and its velocity depends on:

- the rate of loading
- the amplitude of loading
- the age of the concrete at the time of loading
- if the concrete is loaded for the first time or not

Under constant conditions, the deformation due to creep increases when:

- water/cement-ratio increases
- stiffness or the amount of aggregates decreases
- hardening time of concrete is decreased
- relative humidity decreases
- the thickness of the structural element is smaller
- the humidity content of the concrete at loading is higher
- the temperature increases
- age of the concrete at loading decreases
- increase of load occurs

The most evident effect that can be observed due to creep is the increased deformation of concrete structures. But there are also other effects that are of high interest. With time the concrete will become softer. This results in redistribution of stresses in the reinforced concrete, so that the steel stresses increase with time and the concrete stresses decrease. With time the concrete also will tend to adapt itself to constraints due to creep, which eventually will lead to reduced restraint stresses, Engström (2006).

2.3.3.1 Example of creep deformation

The total deformation at a time t may be estimated by using linear dependence and neglecting shrinkage can be performed by using equations given in CEB (1997) and Eurocode 2.

$$\varepsilon(t, t_0) = \varepsilon_c(t_0) \cdot (1 + \varphi(t, t_0)) \quad (2.18)$$

where $\varphi(t, t_0)$ = creep coefficient

The creep coefficient at time t can be calculated according to equation (2.19)

$$\varphi(t, t_0) = \varphi_0 \cdot \beta_c(t, t_0) \quad (2.19)$$

For estimation of the notional (final) creep coefficient, the following expression may be used.

$$\varphi_0 = \varphi_{RH} \cdot \beta(f_{cm}) \cdot \beta(t_0) \quad (2.20)$$

where φ_{RH} = factor which considers the relative humidity, see equation (B.1) or equation (B.2).

$\beta(f_{cm})$ = factor which considers the concrete strength class, see equation (B.4).

$\beta(t_0)$ = factor which considers the age when the concrete was loaded, see equation (B.5).

$\beta_c(t, t_0)$ = time function of the creep coefficient

How to calculate all the factors is described in APPENDIX B and a comparison between Eurocode 2 and BBK 04 is made in APPENDIX D.

2.3.4 Creep and shrinkage according to Swedish code BBK 04

In the Swedish handbook BBK 04, Boverket (2004), the creep and shrinkage strain are estimated in a simplified way. The creep coefficient φ and final shrinkage strain ε_{cs} is chosen as one of the values listed in Table 2.1. A comparison of creep and shrinkage strain is presented in APPENDIX C and APPENDIX D.

Table 2.1 Creep coefficient and mean value of the final shrinkage strain ε_{cs} for different environments according to the Swedish handbook BBK 04, Boverket (2004).

Environment	RH [%]	φ	ε_{cs}
Indoor heated premises	55	3	$0.40 \cdot 10^{-3}$
Normally outdoors and outdoor in non heated premises	75	2	$0.25 \cdot 10^{-3}$
Very moisture environment	≥ 95	1	$0.10 \cdot 10^{-3}$

The creep coefficient can be adjusted with respect to degree of maturity when the first load is applied according to Table 2.2.

Table 2.2 Factor for adjustment of the creep coefficient φ .

a [%]	factor
40	1.4
70	1.3
85	1.1

The adjustment factor a , consider the strength maturity when the first load is applied. The factor a , denote the current strength as a percentage of the requested strength.

3 Material and bond behaviour

3.1 Concrete

For concrete, focus will in this thesis be on the tensile side, since the boundary conditions and the load used in the studies (see Chapters 4, 5 and 6) in general not will generate compression in the concrete.

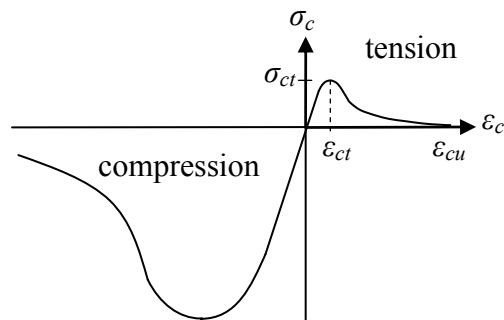


Figure 3.1 Total material response for concrete.

The post-cracking behaviour, $\varepsilon > \varepsilon_t$, is based on the fracture energy, which is the strain energy converted to heat during the fracture process, represented by the area under Figure 3.2 (c) which also refers to different stages in Figure 3.3 (a)-(e). Figure 3.3 (a)-(c) represents the response shown in Figure 3.2 (b). Figure 3.3 (d) and (e) represents the post cracking behaviour seen in Figure 3.2 (c).

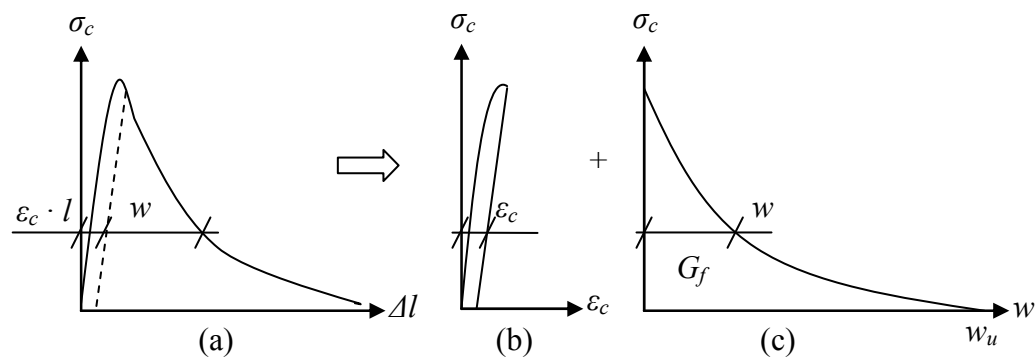


Figure 3.2 (a) mean concrete stress-displacement relation for uniaxial tensile test specimen. The displacement is separated into (b) stress-strain relation and (c) stress-crack opening relation. The area under the softening curve in (c) represents the fracture energy G_f . Based on Plos (2000).

Figure 3.3 (a-e) shows a fracture development in a concrete specimen when loaded in tension. Microcracks are formed in weak points. These will not grow significantly as long as the tensile strength is less than approximately 70% of the tensile strength and until then the stress-strain relationship is found to be linear. When the stress increases further, a critical state is reached and the microcracks connect. A continuous and open crack is formed and finally no further stress can be transferred across the crack. The concrete stress disappears and the crack opening w is greater than the ultimate crack opening w_u .

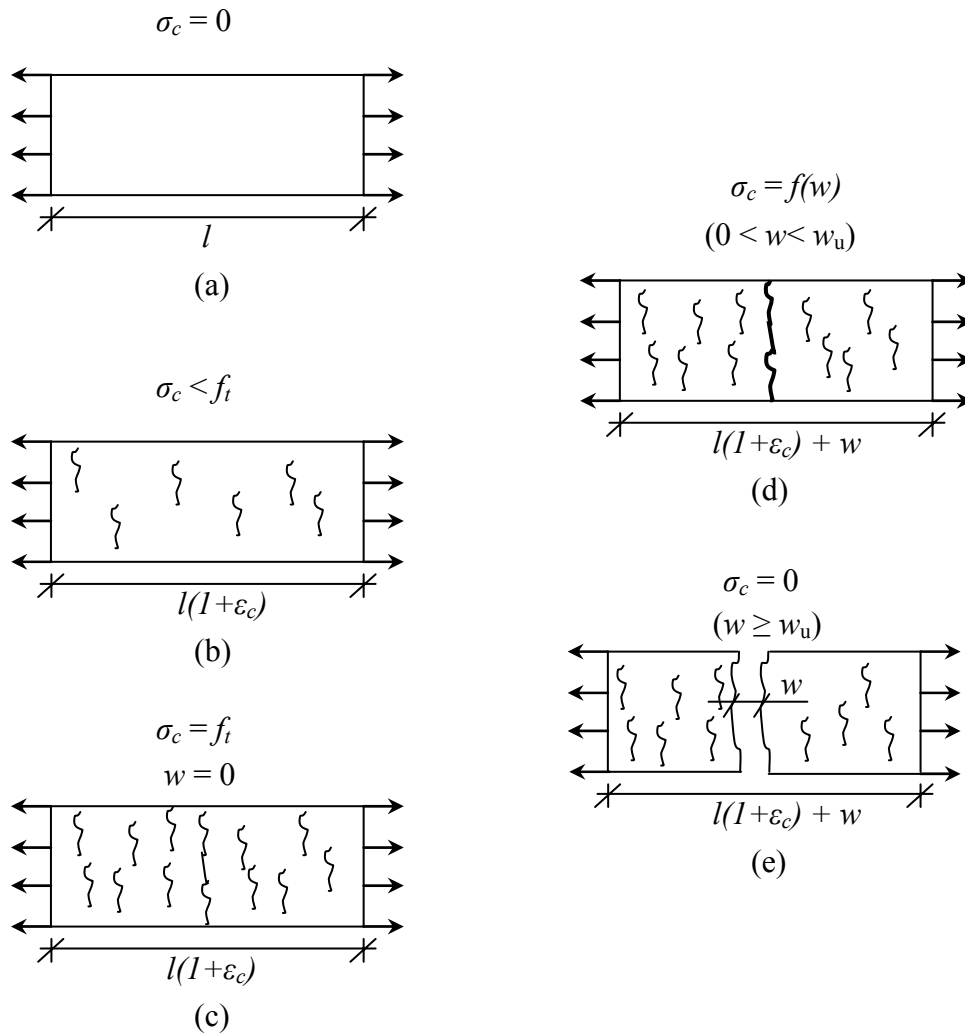


Figure 3.3 Stages in crack formation of a concrete element subjected to increased elongation. Based on Johansson (2000).

3.1.1 Modelling in FE-analysis

Concrete has a characteristic behaviour both in compression and in tension. To be able to use the material in a proper manner in FE-analyses, some simplifications and clarifications have to be made. In the commercial software ADINA a predefined model can be used, called CONCRETE, ADINA (2005). This model simulates a non-linear response in both tension and compression, where the response in the former is bilinear, as shown in Figure 3.4 (a).

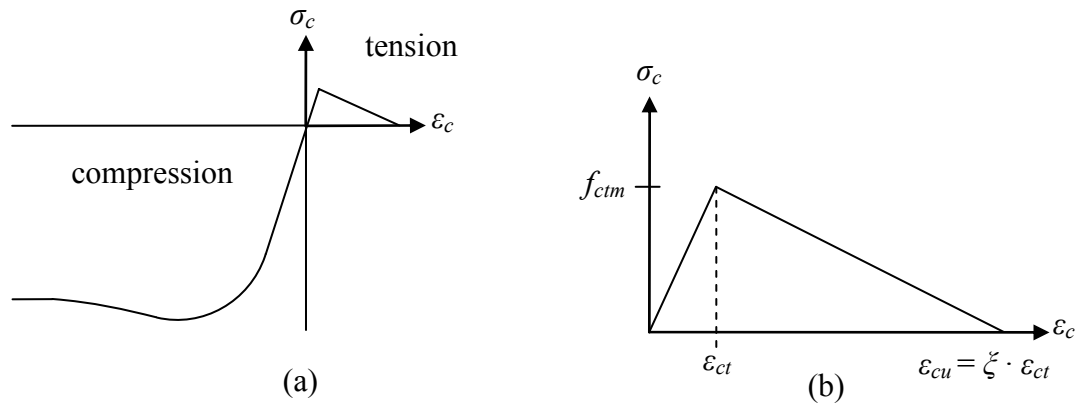


Figure 3.4 (a) total material response in ADINA and (b) details for tensile response.

The post-cracking behaviour of concrete in this case can be described as shown in Figure 3.4, by implementing a relation between the strain at tensile failure, ϵ_{ct} and the ultimate tensile strain, $\epsilon_{cu} = \zeta \cdot \epsilon_{ct}$, described in Section 6.2.2. This method is preferred instead of implementing the actual value of the fractural energy G_f which is described in Section 3.1 and also Section 6.2.2.

3.1.2 Modelling with analytical methods

When using concrete material in hand calculation and analytical tools the response normally is modelled according to Figure 3.5. This means that the concrete will not be able to transfer any stresses after the stress has reached the tensile strength.

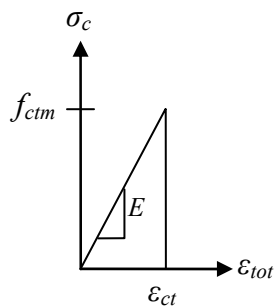


Figure 3.5 Response in tension for hand calculations.

In Section 3.3 an expression for the bond slip relation is presented, see equation (3.2). From this relation the analytical expression for the crack width in equation (3.1), can be derived, Engström (2006).

$$w = 0.420 \left(\frac{\phi \cdot \sigma_s^2}{0.22 f_{cm} \cdot E_s \left(1 + \frac{E_s}{E_c} \cdot \frac{A_s}{A_{ef}} \right)} \right)^{0.826} + \frac{\sigma_s}{E_s} \cdot 4\phi \quad (3.1)$$

where 4ϕ as can be seen in equation (3.1) relates to the local bond failure seen in Figure 3.10.

3.2 Steel

In this thesis it is assumed that the reinforcing steel acts as a bilinear material, also called elastic-plastic material. In reality the stress-strain relation of steel is more complex, according to Figure 3.6 (a). However, in the stress-strain relation of the reinforcement a simplified method is used. The material property is modelled according to Figure 3.6 (b) and (c).

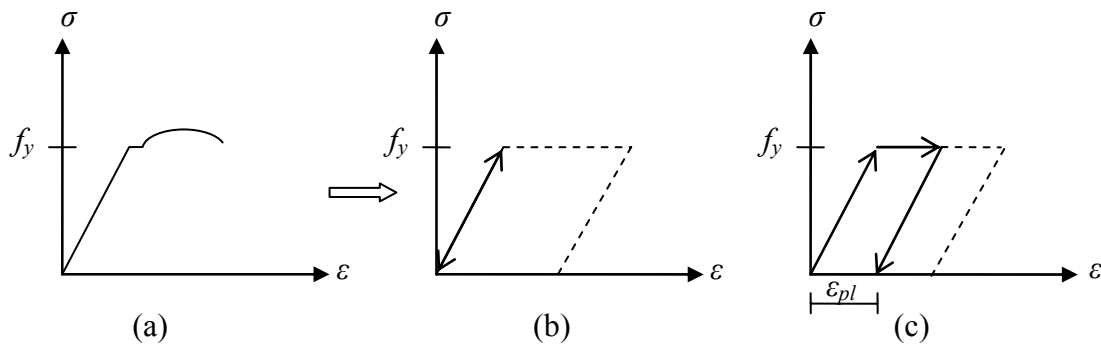


Figure 3.6 (a) Theoretical response of reinforcing steel. (b) Simplified response when unloading just before reaching yield stress in the reinforcing steel. (c) Unloading after yield stress is reached in reinforcing steel.

If the load is removed before the yield stress has been reached, the material still acts as a fully elastic material, i.e. there will be no remaining deformations. If the yield stress has been reached, some plastic deformation will remain after unloading, see Figure 3.6 (c). In the analysis carried out in this thesis, the reinforcement only acts in the linear part of the response curve due to the small loads in the service state.

3.3 Bond behaviour

Bond stress is the stress in the interface between concrete and steel, describing the interaction between the two materials. Bond stress is a type of shear stress and is denoted τ_b . The magnitude of the bond stress increases to a certain value, as the slip s between steel and concrete increases.

A typical relationship between bond stress τ_b and slip s for ribbed bars in well confined concrete is shown in Figure 3.7, adopted from Soroushian and Choi (1989). Based on such relations, schematic relations between bond stress and slip have been proposed in CEB-FIP Model Code 90, CEB (1991), see Figure 3.8.

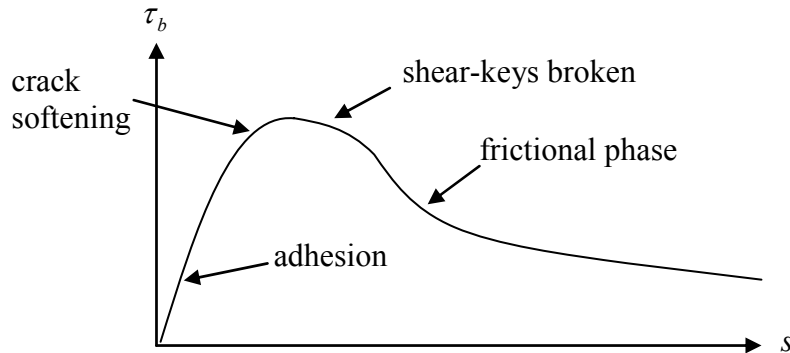


Figure 3.7 General bond slip relation at pull out failure.

The bond behaviour is a combination of mechanical interlock and friction. Bond failure may occur by pulling out the bar or by longitudinal splitting of the concrete cover. The first plateau of the schematic bond stress-slip relation is assumed to be constant between 1 - 3 mm and then decreasing according to Figure 6.12, see CEB Bulletin-235, CEB (1997).

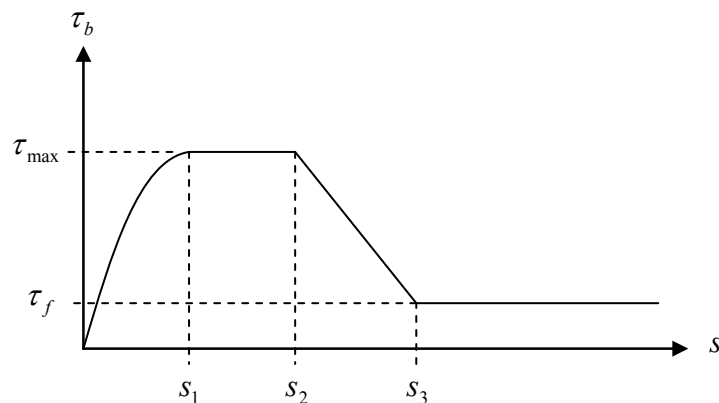


Figure 3.8 Schematic relationship between bond stress and slip according to CEB-FIP Model Code 90.

For analysis in the service state it is normally only the first branch of the bond stress-slip relationship that needs to be considered. The following expression proposed, is valid for both normal strength and high strength concrete in service state, CEB (1997).

$$\tau_b(s) = 0.22 \cdot f_{cm} \cdot s^{0.21} \quad s \leq s_1 \quad (3.2)$$

With this relation it is possible to predict how crack widths and transfer lengths depend on, among other things, the steel stress.

3.4 Crack distribution

Where bond stresses act along a reinforcement bar, force is transferred from the steel to the surrounding concrete. The maximum transfer length $l_{t,max}$ is the transfer length needed to develop tensile stresses in the concrete equal to the tensile strength, see Figure 3.9. A further increase of the concrete stress would result in cracking.

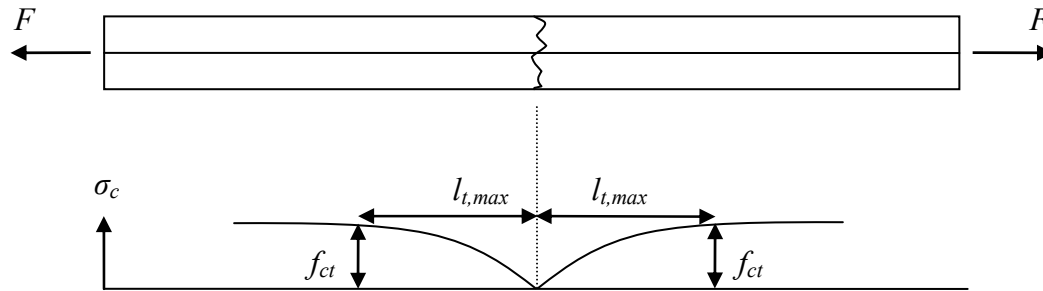


Figure 3.9 Concrete stress after first crack according to Ghali and Favre (1994).

Within this maximum transfer length $l_{t,max}$ no new cracks can appear as the concrete stress is below the tensile strength. The distance between two cracks can on this basis vary between $s_{r,min}$ and $s_{r,max}$ according to equation (3.3) and (3.4).

$$s_{r,min} = l_{t,max} \quad (3.3)$$

$$s_{r,max} = 2 \cdot l_{t,max} \quad (3.4)$$

The maximum crack distance $s_{r,max}$ is the theoretical maximum distance between two cracks in which the concrete stress almost reaches the concrete tensile capacity. Hence, a further crack within this region is not possible.

When taking a possible local bond failure into consideration according to Figure 3.10, the expression for the crack spacing will increase with a bond-free length Δr which is shown in equations (3.5) and (3.6). Local bond failure is the mechanism that occurs in a free end or at a primary crack when the bond between steel and concrete is reduced or even destroyed. This is explained by the fact that the bond stresses act towards a free end of the element.

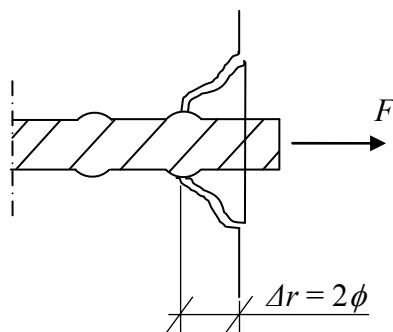


Figure 3.10 Local bond failure.

$$s_{r,\min} = l_{t,\max} + \Delta r \quad (3.5)$$

$$s_{r,\max} = 2 \cdot l_{t,\max} + 2 \cdot \Delta r \quad (3.6)$$

The concrete stress depends on the stresses transferred from the reinforcement bar along the transfer length, as described in equation (3.7), at the moment just before the concrete cracks.

$$f_{ct} \cdot A_c = \tau_{bm} \cdot l_{t,\max} \cdot \pi \cdot \phi \quad (3.7)$$

$$\text{where } \tau_{bm} = \frac{\int_0^{l_{t,\max}} \tau_b(x)}{l_{t,\max}}$$

By dividing equation (3.7) with A_s and inserting ρ_r , the transfer length can be solved as shown in equation (3.8).

$$l_{t,\max} = \frac{1}{4} \cdot \frac{f_{ct} \cdot \phi}{\rho_r \cdot \tau_{bm}} \quad \rho_r = \frac{A_s}{A_c} \quad (3.8)$$

The mean value for the crack distance is shown in equation (3.9), as a result from equations (3.5), (3.6) and (3.8).

$$s_{rm} = \frac{s_{r,\min} + s_{r,\max}}{2} = 1.5 \cdot \Delta r + \frac{3}{8} \cdot \frac{f_{ct} \cdot \phi}{\rho_r \cdot \tau_{bm}} \quad (3.9)$$

In the Swedish handbook BBK 04, Boverket (2004), a similar expression is given, see equation (3.10), for the mean crack spacing in case of pure tension and high bond reinforcement bar, where $\kappa_1 = 0.8$ and $\kappa_2 = 0.25$.

$$s_{rm} = 50 + \kappa_1 \cdot \kappa_2 \cdot \frac{\phi}{\rho_r} \quad (3.10)$$

When comparing equation (3.9) and equation (3.10) it is possible to identify an expression for the mean value of the bond stress in case of pure tension, see equation (3.11).

$$\tau_{bm} = \frac{3}{2 \cdot \kappa_1} \cdot f_{ct} \quad (3.11)$$

For estimation of the crack width, equation (3.12) may be used, where it should be noted that it is an upper limit for calculation of the crack width and will not consider the tensile stress in the concrete between the cracks.

$$w = s_{rm} \cdot \frac{\sigma_s}{E_s} = s_{rm} \cdot \epsilon_s \quad (3.12)$$

Based on the bond behaviour, equation (3.2), the analytical expression for the crack width may be calculated according equation (3.1) and the transfer length can be derived as follows.

$$l_t = 0.443 \frac{\phi \cdot \sigma_s}{0.22 f_{cm} \cdot w_{net}^{0.21} \left(1 + \frac{E_s}{E_c} \frac{A_s}{A_{ef}} \right)} + 2 \cdot \phi \quad (3.13)$$

In equation (3.13) the contribution from the local bond failure is given as 2 times the bar diameter ϕ . The expression w_{net} , equation (3.14), is the crack width where the contribution of the local bond failure is not included.

$$w_{net} = 0.420 \left(\frac{\phi \cdot f_{yk}^2}{0.22 f_{cm} \cdot E_s \left(1 + \frac{E_s}{E_c} \cdot \frac{A_s}{A_{ef}} \right)} \right)^{0.826} \quad (3.14)$$

In equation (3.13) the contribution from the local bond failure to the transfer length is half of the contribution to the crack width, shown in equation (3.1), Engström (2006).

4 Parameters influencing the risk of cracking

In order to better understand the influence of different parameters regarding the distribution of stresses and strains and risk of cracking, a parametric study was carried out. The aim of this study was to make it easier to understand which data were to be used in further analyses.

The basis for the geometry upon on which further studies will be done comes from a wall with longitudinal reinforcement, as shown in Figure 4.1.

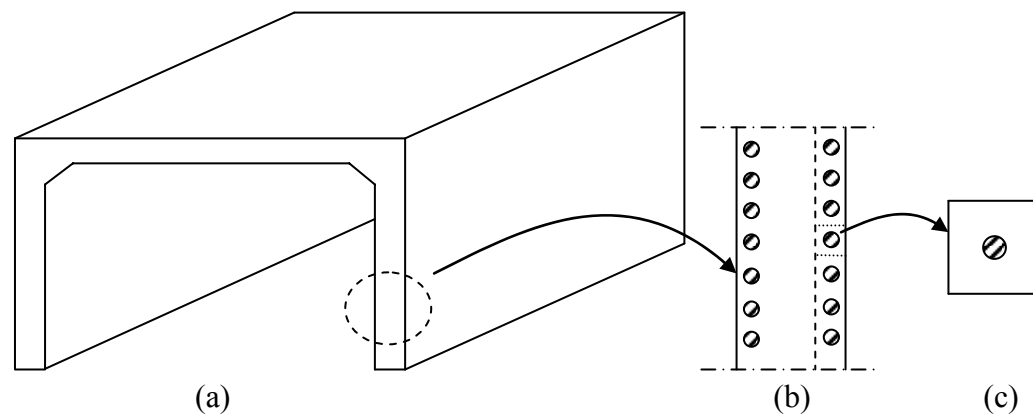


Figure 4.1 Background for chosen geometry.

Figure 4.1 (b) is to be compared with Figure 2.4 (b). As an assumption is made concerning that the structure will crack if the surface region cracks, a prism as shown in Figure 4.1 (c) is to be further studied. This prism will not correspond fully to the real case, but it is a step towards understanding the behaviour of reinforced concrete subjected to restraint forces. To choose the geometry of the prism the requirement of minimum reinforcement has to be fulfilled according to equation (4.1), Eurocode 2, CEN (2004).

$$A_{s,min} \cdot \sigma_s = k_c \cdot k \cdot f_{ct,eff} \cdot A_{ct} \quad (4.1)$$

where k_c and k are factors that in this case can be assumed to 1.0.

If $A_{ct} = 100 \times 100 \text{ mm}^2$, $f_{ct,eff} = 2.9 \text{ MPa}$ and $\sigma_s = f_{yk} = 500 \text{ MPa}$ the minimum reinforcement area is calculated to $A_{s,min} > 58 \text{ mm}^2$. This refers to a bar diameter of approximately $\phi \geq 8.6 \text{ mm}$. For usage of standard dimension, a minimum bar diameter of 10 mm will be used further on.

4.1 Specimen and basic input parameters

In this first study the response in means of concrete stress was studied in the uncracked stage. Therefore the concrete was treated as in state I and transformed concrete sections were used in the calculations. The calculations were carried out with analytical models for the material response, see Chapter 3 and APPENDIX H. By using varied input data for the parameters, the influence on the response was studied by means of concrete stress and risk of cracking.

The following assumptions were used for the specimen in case of default values in the study:

Material:

$$f_{ct} = 2.9 \text{ MPa}$$

$$E_{cm} = 33 \text{ GPa}$$

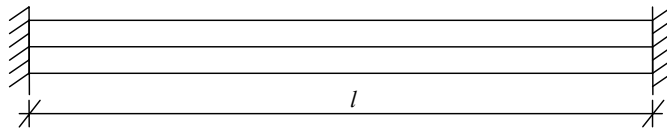
$$f_{yk} = 500 \text{ MPa}$$

Dimensions:

$$A_c = h \cdot b = 100 \times 100 \text{ mm}^2$$

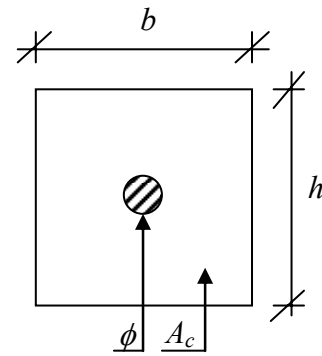
$$\phi = 16 \text{ mm}$$

$$l = 2 \text{ m}$$



Restraint degree:

$$R = 60\%$$



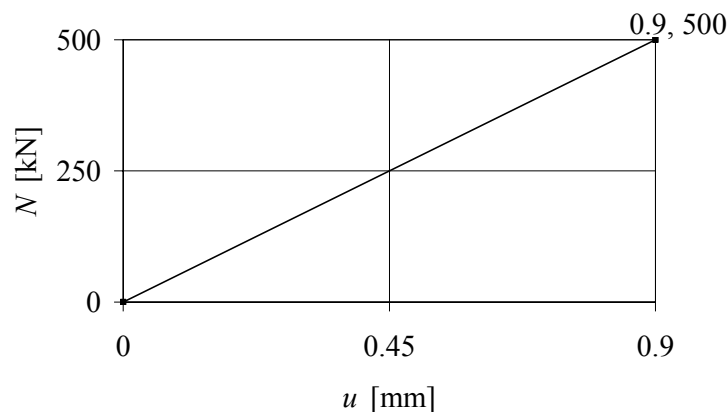
Load condition:

A negative change of a uniformly distributed temperature by $\Delta T = -10\Delta^\circ\text{C}$.

Thermal expansion coefficient is: $\alpha_e = 10.5 \cdot 10^{-6} \text{K}^{-1}$.

Support condition:

According to the default values for the study a restraint degree is chosen to $R = 60\%$ and the value of the stiffness S is derived according to equation (2.13) This value will then be used if nothing else is mentioned. Hence, it is important to note that since the support stiffness S will be constant, the restraint degree will vary during the study.



$$S = \frac{N}{u} = \frac{500}{0.9} = 555.6 \frac{\text{MN}}{\text{m}}$$

Figure 4.2 Chosen stiffness at each support.

Material behaviour:

The concrete is assumed to be uncracked with a linear elastic short-term response without creep. The number of reinforcement bars is set to 1.

The influence of the following parameters was examined:

- diameter of reinforcement bar, ϕ .
- area of concrete cross section, A_c .
- length of specimen, l .
- restraint degree, R .

For each parameter, the influence on the resulting concrete stresses was studied. The results are presented in the following section.

4.2 Results

4.2.1 Influence of bar diameter

When increasing the diameter of the reinforcement bar, and therefore also the reinforcement ratio, the concrete stress decreases since the calculated value of the transformed concrete area A_I in state I, increases, see equation (4.2).

$$A_I = (h \cdot b) + (\alpha - 1) \cdot n \cdot A_{si} \quad (4.2)$$

When calculating the concrete strain using the constitutive relationship, the strain will be reduced as the transformed concrete cross-section A_I increases. This results in reduced stresses within the transformed concrete area, according to equations (4.5) and (4.6). Reduced risk of cracking is to be expected when the bar diameter increases.

$$R = \frac{\varepsilon_c}{-\varepsilon_{cT}} \quad (4.3)$$

$$R = \frac{1}{1 + \frac{2 \cdot E_{cm} \cdot A_I}{S \cdot l}} \quad (4.4)$$

$$\varepsilon_c = \frac{-\varepsilon_{cT}}{1 + \frac{2 \cdot E_{cm} \cdot A_I}{S \cdot l}} \quad (4.5)$$

$$\sigma_c = E_{cm} \cdot \varepsilon_c \quad (4.6)$$

However, increasing the bar diameter must not be made on the expense of the concrete cover or minimum distance between bars.

Figure 4.3 shows the result when using various bar diameter, while keeping the concrete section constant. The concrete stress is compared to the 5%-fractile of the concrete tensile strength.

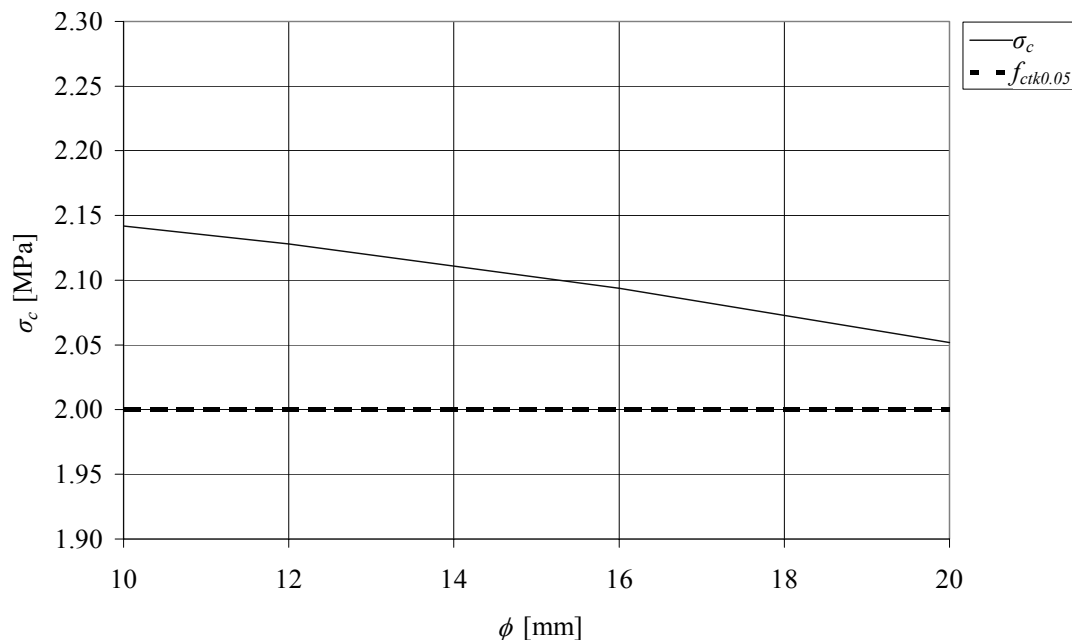


Figure 4.3 Concrete stress calculated for various bar diameter.

The result shows that by using default dimensions of steel bars it is a risk of cracking for the actual loading condition. However, it is not appropriate to increase the bar diameter in order to avoid cracks. Note that the scale on the vertical axis is relatively small. If the steel area is increased with 100%, the concrete stress will decrease with approximately 2%, see Figure 4.3.

4.2.2 Influence of concrete cross section area

By increasing the area of the concrete cross section, the transformed concrete area in state I will increase according to equation (4.2). According to equation (4.5) and equation (4.6) the concrete stresses will decrease. The effect in this case, regarding the risk of cracking, is much larger than for the various bar diameters. It is important to notice that the restraint degree differs when increasing the cross section area compared to the default parameters. The influence of the cross section A_I affects the restraint degree significantly, according to equation (4.4).

When increasing the concrete cross section and thereby decreasing the restraint degree, consideration must be taken to prescriptions of minimum reinforcement in Eurocode 2. The following results were obtained for variation of the concrete cross sections, see Figure 4.4.

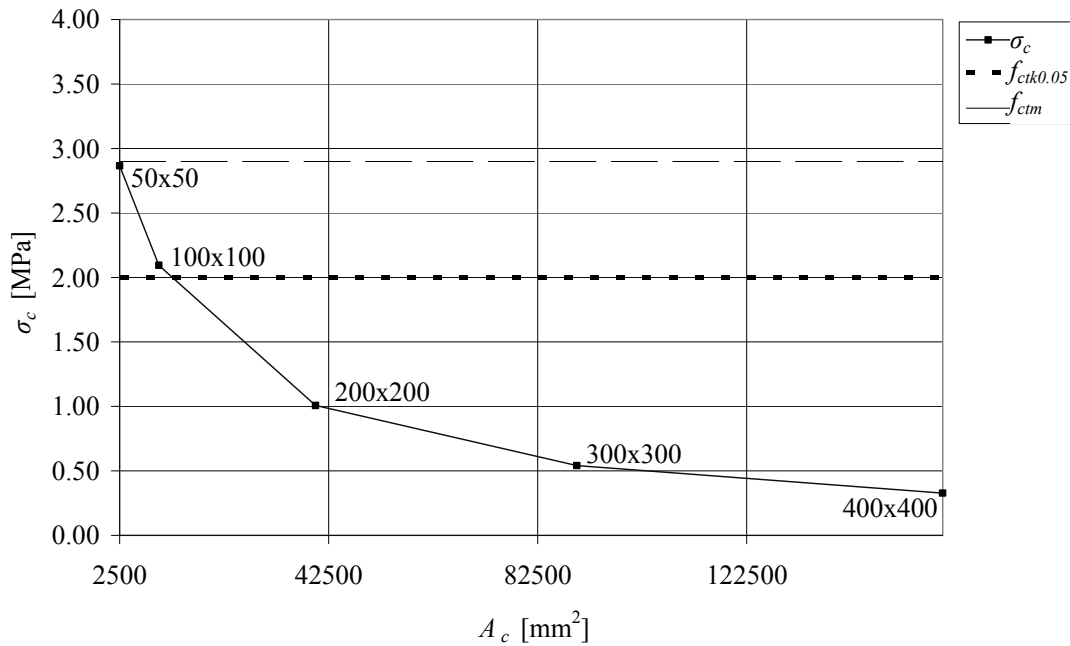


Figure 4.4 Concrete stress calculated for various cross sections.

As shown in Figure 4.4, the stress can decrease significantly as the concrete cross section increases. By increasing the effective area of concrete, shown in Figure 2.4, decreased stresses and therefore decreased risk of cracking will follow. For instance if the cross section area increases with 100%, the concrete stress will decrease with approximately 41%.

4.2.3 Influence of length

As the length of the studied specimen increases, equation (4.5) will change towards equation (4.8) according to equation (4.7).

$$\varepsilon_c = \frac{-\varepsilon_{cT}}{1 + \frac{2 \cdot E_{cm} \cdot A_I}{S \cdot l}} \Rightarrow \frac{-\varepsilon_{cT}}{1 + \frac{2 \cdot E_{cm} \cdot A_I}{S \cdot \infty}} \Rightarrow \frac{-\varepsilon_{cT}}{1 + 0} \Rightarrow -\varepsilon_{cT} \quad (4.7)$$

$$\varepsilon_c = -\varepsilon_{cT} \quad \text{for } R = 1.0 \quad (4.8)$$

The increased concrete strain results in increased concrete stresses. The following results were obtained for various lengths of the specimen, see Figure 4.5. Note that if the length of the element is increased with 100% the stress will increase with approximately 24% in the concrete. Also note that the relation is not linear and that the restraint degree increases with the length.

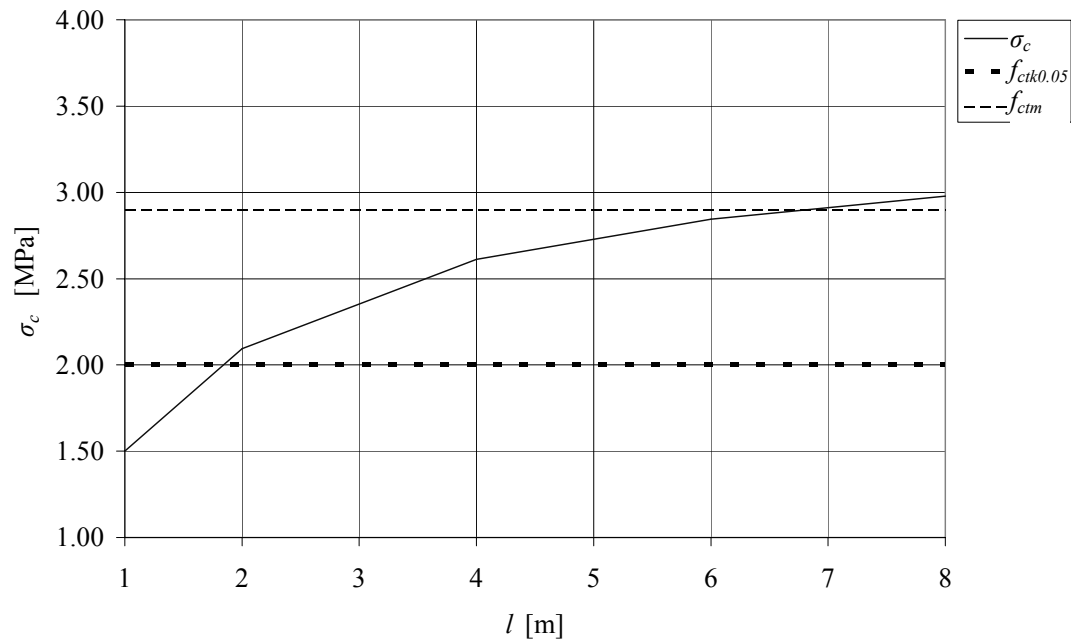


Figure 4.5 Concrete stress calculated for various lengths.

4.2.4 Influence of support conditions

As the element is restrained with different support stiffness, the restraint degree affects the global response. When increasing the stiffness at the support, the element is no longer allowed to move in the same manner as before. This will decrease the concrete strain and hence, increase the concrete stress. As for the case with increased length, equation (4.5) will change towards equation (4.7) resulting in increased risk of cracking and increased support stiffness. This has been done in the previous studies but here it is more systematic and controlled.

The following results were obtained for various restraint degrees at the supports, see Figure 4.6. Note that if the support stiffness increases with 100%, the concrete stress will increase with 100%.

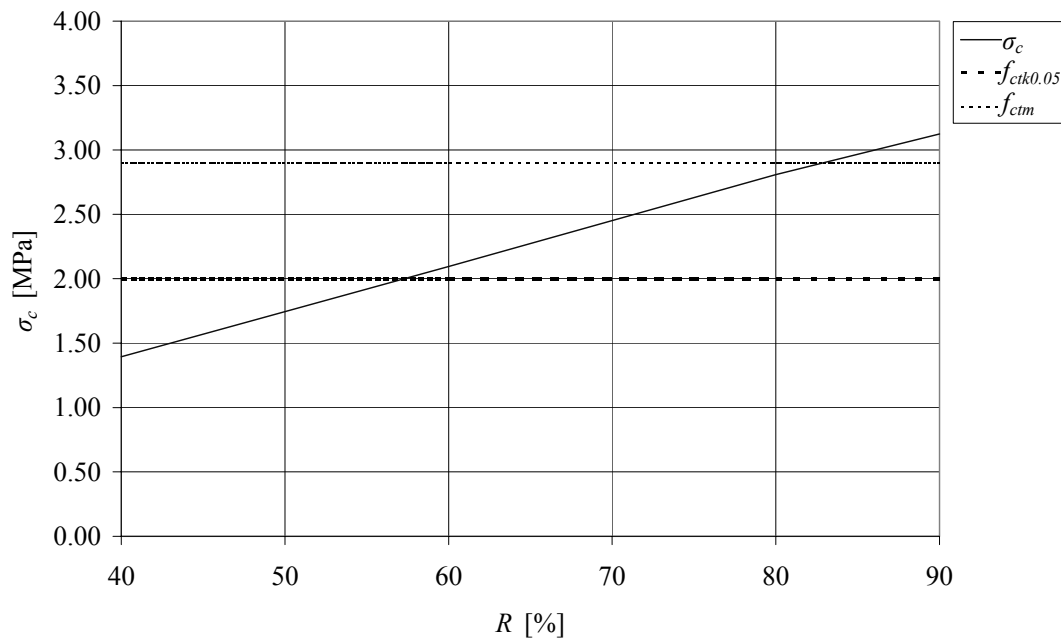


Figure 4.6 Concrete stress calculated for various supports conditions.

4.3 Concluding remarks

This study showed that different parameters have different effects on the concrete stress and the risk of cracking. In addition it is appropriate to present the change of the global stiffness. The material and geometry assumed in this study relate to a specific stiffness, see equation (4.9).

$$k = \frac{E \cdot A}{l} \quad (4.9)$$

The system can be modelled as a combination of stiffness according to Figure 4.7.

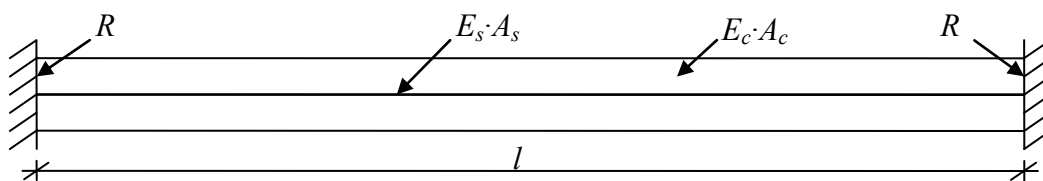


Figure 4.7 Parameters affecting the global stiffness.

When several stiff members are acting together as steel and concrete elements, they can simply be added, but the stiffness at the support has to be considered, according to equation (4.10).

$$k_{tot} = \frac{1}{\frac{1}{k_{R,left}} + \frac{1}{k_c + k_s} + \frac{1}{k_{R,right}}} \quad (4.10)$$

Table 4.1 shows that increasing the concrete cross section area and therefore decreasing the restraint degree is the most preferable option in order to decrease the concrete stress. A more controlled option is to change the restraint at the support but we will not in this study go in deeper on how such an operation would be performed.

Table 4.1 Result from parametric study with different objective.

	σ_c [MPa]	parameter change [%]	$\sigma_{c,new}$ [MPa]	$\Delta\sigma =$ [%]
steel area	2.09	$\Delta A_s = +1$	≈ 2.09	-0.03
concrete area	2.09	$\Delta A_c = +1$	1.54	-26.32
length	2.09	$\Delta l = +1$	2.10	+0.48
restraint	2.09	$\Delta R = +1$	2.11	+0.96

Figure 4.8 shows how the stiffness is affected with regard to a change of a certain parameter. Every bar in the figure relates to an increased or decreased stiffness in percent when a parameter is increased and decreased with 50%. Since the result in almost every parametric study is non-linear, it is important to stress that the concluding result given in the Figure is based on change of from the default geometry, see Section 4.1. Figure 4.8 shows for example that, if the length of the beam is decreased with 50%, the global stiffness of the system will increase with approximately 60%.

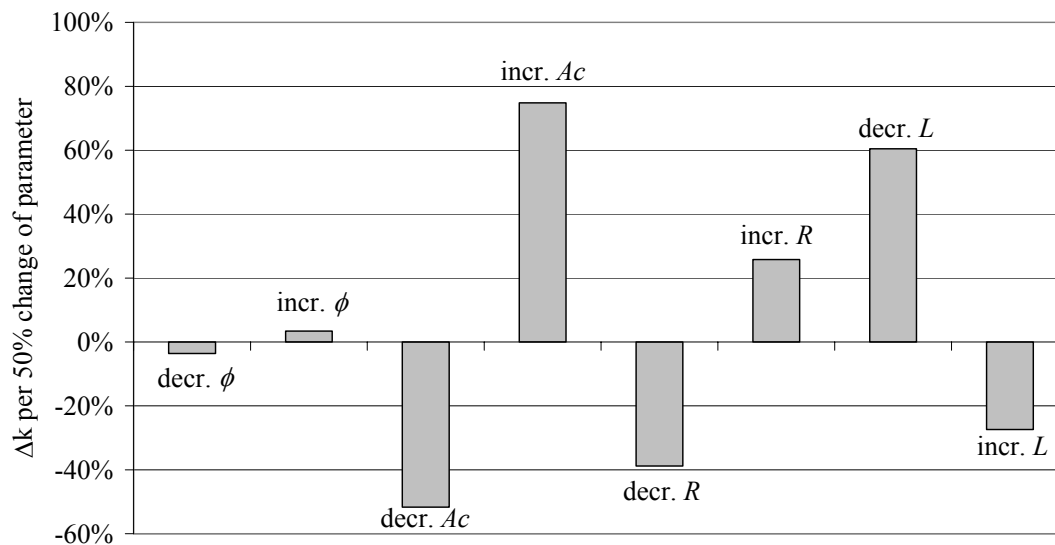


Figure 4.8 Comparison of stiffness contribution at parameter change. The vertical axis shows the amount of percentage change in stiffness when a parameter is increased or decreased with 50%.

5 The cracking process studied by an analytical method

In order to understand the crack propagation after the first crack, a parametric study was made using an analytical method of crack propagation due to restraint forces. Here the cracks were modelled as linear springs, according to Engström (2006) and this approach is hereafter denoted as the *analytical method* and the *analytical model*. The calculations were carried out by means of a numerical stepwise iteration for stresses and deformations caused by a uniform decrease of the temperature, ΔT . The need for thermal deformation, in this case shortening, will result in restraint forces that eventually will cause cracking across the element, see Figure 5.1. The number of cracks that appear depends on the geometry, bond interaction between steel and concrete and the governing material parameters. Further, the maximum number of cracks is limited by the condition that the sum of all crack spacing cannot exceed the total length of the element. For detailed calculations see APPENDIX H and APPENDIX I.

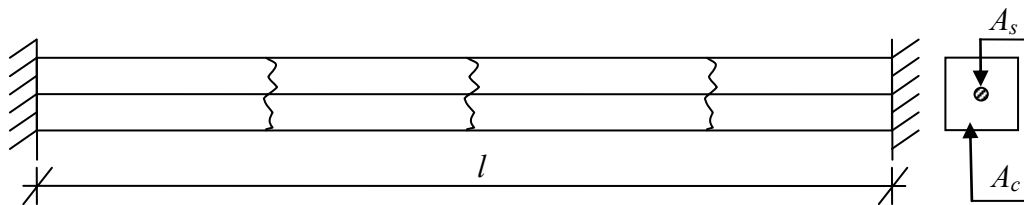


Figure 5.1 Model used in crack propagation study.

5.1 Basic input parameters

The cracking process was studied for a reinforced concrete member as shown in Figure 5.1. A specimen with the following properties was used as a reference case in the parametric study.

Material:

$$f_{ct} = 2.9 \text{ MPa}$$

$$E_{cm} = 33 \text{ GPa}$$

$$f_{yk} = 500 \text{ MPa}$$

Dimensions:

$$A_c = h \cdot b = 100 \times 100 \text{ mm}^2$$

$$\phi = 16 \text{ mm}$$

Length of specimen: $l = 2 \text{ m}$

Loading condition:

A negative change of a uniformly distributed temperature by $\Delta T = -30^\circ\text{C}$.

Thermal expansion coefficient is:

$$\alpha_e = 10.5 \cdot 10^{-6} \text{ K}^{-1}$$

Restraint degree:

$$R = 1$$

In the parametric study one parameter at a time was varied in relation to the reference case. The following parameters were varied in the parametric study with underlined values denoting the reference case.

- diameter of reinforcement bar, ϕ .
 - 10, 12, 16, 20 mm²
- length of specimen, l .
 - 2, 4, 6 m
- concrete cross section area, A_c .
 - 100x100, 200x200, 300x300 mm²
- reinforcement ratio, ρ_r .
 - 1.13% kept constant by variation of geometries
- creep coefficient, $\varphi(\infty, t_0)$.
 - 0, 1, 2, 3

5.2 Calculations

The first assumption was a uniform decrease of the temperature by -30°C. According to the Swedish bridge code BRO 2004, Vägverket (2004), normal production temperature is assumed to be $T_0 = +10^\circ\text{C}$ and a minimum temperature in Gothenburg, Sweden is $T_{min} = -30^\circ\text{C}$. This results in a change of $\Delta T = -40^\circ\text{C}$. Multiplied with a load coefficient, 0.6, results in a change of 24°C. Hence, in this study a maximum change of $\Delta T = 30^\circ\text{C}$ is a relevant choice. Using a coefficient of thermal expansion, $\alpha_e = 10.5 \cdot 10^{-6} \text{K}^{-1}$ this will result in a thermal strain of $\varepsilon_{cT} = \Delta T \cdot \alpha_e = -0.315 \cdot 10^{-3}$. The restraint degree R was set to 1.0 which means that the stress dependent strain in the concrete is equal to the thermal strain with opposite sign, i.e. $\varepsilon_{cT} + \varepsilon_c = 0$.

It was assumed that a new crack appeared when the surface region cracked. The force needed to form a crack in the surface region was calculated according to equation (5.1).

$$N_1 = f_{cm} \cdot [A_{ef} + (\alpha_{ef} - 1)A_s] \quad (5.1)$$

It was assumed that the crack width increased linearly with the steel stress until the yield strength was reached. The crack width at yielding w_y was calculated with regard to the bond stress-slip relation in equation (3.1). The steel stress used in this equation is equal to f_{yk} and is an overestimation when the steel stress in reality is smaller than the yield stress as further discussed in Section 7.2. The response was determined according to the calculations in APPENDIX H.

The deformation condition according to equation (5.2) was used to determine the steel stress and it was assumed that a new crack was initiated when the surface region cracks, according to the following condition.

$$\frac{\sigma_s \cdot A_s \cdot l}{E_{cm} \cdot A_{l,ef}} \cdot (1 + \varphi_{ef}) + n \cdot \frac{\sigma_s}{f_{yk}} \cdot w_y - R \cdot \varepsilon_c \cdot l = 0 \quad (5.2)$$

where n is the number of cracks

$$N(\sigma_s) \geq N_1 \Rightarrow \text{new crack will appear}$$

5.3 Result

The global response for the reference case was found to be as shown in Figure 5.2. The first crack occurred at a negative change of temperature of -8.5°C . As shown in Figure 5.2, the reaction force, F decreased suddenly when the first crack occurred. A similar response was obtained for the following cracks and it corresponds to the expected response described in Figure 2.5 (b). The inclination of the ascending branches shows how the global stiffness decreases for each new crack.

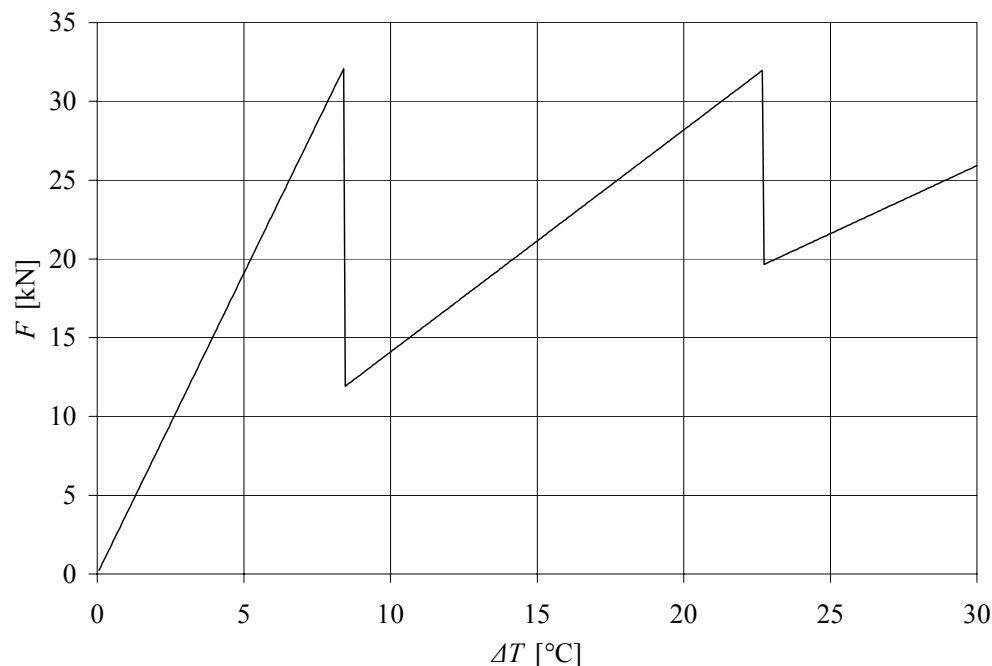


Figure 5.2 Result from default values $\phi = 16 \text{ mm}$, $l = 2 \text{ m}$ and $A_c = 100 \times 100 \text{ mm}^2$.

5.3.1 Influence of bar diameter

When the bar diameter varied, the result appeared as shown in Figure 5.3. When the bar diameter increased, also the surface area, upon which the bond between steel and

concrete acts, increased. The larger bars had an increased ability to transfer the force via bond stresses to the surrounding concrete. In Figure 5.3 it can also be seen that for greater bar diameter the second crack form earlier than for smaller diameter which is positive. Note that it must be studied how the crack widths are affected by this parameter change before a conclusion can be drawn.

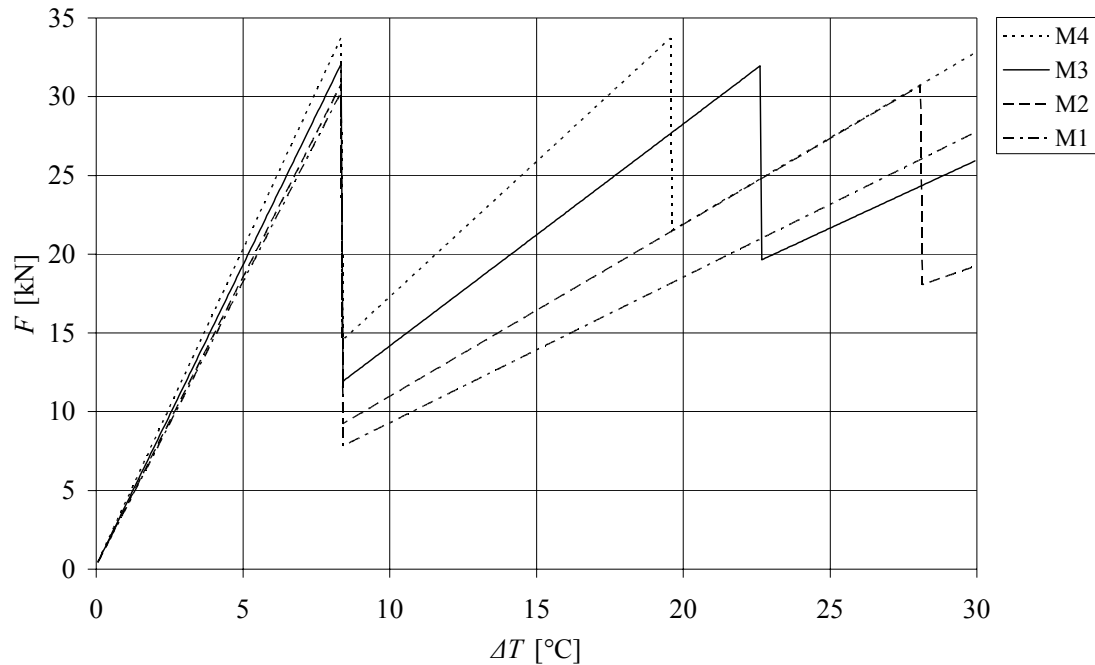


Figure 5.3 Results when the bar diameter varied. $l = 2 \text{ m}$, $A_c = 100 \times 100 \text{ mm}^2$, see Table 5.1 for notations.

The increased tensile capacity in case of larger bars can be explained by equation (5.1), where an increased bar diameter results in an increased transformed concrete area.

From now on the calculations made in the analytical model, and shown in Figure 5.3, are denoted according to Table 5.1. These notations are also further used in order to compare results from Chapter 6.6 in Chapter 7.

Table 5.1 Input for comparison of global response in analytical model.

notation	ϕ [mm]	A_c [mm ²]	$\rho_r = A_s/A_c$ [%]
M1	10	100x100	0.79
M2	12	100x100	1.13
M3	16	100x100	2.01
M4	20	100x100	3.14

5.3.2 Influence of concrete cross section area

The next step in this cracking process study was to increase the concrete cross section. By doing this the transformed concrete area was increased and the expression in equation (5.1) was increased. The reinforcement bar diameter was kept constant, resulting in a decreased reinforcement ratio as the concrete cross section increased. The results are shown in Figure 5.4.

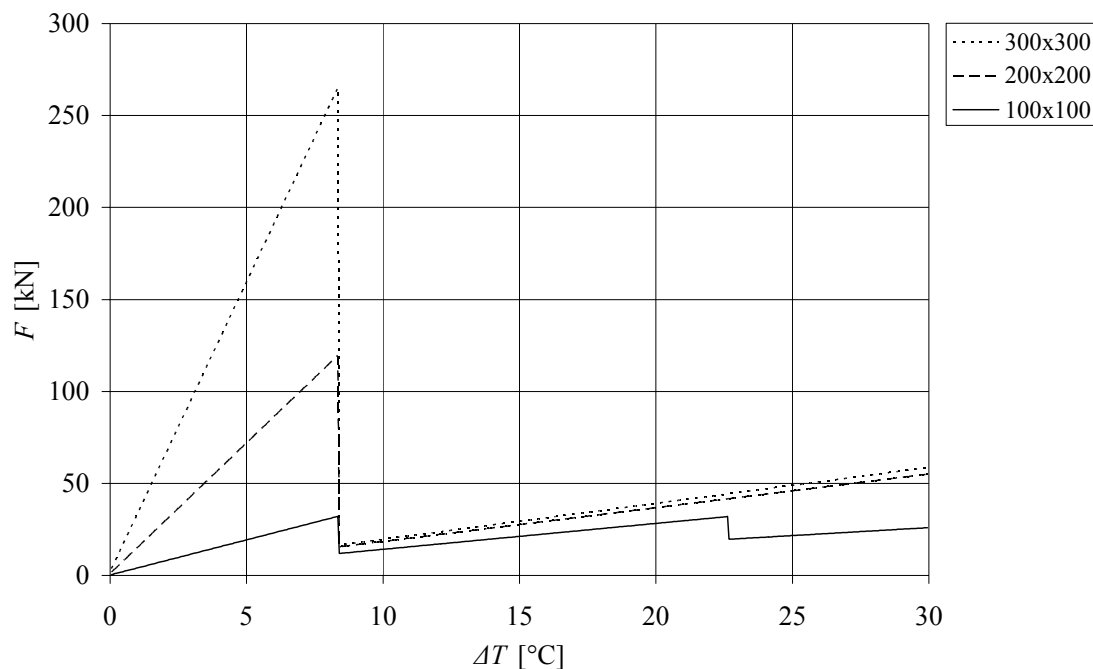


Figure 5.4 Results when the concrete section varied, $A_c = 100 \times 100$, 200×200 , $300 \times 300 \text{ mm}^2$ and $l = 2 \text{ m}$, $\phi 16$.

As mentioned earlier the first crack is to be expected at a temperature load $\Delta T = -8.5^\circ\text{C}$. However as shown in Figure 5.4, the cracking was reduced as the member could take more deformation in the elastic part. Also the cracking force N_I increased when the concrete area was increased, resulting in a need of higher temperature change to achieve further cracks, as shown in Figure 5.4. Important to notice is that if the cracking process is further studied for $A_c = 300 \times 300 \text{ mm}^2$ it is likely that the reinforcement reaches yield stress instead of forming a second crack. For this method controls must be carried out.

5.3.3 Influence of reinforcement ratio

Four specimens with the same reinforcement ratio, but different reinforcement bars and concrete section were studied as shown in Table 5.2. The calculated response is shown in Figure 5.5. Note the deviation from the default values presented earlier. As a reinforcement amount equal to 1% may be considered as a somewhat more normal amount, the case with $\phi 16$ has been exchanged since it results in a reinforcement amount of approximately 2%, see Table 5.2.

Table 5.2 Input for comparison of global response.

notation	ϕ [mm]	A_c [mm ²]	$\rho_r = A_s/A_c$ [%]
M1-2	10	83x83	1.13
M2	12	100x100	1.13
M3-2	16	133x133	1.13
M4-2	20	167x167	1.13

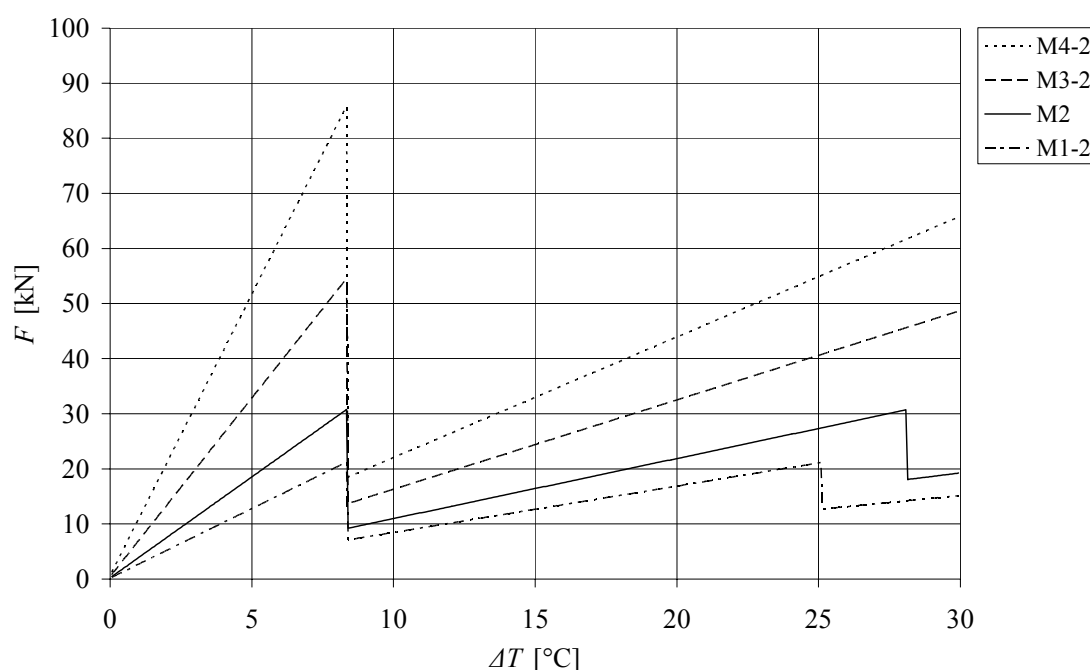


Figure 5.5 Comparison between M1-2, M2, M3-2 and M4-2. Variation of ϕ and A_c while $\rho_r = 1.13\%$ and $l = 2$ m.

Note that the first crack appeared at the same temperature load as for earlier analyses, but when the change increase further, the response varies between the analyses. The $\phi 10$ bar reaches up to a second crack, as for the $\phi 16$ bar there is a need of room for further increased temperature. This shows that when the need of reinforcement is given, a usage of larger bar diameter with larger spacing gives fewer cracks than small bar diameter placed tightly together. This is a result from that the bond increases as larger bar diameter is used.

5.3.4 Influence of creep coefficient

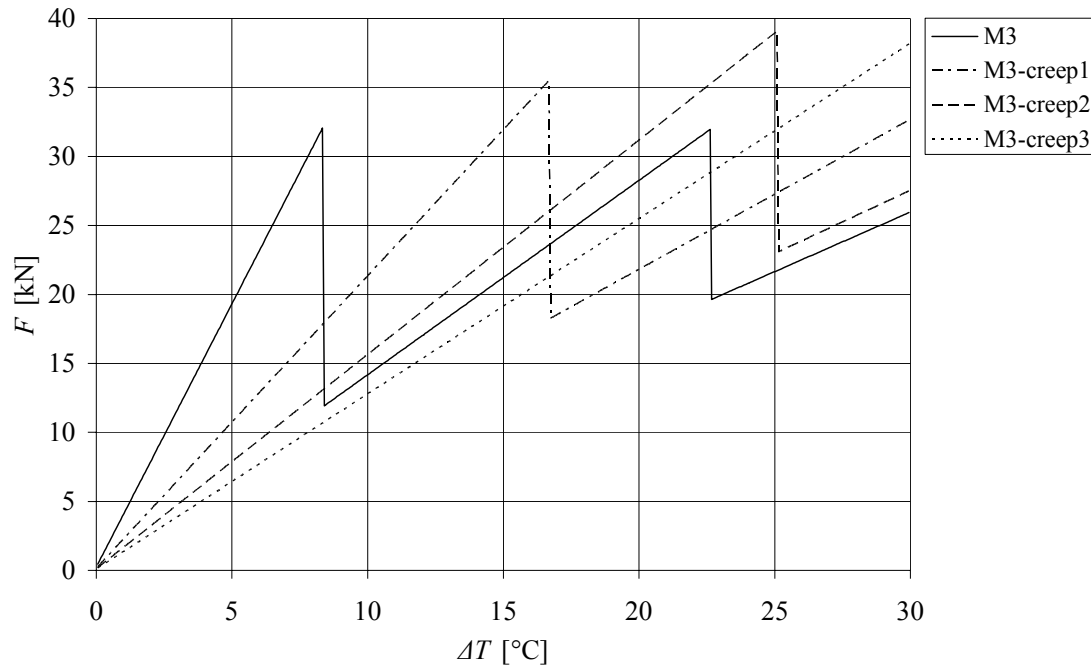


Figure 5.6 Comparison between creep coefficient $\varphi(\infty, t_0) = 0, 1, 2, 3$ for $\phi 16$, $A_c = 100 \times 100 \text{ mm}^2$ and $l = 2 \text{ m}$.

When the creep coefficient increased the effective concrete modulus of elasticity decreased and the global stiffness therefore decreased, as shown in Figure 5.6. Note also that the cracking load increased with increased creep coefficient. This can be explained by the expression for the cracking load, which depends on α_{ef} in the transformed concrete area, see equation (5.1). Note also that when the creep coefficient is increased every crack is formed for higher thermal strain. Hence, fewer cracks will appear and those that do will be wider. Table 5.3 describes the input for analysis M3 with different creep coefficient $\varphi(\infty, t_0)$.

Table 5.3 Notation and details for analyses of creep.

notation	ϕ [mm]	A_c [mm ²]	$\varphi(\infty, t_0)$	ρ_r [%]
M3	16	100x100	0	2.01
M3-creep1	16	100x100	1	2.01
M3-creep2	16	100x100	2	2.01
M3-creep3	16	100x100	3	2.01

5.3.5 Influence of length of specimen

An increased length of the specimen resulted in an increased total deformation. As shown in Figure 5.7, the number of cracks is increased when the length increased from 2 to 6 m. When the length increased, the total need for deformation increased. The increased deformation could not be achieved by the elastic part, hence more cracks had to be developed. The strain for which the first crack occurred remained the same, as shown in Figure 5.3 and Figure 5.7. Further it is shown that the number of cracks per unit length decreases as the length of the specimen increases.

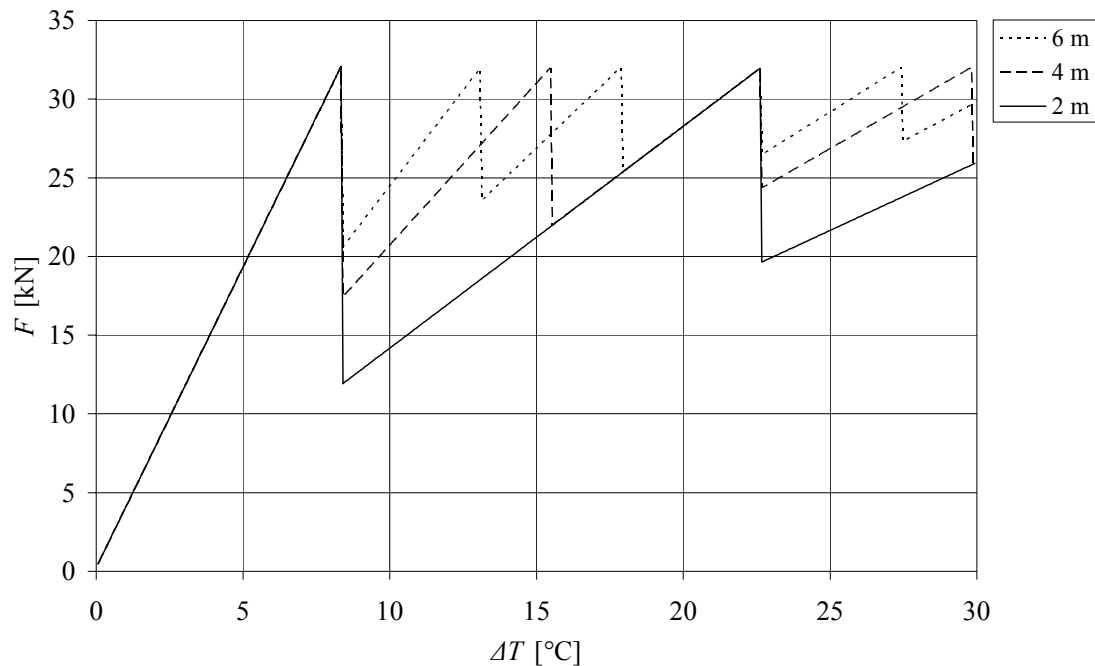


Figure 5.7 Results when the specimen length varied, $l = 2, 4, 6$ m and $\phi 16$, $A_c = 100 \times 100$ mm².

5.4 Concluding remarks

Increasing the bar diameter was found to have a significant influence on the number of cracks that occurs if the element is subjected to the same load. Several cracks were formed for the case with smaller bar diameter ϕ . If the concrete section area increased, fewer cracks appeared for the same load. If also the crack width is of interest, it should be noted that for the case denoted M1-2, a crack width $w_k = 0.35$ mm was achieved compared to $w_k = 0.50$ mm for M4-2 which is preferable, see further in Chapter 7. Finally, in order to optimise the transferred force, it would be preferable to use several smaller bars with same total reinforcement area A_s , since the total surface area in this case is greater. At a specific prescribed thermal strain more cracks is preferable in order to limit each cracks width. Therefore to meet the need of reinforcement with smaller bar diameter results in more but smaller cracks which is a good solution. Increasing the length results in decreased number of cracks per unit length, hence larger cracks are to be expected for increased length of specimen.

6 Finite element analysis

6.1 Modelling approach

In order to study the cracking process due to restraint forces, a more advanced numerical study was made using the finite element method. The general FE-software ADINA (2005) was chosen to perform the analysis. ADINA stands for Automatic Dynamic Incremental Non-linear Analysis and was originally developed to provide one system for comprehensive analyses of structures, fluids and fluid flows with structural interactions.

All inputs for the analyses were taken from the theory presented in the previous chapters and will be discussed further below. When modelling reinforced concrete members subjected to restraint forces, difficulties can be expected. By applying a distributed negative change of temperature and assuming that the reinforcement has the same need for deformation due to the change of temperature, numerical errors may occur. Therefore, in this thesis, the loading condition has been applied in an alternative way. Earlier studied projects also confirm difficulties with thermal loading, Hirschhausen (2000).

Applying the influence of negative change of temperature via a prescribed displacement u , a more reasonable result is to be expected, see Figure 6.1. This load on the other hand must first be evaluated. For further discussion regarding difficulties with thermal load, see APPENDIX E.

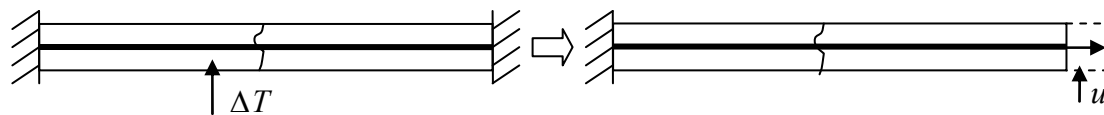


Figure 6.1 Alternative way to apply the loading condition.

6.2 Input data

6.2.1 Geometry

When creating FE-models it is, if possible, preferable to use symmetry in order to utilise the computer capacity fully. The main geometrical modification was the cross section, see Figure 6.2. Due to symmetry only one fourth of the cross section was modelled, so also with the steel cross sectional area. The resulting general model geometries are shown in Figure 6.3 and Figure 6.4.

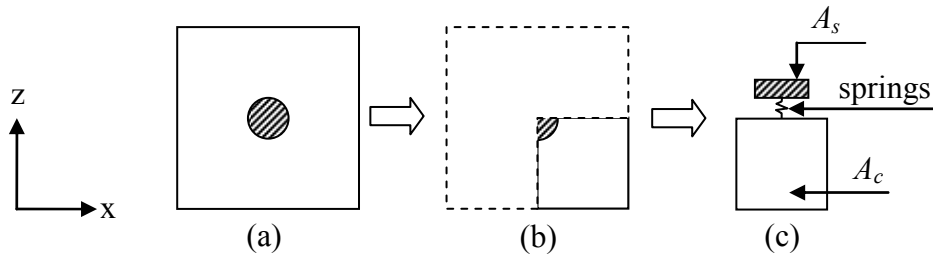


Figure 6.2 Modelling the concrete prism.

As mentioned earlier a low and a high member will represent our main geometries shown in Figure 6.3 and Figure 6.4.

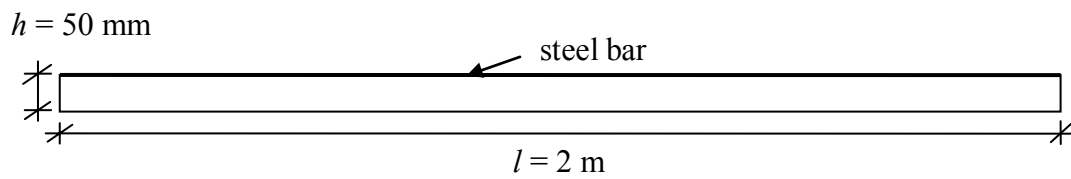


Figure 6.3 Geometry of low model using cross section according to Figure 6.2.

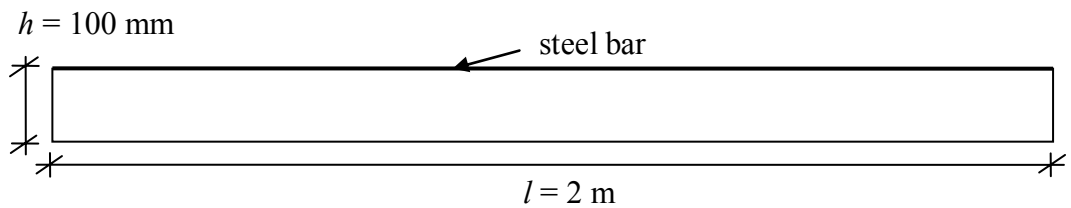


Figure 6.4 Geometry of high model using cross section according to Figure 6.2.

6.2.2 Material models

By applying the material models as described in Chapter 3, an elastic response of the steel is modelled, see Figure 6.5. Since this study only concerns the service state and due to given geometrical conditions, it is controlled that the reinforcing steel will not reach yield stress. However a small strain hardening is modelled in order to avoid possible numerical problems if yielding is reached, see Figure 6.5.

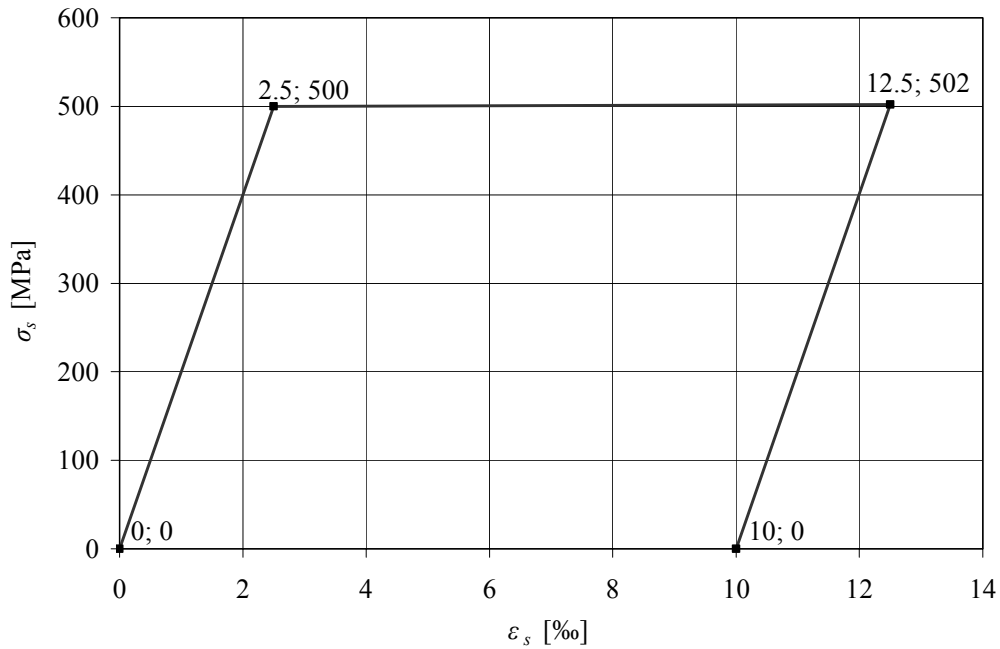


Figure 6.5 Modelled steel response for reinforcing steel B500B.

The response of concrete in compression is not of main interest in this study, but its nonlinear behaviour is inserted to describe the real behaviour of concrete. In tension the cracking response was simplified to a bilinear response in accordance with the present possibilities in ADINA. By using the same value for post-cracking uniaxial cut-off tensile stress σ_{ip} , as for the uniaxial cut-off tensile stress σ_t , numerical problems are most likely to be avoided, see Figure 6.6.

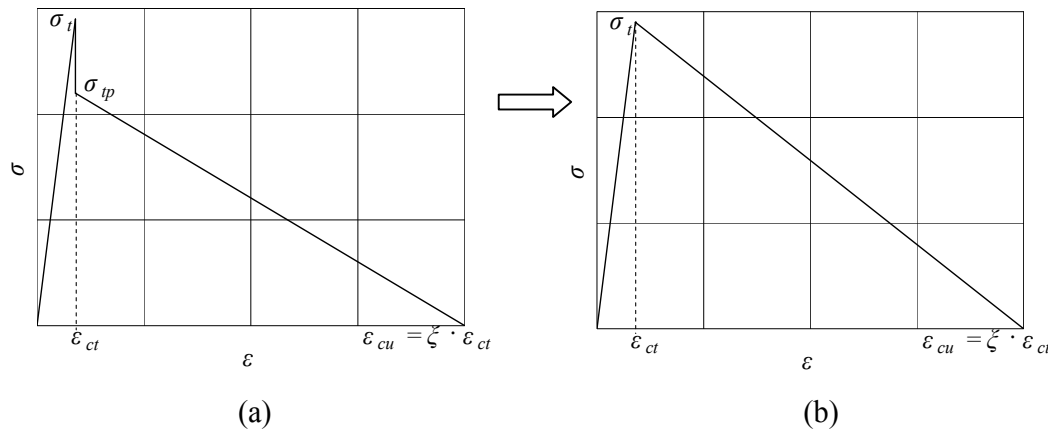


Figure 6.6 Possible approaches to model the concrete at tension in ADINA. Alternative (b) is used in the analysis, i.e. $\sigma_{ip} = \sigma_t$.

In the commercial software ADINA two different post cracking parameters can be applied, either by using the fracture energy G_f , or by calculating a relation ζ , between the uniaxial cut off strain and the ultimate strain see equation (6.1) and Figure 6.7. According to Figure 3.2 and equation (6.1), the fracture energy G_f is the area under the softening curve.

$$G_f = \int_0^{w_u} f(w)dw \quad (6.1)$$

Based on the shape of the softening curve the value of the fracture energy G_f , and the tensile strength f_{ctm} , the value of the ultimate crack width w_u can be determined as:

$$w_u = \frac{2 \cdot G_f}{f_{ctm}} \quad (6.2)$$

In ADINA though, a stress strain relation is needed. This is obtained by dividing the crack width with a length l , i.e.

$$\varepsilon = \frac{w}{l} \quad (6.3)$$

The size of the length l depends on how the interaction between concrete and reinforcement is modelled, Johansson (2006). When modelling the bond it is possible to obtain a full crack location within one element. This is also the case in the analysis performed here, and hence the length l is set to the element length l_{el} , i.e.

$$\varepsilon_u = \frac{w_u}{l_{el}} \quad (6.4)$$

According to Figure 6.6 the ultimate crack strain ε_{cu} is given in ADINA by the parameter ξ :

$$\xi = \frac{\varepsilon_{cu}}{\varepsilon_{ct}} \quad (6.5)$$

and

$$\varepsilon_{ct} = \frac{f_{ctm}}{E_{cm}} \quad (6.6)$$

Equation (6.1) to equation (6.6) results in the expression for ξ , given in equation (6.7).

$$\xi = \frac{2 \cdot G_f \cdot E_{cm}}{l_{el} \cdot f_{ctm}^2} \quad (6.7)$$

Based on experimental results in Johansson (2000) a value of the fracture energy $G_f = 100 \text{ kg/s}^2$ can be used.

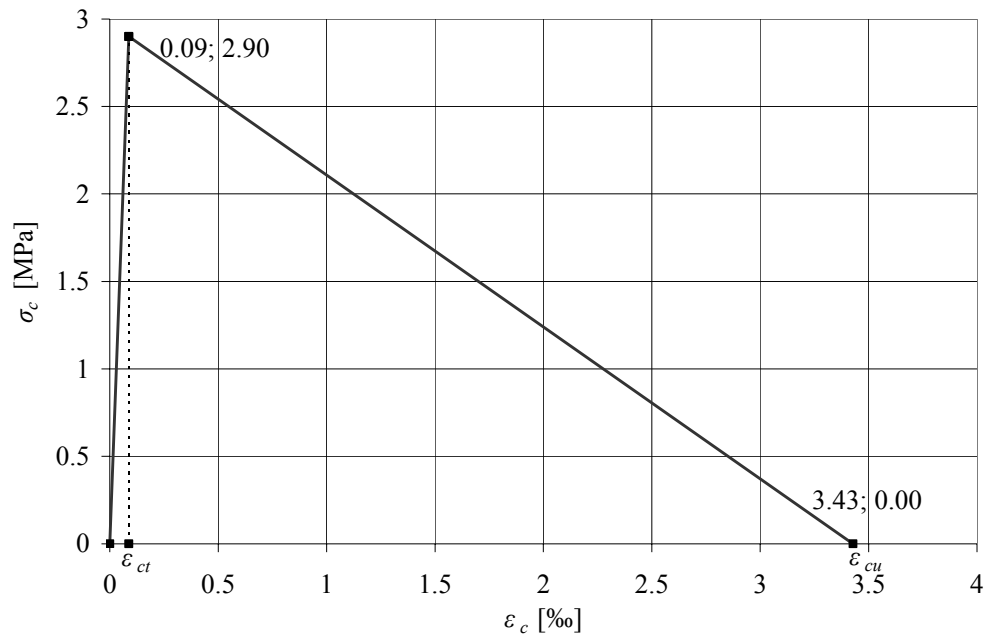


Figure 6.7 Modelled concrete response in tension for element length $l_{el} = 20$ mm.

6.2.3 Boundary conditions and loading

The reinforced concrete member was assumed to have fully fixed boundaries. However, by applying rigid boundaries, high stresses may be expected close to the boundary due to the shape of deformation, see Figure 6.8 (a). In order to avoid these concentrations of stresses in the analyses of the cracking process, boundary conditions according to Figure 6.8 alternative (b) was assumed.

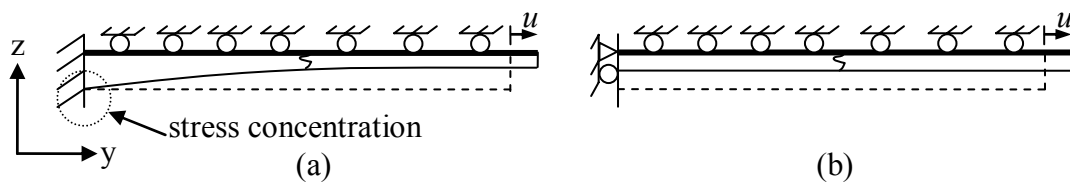


Figure 6.8 Different behaviour due to chosen boundary condition.

In Figure 6.8 (b), a more realistic and uniform stress distribution will be obtained. During analysis the concrete will be free to move in the z -direction around the boundaries except for the upper edge where the reinforcement is located. In the y -direction the concrete will be prohibited to move at the left end. On the upper side, the springs connecting the concrete and steel, will act only in the y -direction. The steel is prohibited to move in the x - and z -direction along the specimen. The boundary conditions for the far left node all translation degrees of freedom will be fixed.

The load is applied as an imposed end displacement, where both the steel and the concrete have the same need of movement at the right boundary.

For the elements close to the boundaries at the short ends a stronger material is applied. By increasing the uniaxial cut-off tensile strength with approximately 3%, cracks close to the boundary are avoided. This modification is made due to difficulties occurred as the model tends to crack at the boundary. Concentrations and errors are avoided by this rather small modification.

6.2.4 Mesh

Four node 2D-solid elements were used for modelling the concrete with a plane stress relation. Plane stress elements are preferable in order to describe stresses and strains in the direction of the loading. The reinforcing steel was modelled as two node truss elements. The software was limited to maximum 900 nodes and therefore the models had to be adjusted to fit this requirement. The elements were 20x16.7 mm for the low member compared to 20 mm and quadratic for the high member.

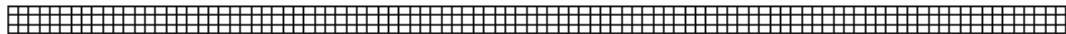


Figure 6.9 Mesh of low member.

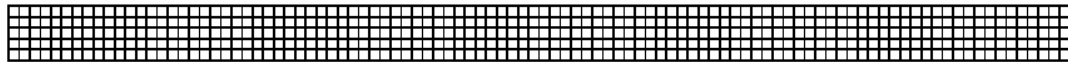


Figure 6.10 Mesh of high member.

6.2.5 Interface behaviour modelled by non-linear springs

In order to describe the bond between steel and concrete, non-linear springs were applied between the two materials. The behaviour of the springs was derived from the bond stress and slip relation shown in Figure 3.8. As the bond acts along the reinforcement, see Figure 6.11, it can be derived to a spring force, as shown in equation (6.8).

$$F = \tau_b \cdot \frac{\pi \cdot \phi}{4} \cdot l_{el} \quad (6.8)$$

where l_{el} = element length

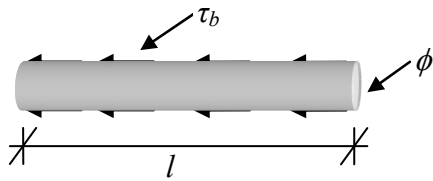


Figure 6.11 Bond stress along the reinforcement

The bond force transferred between the reinforcement and the concrete, is the sum of the bond stress along the elements length. Since the bond stress acts around the whole reinforcement the sum will be influenced by the reinforcement diameter and the element length. The bar circumference combined with the element length will result in an area, also called interface area. Since the model in ADINA corresponds to one fourth of the whole model, see Figure 6.2, the bonded area is reduced to one quarter.

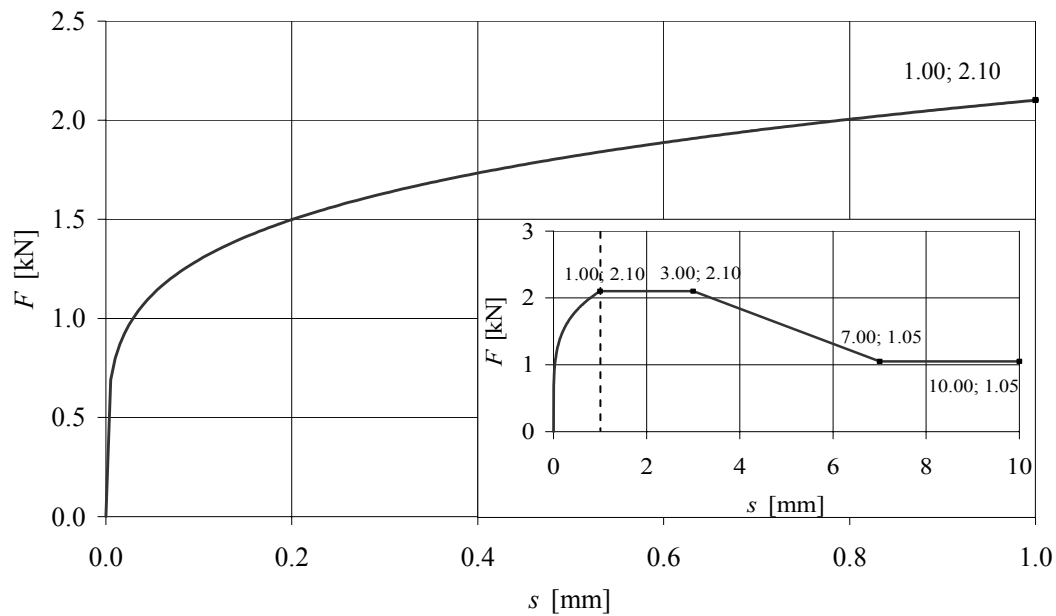


Figure 6.12 Bond force relation used in the analyses for element length of 20 mm and $\phi 16$.

The springs were modelled with the same properties in both tension and compression since the bond was assumed to work in the same manner irrespective of the direction. The response for a displacement of 1 mm is given from equation (3.2) and equation (6.8).

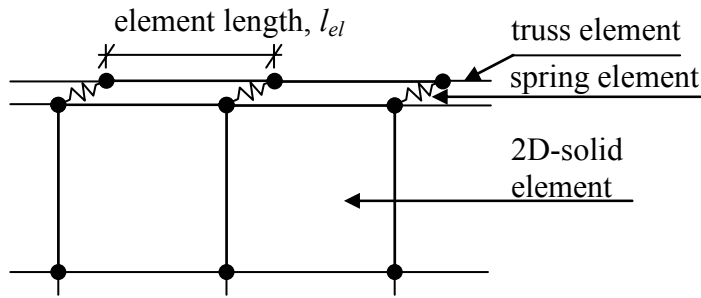


Figure 6.13 Schematic figure of how the concrete, steel bars and springs are generated in the analyses. Note, in the model the truss elements are only displaced in the longitudinal direction

As can be seen in Figure 6.13, the reinforcing steel was modelled with a slight displacement to the right. The purpose with that is to model the bond behaviour using non-linear springs, which has to work in the direction of loading.

6.3 Solution process

6.3.1 Classification with regard to type of analysis

The type of analysis to be preferred is not obvious. In the performed analyses both static and dynamic direct integration were used to be able to discretize the given problem. The main difference in these two approaches is the meaning of time. The experience from the dynamic direct integration was that it gave a softer and more stable response. This softer response is probably due to the applied damping that was needed to find convergence. In both approaches the loading was applied by small increments up to the full displacement, called displacement controlled procedure, see Figure 6.14. The opposite could have been a load controlled procedure, see Figure 6.15. When using the dynamic approach, every solution is influenced by how long time, and at which time the increment of load is applied. In this thesis however, the static analysis were mainly used.

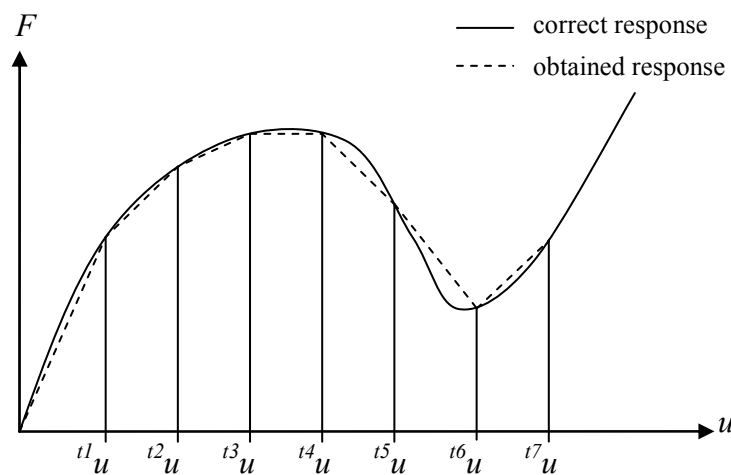


Figure 6.14 Deformation controlled incremental procedure.

By using the load controlled incremental procedure, the correct response may be overseen, hence the deformation controlled incremental procedure is preferable.

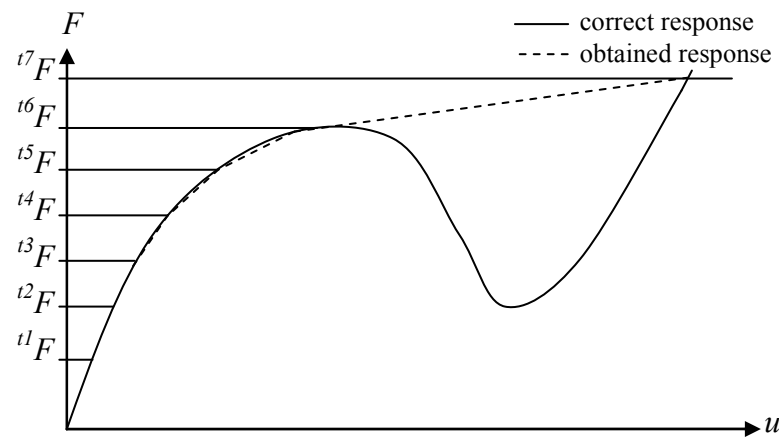


Figure 6.15 Load controlled incremental procedure.

6.3.2 Iteration method

While performing a non-linear analysis the solution vector can not be found by an equilibrium condition as for a linear problem. The loading history is applied as a deformation with small increments. Equilibrium conditions are hereby found after every increment by iteration.

There are several iteration procedures available in ADINA. The most common ones are Newton-Raphson, Quasi-Newton and Constant-Stiffness methods. The main difference is how the stiffness matrices are established.

Quasi-Newton or Secant-Stiffness methods are modified methods in order to establish stiffness matrices in case of softening material behaviours. These methods establish their stiffness matrices from a previous solution and update these continuously to be able to find the softening response. A well-known method is the Broyden, Fletcher, Goldfarb, Shanno or BFGS-Method, see Figure 6.16. This method was also used in the analyses carried out in this thesis.

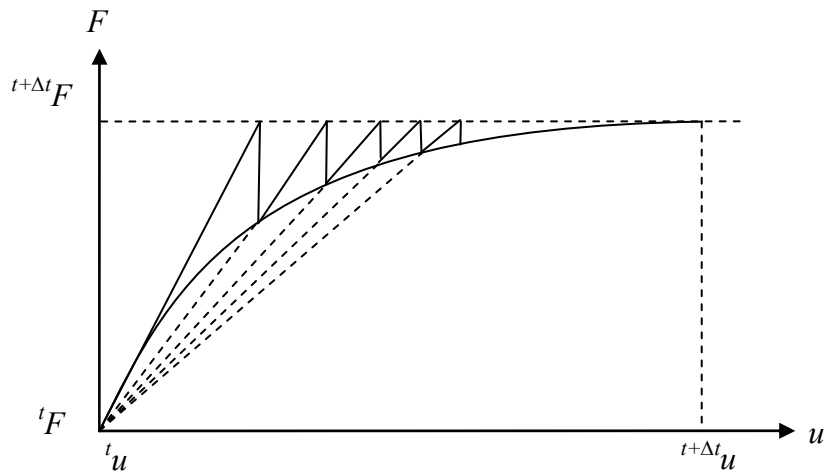


Figure 6.16 BFGS-Secant-Method in load controlled loading.

6.3.3 Time step and tolerances

To reach a solution with limited computer force, it is important with proper time stepping and reasonable tolerances. In the analyses energy convergence tolerance, ETOL, with line search convergence tolerance, STOL were used in order to find convergence. The following values were used according to ADINA:

$$\text{ETOL} = 0.001$$

$$\text{STOL} = 0.5$$

$$\text{Number of steps} = 1000$$

In ADINA manually controlled tolerances must be done with caution since every input regarding tolerances depends on norms and reference values. This difficulties are treated further in APPENDIX E.2 .

6.4 Verification

In order to verify if the input and also the material parameters were correct a simple model was generated, see Figure 6.17. The model consisted of one element only and was subjected to a tensile force to verify the stress-strain relation for the concrete model.

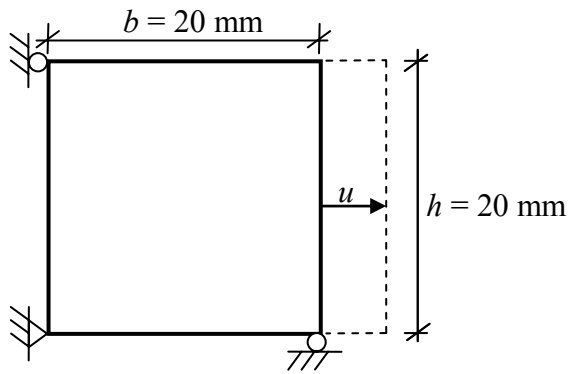


Figure 6.17 Verification model.

As seen in Figure 6.18 the verifying model responded as expected. The modulus of elasticity, $E = 33 \text{ GPa}$ can be verified by the inclination of the first half of the figure. Also important to notice is that the element has big influence of the post-cracking response. In this case when the element length is 20 mm , the value of $\zeta = 39$, described in Section 6.2.2. The post-cracking behaviour is modelled according to Section 6.2.2.

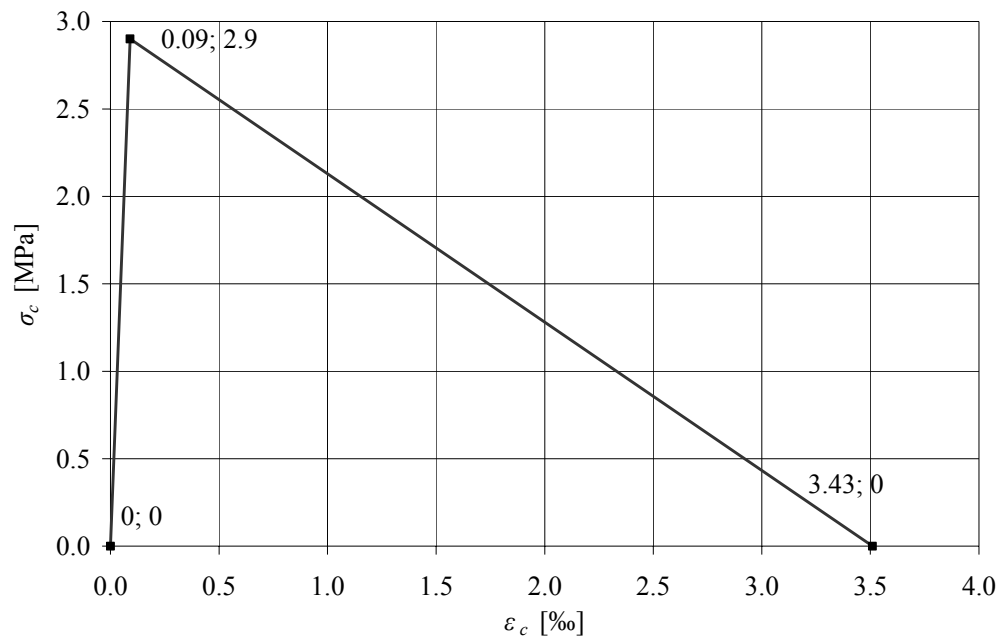


Figure 6.18 Response from verification, $l_{el} = 20 \text{ mm}$.

6.5 Performed analyses

A list of performed analyses is presented in Table 6.1 – Table 6.3. In these, all input data are presented and every analysis is given a notation. The analyses are also divided into blocks which represent different types of studies, see Figure 6.19 A-C. Note that A2 and C2 have the same input data but due to the comparisons they have different notations.

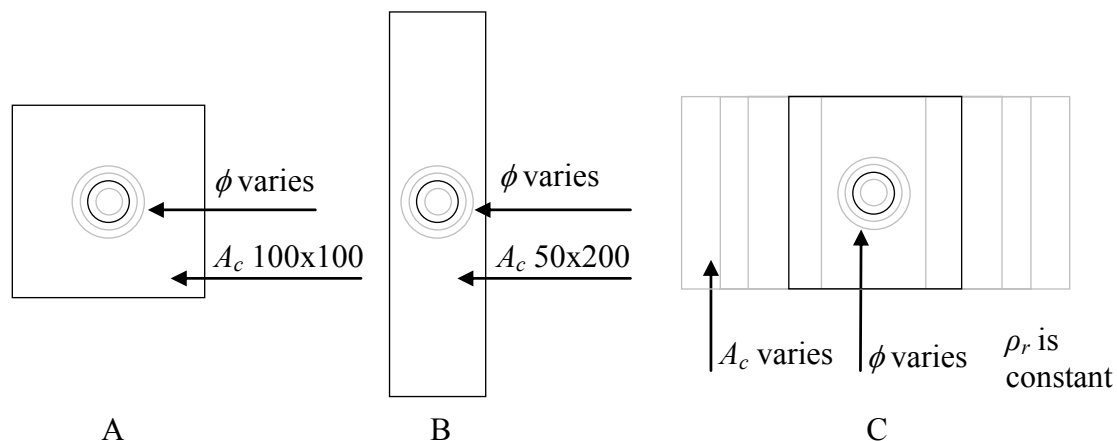


Figure 6.19 Main geometries in parametric study.

A summary of the tables, containing notations for analyses performed in this thesis, is given in APPENDIX L.

Table 6.1 Notation and details for original analyses.

notation	ϕ [mm]	A_c [mm ²]	φ	ρ_r [%]	software	solution category
A1	10	100x100	0	0.79	ADINA	Static
A2	12	100x100	0	1.13	ADINA	Static
A3	16	100x100	0	2.01	ADINA	Static
A4	20	100x100	0	3.14	ADINA	Static

Table 6.2 Notation and details for analyses of high member.

notation	ϕ [mm]	A_c [mm ²]	φ	ρ_r [%]	software	solution category
B1	10	50x200	0	0.79	ADINA	Static
B2	12	50x200	0	1.13	ADINA	Static
B3	16	50x200	0	2.01	ADINA	Static
B4	20	50x200	0	3.14	ADINA	Static

Table 6.3 Notation and details for analyses of prism containing same reinforcement ratio.

notation	ϕ [mm]	A_c [mm ²]	φ	ρ_r [%]	software	solution category
C1	10	69x100	0	1.13	ADINA	Static
C2	12	100x100	0	1.13	ADINA	Static
C3	16	178x100	0	1.13	ADINA	Static
C4	20	278x100	0	1.13	ADINA	Static

6.6 Results

6.6.1 Introduction

As expected, significant differences were found depending on the actual parameters in the analyses. Several results from the performed analyses are presented in APPENDIX F and every analysis has its own notation, see Chapter 6.5. As already discussed in Sections 4.2 and 4.3 geometrical variations have considerable influence on the global response.

The results are divided into two main objectives of interest: global response and stress and strain development. In these two sections several figures are presented in order to visualise differences of geometry and parameters.

6.6.2 Global response

The global response is the first result visualised. Deformation versus reaction force F , is plotted for every analysis. The four analyses A1-A4 are shown in Figure 6.20.

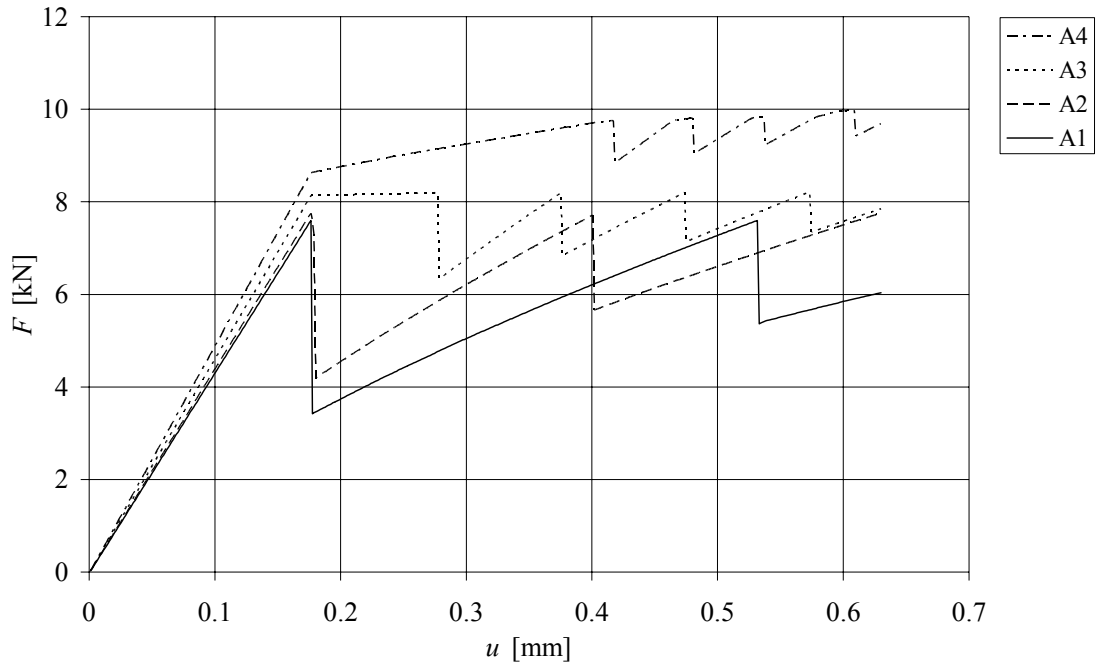


Figure 6.20 Global response for the first four analyses.

Figure 6.20 shows the significant differences in global response at a prescribed displacement of 0.63 mm, which represents a temperature decrease of $\Delta T = -30^\circ\text{C}$. The most apparent differences between results obtained, are when the cracks form and also the number of cracks. Analyses A3 and A4 generates a plateau before the first crack is fully opened. This behaviour may be explained by the mutual forming of several cracks along the specimen at the same time. This behaviour, in turn, is due to the numerical solution process when the program tries to find the first crack. During the plateau several small stress raisers in the concrete were located along the connection to the reinforcement bar before one element row was fully opened, see the small peaks in Figure 6.22.

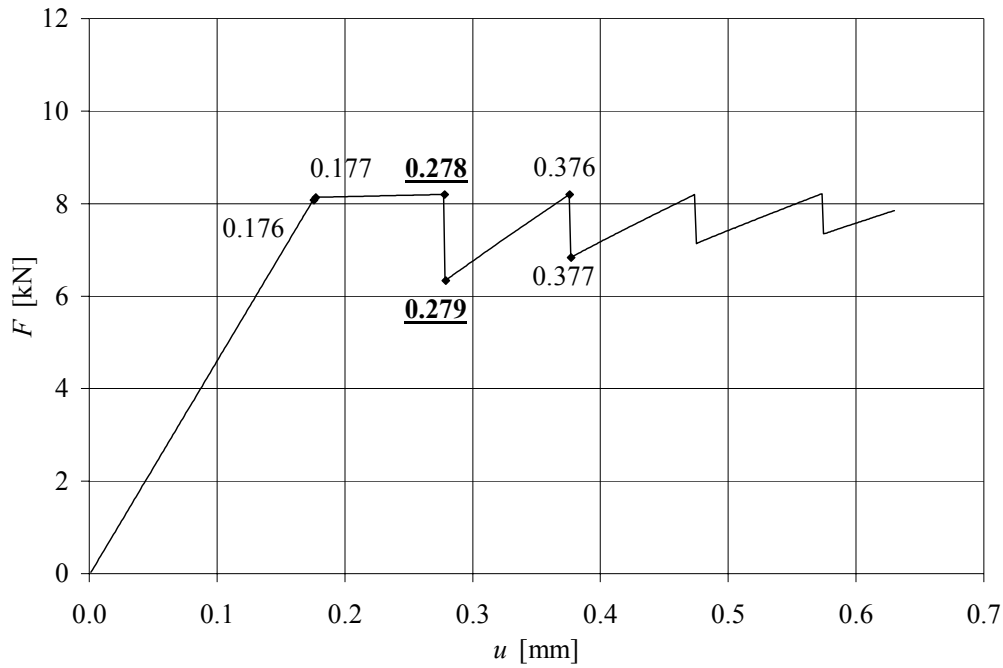


Figure 6.21 Points of interest for stress distribution in A3.

The response of the default analysis, A3 is shown in Figure 6.21. Six points of interest is marked with its load of displacement. These points are further studied in order to examine the behaviour within the plateau, see APPENDIX F.1.5. In Figure 6.22 one of these points is shown, regarding the concrete stress and the steel stress.

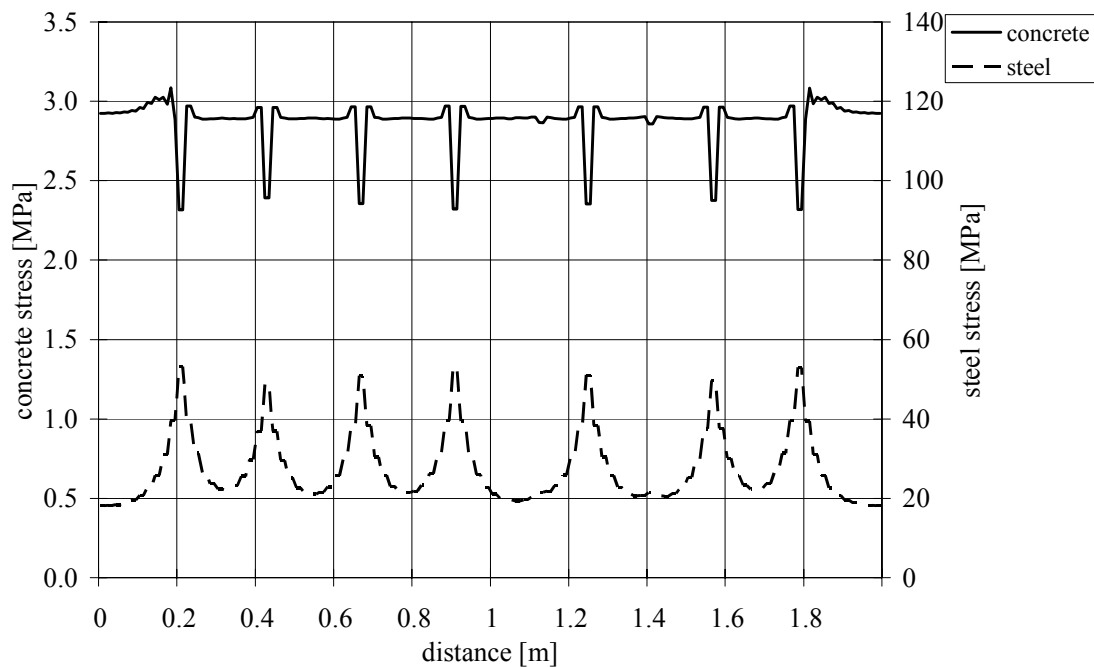


Figure 6.22 Steel and concrete stress along the specimen during the plateau. The displacement is 0.278 mm in A3.

Figure 6.22 shows the small peaks where the force has been transferred to the steel at several locations. In these locations the concrete stress has begun to decrease. Notable in Figure 6.22 is that the concrete stresses close to the boundaries are greater than 2.9 MPa. This is due to the linear elastic materials with slightly increased capacity inserted close to the boundaries, as described in Section 6.2.3.

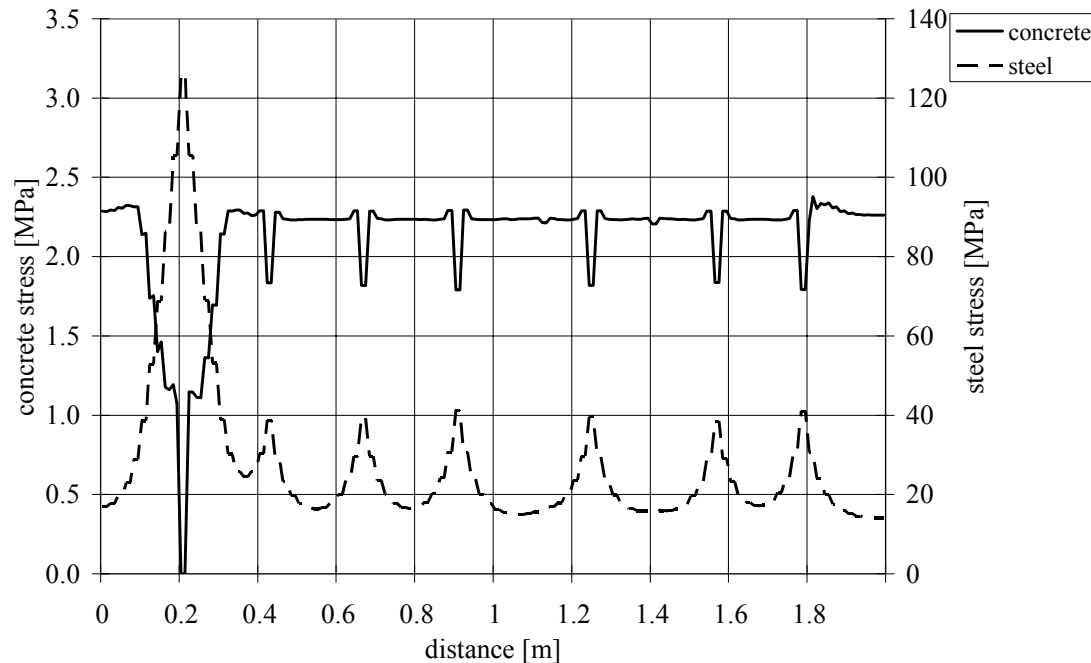


Figure 6.23 Steel and concrete stress along the specimen after the plateau. The displacement is 0.279 mm in A3.

As the load increases to 0.279 mm, the first fully opened crack appears, as shown in Figure 6.21 and Figure 6.23. When the first crack opens, the concrete stress is reduced, when the steel stress increases considerably as a result from that the reinforcement has to carry the load.

In order to evaluate the reason for the behaviour with the plateau, the bond resistance was reduced. The results obtained from the new analyses were significant, as shown in Figure 6.24. When the bond between concrete and reinforcement was reduced with 10%, the problem with the plateau found earlier more or less disappeared, resulting in that the peaks of stress shown in Figure 6.22 and Figure 6.23 are no longer to be found. Still, whether this is a numerical problem in the FE-program was not further investigated.

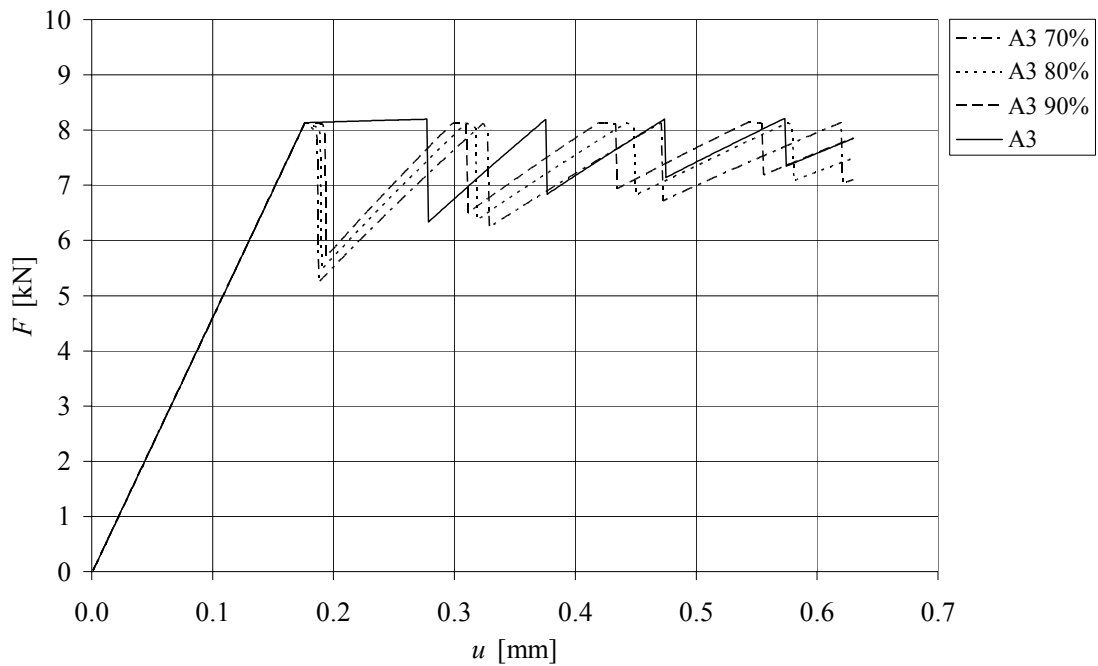
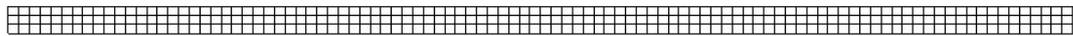


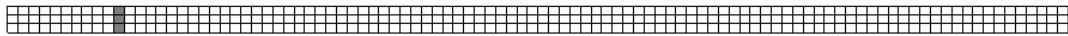
Figure 6.24 Global response for various bond conditions.

In Figure 6.25 the cracks that appeared in the FE-model for the examined member A3 are shown for five loads, u of interest.

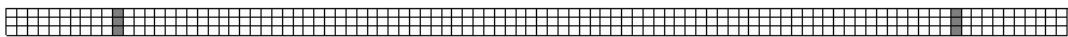
$$u \leq 0.278$$



$$u = 0.279$$



$$u = 0.377$$



$$u = 0.475$$



$$u = 0.575$$

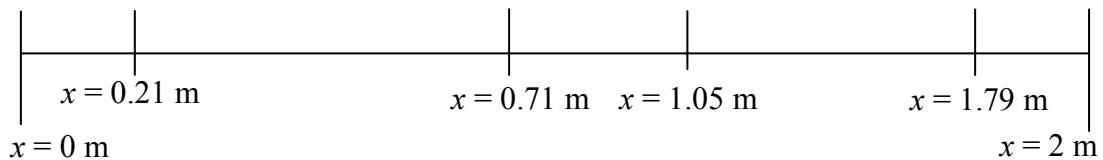
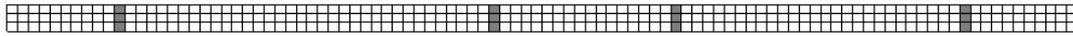


Figure 6.25 Crack propagation in a concrete prism for analysis A3. Grey areas indicate fully opened cracks.

Now the height is increased according to Table 6.2 and the results from the four analyses B1-B4 are shown in Figure 6.26. In order to see the differences compared to the original analyses it is preferable to visualise them together according to Figure 6.27. The figure only shows one analyses with similar geometry, A2 and B2.

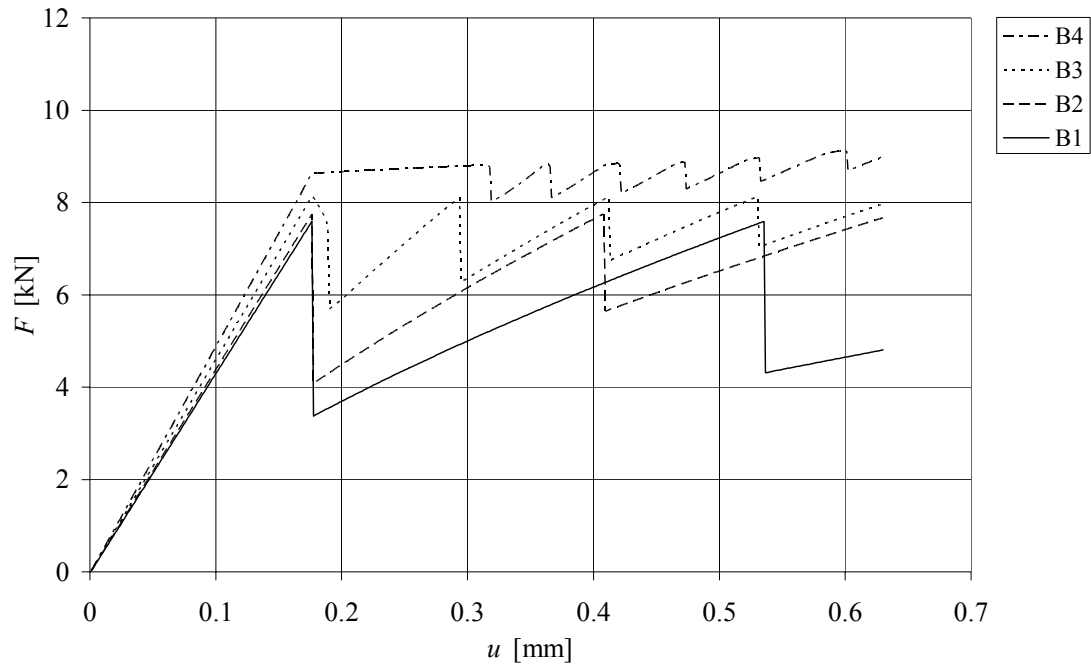


Figure 6.26 Global response from analyses of high member.

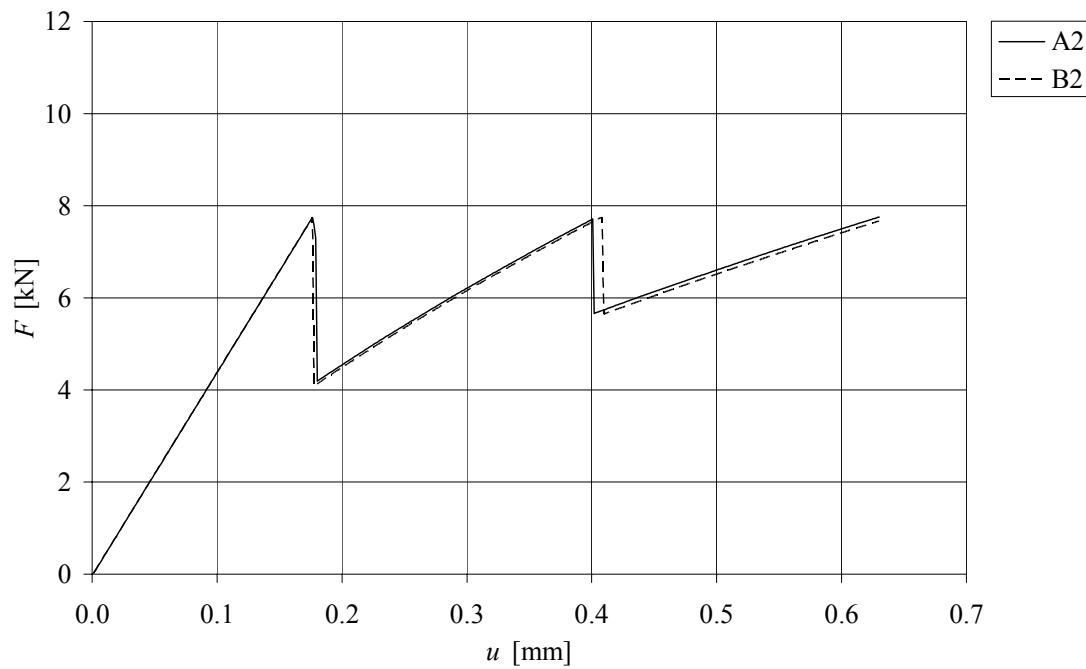


Figure 6.27 Comparison between low (A2) and high (B2) member.

By comparing the global response from a low member A2 with the global response from a high member B2, see Figure 6.27, the results indicate that the whole concrete height is within the effective area. By introducing a further increment of the height, an evaluation of what concrete amount to take into consideration as effective area, may be carried out. However, such an investigation is not within the scope of this study and is hence not further studied, see Section 8.2.

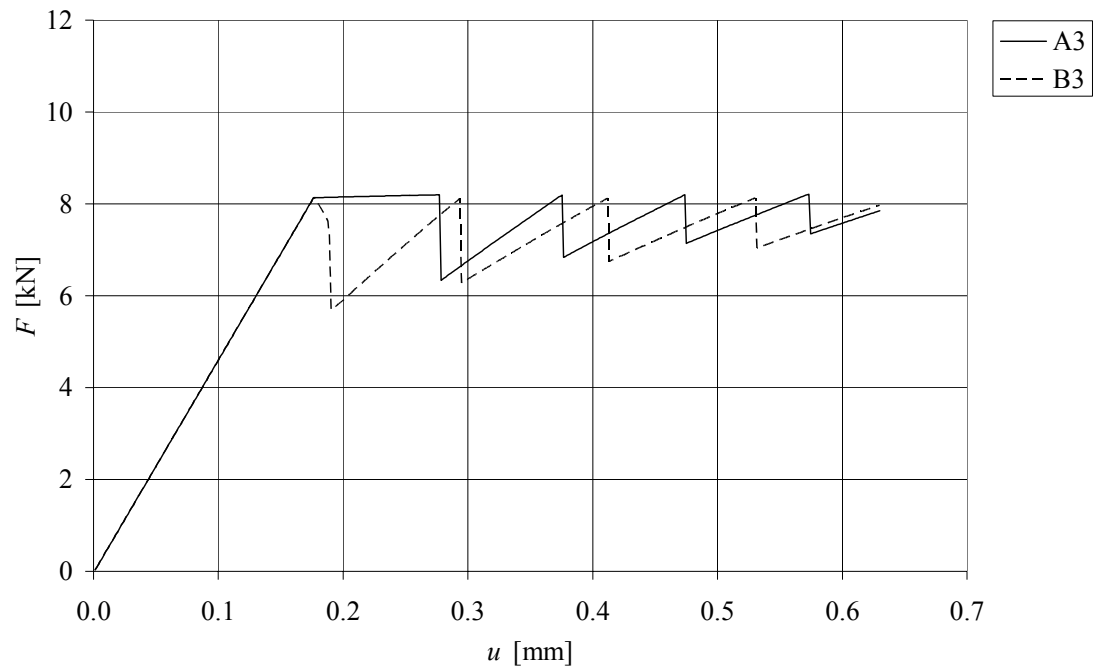


Figure 6.28 Results from low (A3) and high (B3) member.

When comparing the result obtained from the low member A3 with the high member B3, it is notable that the plateau is reduced. As the first crack opens the response in B3 is smoother than for the following cracks, but the plateau to be found in A3 does not appear for B3, see Figure 6.28.

In a real design stage the reinforcement ratio needed can be specified in order to oblige the limits of ductility, load bearing capacity and crack width. The reinforcement ratio can be fulfilled with different geometries of concrete cross section area and reinforcement bar dimension. The following analyses are based on a specific reinforcement ratio and constant height of the concrete cross section, see Figure 6.29 and Table 6.4.

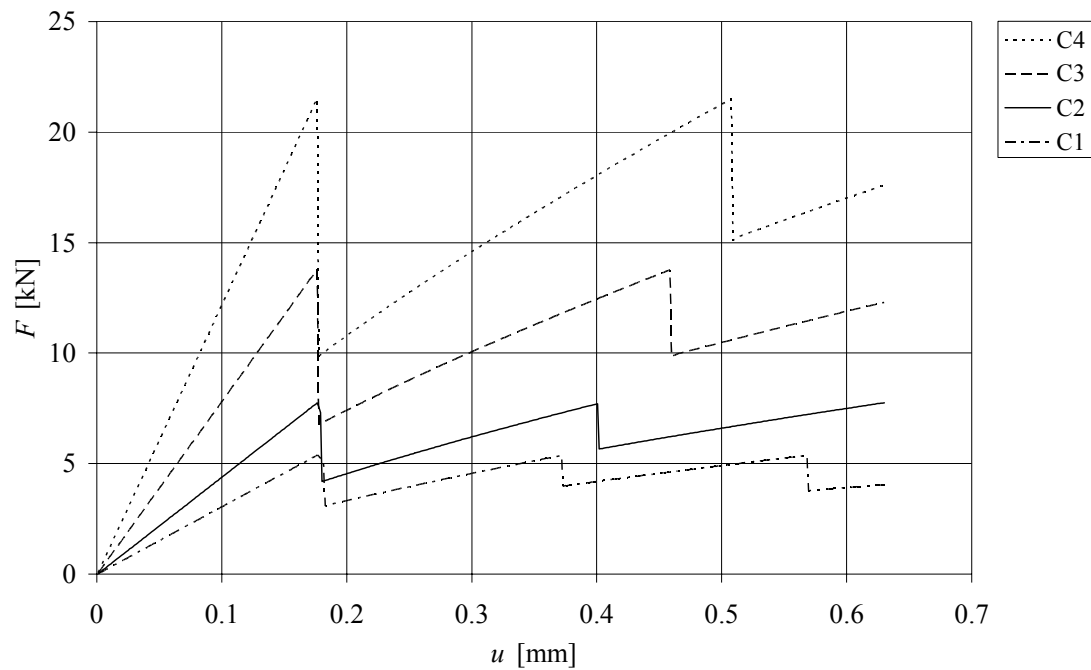


Figure 6.29 Analyses for different sections with constant reinforcement ratio, ρ_r .

For the various analyses given in Figure 6.29, cross sectional geometry according to Table 6.4 were used.

Table 6.4 Input for given analyses.

notation	ϕ [mm]	A_c [mm ²]	ρ_r [%]
C1	10	69x100	1.13
C2	12	100x100	1.13
C3	16	178x100	1.13
C4	20	278x100	1.13

By increasing the bar diameter and the concrete section such that the reinforcement ratio was kept constant, the global responses as shown in Figure 6.29 were obtained. The first crack appeared at the same displacement in all studied cases. When cracking started, various results were obtained. The increased concrete cross section resulted in an increased cracking load in Figure 6.29. The number of cracks and for which load they occurred varied between the analyses. That is, an increased number of cracks were obtained for a decreased value of the bar diameter.

6.6.3 Stress and strain development

As the displacement increased, the stress increased in the materials according to linear material response. When cracks appeared, the concrete was no longer capable to carry stress in this section, hence all stress in the cracks had to be taken by the reinforcement. The plateau described in Figure 6.20 and Figure 6.22, is also to be found in Figure 6.30, where four of the peaks have developed to fully opened cracks.

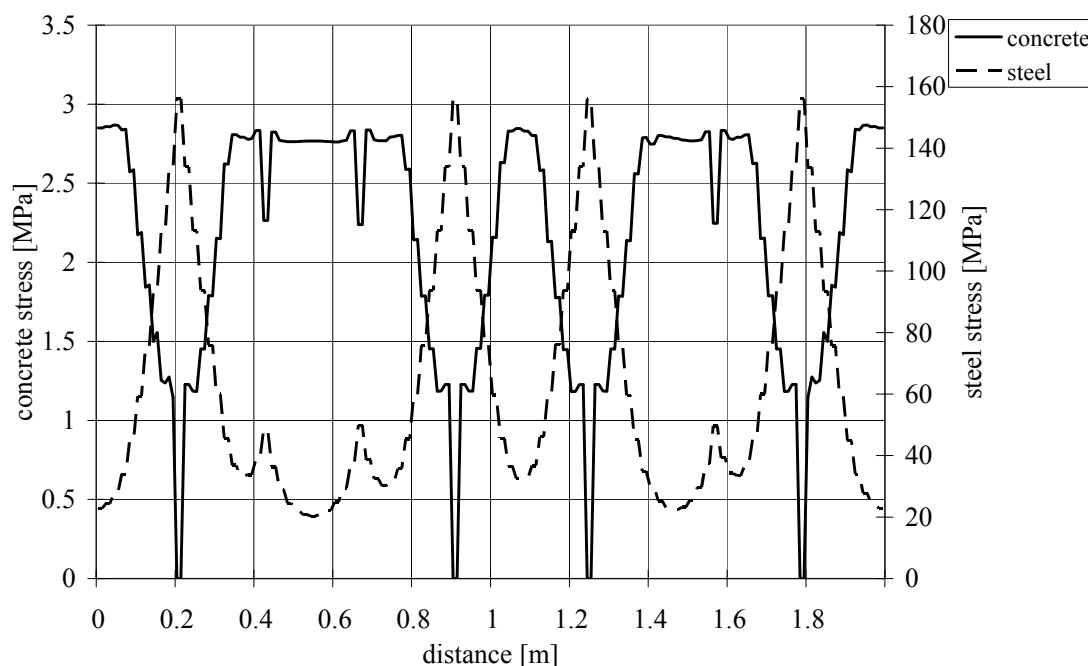


Figure 6.30 Steel and concrete stress along the specimen when the full displacement is applied, $u = 0.63\text{mm}$, for analysis A3.

When comparing the stress distribution for a case with lower reinforcement ratio, the behaviour with small stress peaks was not to be found, see Figure 6.31. This response has earlier been described as a result caused by the numerical solution process, now showing to be influenced by the reinforcement amount. As a result from changing the reinforcement amount, the bond between concrete and steel is changed. With smaller reinforcement ratio, as described in Figure 6.24, the plateau was eliminated. By eliminating the plateau, the stress distribution moves towards the distribution shown in Figure 6.31.

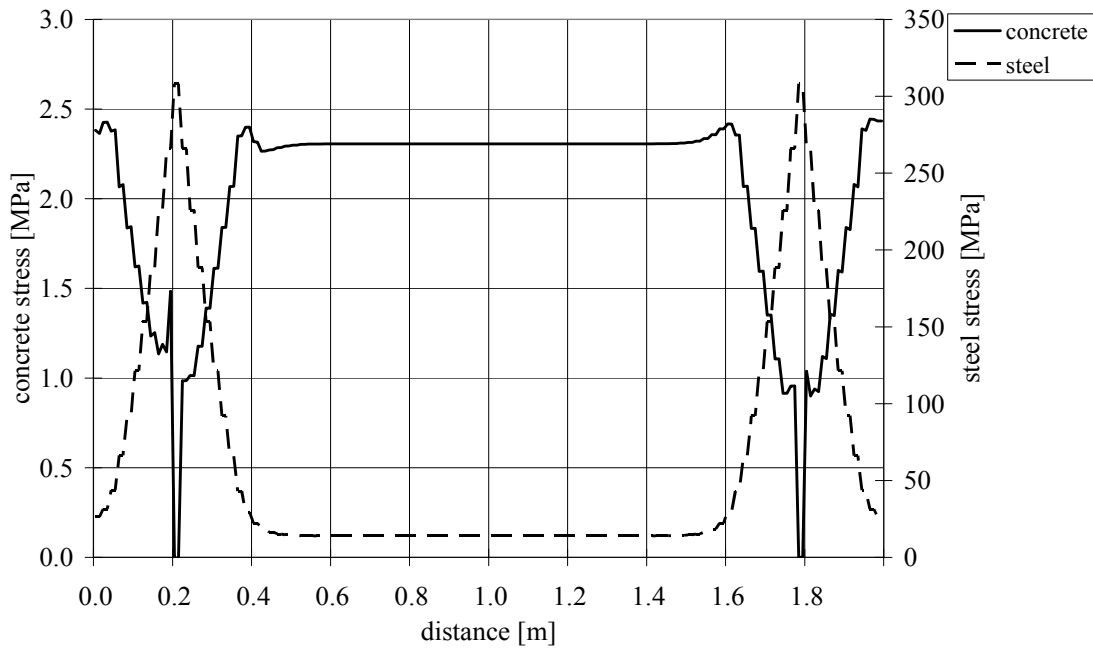


Figure 6.31 Steel and concrete stress along the specimen when the full displacement is applied, $u = 0.63\text{mm}$, for analysis A1.

One assumption that was made in the analytical method was that all cracks have the same crack width. This result is also obtained in the numerical analyses in ADINA. In the comparison of four developed cracks shown in Figure 6.32, it can be seen that the strain develops simultaneously. Also here the plateau, as described in Figure 6.22, was found between the load displacements of 0.18-0.28 mm.

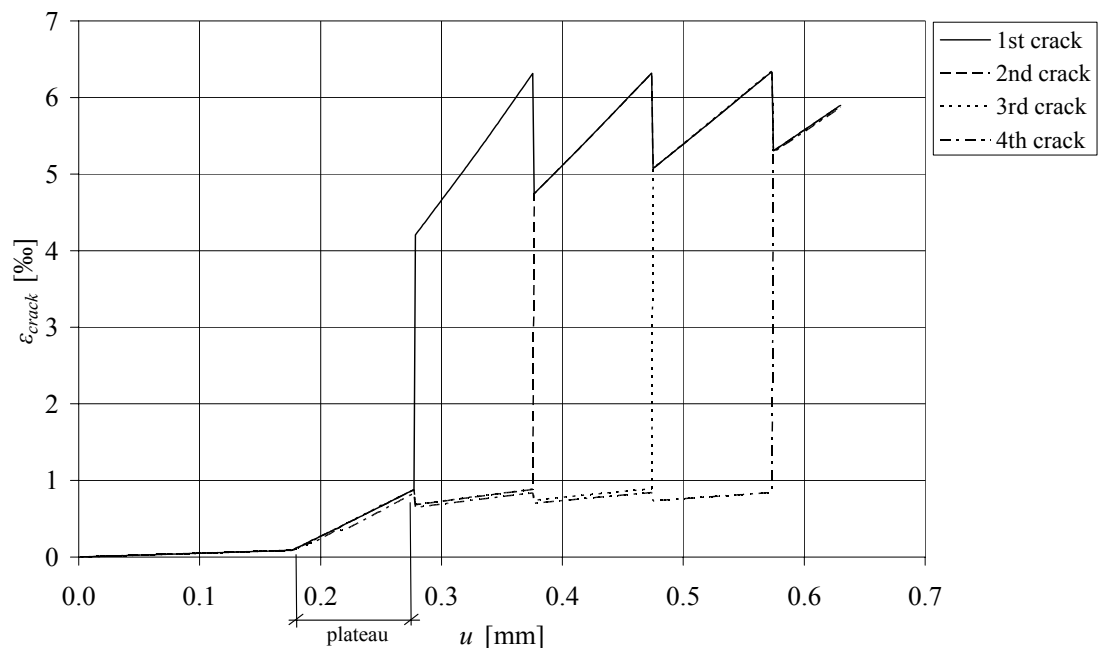


Figure 6.32 Strain in crack versus applied deformation for analyses A3.

By increasing the depth of the prism, as described in Table 6.2, the response regarding crack width was changed. The plateau earlier found for analysis A3 is not obtained for

analysis B3, containing the same concrete area and reinforcement ratio as A3. As shown in Figure 6.33, the strain for the second, third and fourth crack was not increased as they were in the peaks for analysis A3.

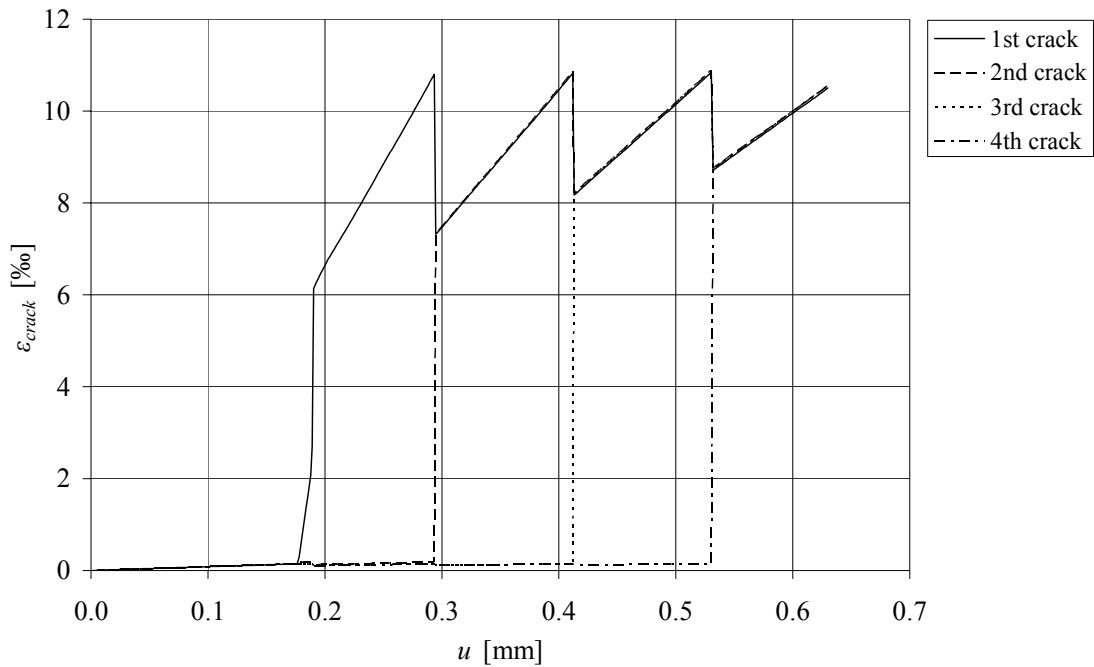


Figure 6.33 Strain in crack versus applied deformation for analysis B3.

By comparing the analyses A3 and B3 in Figure 6.34, it is clear that the crack development is influenced by the peaks obtained in the plateau.

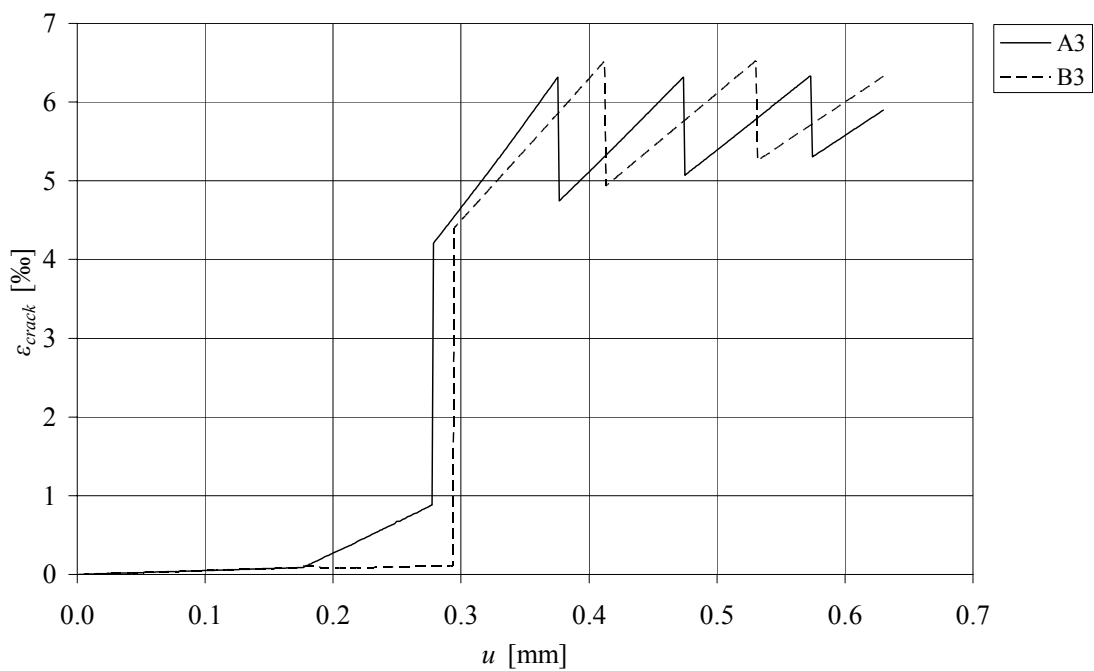


Figure 6.34 Strain in crack versus applied deformation for analyses A3 and B3.

A study with a constant reinforcement ratio, but with various bar diameter, resulted in a strain development as shown in Figure 6.35.

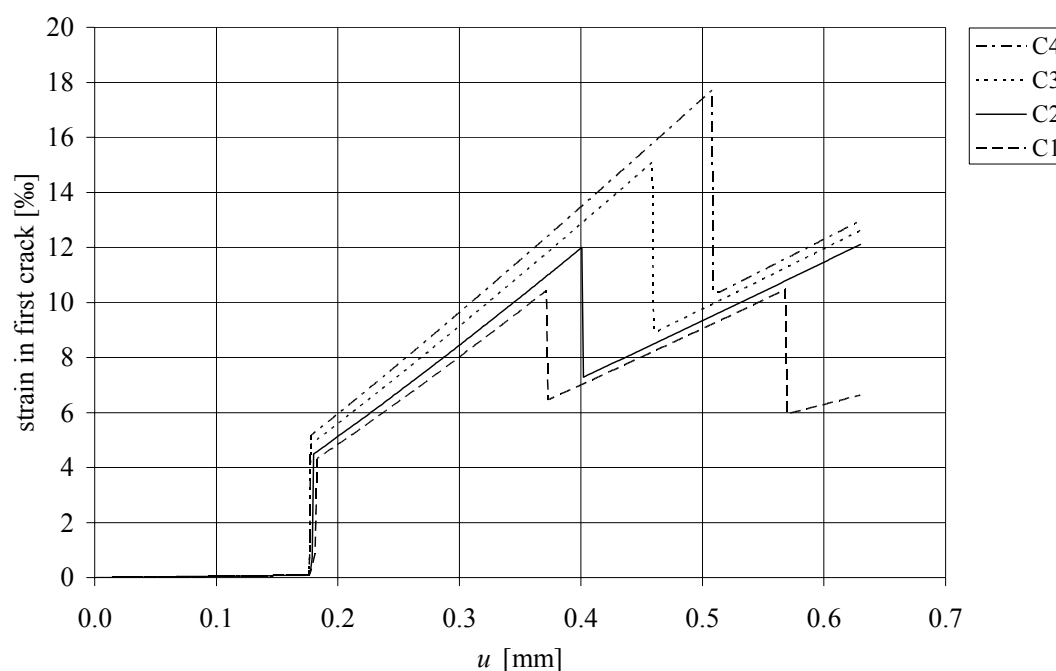


Figure 6.35 Strain in the first crack for different ϕ and constant ρ_r .

One study that is of interest is the comparison between crack widths. For the analyses denoted C3, the maximum crack width was calculated to 0.30 mm. This value should be compared to the one obtained in the case called C2, where the maximum crack width was calculated to 0.24 mm. The global responses in the two cases were rather similar, but for the resulting stresses and strains in the cracks, the two studies varied considerably.

It can be observed from the strain development for the first appeared crack in the four studied cases that the first crack was initiated at the same magnitude of displacement u , see Figure 6.35. The crack developed initially with a slightly increased value on the strains for the larger bar diameter. As the crack width increased, the prism with larger bar diameter reached a larger strain and therefore also a larger crack width. This is a result from an increased bar diameter. As the bar diameter increased, the surface area upon on which the bond between the concrete and steel acts increases. Hence, the value of the spring stiffness increases. However, the increase in steel area is not equivalent with the increase of the transferring bond area. Using larger bar diameter results in a smaller transferring area per unit steel area than for the same steel area using smaller bar dimensions.

7 Comparisons

7.1 External load and restraint forces

7.1.1 Number of cracks

A common approach engineers in Sweden use today, when designing with respect to temperature and internal restraint, is an approach based on external load. The approach described in BBK 04, Boverket (2004), is similar to the one found in Eurocode 2, CEN (2004), where initially a value for the crack spacing, s_{rm} , is calculated from where the crack widths, w_m can be estimated. By doing this, it is assumed that all cracks will appear according to equation (7.1) – (7.7), resulting in more cracks than found by means of the FE-model.

The concrete is assumed to be uncracked under the condition described in equation (7.1), where ζ in this case is set to 1.0.

$$\sigma_c \leq \frac{f_{ctm}}{\zeta} \quad (7.1)$$

The characteristic crack width is given from the mean value of the crack width according to equation (7.2).

$$w_k = 1.7 \cdot w_m \quad (7.2)$$

The mean value of the crack width can be calculated from equation (7.3).

$$w_m = \nu \cdot \frac{\sigma_s}{E_s} \cdot s_{rm} \quad (7.3)$$

By the factor ν , the concrete in tension between cracks is taken into consideration. With regard to the studies carried out where temperature and end displacement were used, the response for this load case is assumed as shown in Figure 7.1. Hence, when the first crack appears, the steel stress is to be set equal to the final steel stress, assuming that the load does not increase after the last crack has developed.

$$\nu = 1 - \frac{\beta}{2.5 \cdot \kappa_1} \cdot \frac{\sigma_{sr}}{\sigma_s} \quad (7.4)$$

where $\beta = 1.0$

$$\kappa_1 = 0.8$$

In this case the ratio σ_{sr}/σ_s , may be assumed to be equal to 1.0 since the response for a perfect material will be as described in Figure 7.1. The steel stress for the first crack can be calculated according to equation (7.5).

$$\sigma_{sr} = \frac{f_{ct} \cdot A_l}{A_s} \quad (7.5)$$

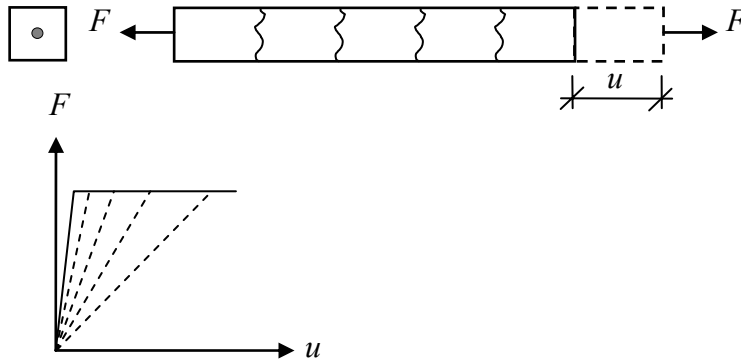


Figure 7.1 Global response for external force with perfect material.

The response shown in Figure 7.1 is to be compared to the response described in Figure 2.5. The mean value for the crack spacing can be calculated according to equation (7.6).

$$s_{rm} = 50 + \kappa_1 \cdot \kappa_2 \cdot \frac{\phi}{\rho_r} \quad (7.6)$$

For the total need of deformation, according to a change in temperature of -30°C , the corresponding number of cracks can be estimated according to equation (7.7).

$$n = \frac{l}{s_{rm}} + 1 \quad (7.7)$$

7.1.2 Simple example using Swedish code BBK 04

$$A_c = 100 \times 100 \text{ mm}^2$$

$$f_{ctm} = 2.9 \text{ MPa}$$

$$\phi = 12 \text{ mm}$$

$$f_{yk} = 500 \text{ MPa}$$

$$l = 2 \text{ m}$$

$$\text{Applied deformation: } u = 0.63 \text{ mm}$$

$$\text{Applied load: } F = f_{ctm} \cdot A_l$$

The results from the calculations, according to the Swedish handbook BBK 04, show a mean crack width of $w_m = 0.18 \text{ mm}$ and a characteristic crack width of $w_k = 0.30 \text{ mm}$. The mean value for the crack spacing is $s_{rm} = 262 \text{ mm}$, hence the number of cracks for a 2 m long specimen is $n = 8$.

Results from using the Swedish handbook BBK 04 are to be compared with results from the FE-analysis A2, where $n = 2$ cracks were found with maximum crack width of $w = 0.24 \text{ mm}$. By using Eurocode 2, the characteristic crack width can be

calculated to $w_k = 0.42$ mm and the maximum crack spacing to $s_{rmax} = 510$ mm. In order to find the same number of cracks obtained in calculations according to the Swedish handbook, a change in temperature of approximately -110°C in the improved analytical method is needed, see Figure 7.2. For calculations, see APPENDIX I.

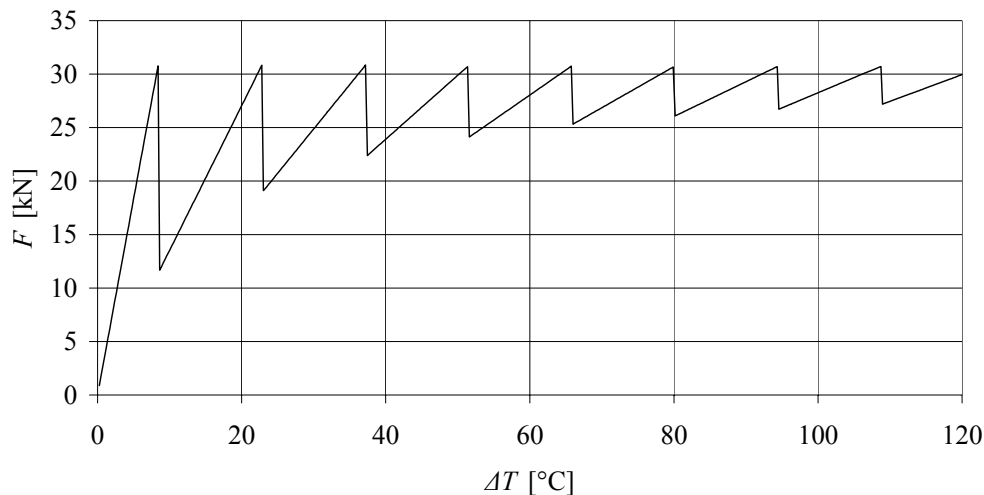


Figure 7.2 Global response in order to find 8 cracks in specimen subjected to thermal loading.

To sum up, using an approach derived for a load case with external response, several mistakes can be made. To start with, the global response differs a lot compared to a load case with imposed end displacement. When the crack develops the reaction force in the boundary decreases and the end displacement is kept constant with imposed end displacement. For the external load case the reaction force, equal to the acting force, will be constant when the crack develops and the displacement will suddenly increase, see Figure 2.5, hence the stress distribution will not be the same for the two cases. Further, assuming that many cracks appear and distributing the total need of deformation, according to equation (7.8), lead to an underestimation of the crack width.

$$u_{tot} = 10.5 \cdot 10^{-6} \left[\frac{1}{^\circ\text{C}} \right] \cdot 30 [^\circ\text{C}] \cdot 2000 [\text{mm}] = 0.63 \text{ mm} \quad (7.8)$$

Hence, distributing the needed deformation $u = \text{mm}$ in the assumed crack amount of 8 cracks result in a crack width of 0.08 mm. This value can be compared to the crack width obtained in analysis A2 which measure 0.24 mm.

In Figure 7.3 the four studied cases with the same reinforcement amount are presented with the corresponding load in temperature and response in crack width, comparable with the result in Figure 6.35.

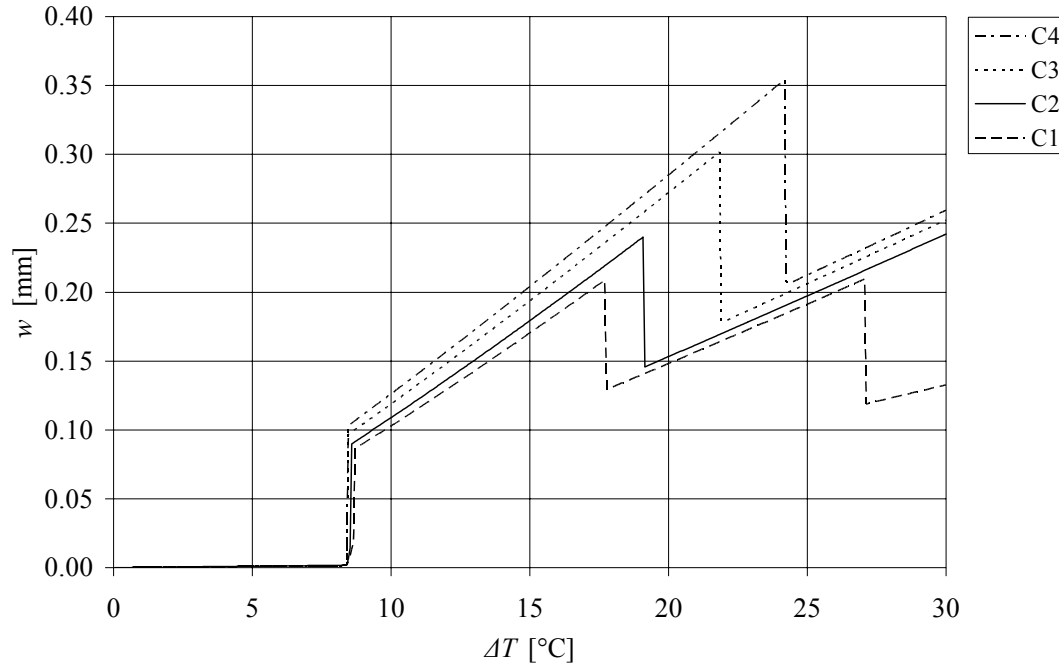


Figure 7.3 Crack width for the first crack, different ϕ and constant ρ_r .

As can be seen in Figure 7.3, the crack width varied when using different bar diameters. By inserting a larger bar diameter with a larger bar spacing, larger cracks are to be expected. But by inserting smaller bar diameter with a smaller bar spacing, the expected number of cracks is increased, and hence, the crack widths are decreased.

7.2 Improved analytical model

When the global response is calculated using the analytical model and assuming a linear response of the cracks, it is noticeable that the same response is found when comparing the reaction force and the linear-elastic behaviour with the result from the FE-analysis, see Figure 7.4. But as the crack propagation starts, differences in response are found. In order to improve the analytical model a way of iteration is described in the following paragraphs.

When using the analytical model, an assumption that the steel stress is equal to the ultimate tensile stress is made and used for estimation of the maximum crack width, according to equation (7.9).

$$w_y = 0.420 \left(\frac{\phi \cdot f_{yk}^2}{0.22 f_{cm} \cdot E_s \left(1 + \frac{E_s}{E_c} \cdot \frac{A_s}{A_{ef}} \right)} \right)^{0.826} + \frac{f_{yk}}{E_s} \cdot 4\phi \quad (7.9)$$

Instead of continuing the calculation according to this simplification, the maximum steel stress can be calculated from equation (5.2). As a new value for the maximum

steel stress is calculated, the estimated value for the maximum crack widths may be recalculated. The result in Figure 7.4 shows that, from one iteration, the result converge towards the behaviour found in the FE-model. By doing this small step in the calculations, a more accurate estimation will be achieved compared to the FE-model. As shown in Table 7.1, both the transfer length and crack width has noteworthy variation as one iteration has been done.

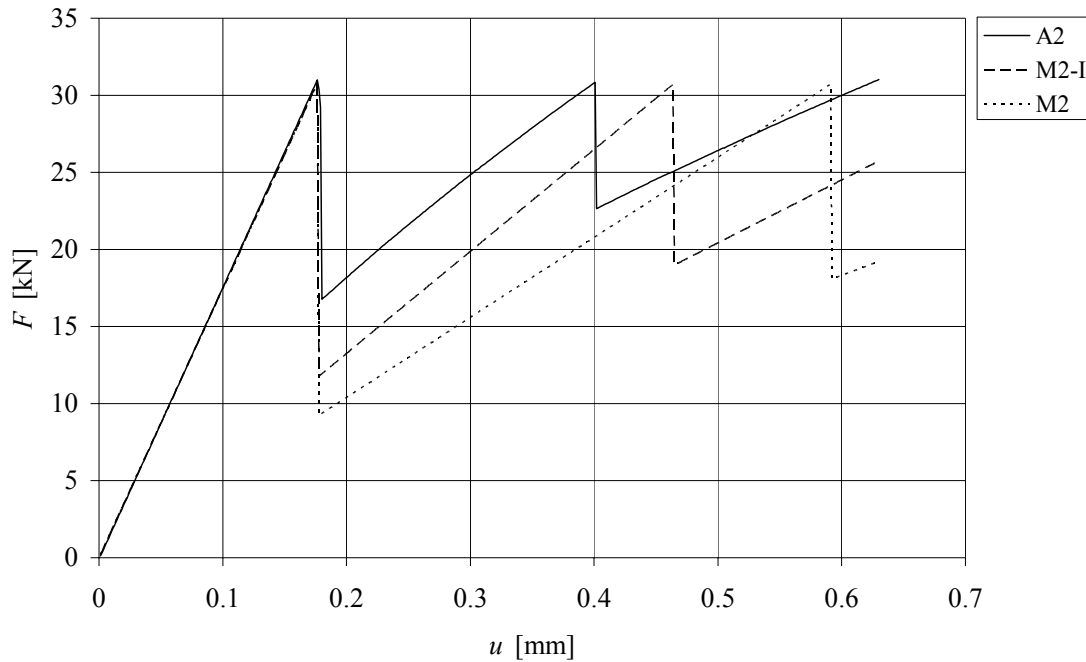


Figure 7.4 Global response from one iteration in analytical model compared with result from the FE-model.

Table 7.1 Differences in results when iteration was performed in the analytical model.

notation	M2	M2-I
maximum steel stress [MPa]	500	272
transfer length [mm]	350	243
crack width [mm]	0.764	0.301

For the two results shown in Figure 7.4, denoted M2 and M2-I, the only variation is the used value for the maximum steel stress, shown in Table 7.1, for calculation of w_y and l_t .

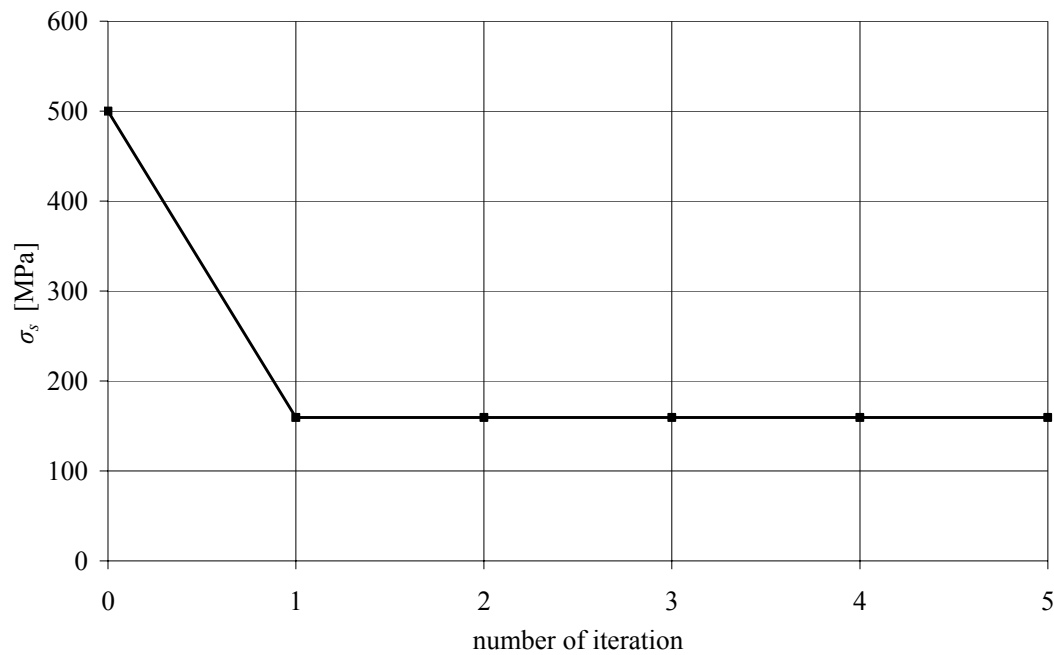


Figure 7.5 Steel stress from 5 iterations.

As shown in Figure 7.5, the iteration process converges very fast. By only using the calculated value for the maximum steel stress from the first calculation instead of f_{yk} , the calculated response will be more like the result from the FE-model. Comparing the results in Figure 7.4 and Figure 7.5 it is easy to understand that, by using the new calculated steel stress, the analytical model is a good tool in order to find the response of reinforced concrete.

7.3 Improved analytical and FE-model

When using a time consuming FE-model, the obtained response has a high credibility compared to the real structural behaviour of a specimen. The analytical method has not the same credibility due to the assumption of linear behaviour in the cracks. But as can be seen in Figure 7.6, the response obtained in the improved analytical method was a good estimation compared to the FE-model. Notable in the comparison is the response as the crack was initiated. For the improved analytical method the drop was larger than for the FE-model. This behaviour may be described as a result from that the post cracking response in the two analyses differs, as mentioned in Sections 3.1.1 and 3.1.2. A short evaluation whether this is a result from the fracture energy or assumption of linear response in cracks is to be found further on in this chapter.

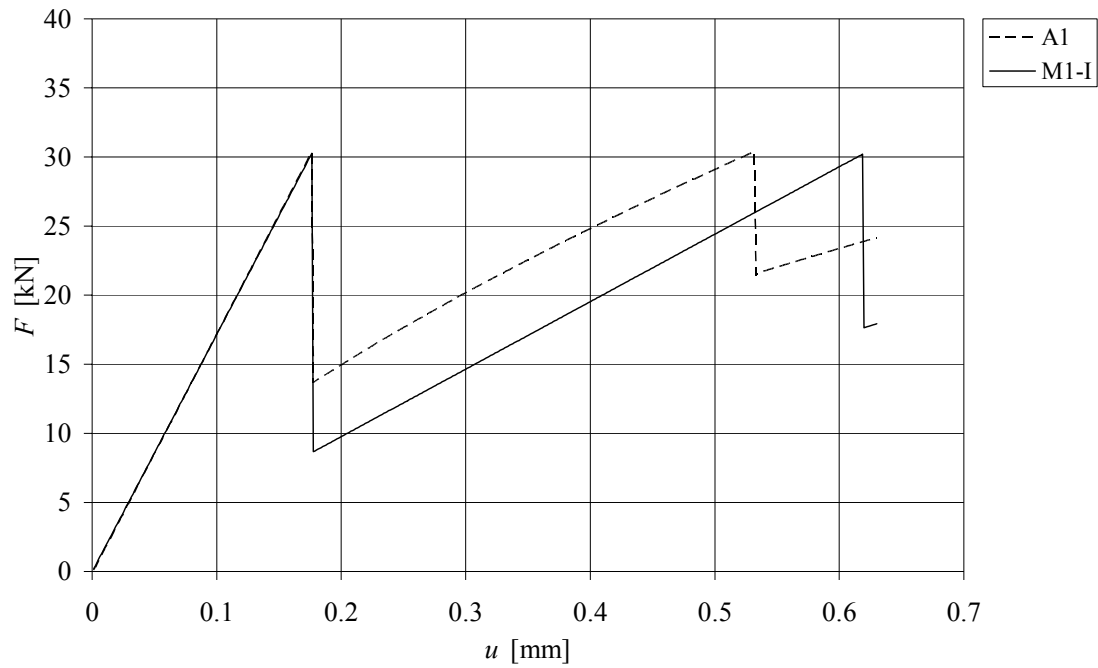


Figure 7.6 Improved analytical method M1-I, compared with FE-model A1.

In an early design stage the improved analytical method is a very good tool in order to estimate the cracking of reinforced concrete. As can be seen in Figure 7.6 - Figure 7.8, the linear elastic response are identical in the analytical method compared to the FE-model.

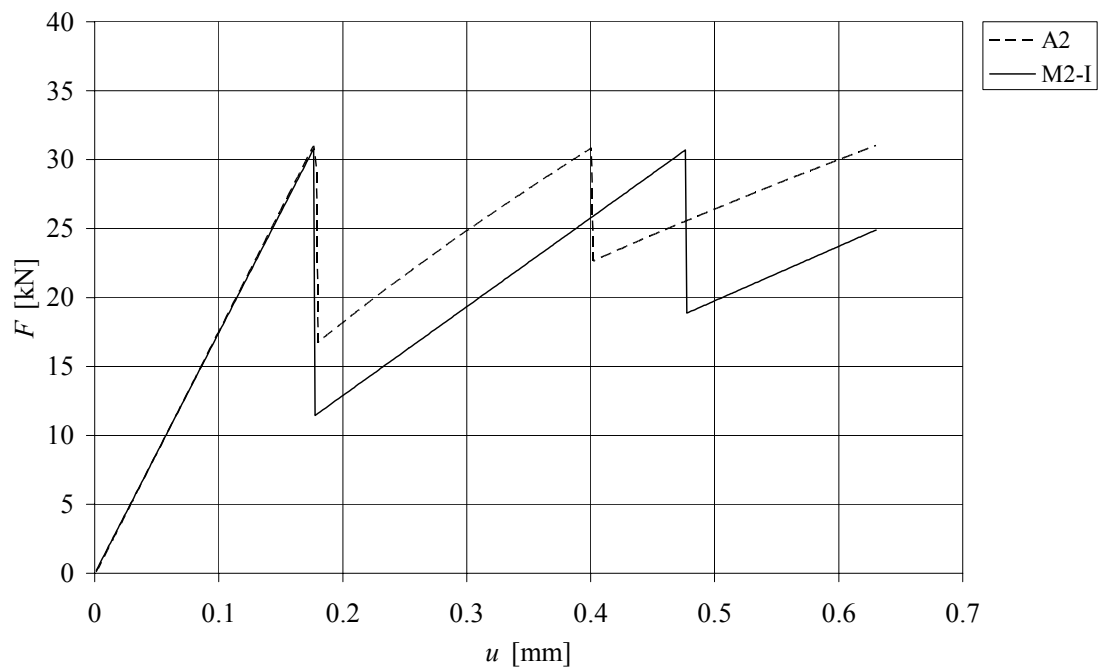


Figure 7.7 Improved analytical method M2-I, compared with FE-model A2.

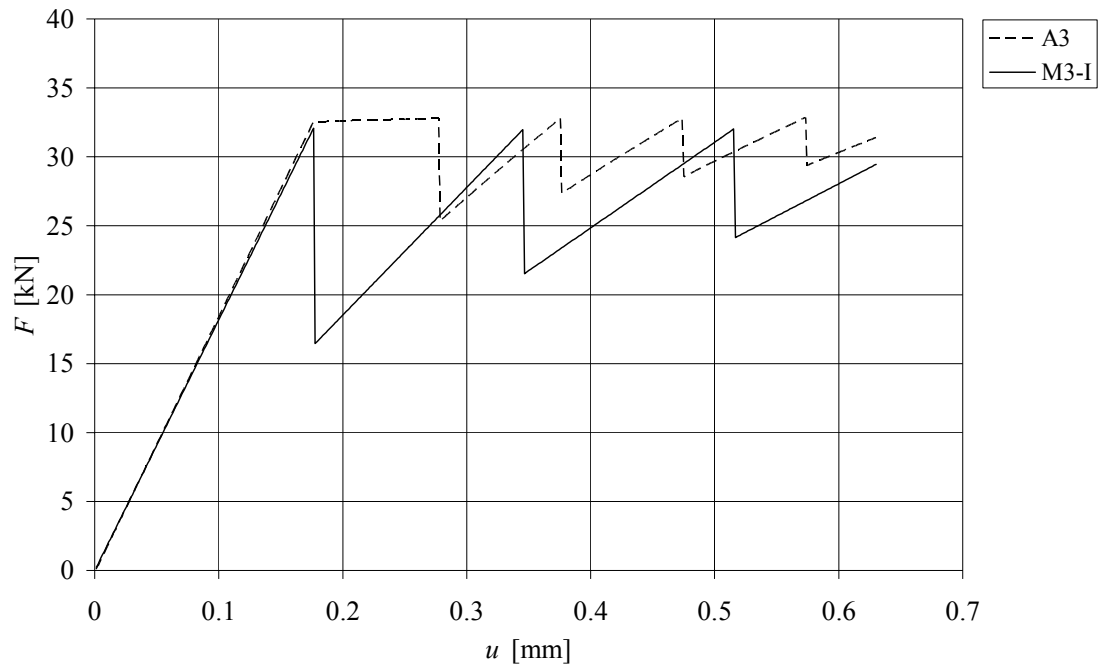


Figure 7.8 Improved analytical method M3-I, compared with FE-model A3.

When the reinforcement ratio was increased, by means of increased bar diameter, the response in the FE-model changed significantly. The plateau obtained in the FE-model was not to be found in the improved analytical method, resulting in increased differences between the analysis methods, see Figure 7.8.

When comparing the response from the improved analytical method with the FE-model in means of crack width, the results are showing notable similarities, see Figure 7.9.

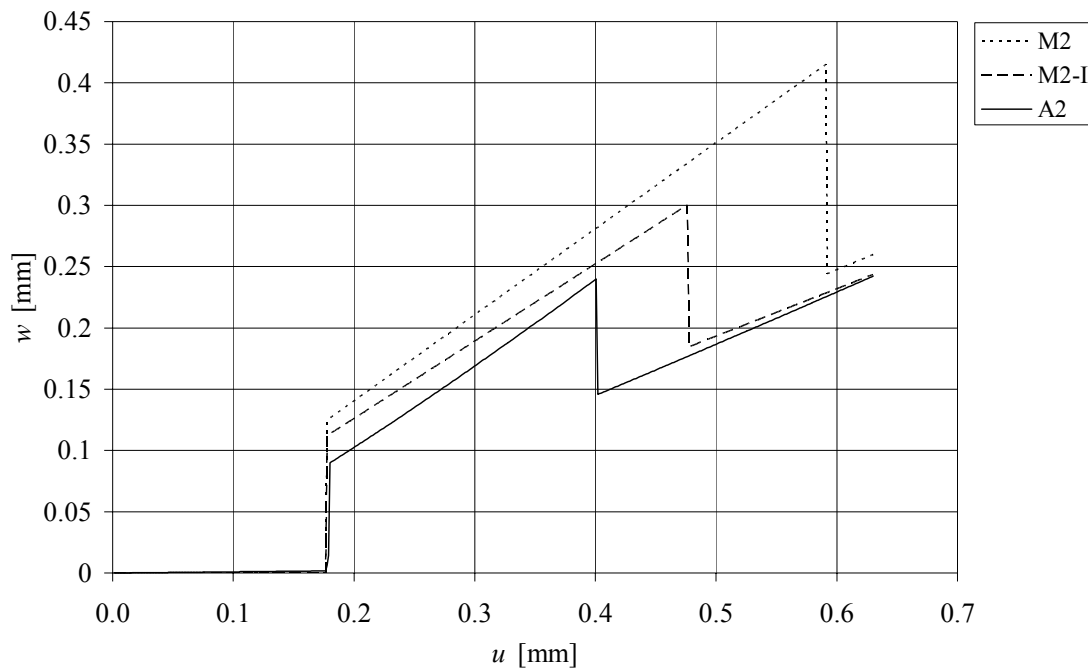


Figure 7.9 Improved analytical method M2-I and analytical method M2, compared with FE-model A2.

The maximum crack width obtained from the improved analytical method was 0.30 mm compared with 0.24 mm obtained from the FE-model. Still, the crack width in the improved analytical method is overestimated. But as can be seen in Figure 7.9, the improved analytical method must be considered as a good tool compared to the FE-model and the analytical method without any improvement.

In the improved analytical method, the linear response of the crack width is calculated with a contribution from the local bond failure, shown in Figure 3.10. In the FE-model this contribution is not considered, why an evaluation by deleting this contribution in the improved analytical method was carried out and shown in Figure 7.10.

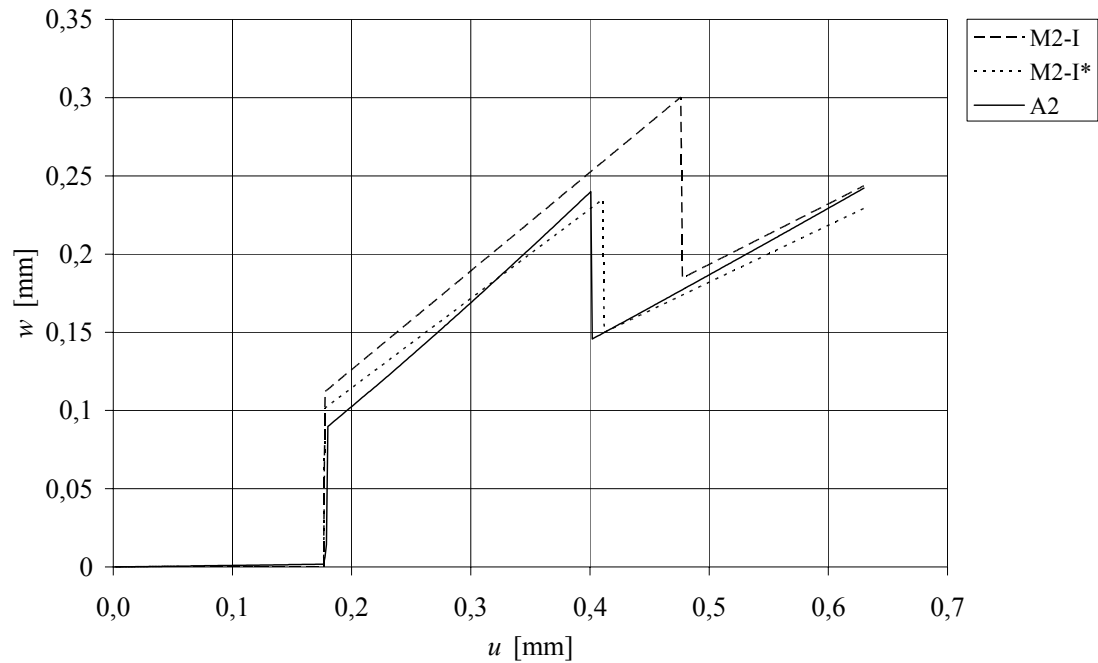


Figure 7.10 Improved analytical method M2-I, improved analytical method without the contribution of local bond failure M2-I* and FE-model A2.

The results show that by not introducing the local bond failure in the improved analytical method, the response is significantly improved towards the FE-model by means of crack width. The FE-model does not take the local bond failure in consideration, hence the analytical method can better describe the failure mechanism near a crack.

By comparing the results by means of global response the improved analytical method without taking in consideration the local bond failure shows good similarities with the FE-model, see Figure 7.11.

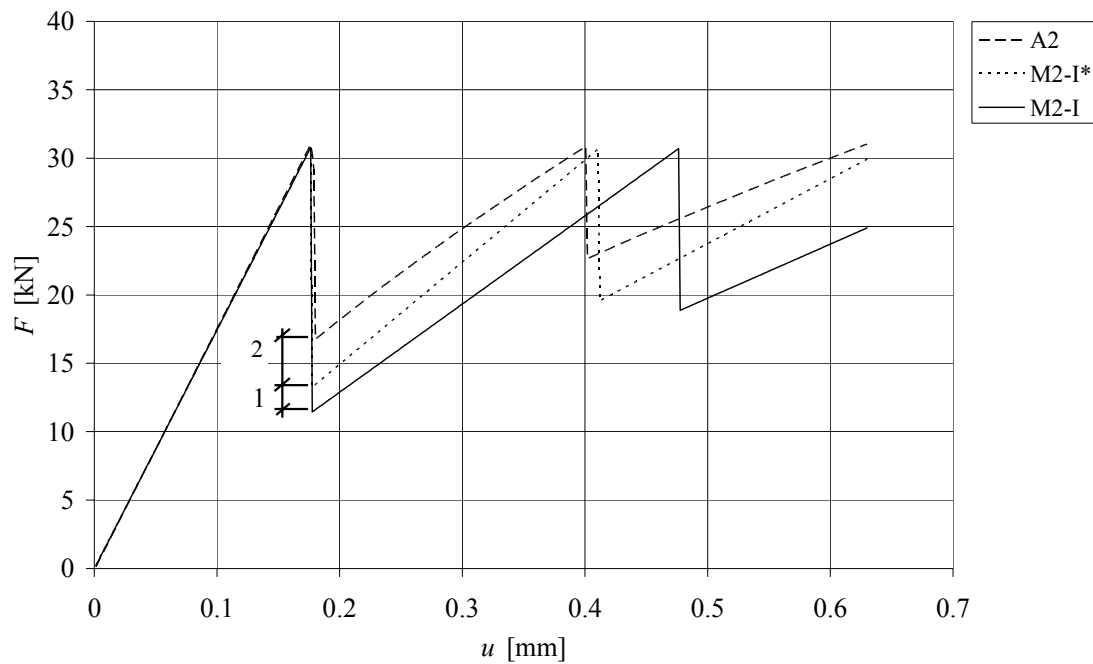


Figure 7.11 Improved analytical method M2-I, improved analytical method without the contribution of local bond failure M2-I* and FE-model A2.

In Figure 7.11 the difference in the response between the improved analytical method and the FE-model may be divided into two reasons, (1) the local bond failure and (2) the fracture energy G_f . As the improved analytical method is used without the contribution of the local bond failure, the response once again moves towards the response obtained in the FE-model. The response obtained as the crack appears still shows some difference between the two approaches, but as the specimen reaches the second crack the difference is comparatively negligible.

8 Conclusions

8.1 General

In this thesis, an analytical method with linear assumptions of the crack response has been used in order to describe the cracking behaviour of a reinforced concrete specimen. The analytical method have been improved and compared with a non-linear FE-model. Further, the analytical method and a FE-model have been used in order to verify if the common approach upon which Swedish designers today regard situations with thermal strain as governing load on reinforced concrete is appropriate or not.

Firstly it is stated that the model, for external load in BBK 04, often used by Swedish designers today regarding the number of cracks and crack distribution in concrete structures subjected to restraint situations is not suitable. This can be verified both by using FE-models and the analytical model. The approach based on external load will not give any hints on how the cracks are distributed and it is wrong to assume that the cracks are evenly distributed in a restrained structure. Cracks will be initiated in locations of deviant material capacities. The analyses showed that, an applied temperature of very high magnitude is needed in order to generate the number of cracks corresponding to such a crack distribution. Important to highlight in this discussion is that several cracks with smaller crack widths can be considered as less dangerous than fewer cracks with large crack widths.

The non-linear FE-model describes a more realistic behaviour than the analytical model where the response in concrete of post-cracking is considered. When comparing the strain in the first crack by using the same reinforcement ratio, the first crack will appear as earlier described for the same load, in this thesis described as an imposed end deformation. The differences are the crack width which for the larger bar diameter will be greater. The total deformation for the element is kept constant, but for smaller bar diameter several and smaller cracks are to be expected. Hence, smaller bar diameter with smaller spacing is to prefer in order to avoid large cracks.

When comparing the results from the FE-model and the improved analytical model, it can be stated that the crack propagation obtained in the improved analytical model may be suitable for the global response. Using a time demanding but powerful FE-model for this analysis may be hard to justify from an economical point of view. However, FE-models are a useful tool in order to verify the correctness of inputs for analytical models.

8.2 Further investigations

The assumption that the structure will crack if the surface region cracks, is the base for this study. However, studying a larger structure results in consequences for the contribution of concrete and not only by the surface regions. This may result in an additional restraint for the concrete in the surface region and a more real scenario is obtained.

When increasing the depth of the studied concrete structure the effective area will have significant influence. In order to understand the influence of the surrounding concrete, further investigation of crack propagation is of interest focusing on different heights, see Figure 8.1.

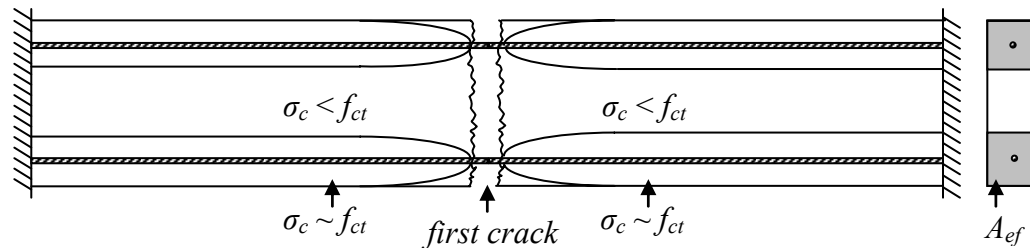


Figure 8.1 Evaluation of effective area near first crack.

When studying a concrete slab cast on, i.e. a foundation of friction soil, a new restraint is introduced to the system. Longitudinal external restraint is a case often to be found in real situations. The slab, as well as the increased depth, results in additional restraint acting along the member. Introducing this restraint is a step towards modelling a more real situation.

In this thesis the concrete shrinkage has been mentioned, but not further studied. As a load case, shrinkage of concrete will have different effects on the structure compared to thermal shrinkage of the whole structure. Since the steel will have no need for deformation, the restraint by the reinforcement on the surrounding concrete will be increased. What influence this internal restraint has on the structural response has to be further studied.

Furthermore, the effect of relaxation by implementing long term effects such as creep may have positive effects on the stress distribution. This effect has not been carefully studied in this thesis, why it is of interest in a further investigation.

By introducing different temperature gradient applied over the height of a concrete member, the stress distribution may be changed. The case of pure tension may be replaced by a case of both tension and compression. The new temperature distribution result in a case of bending moment. Due to the new stress distribution, equations will be in need of different coefficients according to national and European standards. In the end, the response of crack propagation will differ for the new temperature distribution.

When introducing deviant material properties in the FE-model, a more realistic reinforced concrete specimen will be modelled as the specimen in reality can not be considered to have the same properties for all sections. In case of deviant material properties, the length used in order to determine the fracture energy must be evaluated by means of whether the element length is proper to use.

9 References

- ADINA (2005): *Theory and Modelling Guide, Vol. 1: ADINA Solids & Structures*, Report ARD 05-7, ADINA R & D, Inc. Watertown, USA, (2005).
- Boverket (2004): *Boverkets handbok om betongkonstruktioner, BBK 04*, (Boverket's handbook on Concrete Structures, BBK 04. In Swedish), Boverket, Karlskrona, Sweden.
- CEB (1991): *CEB-FIP Model Code 1990*, Bulletin d'information Nr.203, Lausanne Switzerland, (1991).
- CEB (1997): *Serviceability Models, Behaviour and modelling in serviceability limit state including repeated and sustained loads*, CEB Bulletin 235, Lausanne Switzerland, (1997).
- CEN (2004): Eurocode 2: Design of concrete structures, Part 1-1, General rules and rules for buildings. European Committee for Standardization, Brussels, 225 pp.
- Engström B. (2006): Restraint cracking of reinforced concrete structures. Chalmers University of Technology, Division of Structural Engineering, Göteborg, Sweden, 2006.
- Engström B. (1997): *Beräkning av betong och murverkskonstruktioner – Del II Beräkningsmodeller*, (Calculations of concrete and concrete structures – Part II Models for calculation) . Chalmers University of Technology, Division of Structural Engineering, Göteborg, Sweden, 1997.
- Ghali A., Favre R. (1994): *Concrete structures, Stresses and deformations – Second edition*. E & FN SPON, London, 444 pp.
- Hirschhausen, v H. (2000): *Crack control of Restrained Concrete Structures*. Master Thesis 99:6. Chalmers University of Technology, Division of Concrete Structures. Göteborg, Sweden, 2000.
- Johansson, M. (2000): *Structural Behaviour in Concrete Frame Corners of Civil Defence Shelters*. Ph.D. Thesis. Department of Structural Engineering, Chalmers University of Technology, 00:2., Göteborg, Sweden, 2000, 145 pp.
- Jonasson J.-E., Embrg M., Bernander S. (1994): *Temperatur, mognadsgradsutveckling och egenspanningar i ung betong. Betonhandbok – Material* (Temperature, maturity development and eigenstresses in young concrete, Concrete handbook – Material. In Swedish), Byggtjänst, Stockholm, Sweden, Chapter 16, pp. 557-607.
- Plos M. (2000): *Finite element analyses of reinforced concrete structures*. Chalmers University of Technology, Department of Structural Engineering, *Concrete structures*, Göteborg, Sweden, 2000
- Soroushian P., Choi K.-B. (1989): Local bond of deformed bars with different diameters in confined concrete, *ACI Journal*, V. 86, No. 2, 1989.

Vägverket (2004): BRO 04 – Allmän teknisk beskrivning (Bridge 04 – General Technical Descriptions for Bridges. In Swedish). Publication 2004:56, Borlänge, Sweden.

APPENDIX A Calculation of shrinkage

According to CEN (2004), the shrinkage strain, ε_{cs} can be determined from:

$$\varepsilon_{cs}(t) = \varepsilon_{cd}(t) + \varepsilon_{ca}(t) \quad (\text{A.1})$$

where ε_{cd} and ε_{ca} are drying shrinkage strain and autogenous shrinkage strain of concrete.

In order to estimate the drying shrinkage, the following equations can be found in CEN (2004).

$$\varepsilon_{cd}(t) = \beta_{ds}(t) \cdot \varepsilon_{cd}(\infty) \quad (\text{A.2})$$

where $\beta_{ds}(t)$ = time function for drying shrinkage, see Figure A.2 and Figure A.3.

$\varepsilon_{cd}(\infty)$ = final value of drying shrinkage

$$\varepsilon_{cd}(\infty) = k_h \cdot \beta_{RH} \cdot \varepsilon_{cdi} \quad (\text{A.3})$$

where k_h = coefficient that considers the notional size of the section, see Table A.1.

Table A.1 Factor k_h that considers the notional size of the section.

h_0 [mm]	k_h
100	1.0
200	0.85
300	0.75
≥ 500	0.70

where h_0 is calculated according to equation (A.5).

β_{RH} = factor that considers the ambient relative humidity, see Figure A.1.

ε_{cdi} = starting value to determine the drying shrinkage strain, see Table 6.1 in Engström (2006).

$$\beta_{RH} = 1.55 \cdot \left(1 - \left(\frac{RH}{(RH)_0} \right)^3 \right) \quad (\text{A.4})$$

where RH = ambient relative humidity [%]

$$(RH)_0 = 100\% \text{ (reference value)}$$

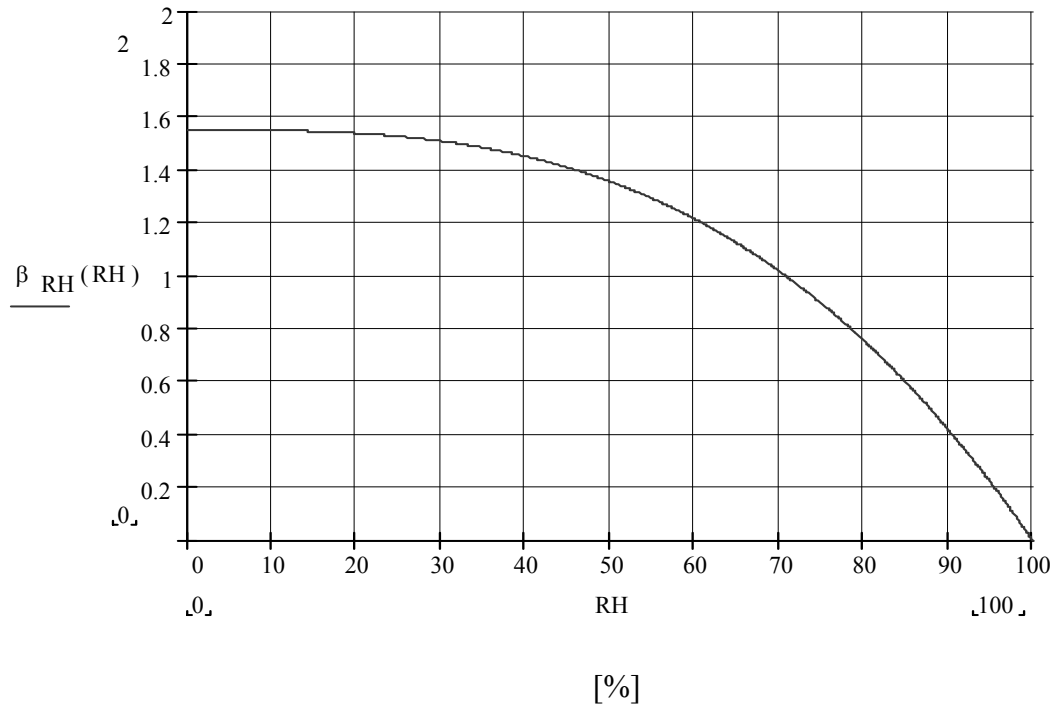


Figure A.1 The factor β_{RH} that considers the ambient relative humidity RH .

$$h_0 = \frac{2 \cdot A_c}{u} \tag{A.5}$$

where A_c = gross concrete cross sectional area

u = perimeter of that part of the cross section which is exposed to drying

The time function that describes the development of the drying shrinkage strain can be determined from

$$\beta_{ds}(t, t_s) = \frac{(t - t_s)}{(t - t_s) + 0.04\sqrt{h_0^3}} \tag{A.6}$$

where h_0 is to be inserted in mm

t = actual age of the concrete [days]

t_s = age of the concrete when drying starts [days]

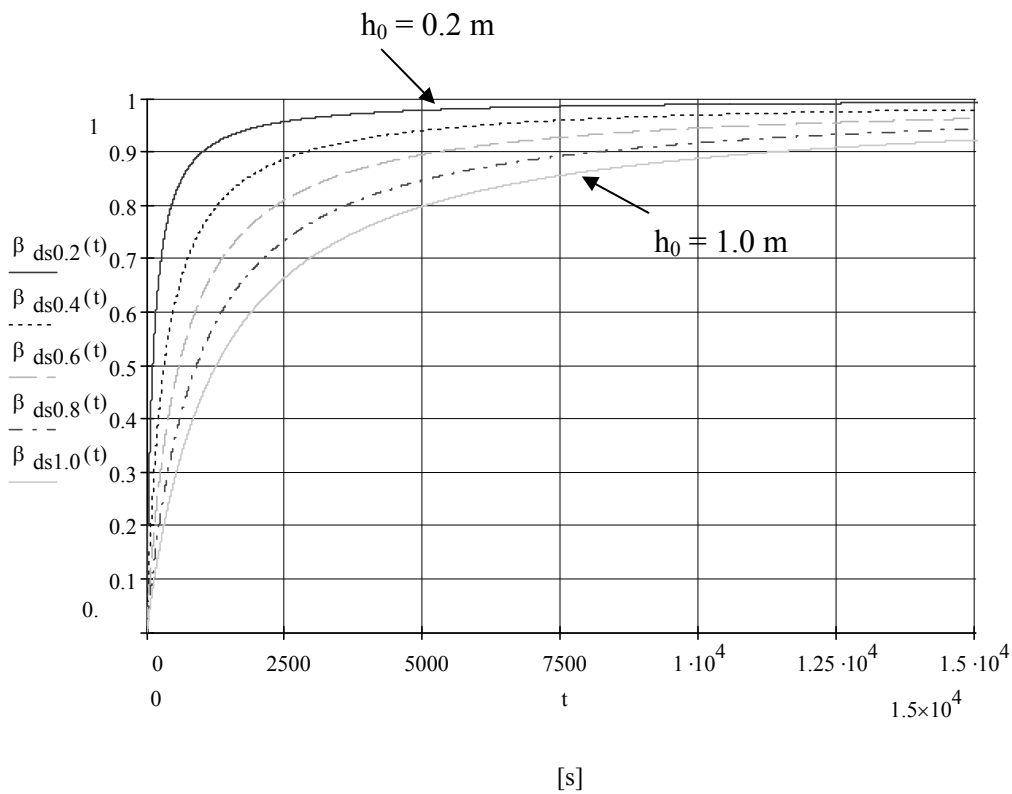


Figure A.2 The factor $\beta_{ds}(t)$ that describes the development of the drying shrinkage strain, linear scale on the x-axis.

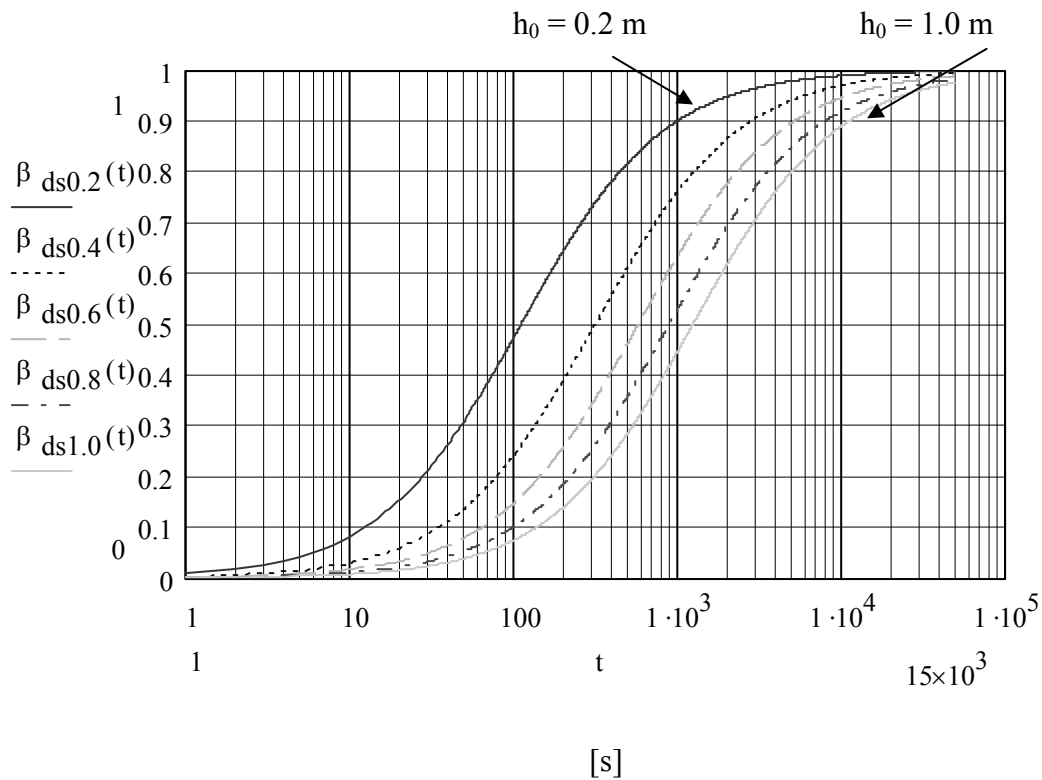


Figure A.3 The factor $\beta_{ds}(t)$ that describes the development of the drying shrinkage strain, logarithmic scale on the x-axis.

APPENDIX B Calculation of creep

Following calculations are based on Eurocode 2, CEN (2004).

The factor which considers the relative humidity ϕ_{RH} can be determined from

$$\phi_{RH} = 1 + \frac{1 - RH / 100}{0.1 \cdot \sqrt[3]{h_0}} \quad \text{for } f_{cm} \leq 35 \text{ MPa} \quad (\text{B.1})$$

$$\phi_{RH} = \left[1 + \frac{1 - RH / 100}{0.1 \cdot \sqrt[3]{h_0}} \cdot \left[\frac{35}{f_{cm}} \right]^{0.7} \right] \cdot \left[\frac{35}{f_{cm}} \right]^{0.2} \quad \text{for } f_{cm} > 35 \text{ MPa} \quad (\text{B.2})$$

where RH = relative humidity of the ambient environment in [%]

h_0 = notional size of the concrete section [mm]

f_{cm} = mean compressive strength of concrete [MPa] at an age of 28 days

The notional size of the concrete section is the thickness of an equivalent wall that is exposed to drying at both main faces. The notional size can be determined from

$$h_0 = \frac{2 \cdot A_c}{u} \quad (\text{B.3})$$

where A_c = gross concrete cross sectional area.

u = perimeter of that part of the cross section which is exposed to drying.

The factor which considers the concrete strength class $\beta(f_{cm})$ can be determined from:

$$\beta(f_{cm}) = \frac{16.8}{\sqrt{f_{cm}}} \quad (\text{B.4})$$

f_{cm} is the mean compressive strength of concrete [MPa] at an age of 28 days.

$$\beta(t_0) = \frac{1}{0.1 + t_0^{0.20}} \quad (\text{B.5})$$

t_0 = age of concrete when load is applied [days].

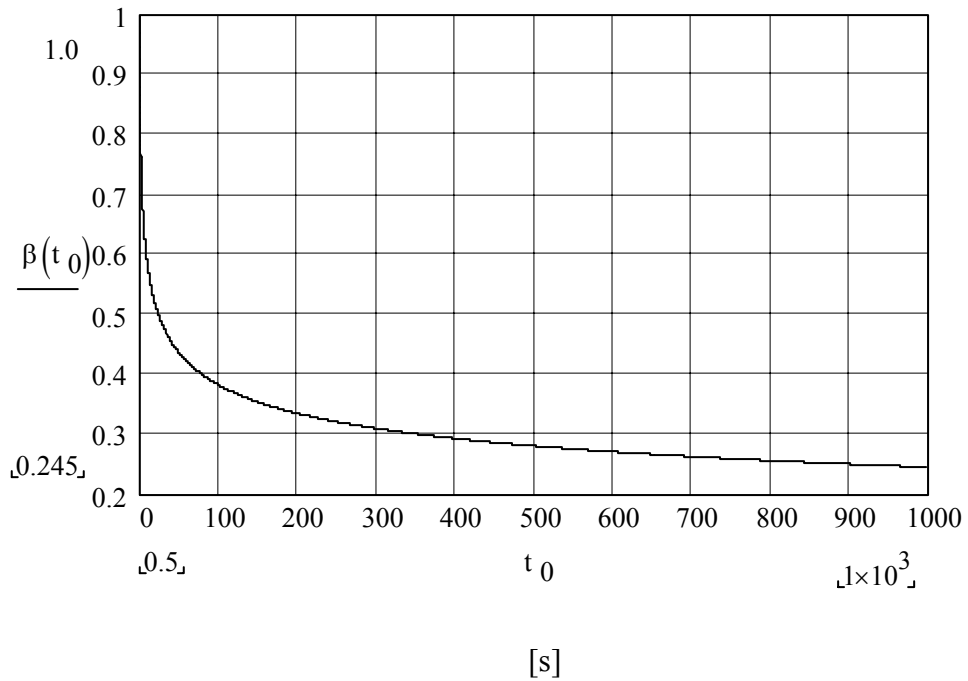


Figure B.1 The factor β_{t_0} that considers the concrete age when load is applied, linear scale on the x-axis.

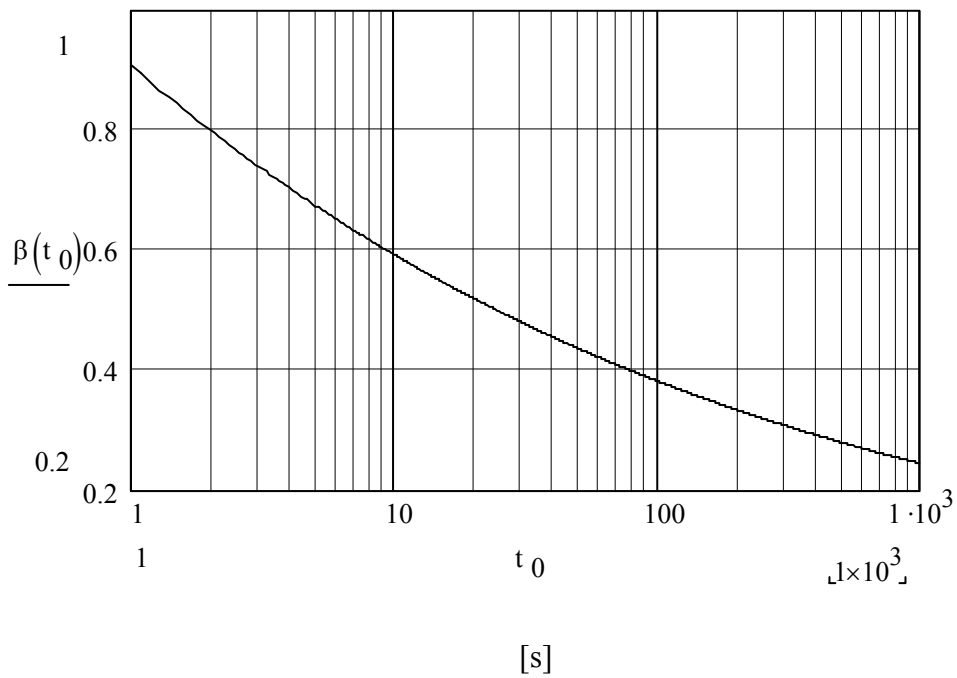


Figure B.2 The factor β_{t_0} that considers the concrete age when load is applied, logarithmic scale on the x-axis.

The development of creep with time is given by:

$$\beta_c(t, t_0) = \left[\frac{(t - t_0)}{\beta_H + (t - t_0)} \right]^{0.3} \quad (\text{B.6})$$

where t = age of concrete at the moment considered (days)

t_0 = age of concrete at time of loading (days)

$t - t_0$ = the non-adjusted duration of loading (days)

β_H = coefficient depending on the ambient relative humidity and the notional size h_0

The factor which considers the ambient relative humidity and the notional size of the section β_H can be determined from:

$$\beta_H = 1.5 \cdot \left[1 + (0.012 \cdot RH)^{18} \right] \cdot h_0 + 250 \leq 1500 \quad (\text{B.7})$$

for $f_{cm} \leq 35\text{MPa}$

$$\beta_H = 1.5 \cdot \left[1 + (0.012 \cdot RH)^{18} \right] \cdot h_0 + k_1 \leq k_2 \quad (\text{B.8})$$

where $k_1 = 250 \cdot \left[\frac{35}{f_{ck} + 8} \right]^{0.5}$

$$k_2 = 1500 \cdot \left[\frac{35}{f_{ck} + 8} \right]^{0.5}$$

for $f_{cm} > 35\text{MPa}$

The effect of type of cement on the creep coefficient of concrete may be taken into account by modifying the age of loading t_0 by:

$$t_0 = t_{0,T} \cdot \left(\frac{9}{2 + t_{0,T}^{1.2}} + 1 \right)^\alpha \geq 0.5 \quad (\text{B.9})$$

where $t_{0,T}$ = is the temperature adjusted age of concrete at loading adjusted according to:

$$t_T = \sum_{i=1}^n e^{-(4000/[273+T(\Delta t_i)]-13.65)} \cdot \Delta t_i \quad (\text{B.10})$$

where t_T = the temperature adjusted concrete age which replaces t in the corresponding equations.

$T(\Delta t_i)$ = the temperature in °C during the time period Δt_i .

Δt_i = the number of days where a temperature T prevails.

The mean coefficient of variation of the above predicted creep data, deduced from a computerised data bank of laboratory test results, is of the order of 20%.

APPENDIX C Differences in codes regarding shrinkage

Example 1

Concrete C70/85	Load applied at early age (28 days)
RH 55%	Load stays for 100 days
h_0 1.0 m	

EC2	BBK 04
$\varepsilon_{cs} = 0.14 \cdot 10^{-3}$	$\varepsilon_{cs} = 0.40 \cdot 10^{-3}$

Example 2

Concrete C20/25	Load applied at early age (28 days)
RH 55%	Load stays for 100 days
h_0 1.0 m	

EC2	BBK 04
$\varepsilon_{cs} = 0.04 \cdot 10^{-3}$	$\varepsilon_{cs} = 0.40 \cdot 10^{-3}$

Example 3

Concrete C20/25	Load applied at high maturity
RH 55%	Load stays for long
h_0 1.0 m	

EC2	BBK 04
$\varepsilon_{cs} = 0.32 \cdot 10^{-3}$	$\varepsilon_{cs} = 0.40 \cdot 10^{-3}$

Example 4

Concrete C20/25

Load applied at an age of 28 days.

RH 95%

Load stays for long.

h_0 0.1 m

EC2

BBK 04

$$\varepsilon_{cs} = 0.10 \cdot 10^{-3}$$

$$\varepsilon_{cs} = 0.10 \cdot 10^{-3}$$

The evaluation has been carried out according to the following calculations (values for Example 3):

EC2

BBK 04

$$\varepsilon_{cs}(\infty) = \varepsilon_{cd}(\infty) + \varepsilon_{ca}(\infty)$$

$$\varepsilon_{cs} = 0.4 \cdot 10^{-3}$$

$$\varepsilon_{cd}(\infty) = k_h \cdot \beta_{RH} \cdot \varepsilon_{cdi} = 2.93 \cdot 10^{-4}$$

$$\varepsilon_{ca}(\infty) = 2.5 \cdot 10^{-5}$$

$$\varepsilon_{cs,EC2} = 0.32 \cdot 10^{-3}$$

$$\varepsilon_{cs,BBK04} = 0.40 \cdot 10^{-3}$$

APPENDIX D Differences in codes regarding creep

Example 1

Concrete C70/85	Load applied at early age (28 days)
RH 55%	Load stays for 100 days
h_0 1.0 m	

EC2	BBK 04
$\varphi = 0.61$	$\varphi = 3.00$

Example 2

Concrete C20/25	Load applied at early age (28 days)
RH 55%	Load stays for 100 days
h_0 1.0 m	

EC2	BBK 04
$\varphi = 1.01$	$\varphi = 3.00$

Example 3

Concrete C20/25	Load applied at high maturity
RH 55%	Load stays for long
h_0 1.0 m	

EC2	BBK 04
$\varphi = 1.13$	$\varphi = 3.00$

Example 4

Concrete C20/25

Load applied at an age of 28 days.

RH 95%

Load stays for long.

h_0 0.1 m

EC2

BBK 04

$\varphi = 1.92$

$\varphi = 1.10$

The evaluation has been carried out according to the following calculations (values for Example 3):

EC2

$$\varphi_{RH} = 1.5$$

$$\beta_{fcm} = 3.0$$

$$\beta_{t_0} = 0.25$$

$$\beta_{t,t_0} = 0.25$$

$$\varphi_{EC2} = \varphi_{RH} \cdot \beta_{fcm} \cdot \beta_{t_0} \cdot \beta_{t,t_0}$$

$$\varphi_{EC2} = 1.13$$

BBK 04

$$\varphi_{start} = 3.0$$

$$\alpha = 1.0$$

$$\varphi_{BBK04} = \varphi_{start} \cdot \alpha$$

$$\varphi_{BBK04} = 3.00$$

APPENDIX E Difficulties and approaches in FE-modelling

E.1 Temperature load

As mentioned in Section 6.1, various problems occurred as the load were described as a prescribed negative change of temperature. The first problem found, was that cracks will appear close to the boundary. By introducing a small increase of the tensile strength for the elements close to the boundary, the expected response was received.

When calculating the sum of reaction forces acting at the boundary, the results are not unanimous. The result obtained from the FE-analysis showed a decreased value on the reaction force as the load was applied.

A summation of the reaction force has been carried out by hand. The mean value of the concrete stress for the elements on the boundary, together with the steel stress for the edge element, has been multiplied with the initial area of the corresponding elements. The result is shown in Figure E.1 and compared to the result from the dynamic FE-analysis.

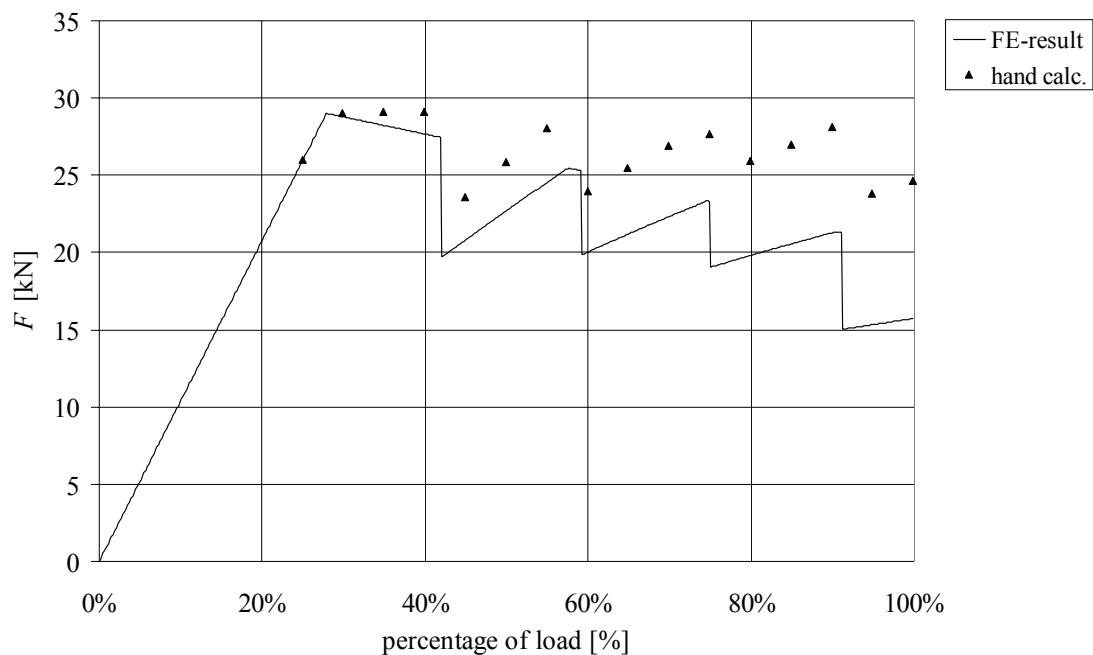


Figure E.1 Sum of reaction force due to temperature loading.

In order to find a solution where this behaviour does not occur, a number of analyses have been carried out to find the expected global behaviour.

For the dynamic analysis, one solution could be that acceleration forces result in a loss of reaction force. The time function was changed from applying the load under a time of 1 second up to 10 second and then up to 1000 seconds. This change showed no

change of response, why the assumption of acceleration forces will be no further investigated.

By applying a Rayleigh damping on the structure of 1% between 1 – 1000 Hz and 1% between 1 – 10000Hz same results were obtained, why this is not the cause to the error.

One solution to this phenomenon might be that the FE-program take in consideration the decrease of concrete cross section and therefore the resulting force will be reduced, according to (E.1).

$$F = \sigma \cdot A \quad (\text{E.1})$$

But the decrease of the cross section area is not as big as the decrease of reaction force in Figure E.1. There is most likely an additional influence to this phenomenon.

A further explanation could be that there is a change in material properties due to changed temperature. But for this FE-analysis, the influence of the temperature is not regarded and there is no data for this in the material properties. Due to lack of experience with this FE-program, no further conclusion can be drawn. There are numerical problems by using a prescribed temperature as load, why this load case will not be further evaluated.

By applying a prescribed end displacement on the element that corresponds to the negative change of temperature, according to equation (E.3), the behaviour is expected to be without numerical errors.

$$\varepsilon_{cs} = \alpha \cdot \Delta T = 10.5 \cdot 10^{-6} \left[\frac{1}{^{\circ}\text{C}} \right] \cdot 30[^{\circ}\text{C}] = 3.15 \cdot 10^{-4} \quad (\text{E.2})$$

$$u = \varepsilon_{cs} \cdot l = 3.15 \cdot 10^{-4} \cdot 2[\text{m}] = 6.3 \cdot 10^{-4} \text{ m} \quad (\text{E.3})$$

By comparing the global response of the two load cases in Figure E.2, it can be observed that the cracks will appear for the same load and that the number of cracks is the same.

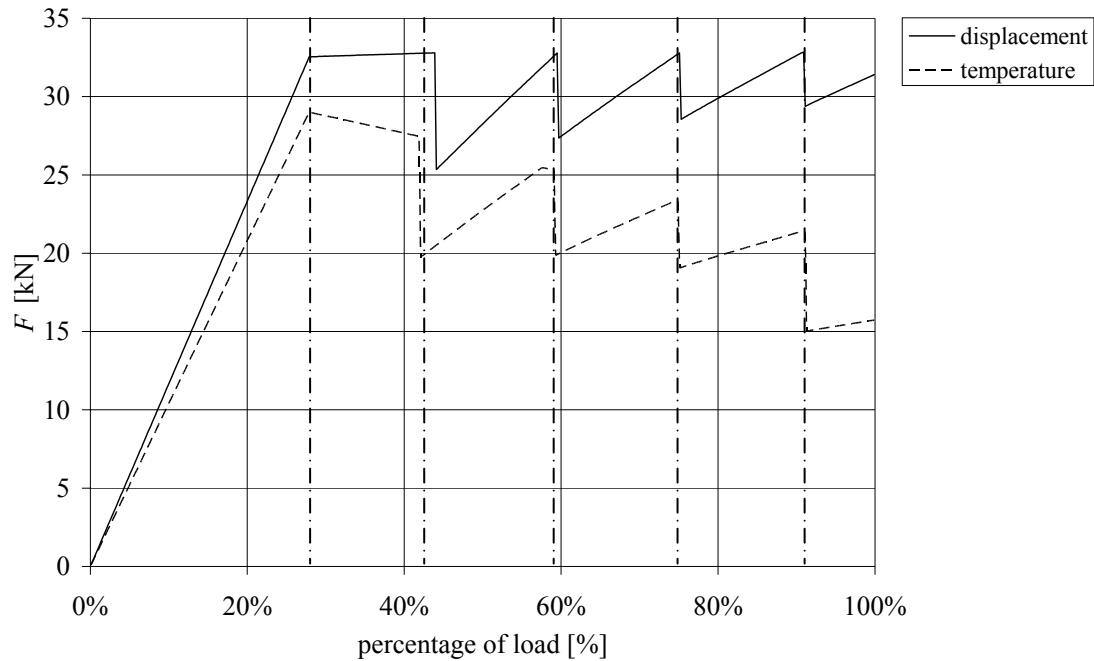


Figure E.2 Global response due to displacement and temperature loading.

By this comparison, the conclusion that it is applicable to model the change of temperature as an end displacement can be drawn, as the response from the shown case is rather similar.

E.2 Iteration difficulties

When modelling non-linear reinforced concrete structures, convergence difficulties are to be expected. This is due to sudden nonlinearities that will take place as a result of cracking of the materials. The overall structural nonlinearities are more pronounced when only small amounts of steel reinforcement are used in the structure. To avoid these problems, the reinforcement ratio has to be considered. Also the size of incremental load step is of importance for the analyses to find convergence in the equilibrium iteration.

In the analyses, in most cases, the static solution category was stable with effective solution times. But in cases where convergence was hard to reach, the dynamic solution category gave more stable results. In this method damping, according to Figure E.3, had to be applied in order to handle small oscillations.

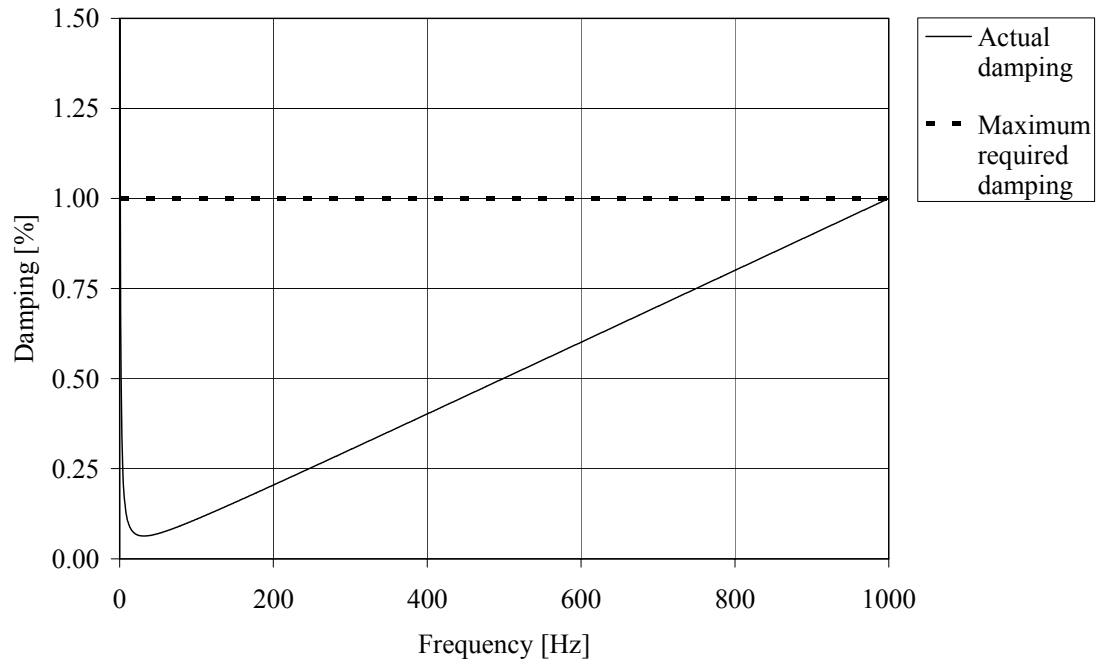


Figure E.3 Graph showing damping between 1 and 1000 Hz.

Further the tolerances have significant influence of the equilibrium iterations. The analysis can be done using several different tolerances. One common is energy tolerance where a limit for the energy ratio has to be reached, called ETOL see equation (E.4), for the equilibrium using a specific number of maximum iterations.

$$\frac{\Delta U^{(i)^T} \left[{}^{t+\Delta t} R - {}^{t+\Delta t} F^{(i-1)} \right]}{\Delta U^{(1)^T} \left[{}^{t+\Delta t} R - {}^t F \right]} \leq ETOL \quad (E.4)$$

Other types of convergence criteria specified in ADINA are: energy and force/moment, energy and translation/rotation, force/moment only and translation/rotation only.

The experience from working with tolerances is that it can be hard to modify these in a proper manner due to numerical instabilities and other parameters such as norms and references values that affecting the result.

E.3 Comparison Static and Dynamic analysis

When comparing the result obtained in the static analysis with the result from the dynamic analysis for A1, there are no differences as shown in Figure E.4.

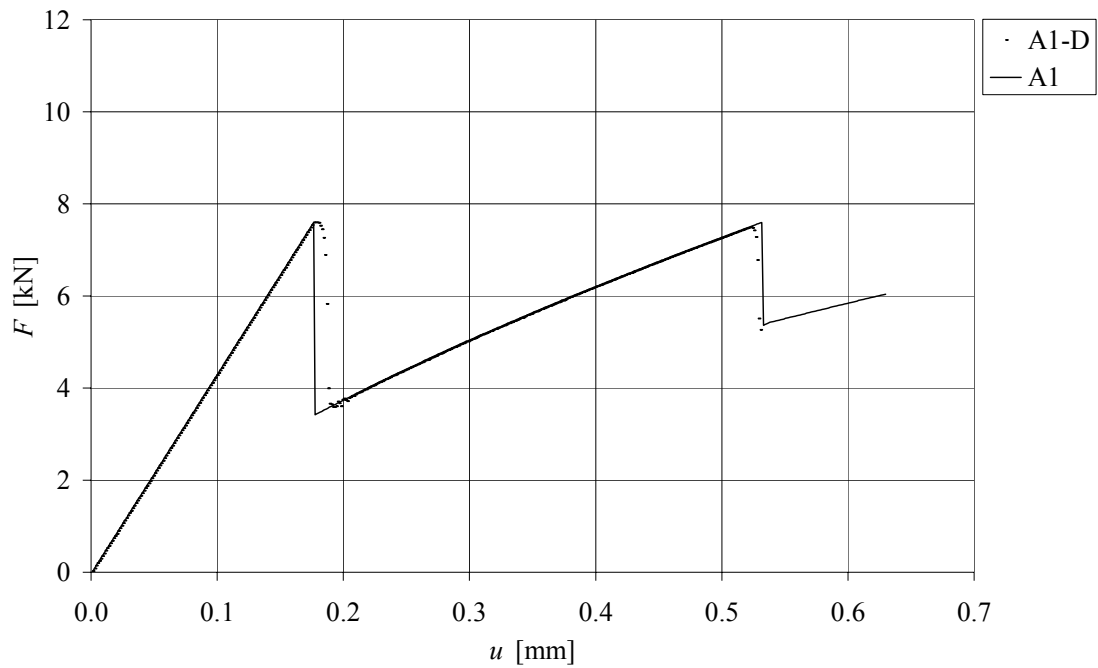


Figure E.4 Results from Static (A1) and Dynamic (A1-D) analysis.

When comparing results from static and dynamic analysis for A2, there are minor differences as the second crack are described, see Figure E.5.

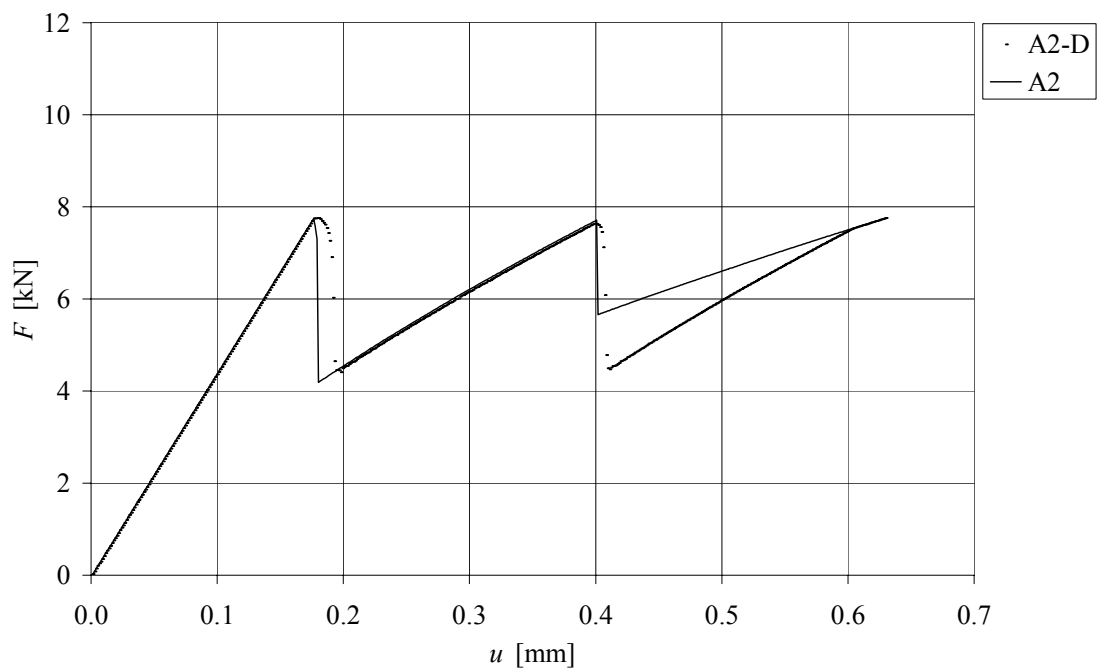


Figure E.5 Results from Static (A2) and Dynamic (A2-D) analysis.

For the analyses A3 and A4, the results from static and dynamic calculations show small but noticeable variations. Using the dynamic analysis resulted in a smoother response, shown in Figure E.6 and Figure E.7.

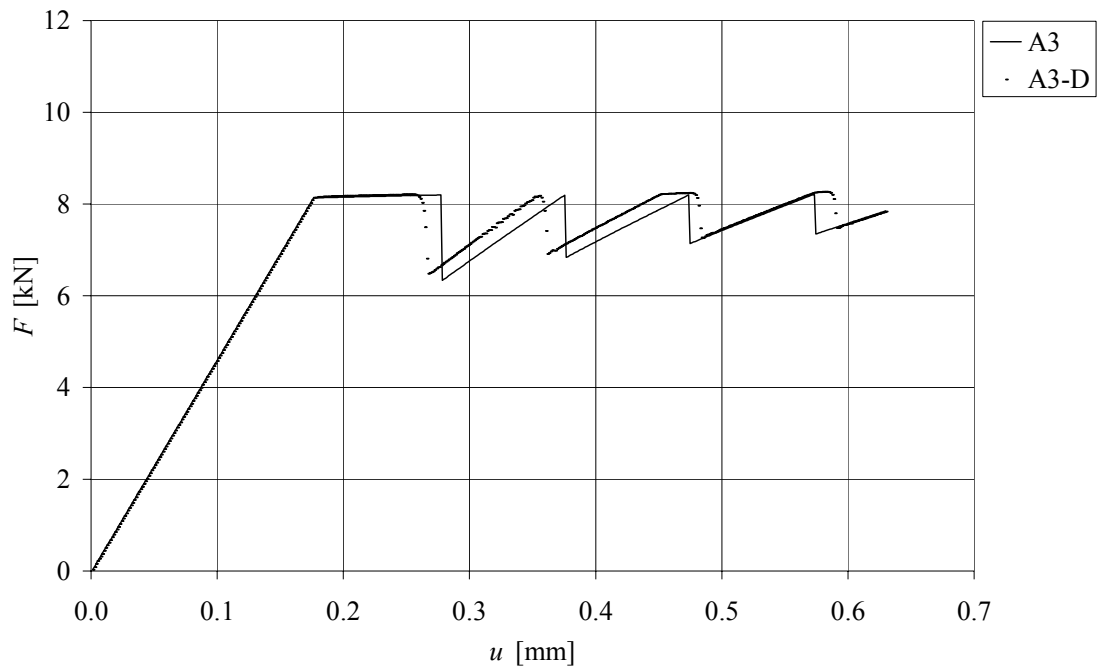


Figure E.6 Results from Static (A3) and Dynamic (A3-D) analysis.

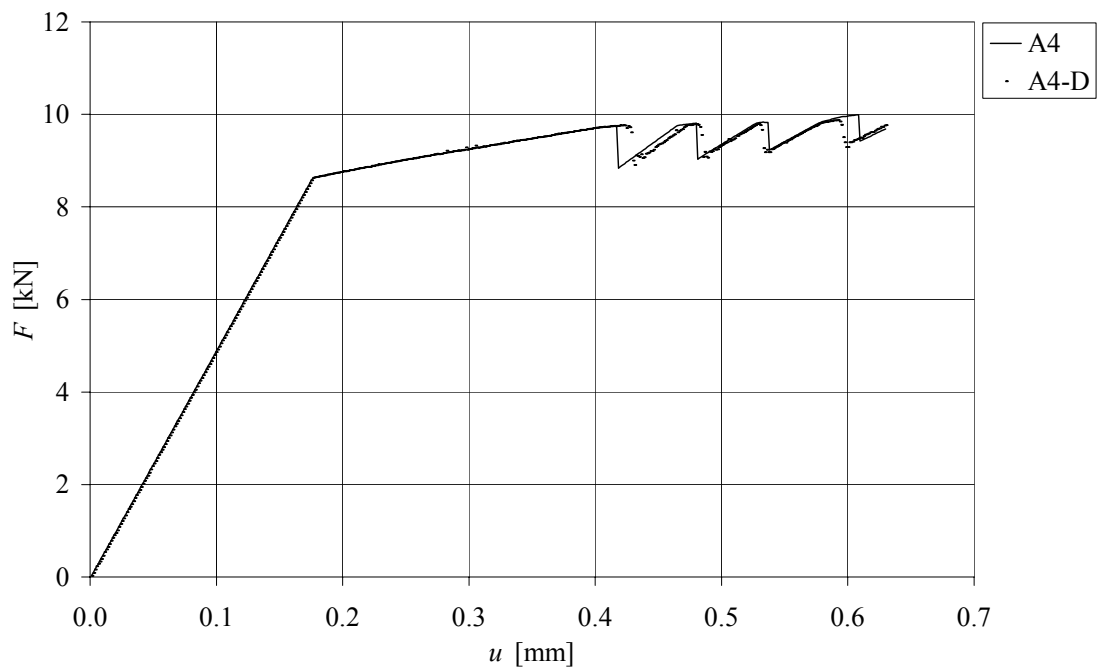


Figure E.7 Results from Static (A4) and Dynamic (A4-D) analysis.

APPENDIX F Results from FE-analysis

F.1 Bar diameter

For this first static analysis a cross section of $100 \times 100 \text{ mm}^2$ has been used. The total length was 2.0 m and the element length is 20 mm. Results from analyses concerning concrete and steel stress, are taken from 10 steps from the loading history. The notation and variation of the tests are as follows:

Table F.1 Notations of performed analyses.

notation	bar diameter [mm]
A1	10
A2	12
A3	16
A4	20

F.1.1 A1

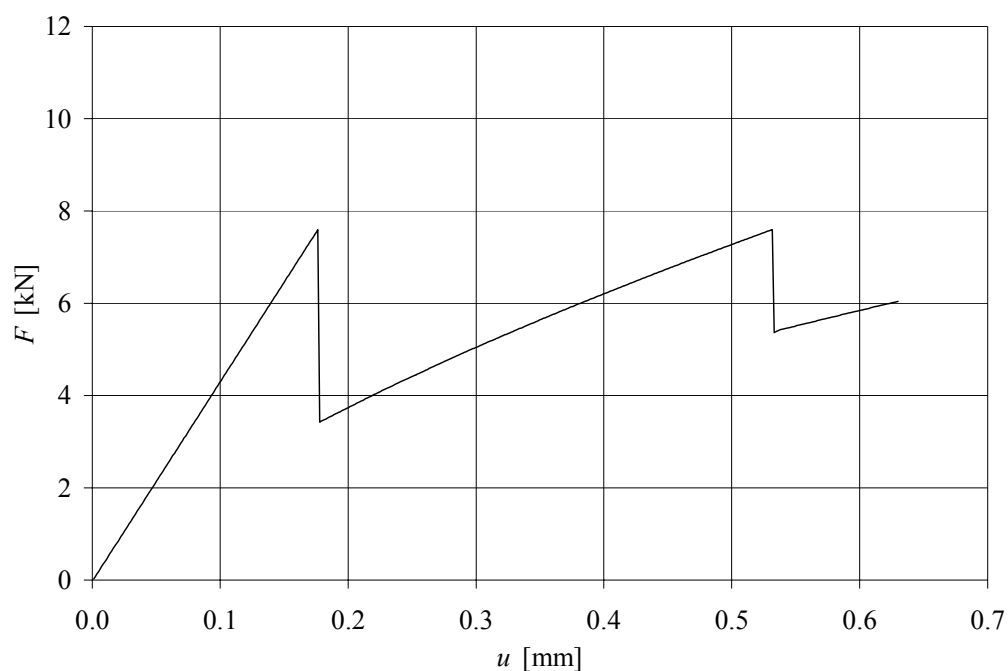


Figure F.1 Global response for A1.

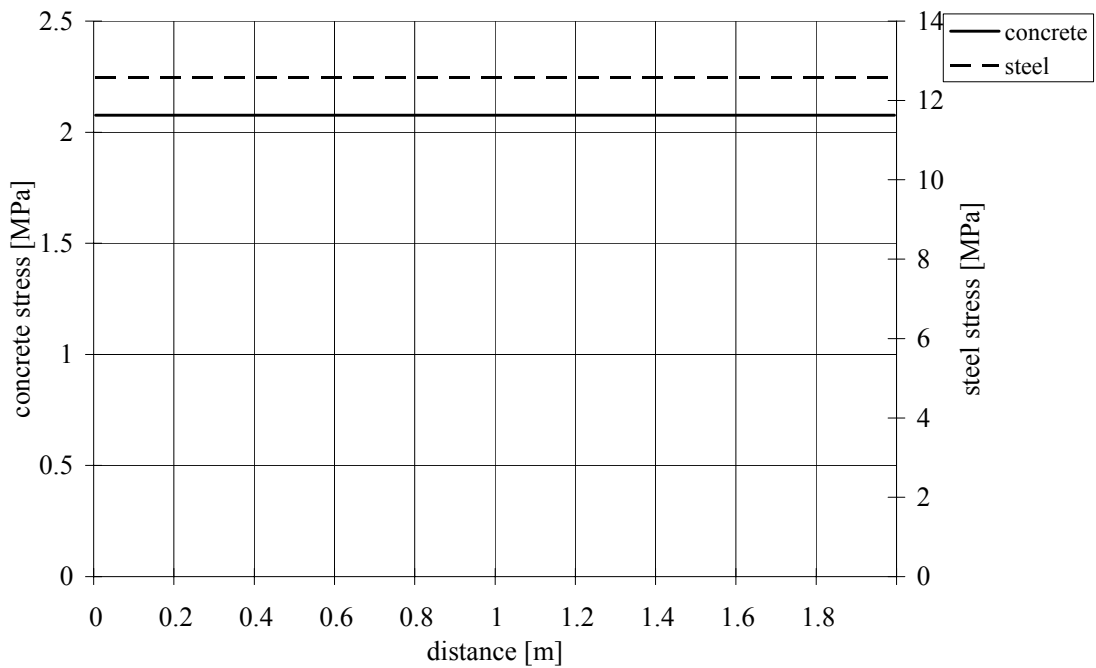


Figure F.2 Concrete stress and steel stress at an imposed end displacement = 0.063 mm, for A1.

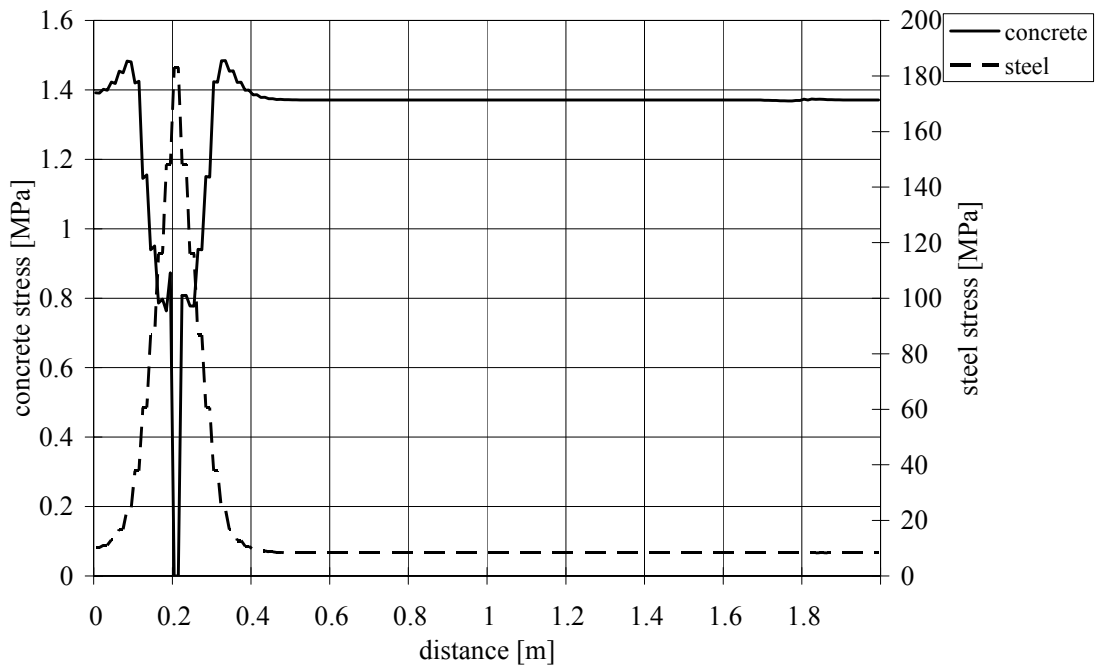


Figure F.3 Concrete stress and steel stress at an imposed end displacement = 0.189 mm, for A1.

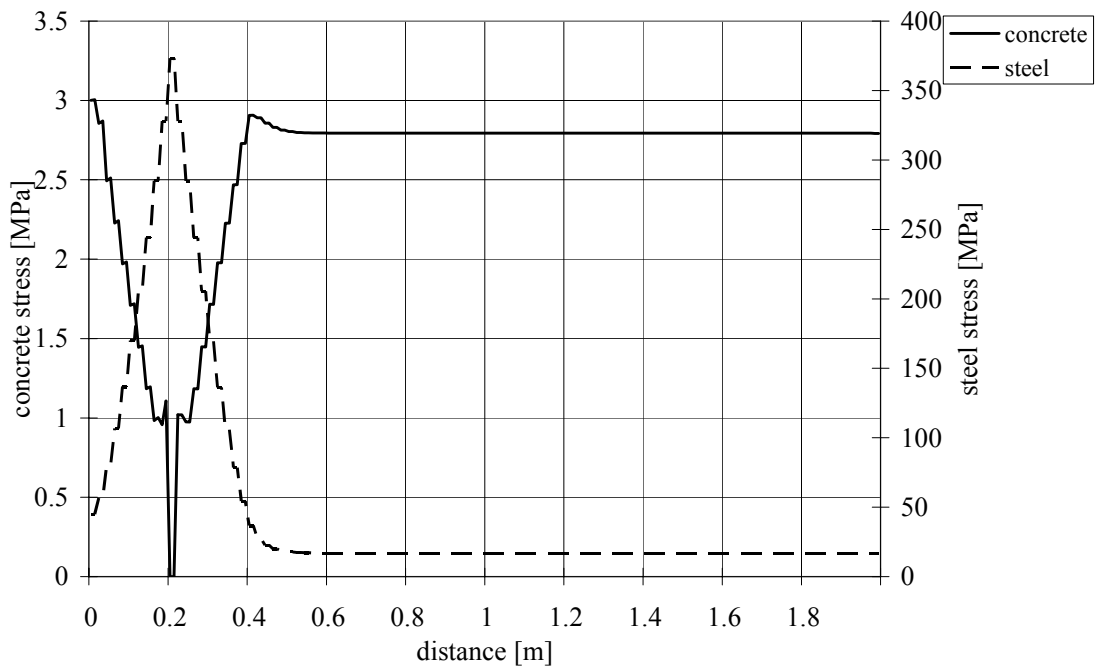


Figure F.4 Concrete stress and steel stress at an imposed end displacement = 0.504 mm, for A1.

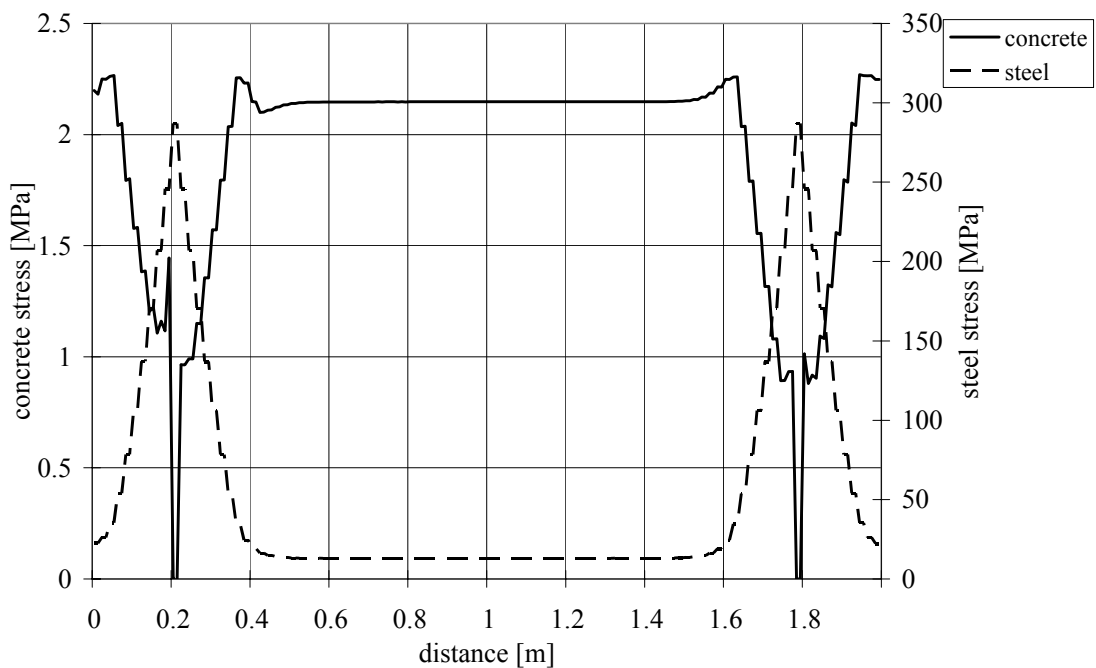


Figure F.5 Concrete stress and steel stress at an imposed end displacement = 0.567 mm, for A1.

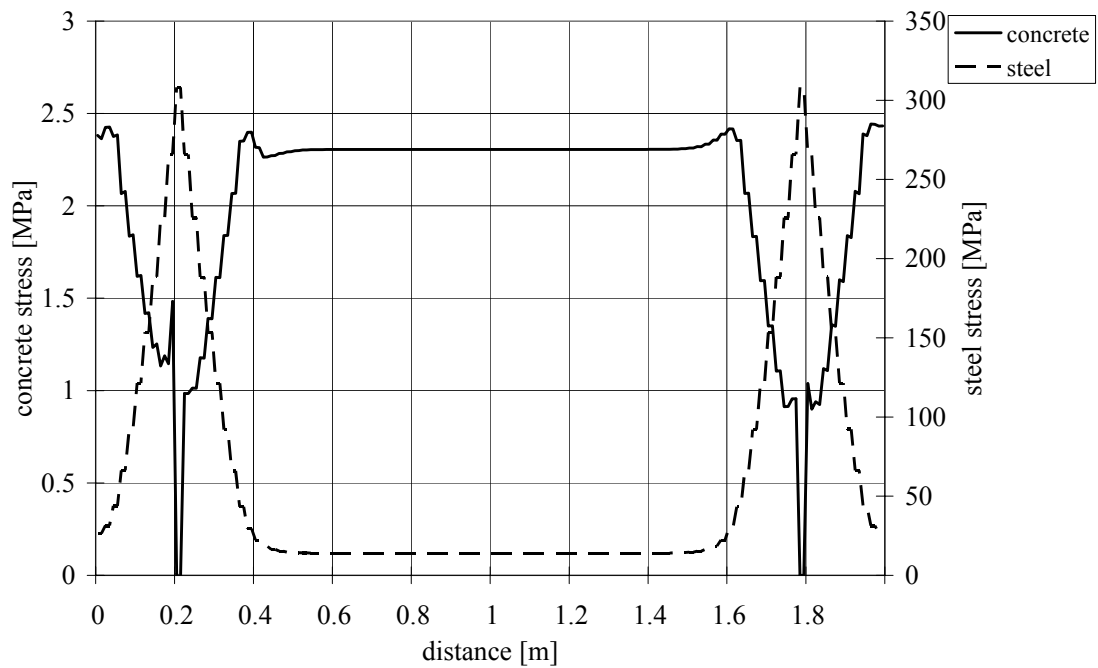


Figure F.6 Concrete stress and steel stress at an imposed end displacement = 0.630 mm, for A1.

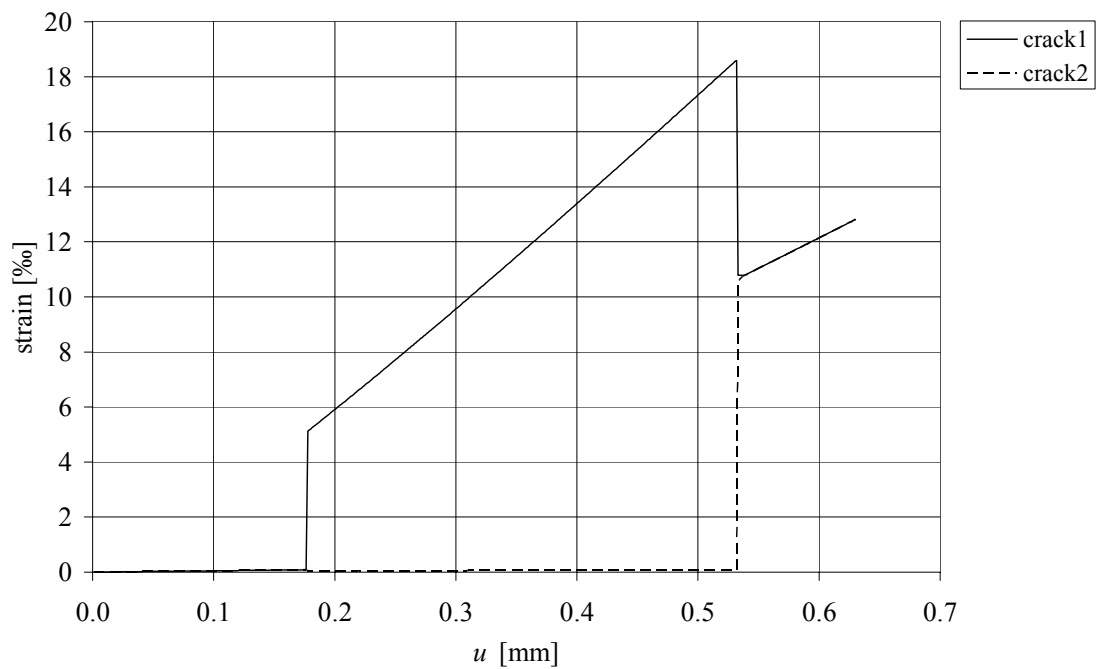


Figure F.7 Strain in cracks, for A1.

F.1.2 A2

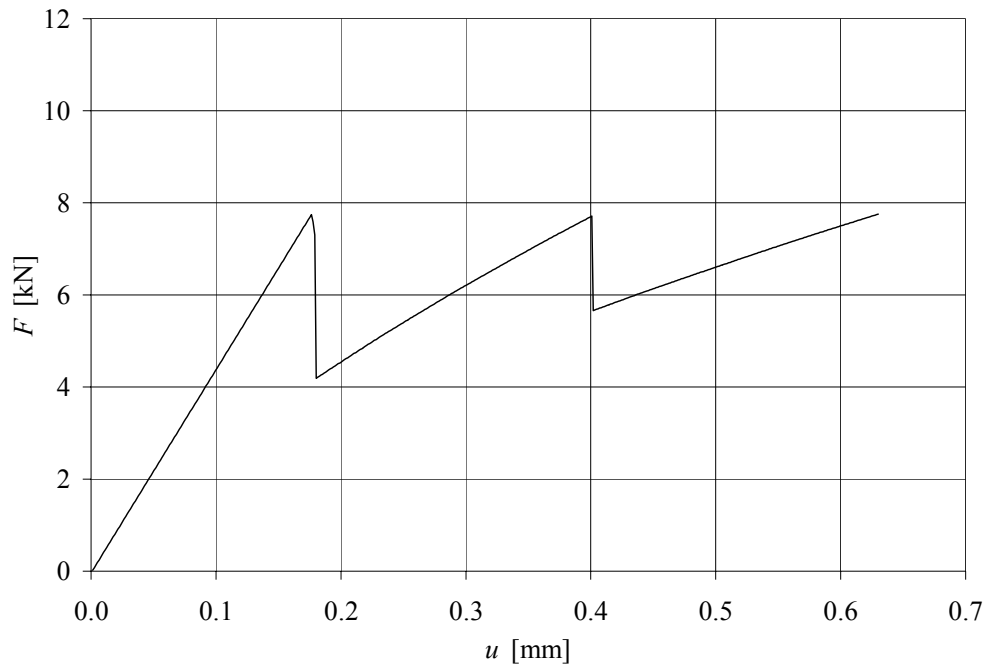


Figure F.8 Global response for A2.

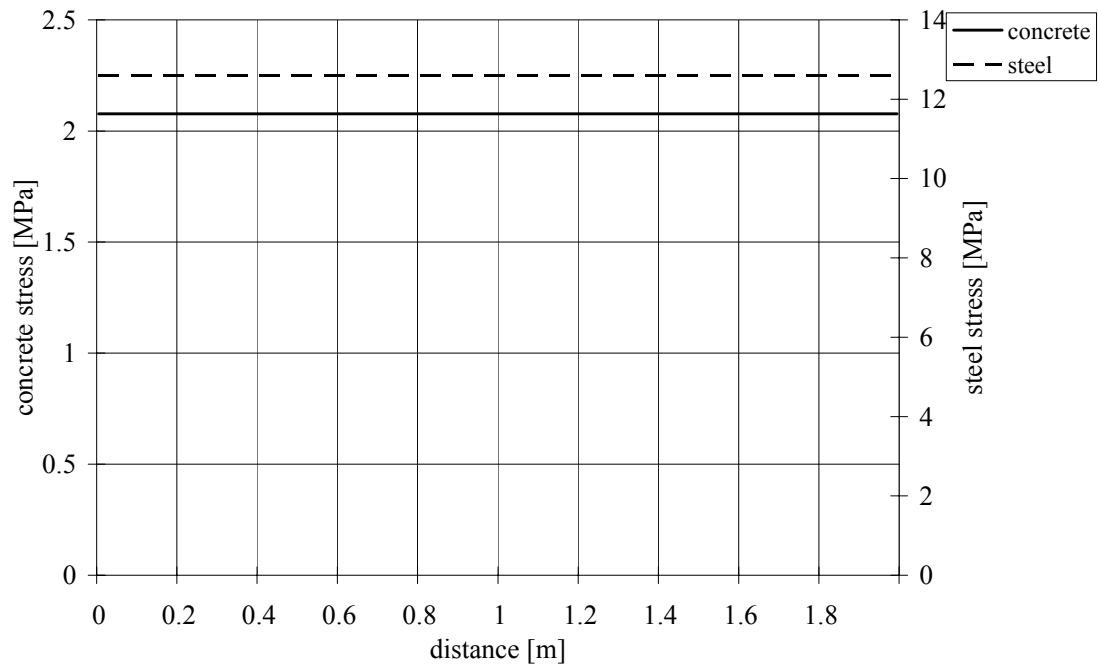


Figure F.9 Concrete stress and steel stress at an imposed end displacement = 0.126 mm, for A2.

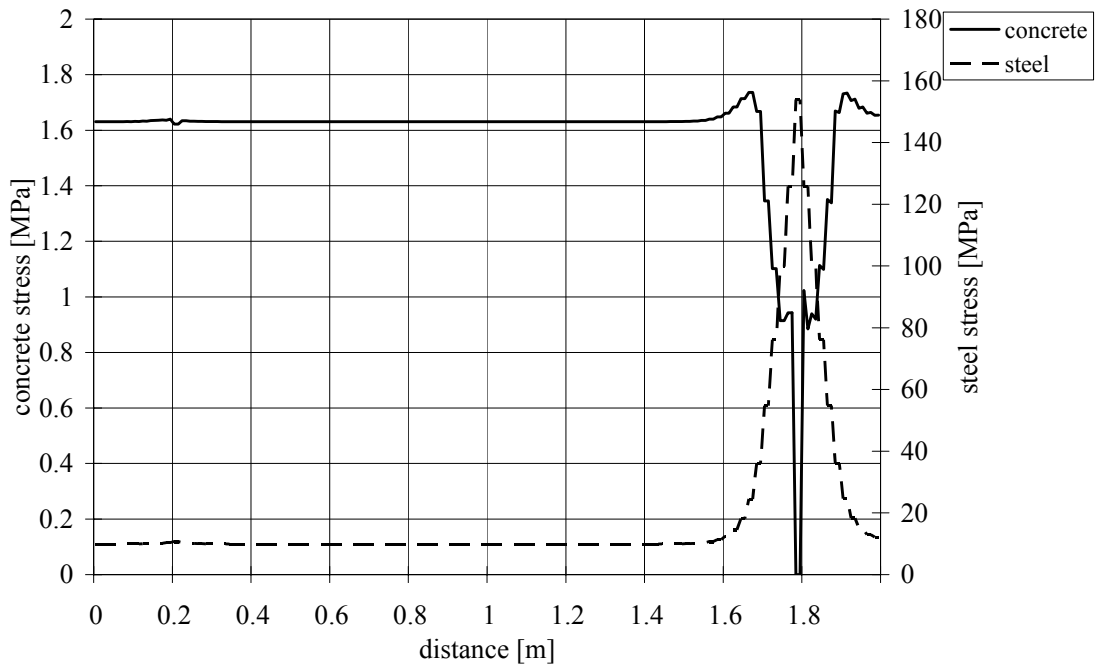


Figure F.10 Concrete stress and steel stress at an imposed end displacement = 0.189 mm, for A2.

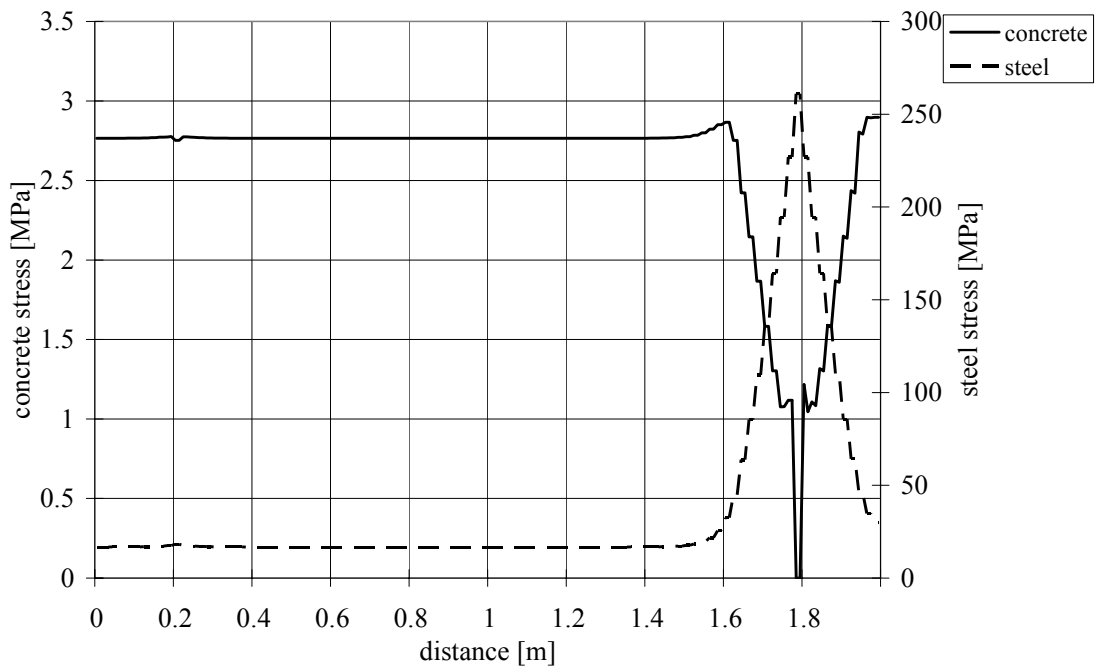


Figure F.11 Concrete stress and steel stress at an imposed end displacement = 0.378 mm, for A2.

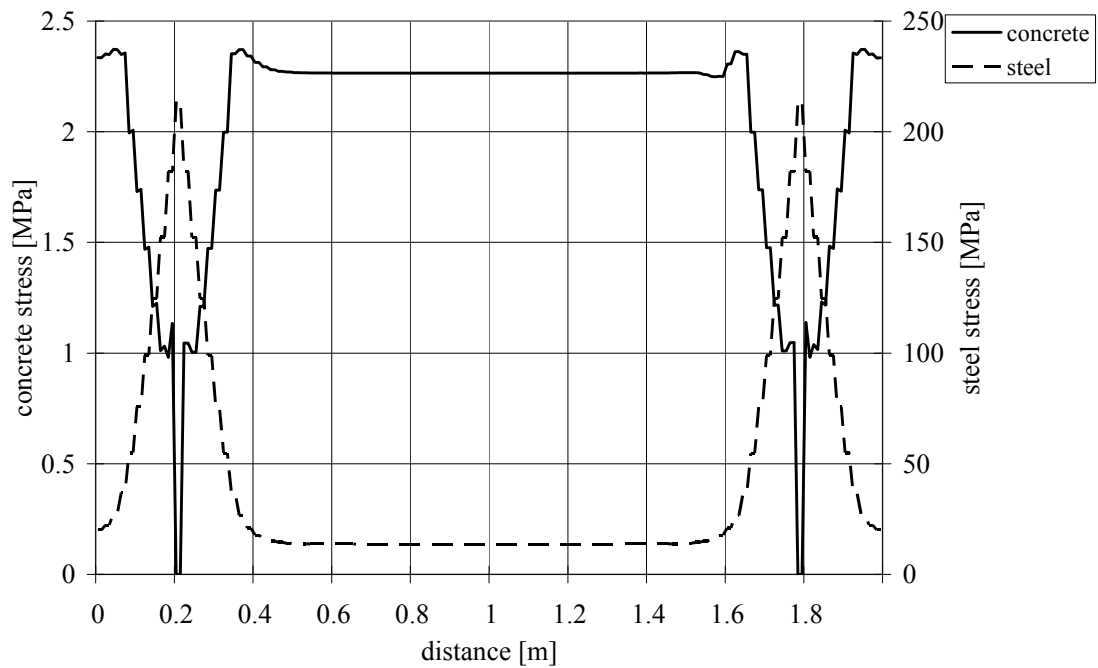


Figure F.12 Concrete stress and steel stress at an imposed end displacement = 0.441 mm, for A2.

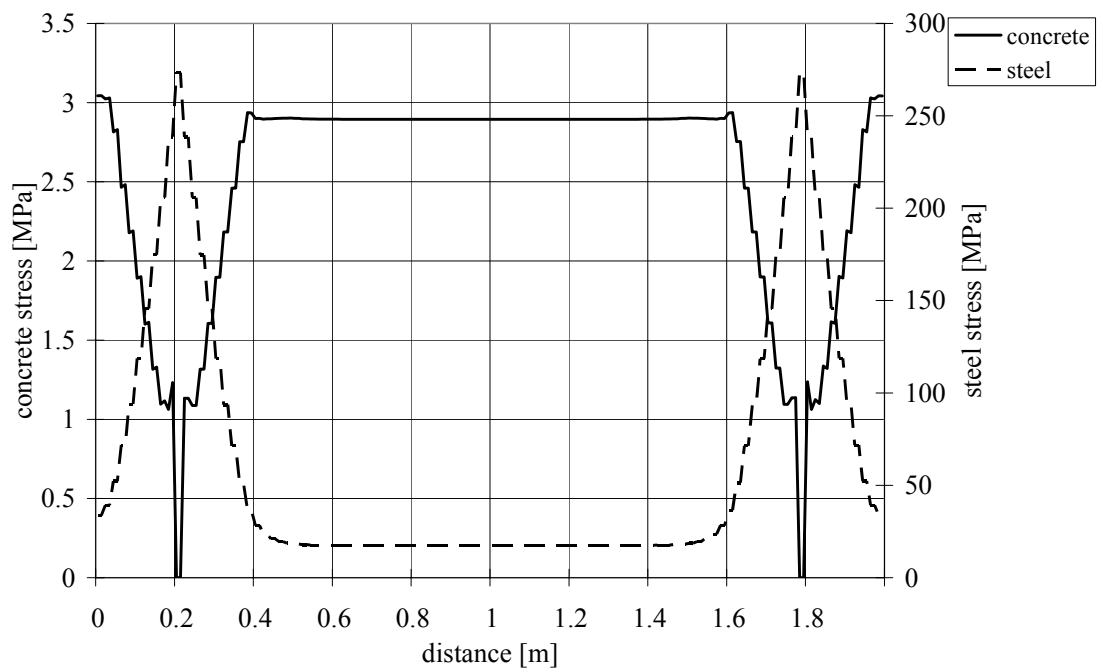


Figure F.13 Concrete stress and steel stress at an imposed end displacement = 0.630 mm, for A2.

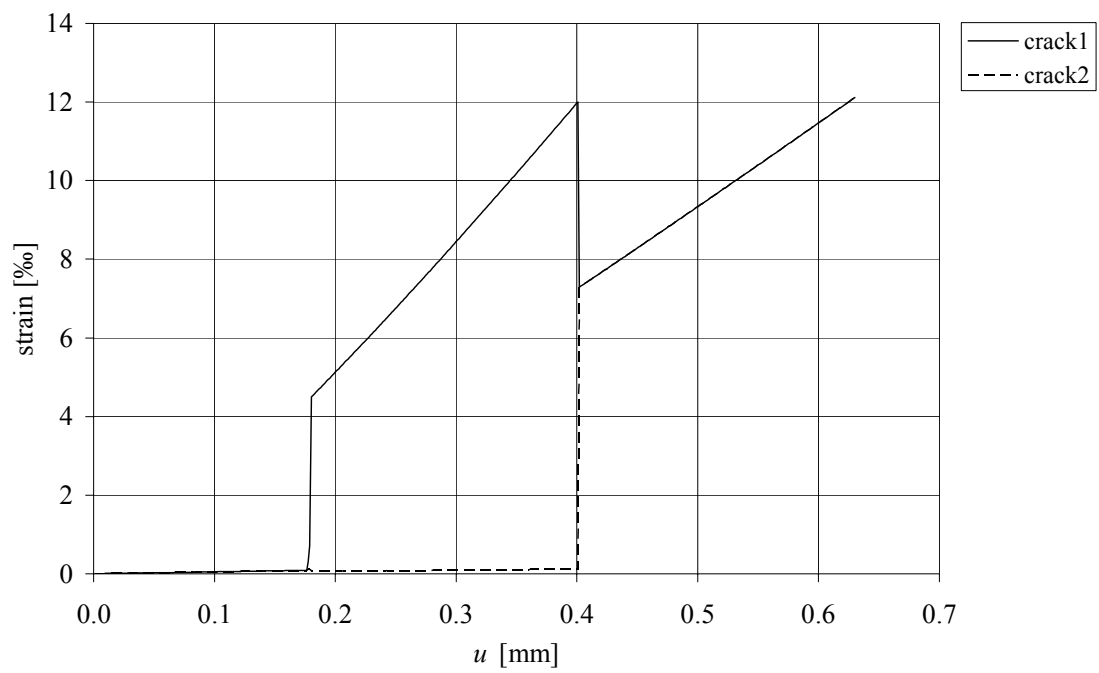


Figure F.14 Strain in cracks for A2.

F.1.3 A3

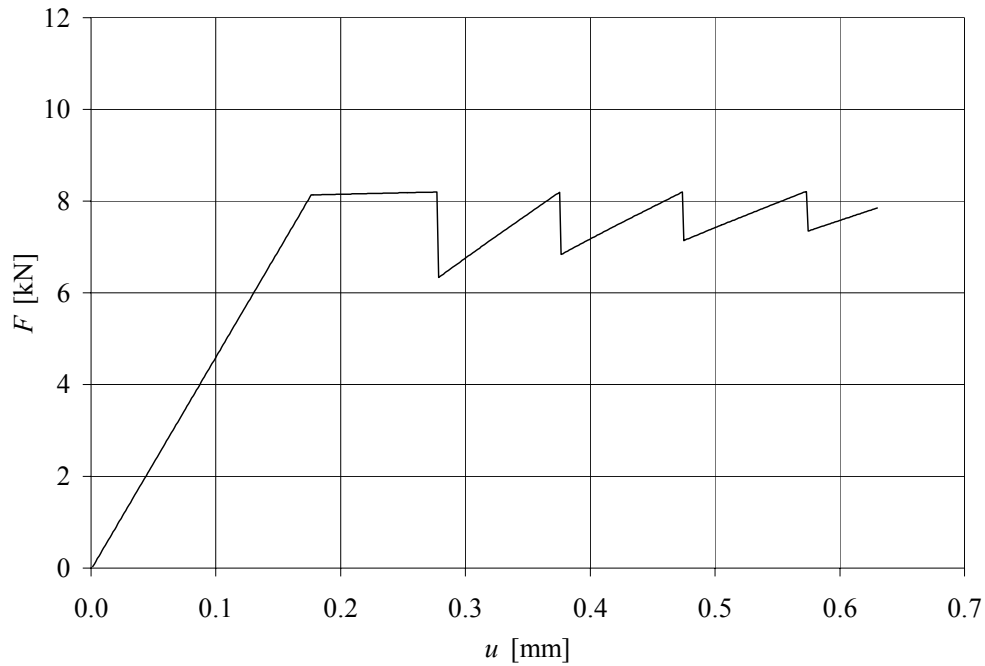


Figure F.15 Global response for A3.

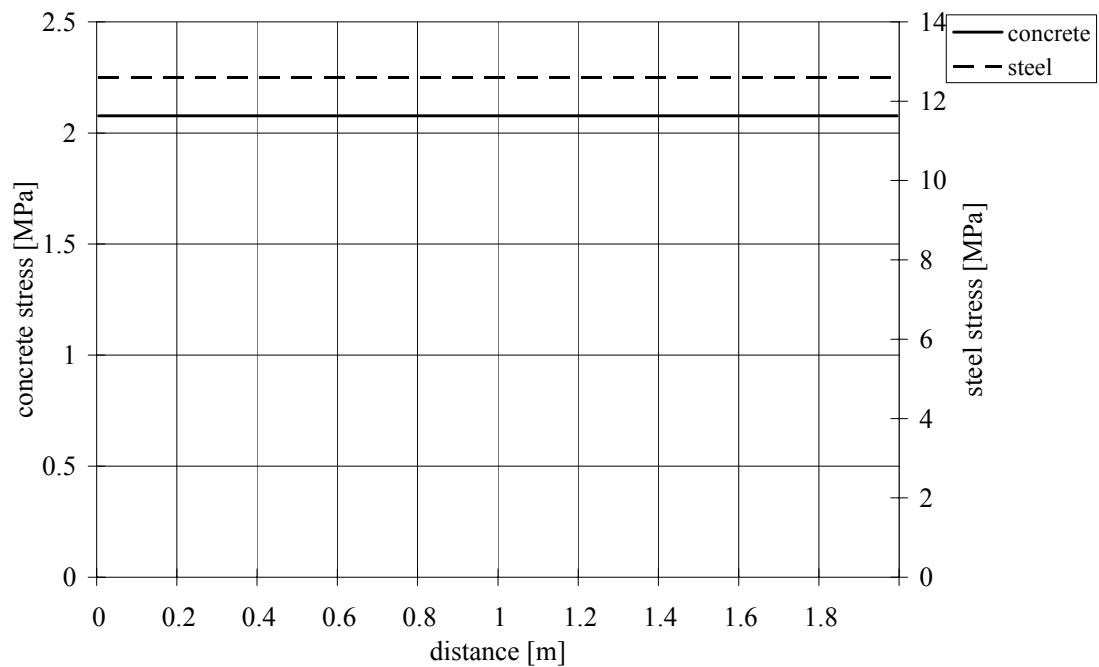


Figure F.16 Concrete stress and steel stress at an imposed end displacement = 0.126 mm, for A3.

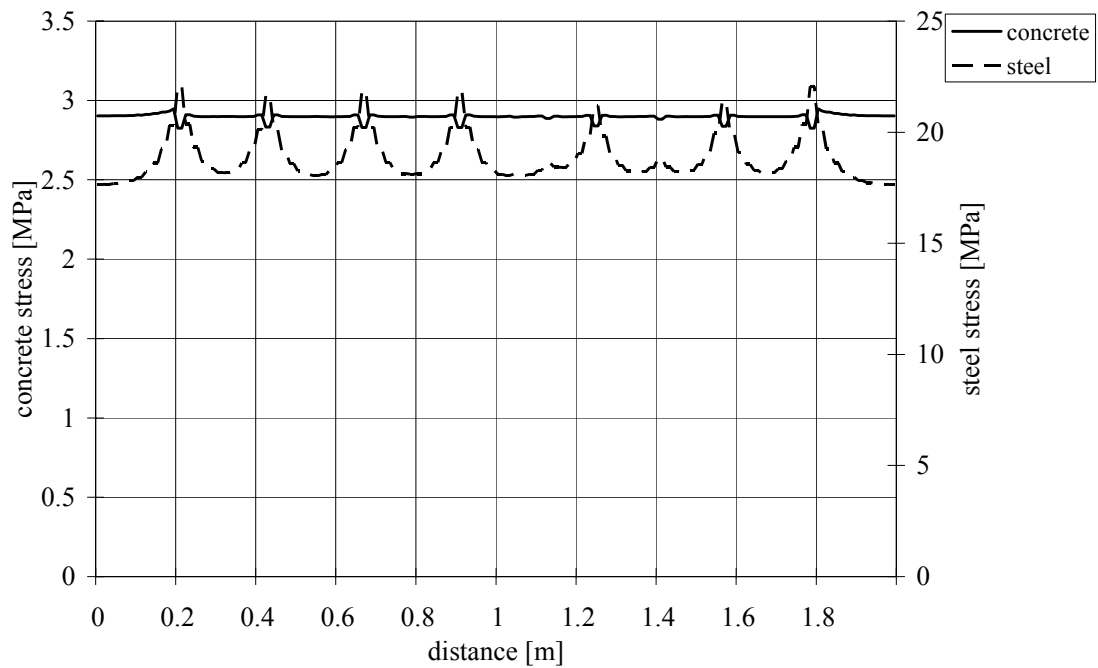


Figure F.17 Concrete stress and steel stress at an imposed end displacement = 0.189 mm, for A3.

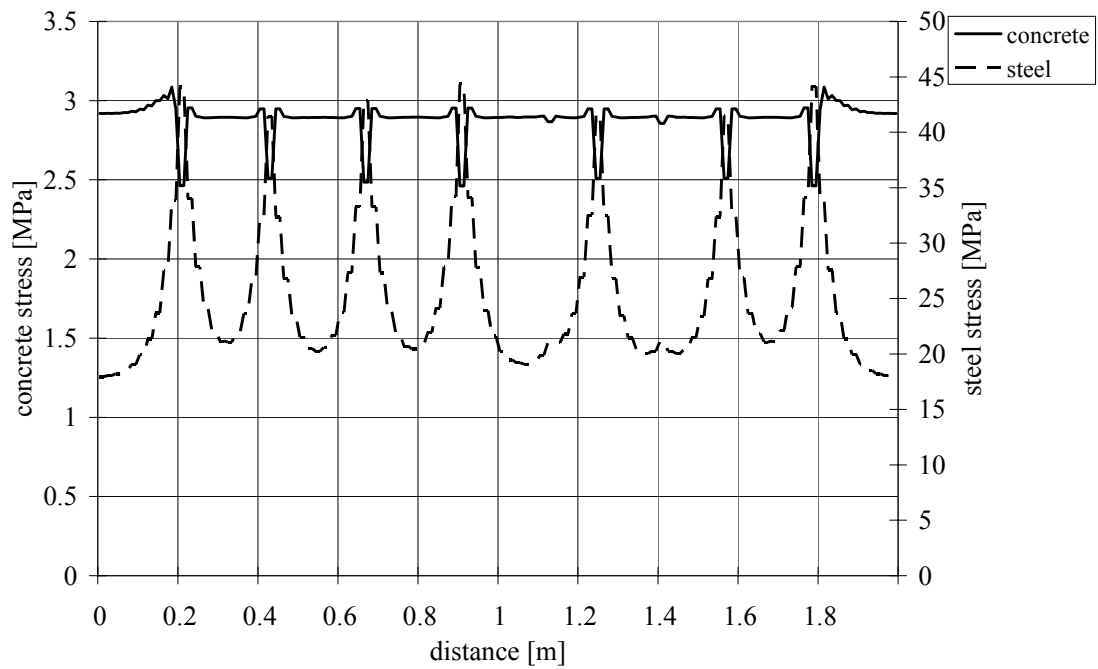


Figure F.18 Concrete stress and steel stress at an imposed end displacement = 0.252 mm, for A3.

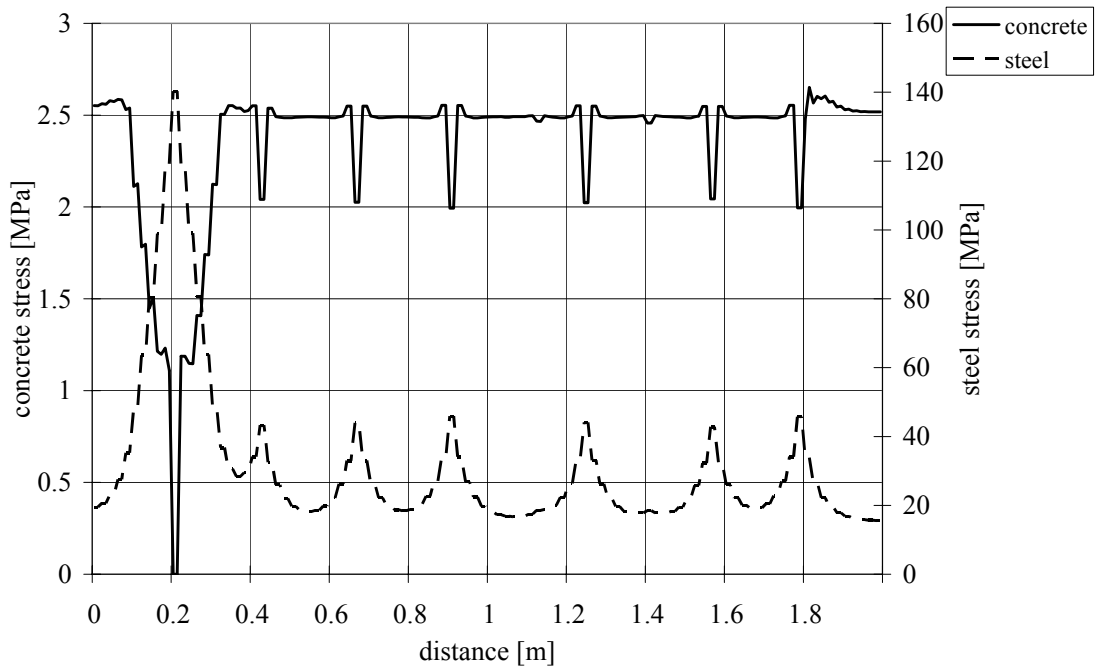


Figure F.19 Concrete stress and steel stress at an imposed end displacement = 0.315 mm, for A3.

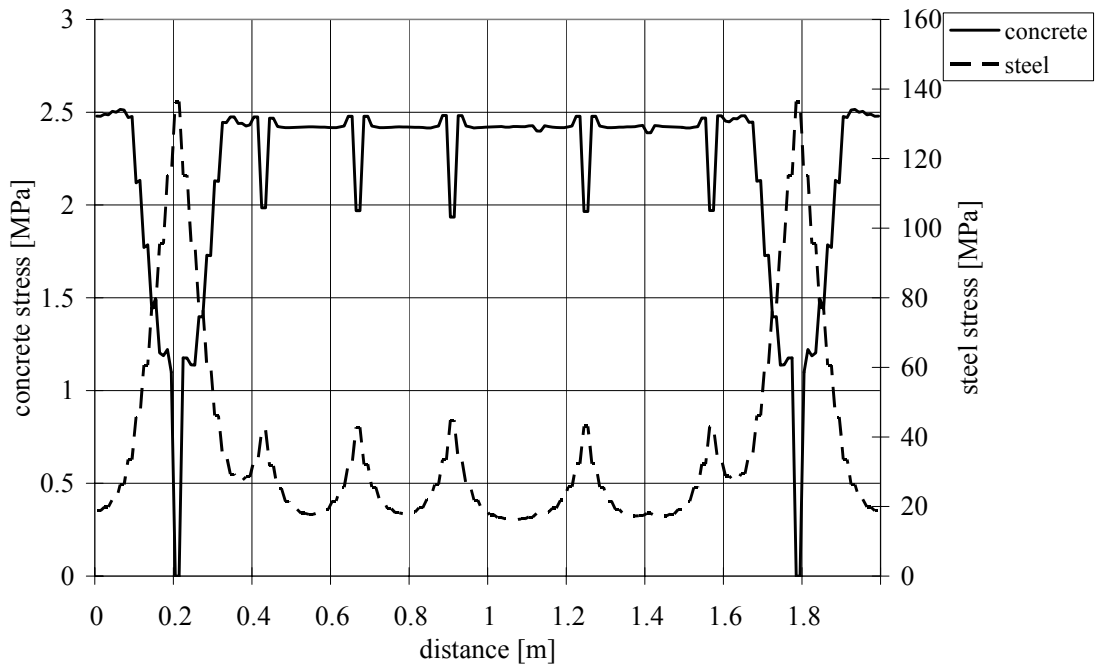


Figure F.20 Concrete stress and steel stress at an imposed end displacement = 0.378 mm, for A3.

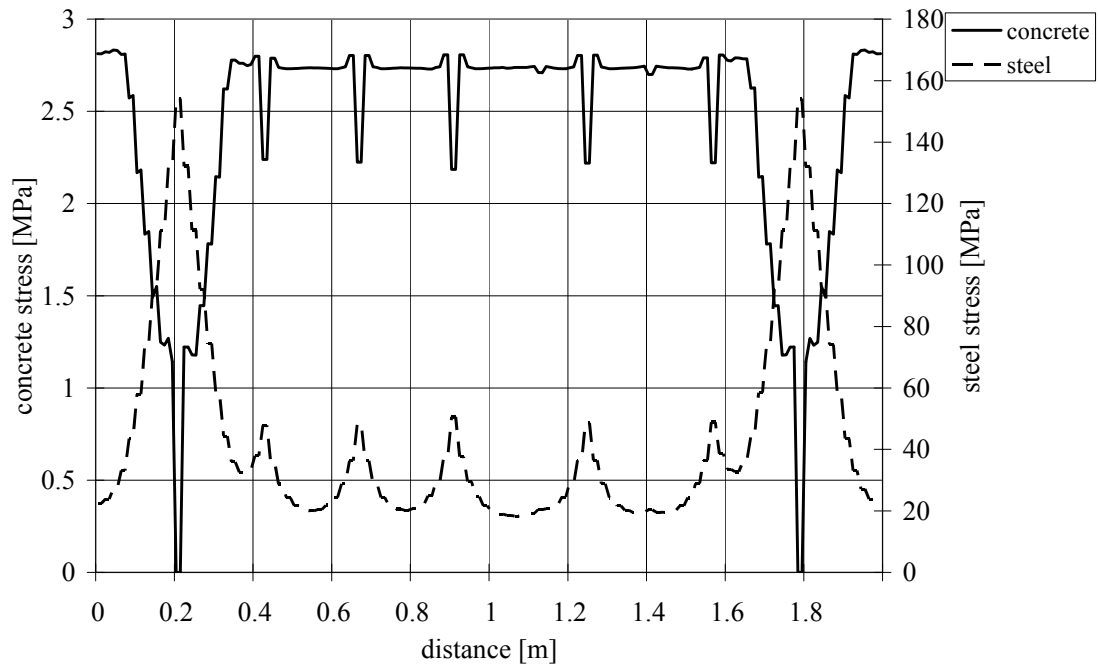


Figure F.21 Concrete stress and steel stress at an imposed end displacement = 0.441 mm, for A3.

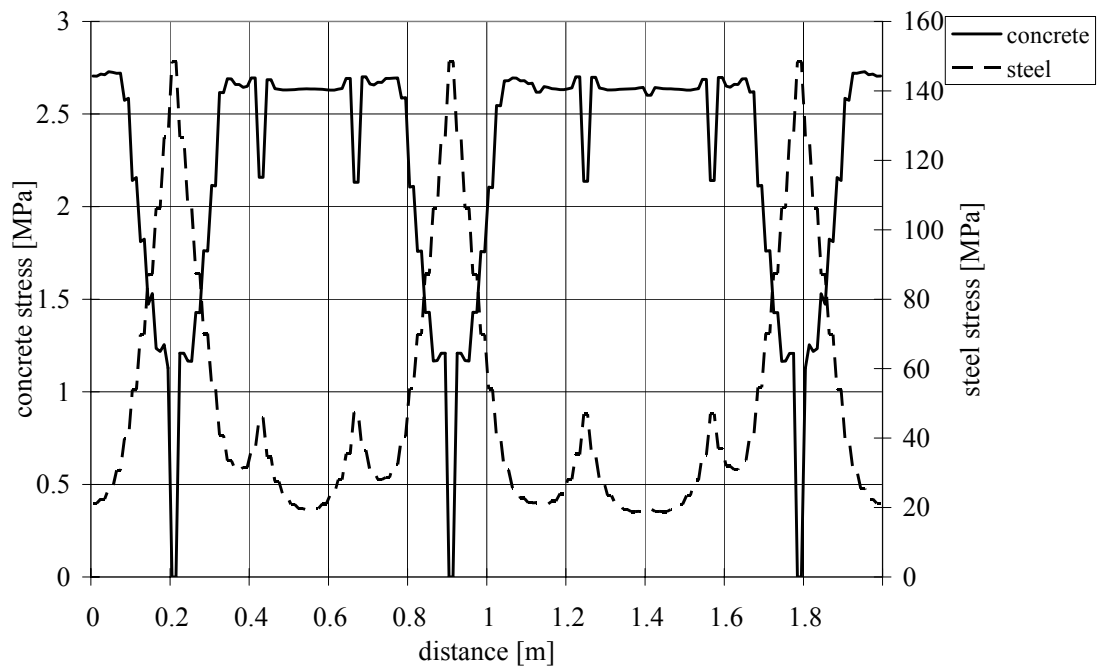


Figure F.22 Concrete stress and steel stress at an imposed end displacement = 0.504 mm, for A3.

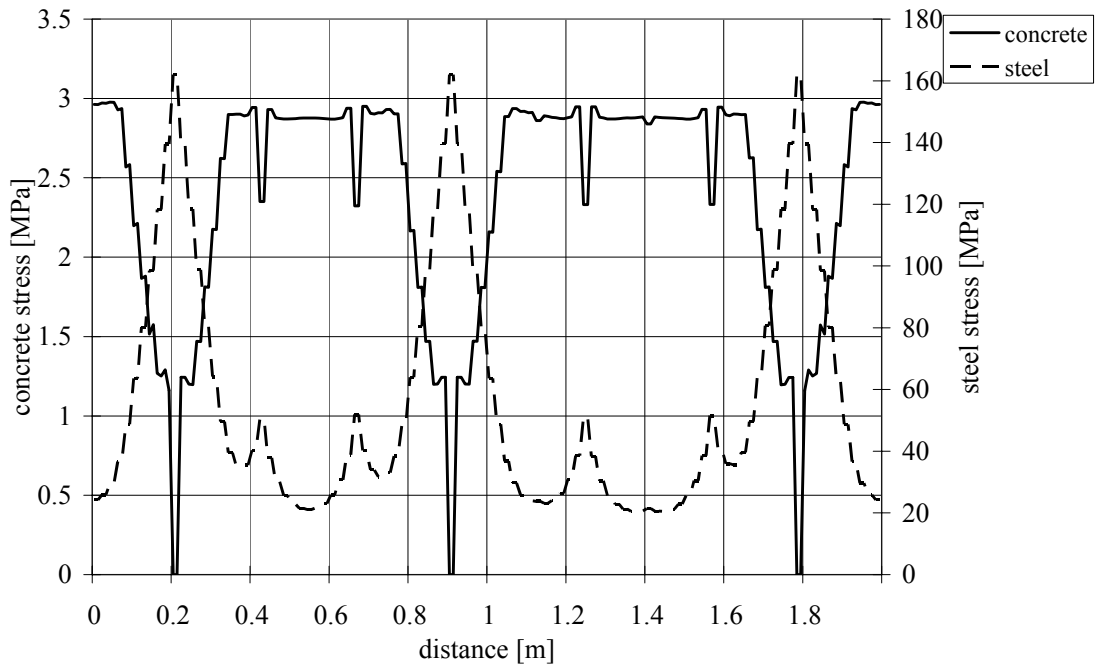


Figure F.23 Concrete stress and steel stress at an imposed end displacement = 0.567 mm, for A3.

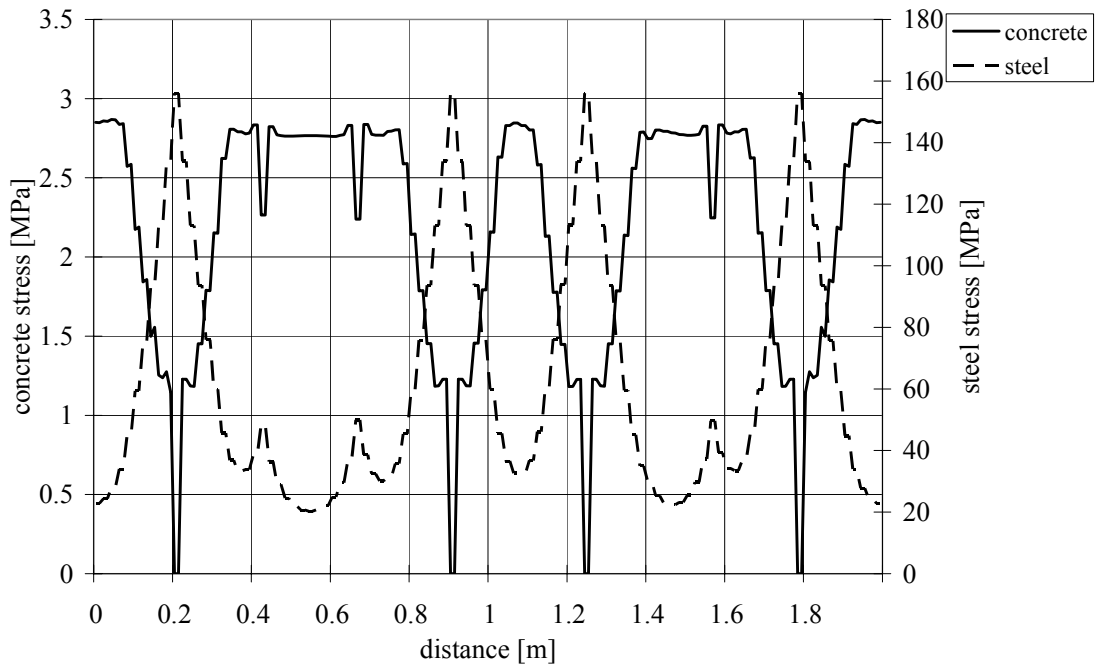


Figure F.24 Concrete stress and steel stress at an imposed end displacement = 0.630 mm, for A3.

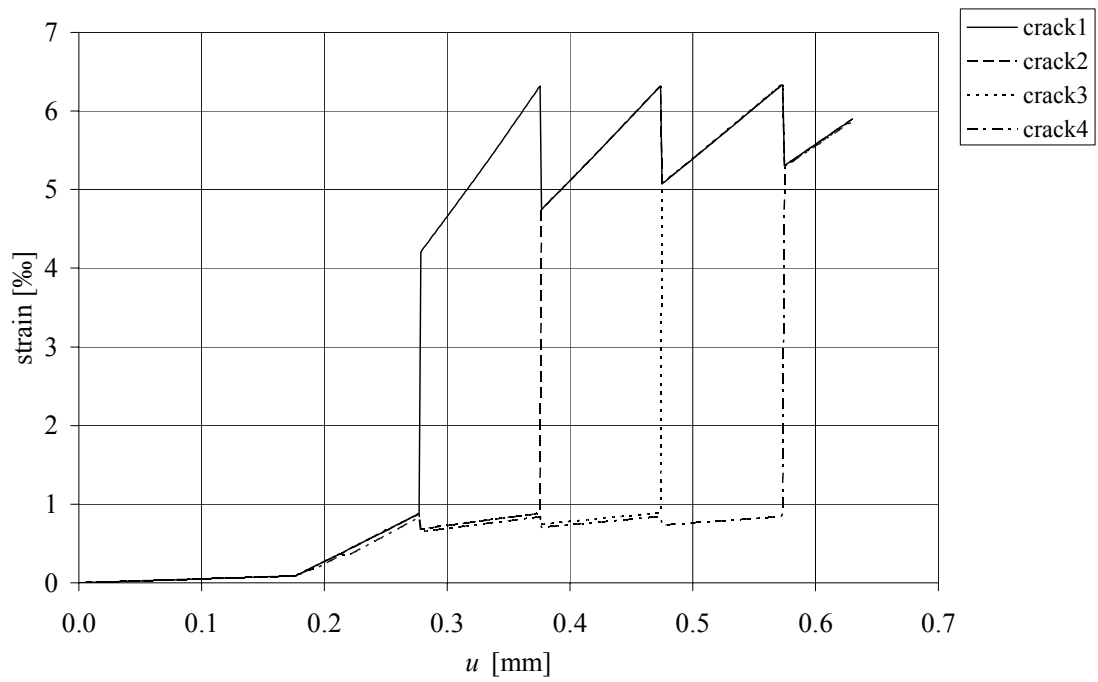


Figure F.25 Strain in cracks for A3.

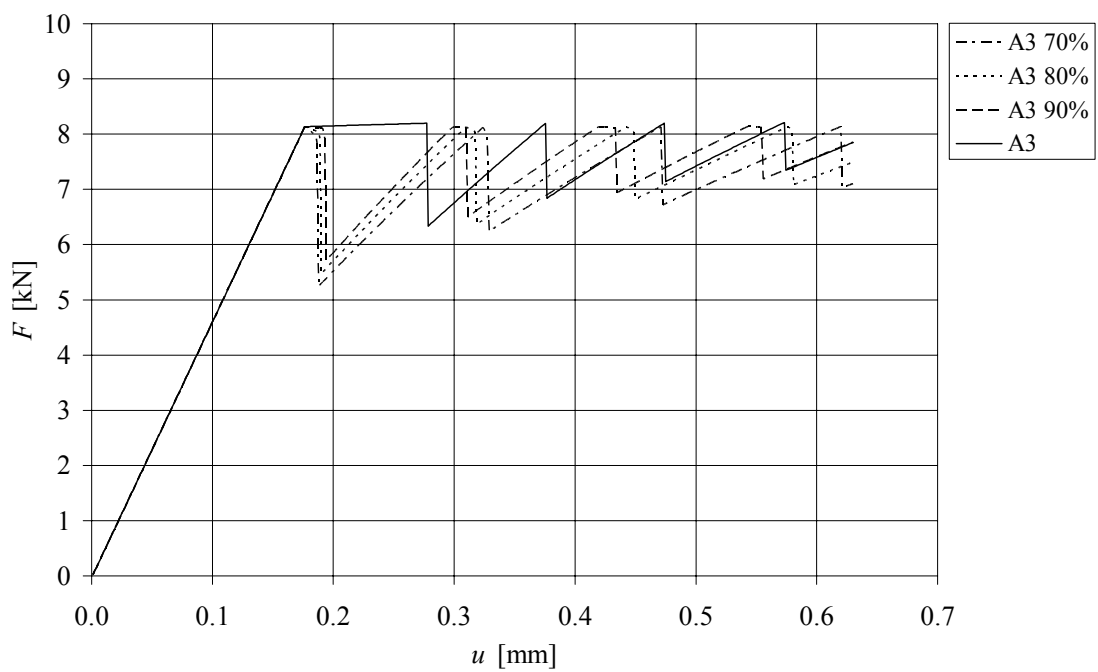


Figure F.26 Results from various bond relations.

F.1.4 A4

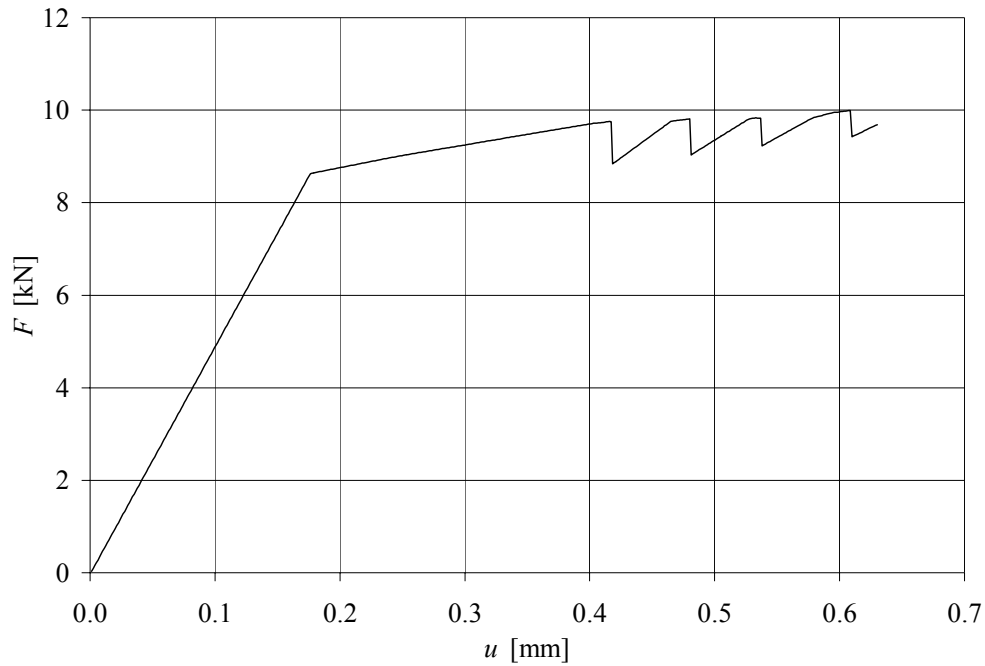


Figure F.27 Global response for A4.

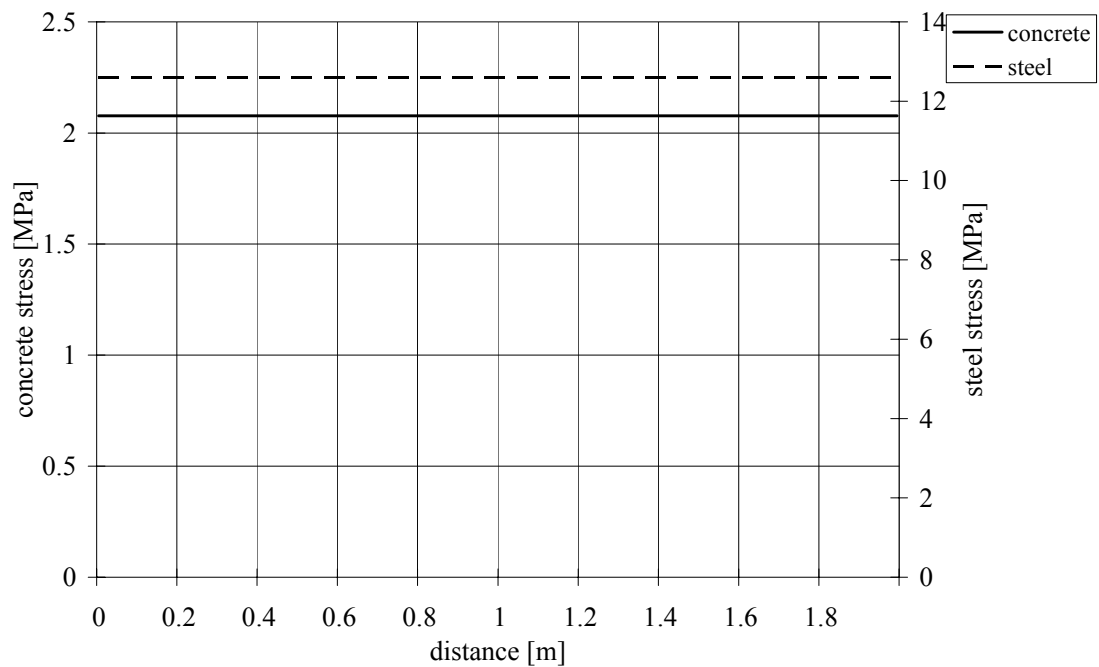


Figure F.28 Concrete stress and steel stress at an imposed end displacement = 0.126 mm, for A4.

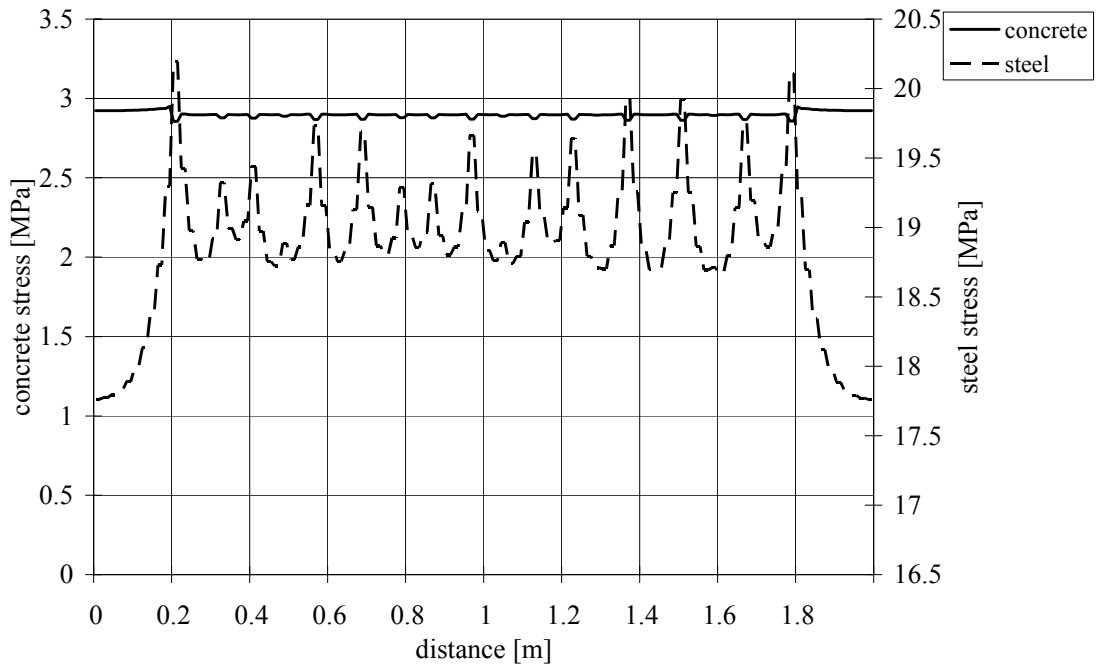


Figure F.29 Concrete stress and steel stress at an imposed end displacement = 0.189 mm, for A4.

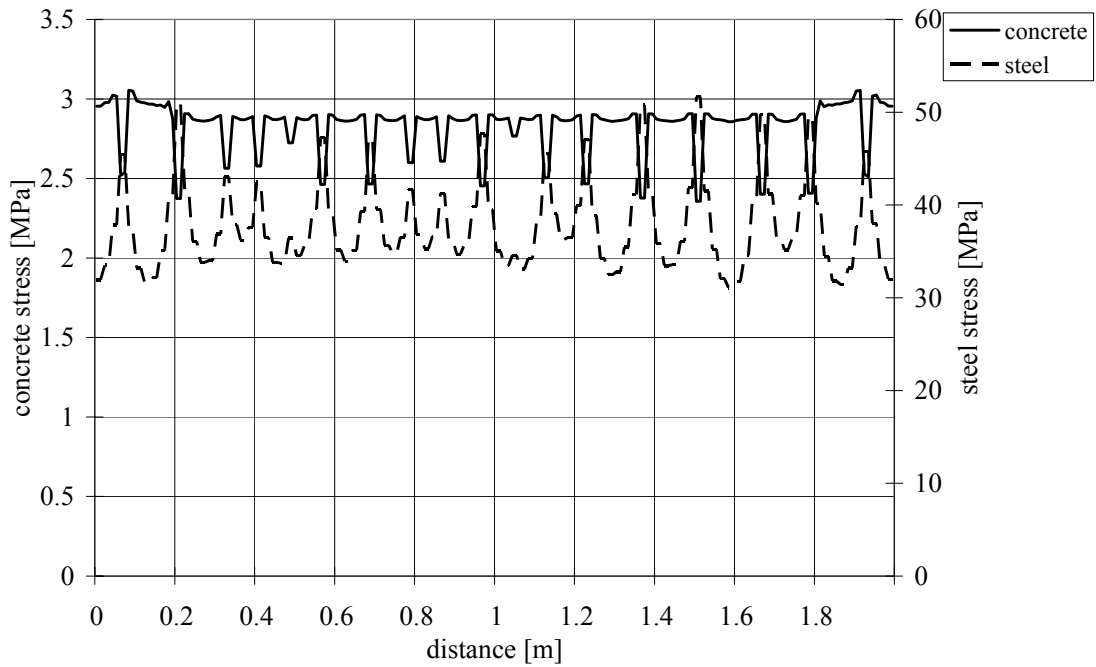


Figure F.30 Concrete stress and steel stress at an imposed end displacement = 0.378 mm, for A4.

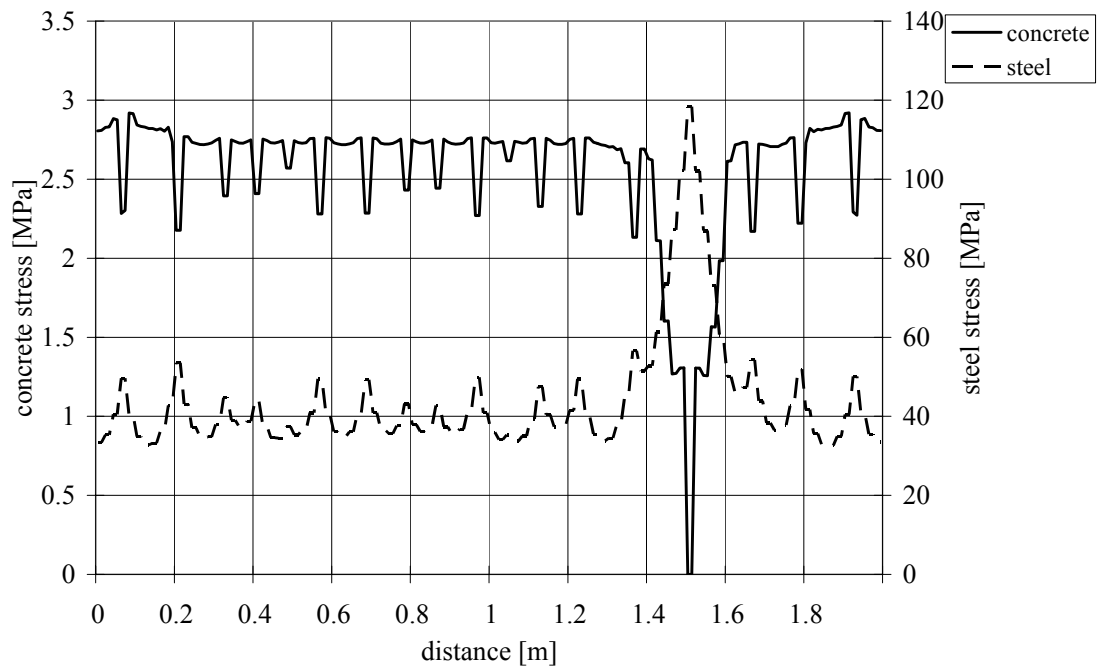


Figure F.31 Concrete stress and steel stress at an imposed end displacement = 0.441 mm, for A4.

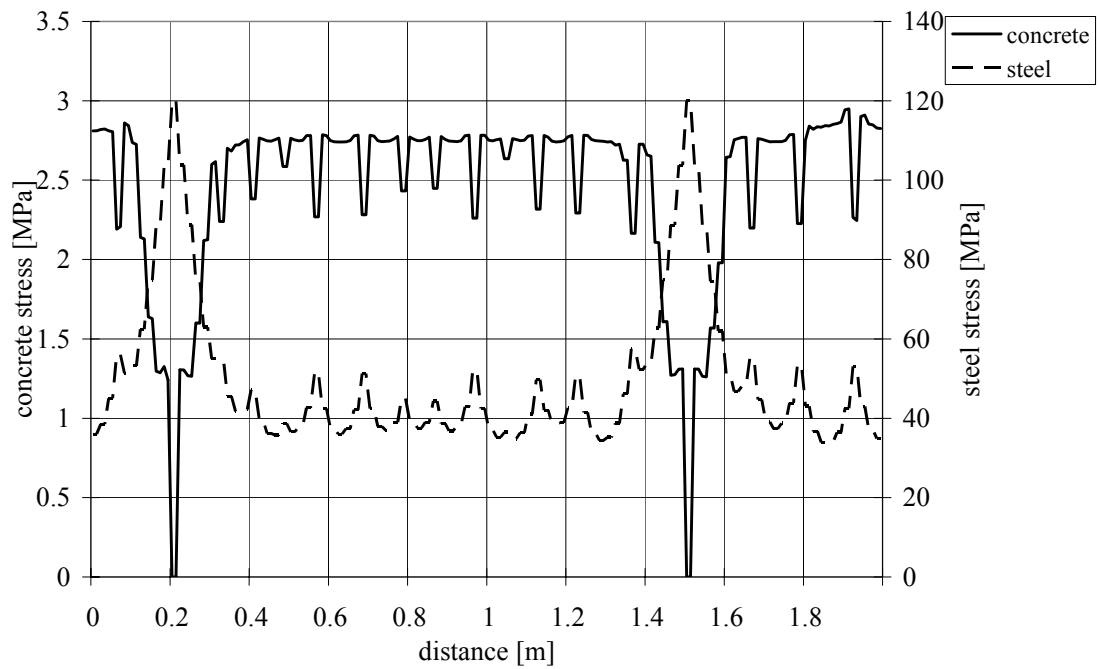


Figure F.32 Concrete stress and steel stress at an imposed end displacement = 0.504 mm, for A4.

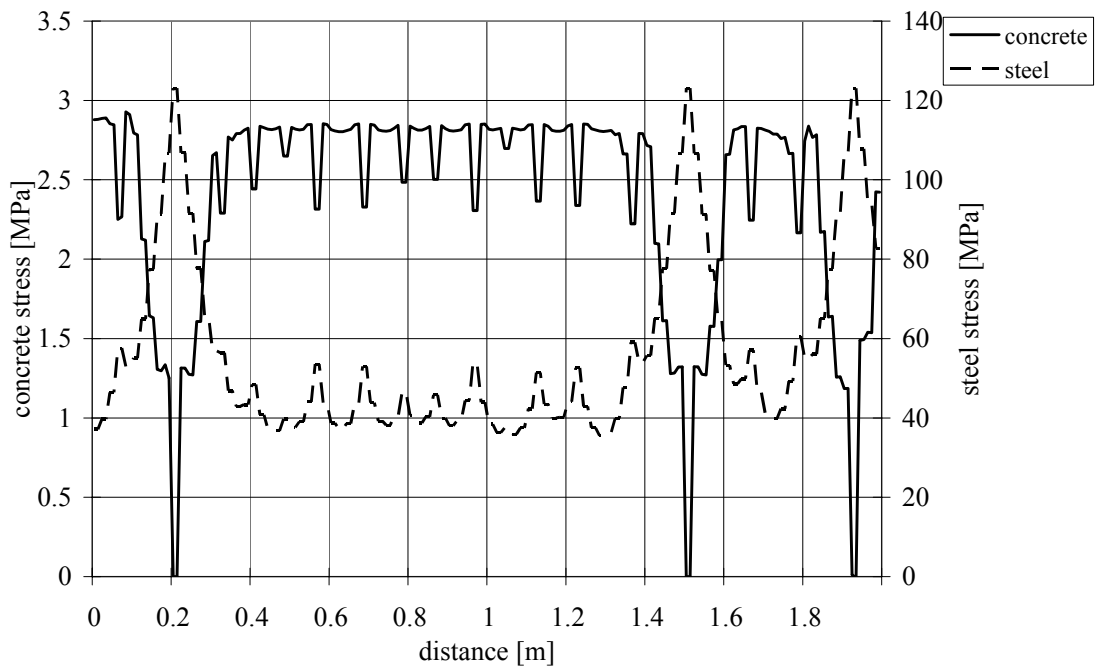


Figure F.33 Concrete stress and steel stress at an imposed end displacement = 0.567 mm, for A4.

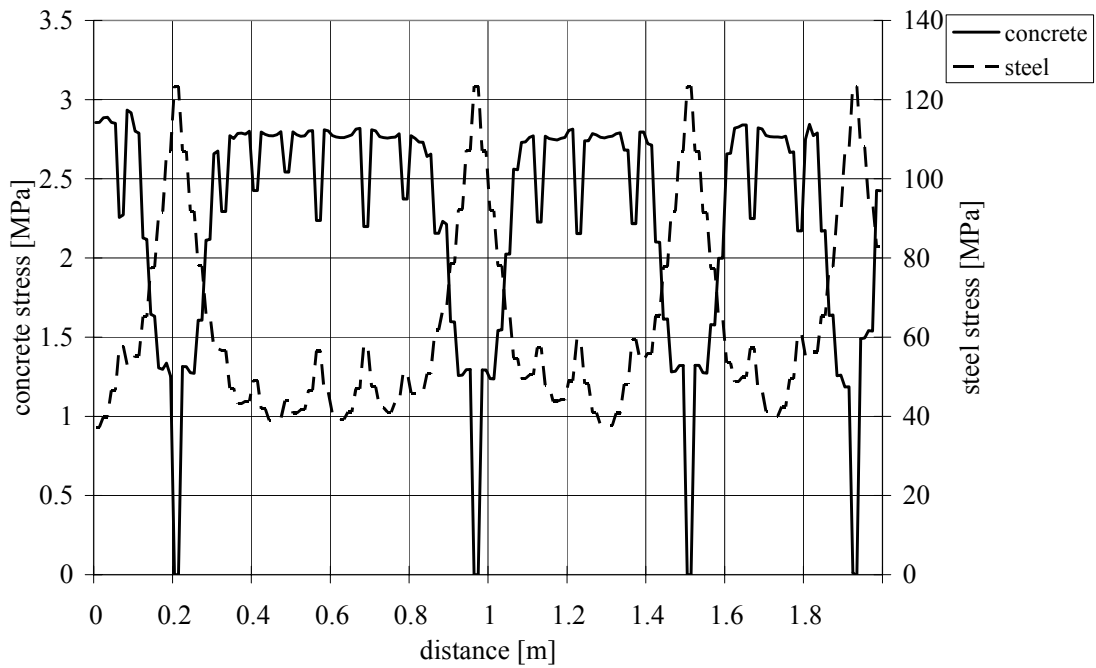


Figure F.34 Concrete stress and steel stress at an imposed end displacement = 0.630 mm, for A4.

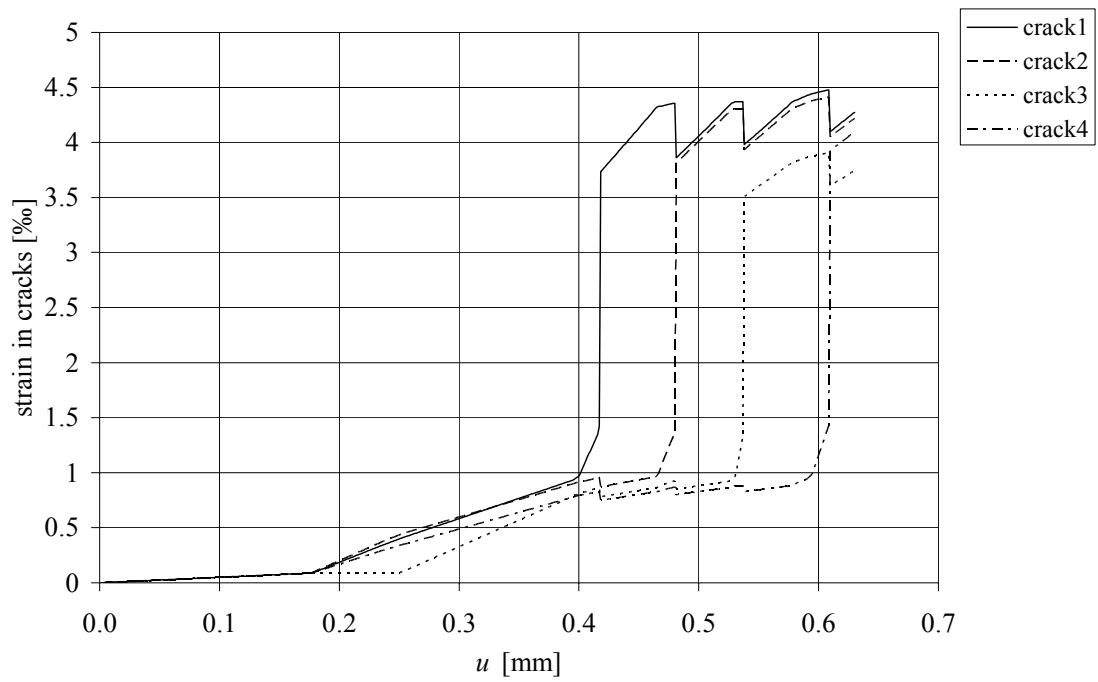


Figure F.35 Strain in cracks for A4.

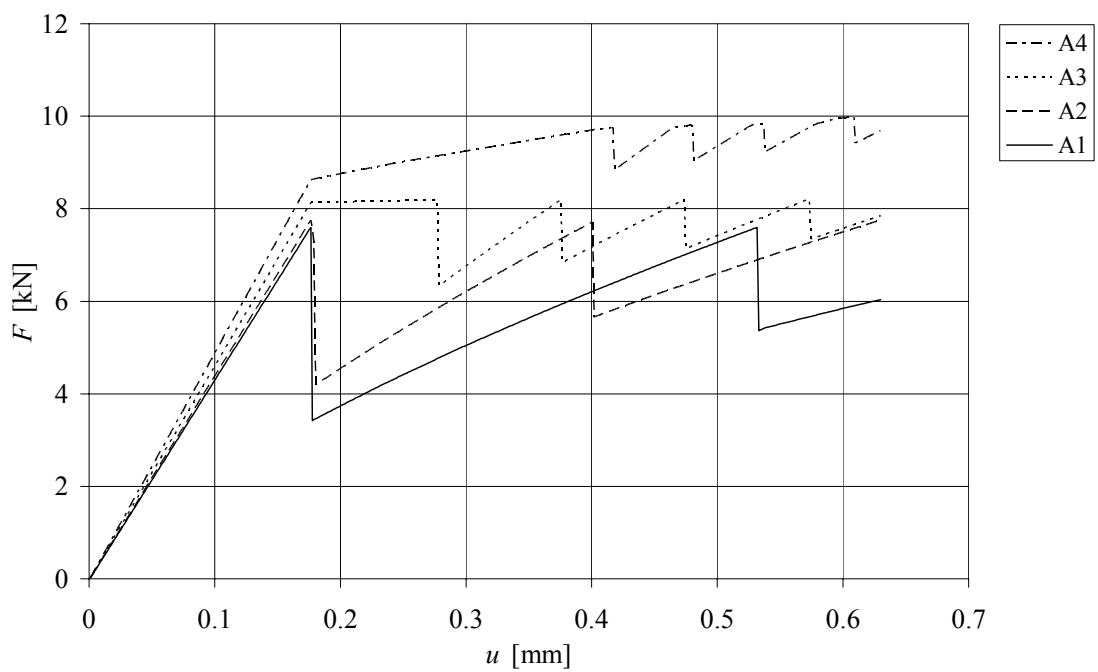


Figure F.36 Global response due to displacement for various bar diameter.

F.1.5 Points of more interest

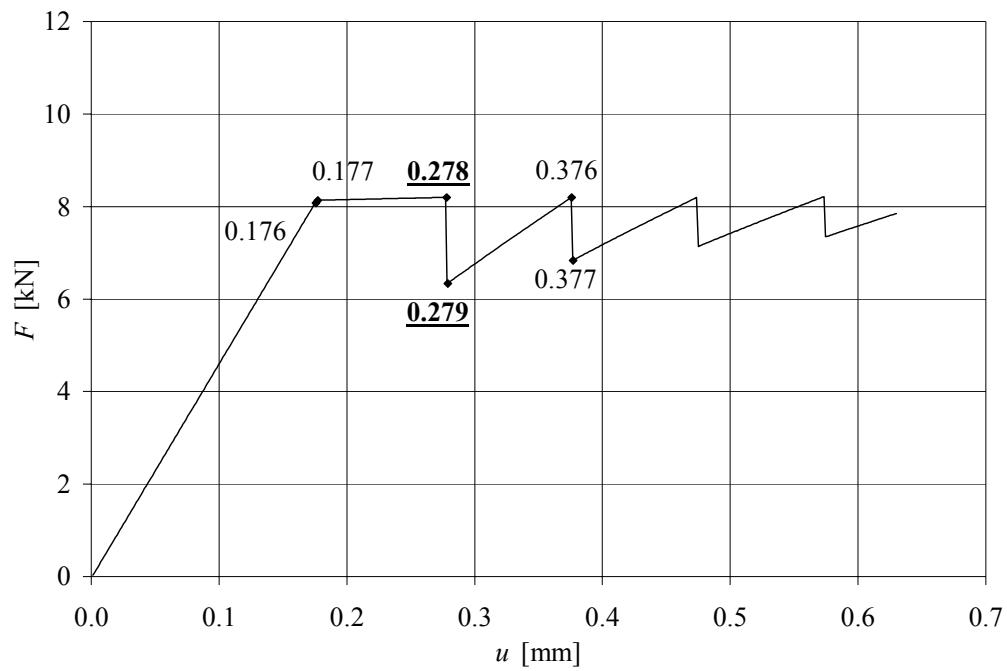


Figure F.37 Six different points from where results will be presented.

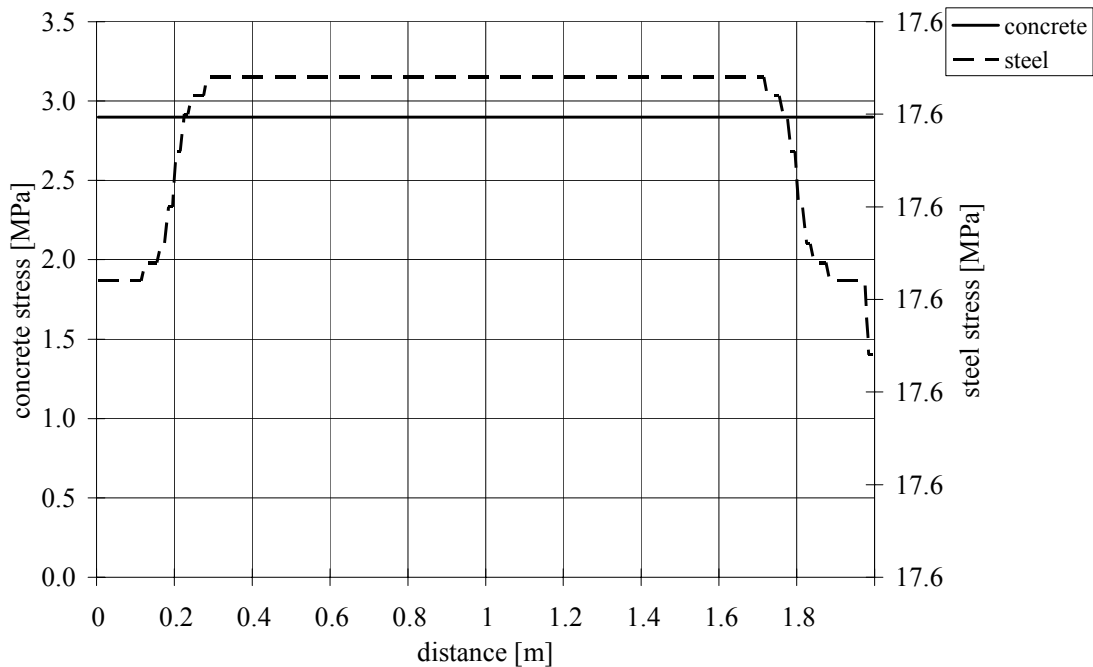


Figure F.38 Stress distribution at an imposed end displacement of 0.176 mm.

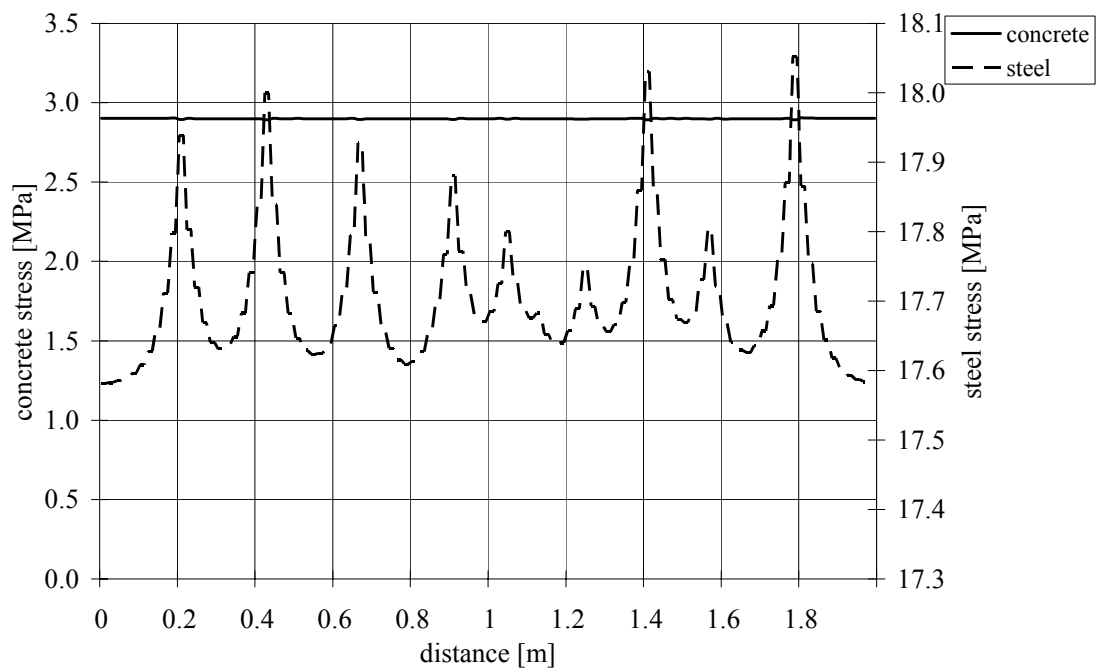


Figure F.39 Stress distribution at an imposed end displacement of 0.177 mm.

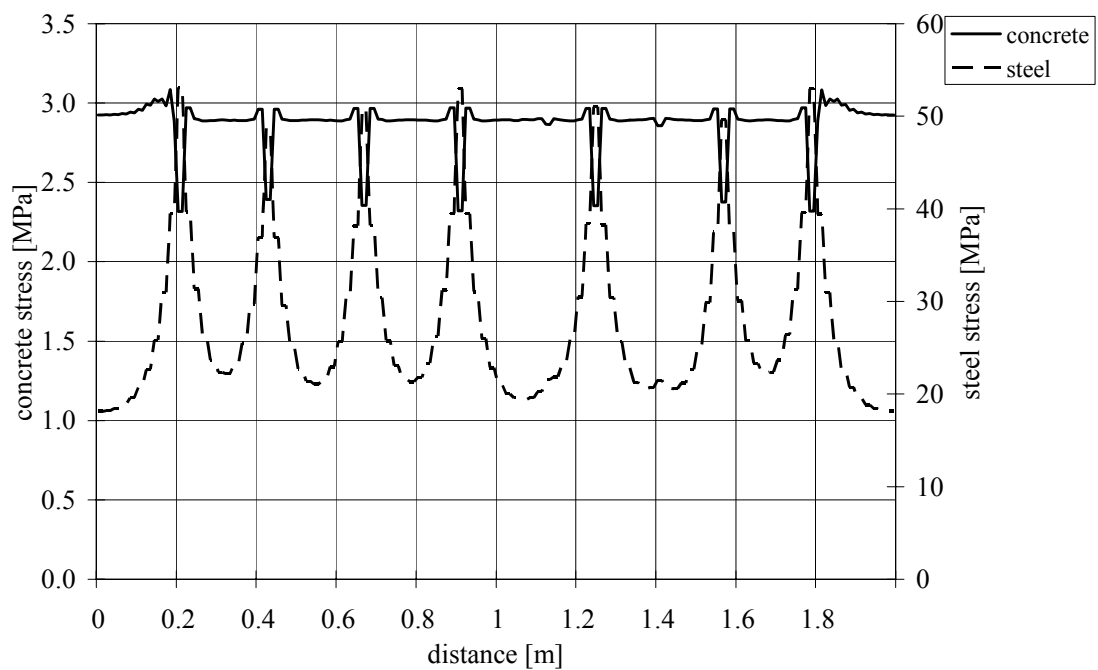


Figure F.40 Stress distribution at an imposed end displacement of 0.278 mm.

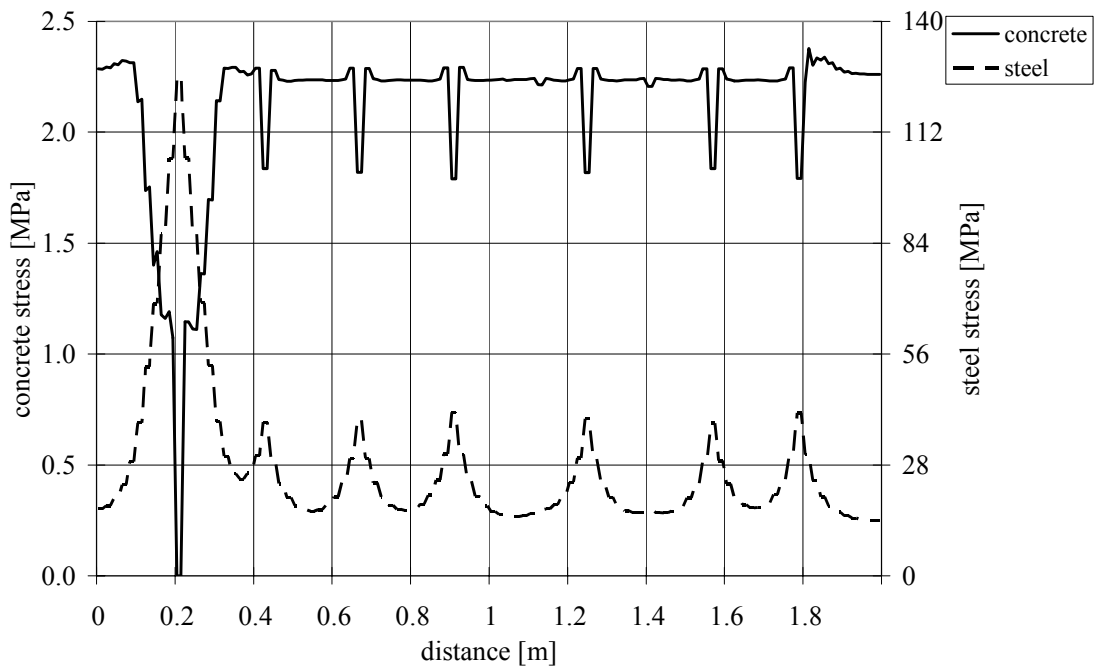


Figure F.41 Stress distribution at an imposed end displacement of 0.279 mm.

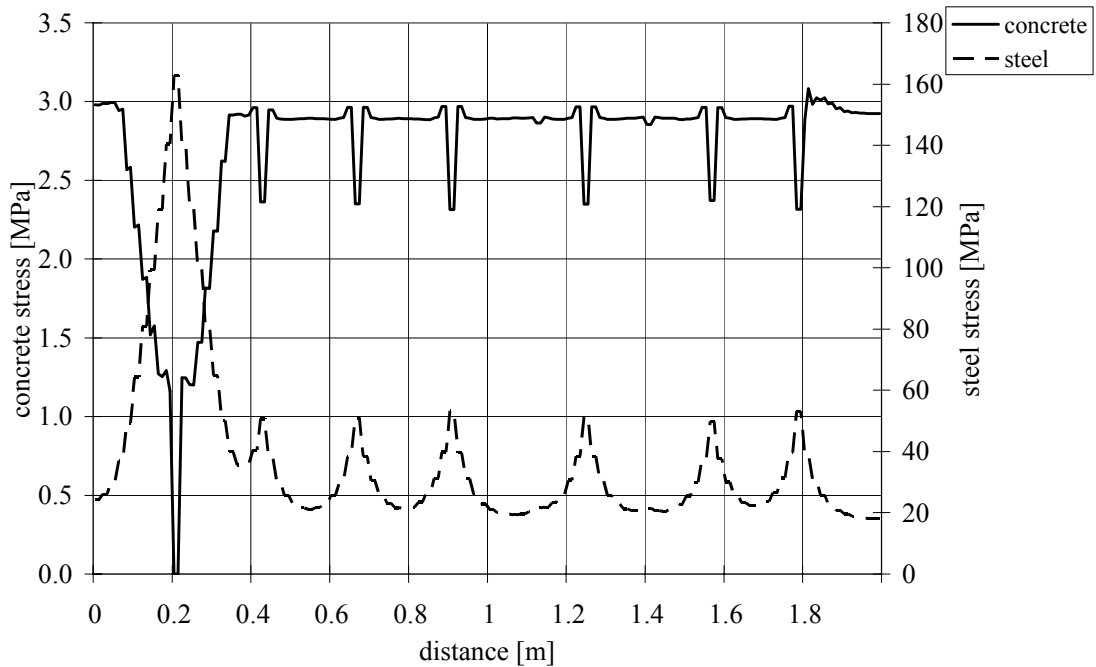


Figure F.42 Stress distribution at an imposed end displacement of 0.376 mm.

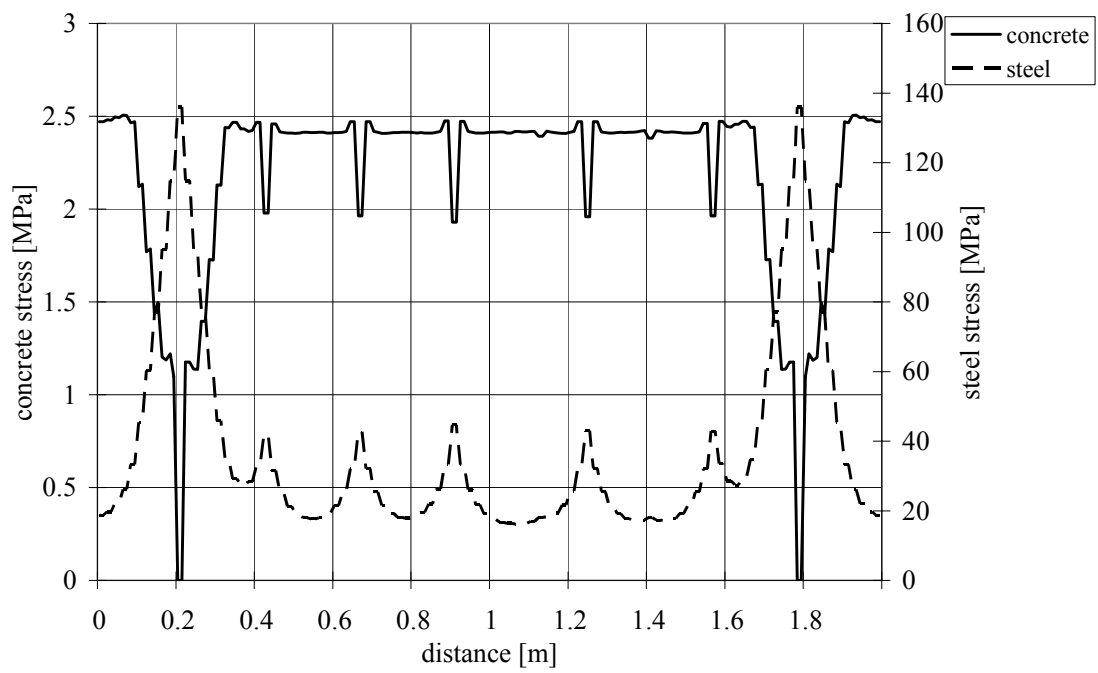


Figure F.43 Stress distribution at an imposed end displacement of 0.377 mm.

F.2 Reinforcement ratio

For this second static analysis a constant reinforcement amount of 1.13% have been used. The total length was 2 m and the element length was 20 mm. The notation and variation of the tests are as follows:

Table F.2 Notations of performed comparisons.

notation	bar diameter [mm]	cross section [mm ²]
C1	10	69x100
C2	12	100x100
C3	16	178x100
C4	20	278x100

The thickness has been altered in order to keep the reinforcement amount constant. The height is still 100 mm in this analysis.

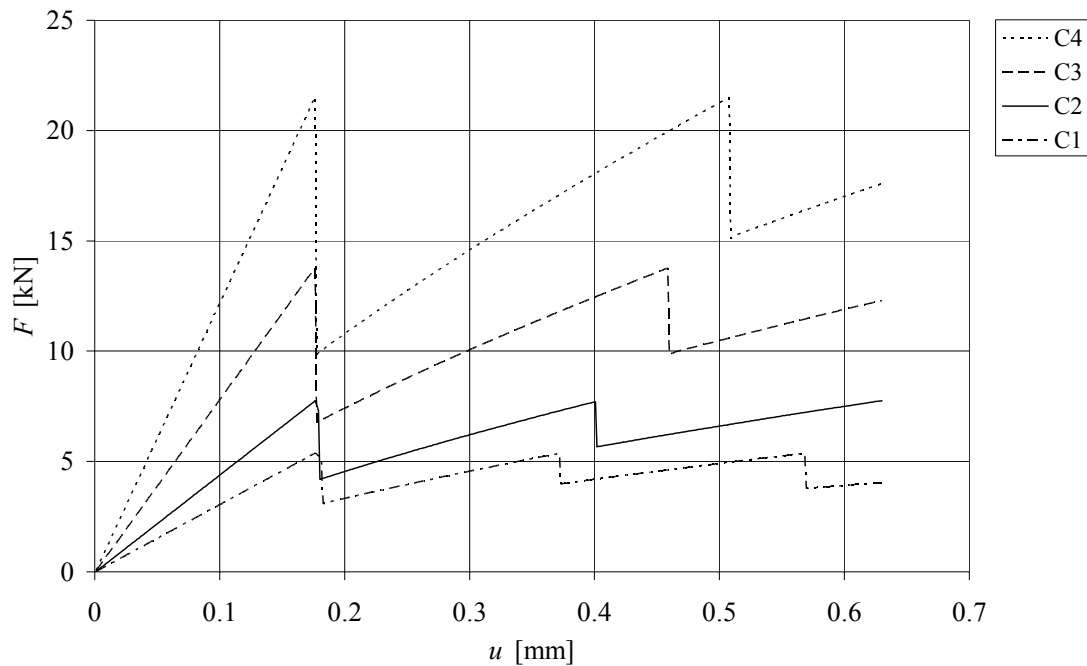


Figure F.44 Sum of reaction force due to displacement for a constant reinforcement amount.

F.3 Comparison MATLAB – ADINA

Table F.3 Notations of performed comparisons between improved analytical method and the FE-model.

notation	ϕ [mm]	software
M1-I	10	MATLAB
A1	10	ADINA
M2-I	12	MATLAB
A2	12	ADINA
M3-I	16	MATLAB
A3	16	ADINA
M4-I	20	MATLAB
A4	20	ADINA

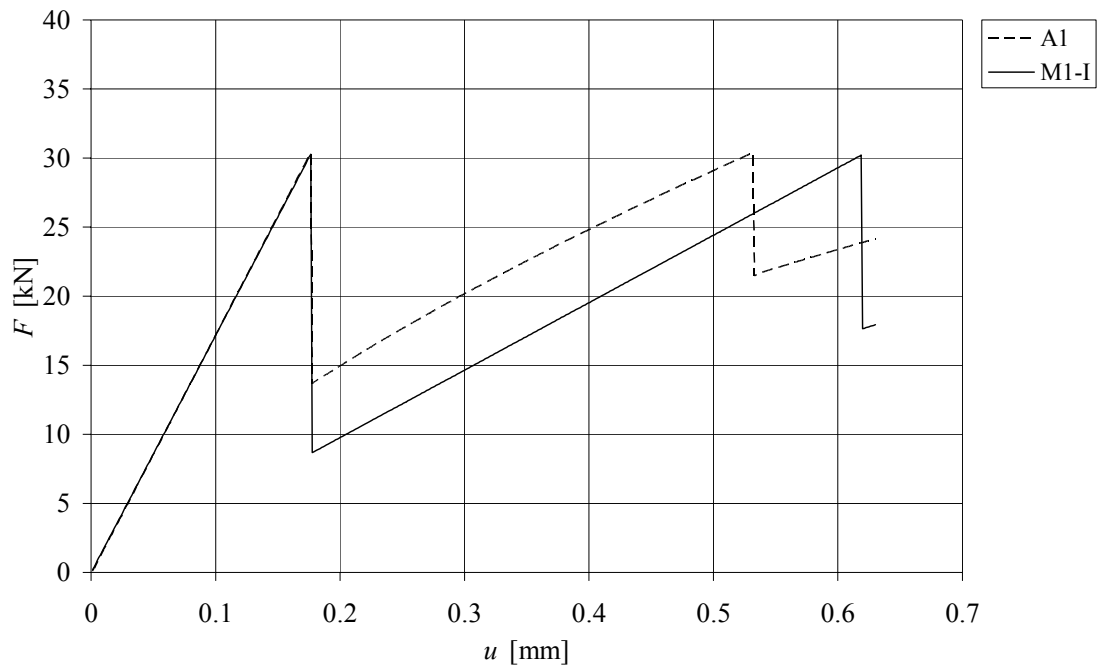


Figure F.45 For ϕ 10 mm.

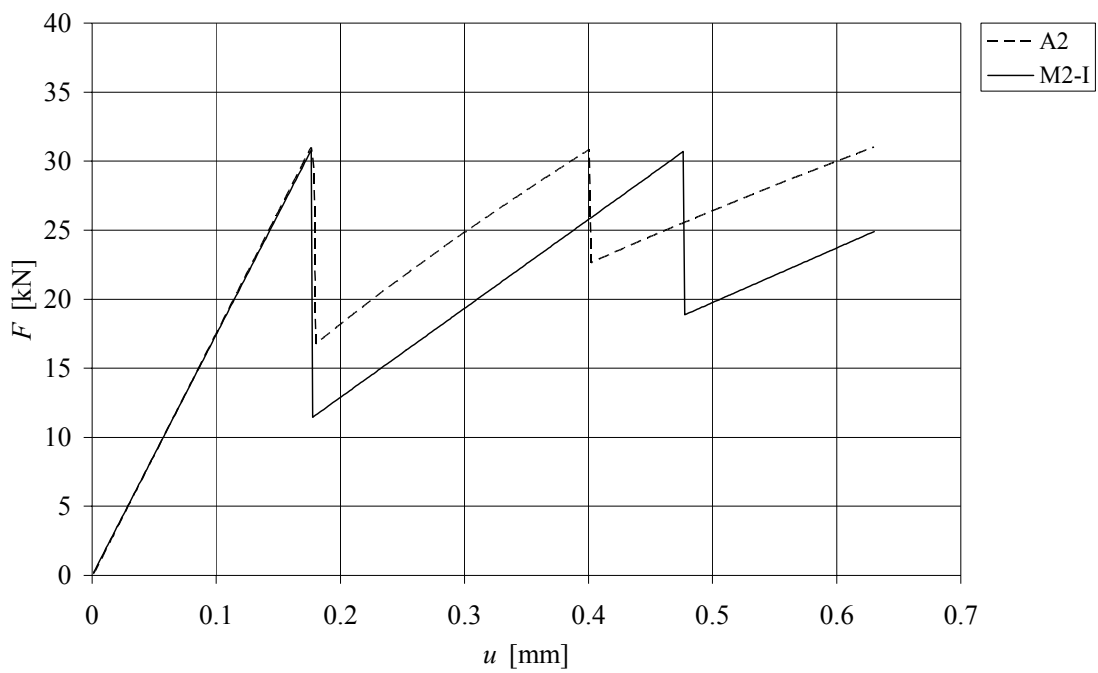


Figure F.46 For $\phi 12$ mm.

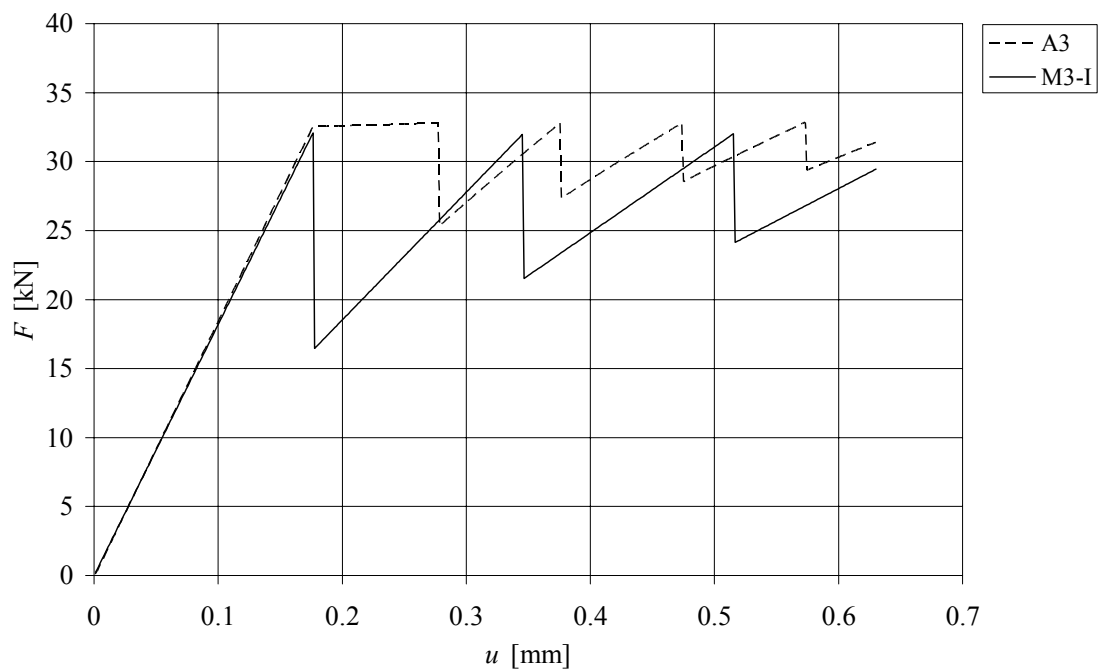


Figure F.47 For $\phi 16$ mm.

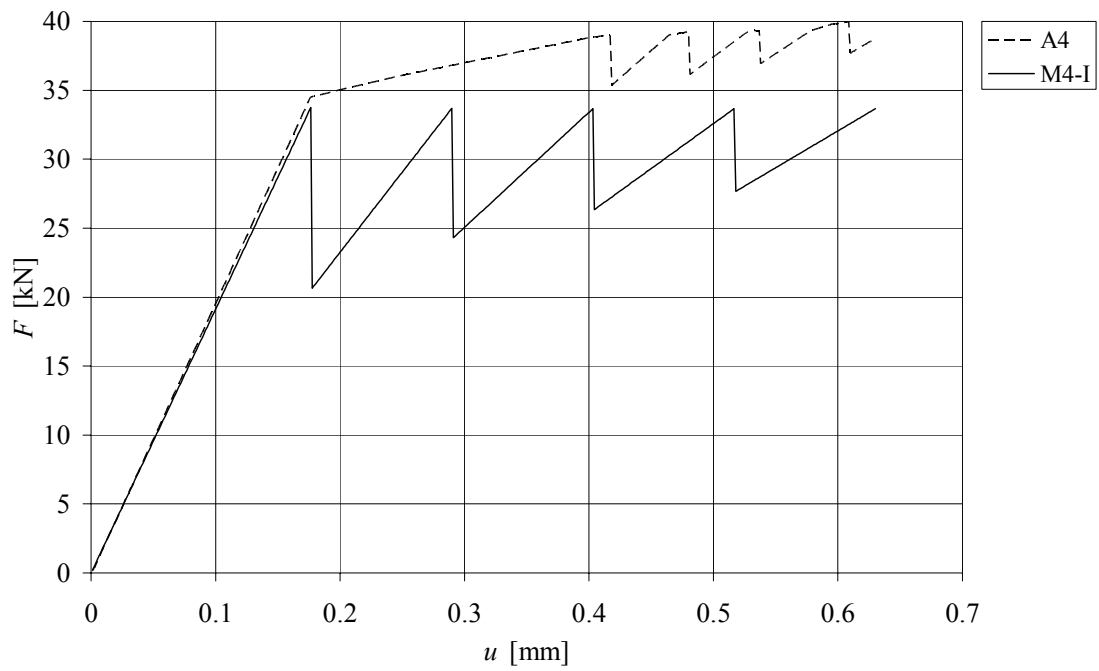


Figure F.48 For ϕ 20 mm.

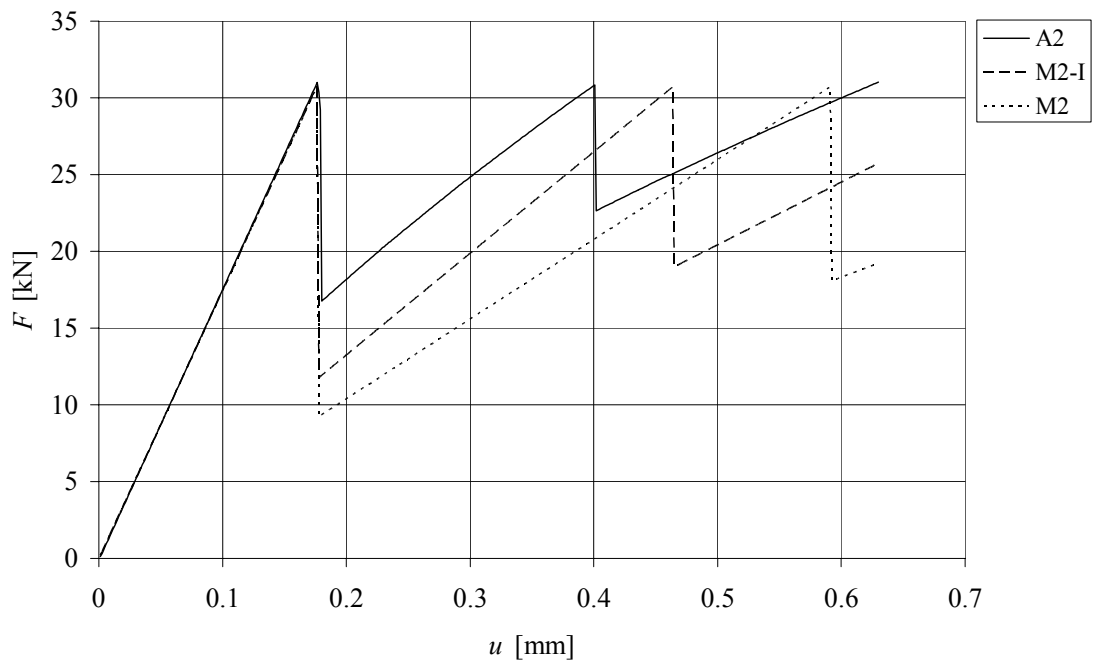


Figure F.49 Results from iteration process in the analytical model compared to FE-analysis. Based on A2.

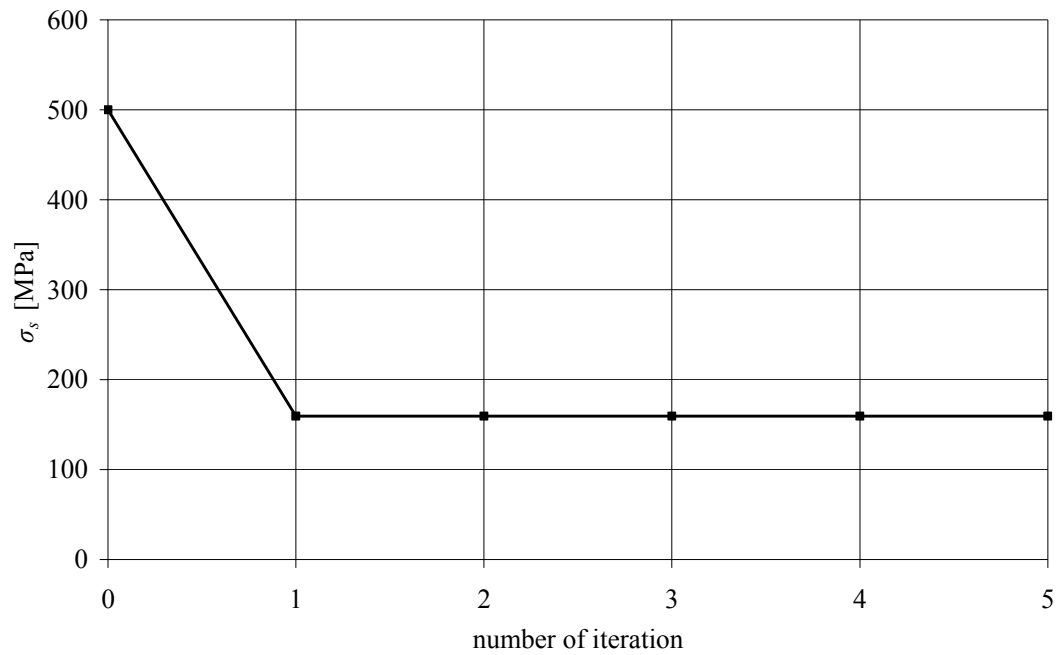


Figure F.50 Steel stress for 5 iterations.

Table F.4 Notations of performed iteration.

notation	M2	M2-I
maximum steel stress [MPa]	500	272
transfer length [mm]	350	243
crack width [mm]	0.764	0.301

F.4 Comparison low and high member

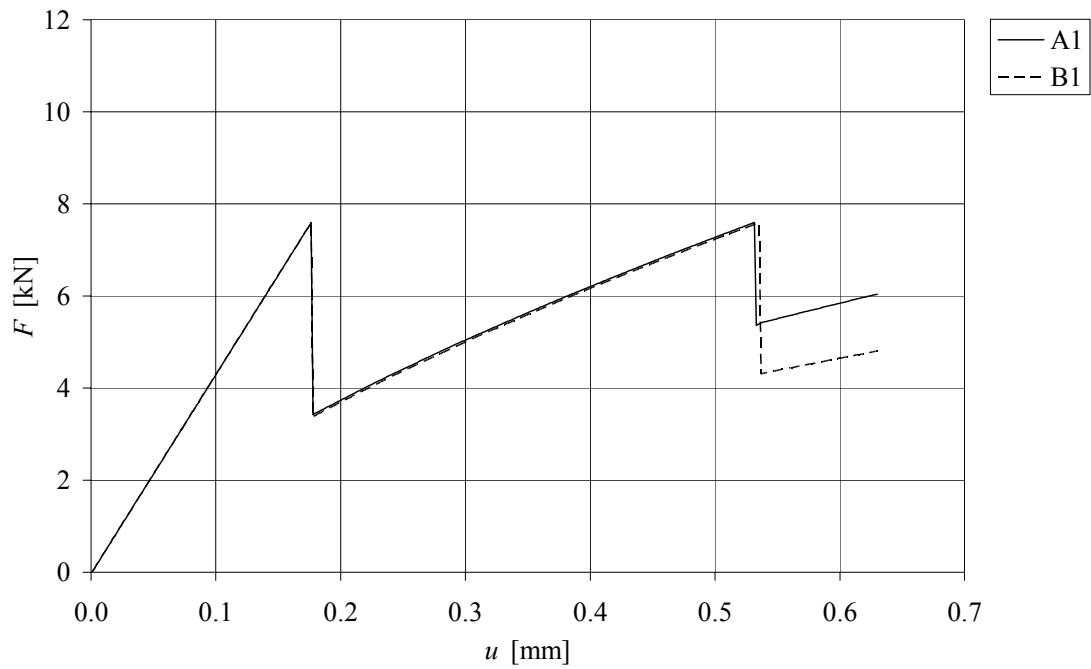


Figure F.51 Results from low (A1) and high (B1) member.

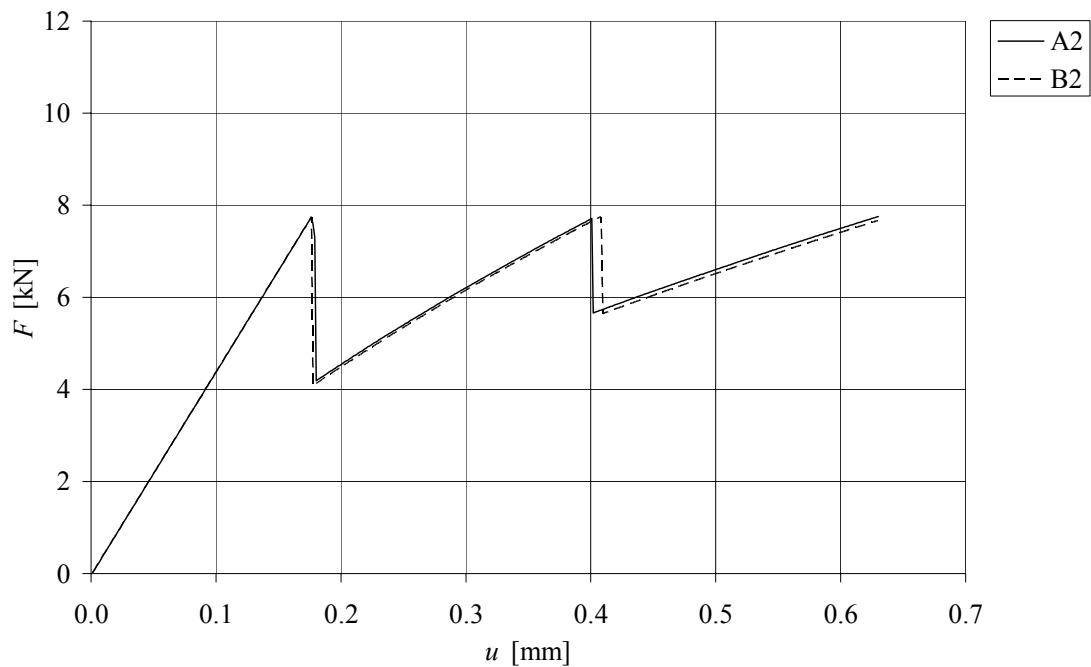


Figure F.52 Results from low (A2) and high (B2) member.

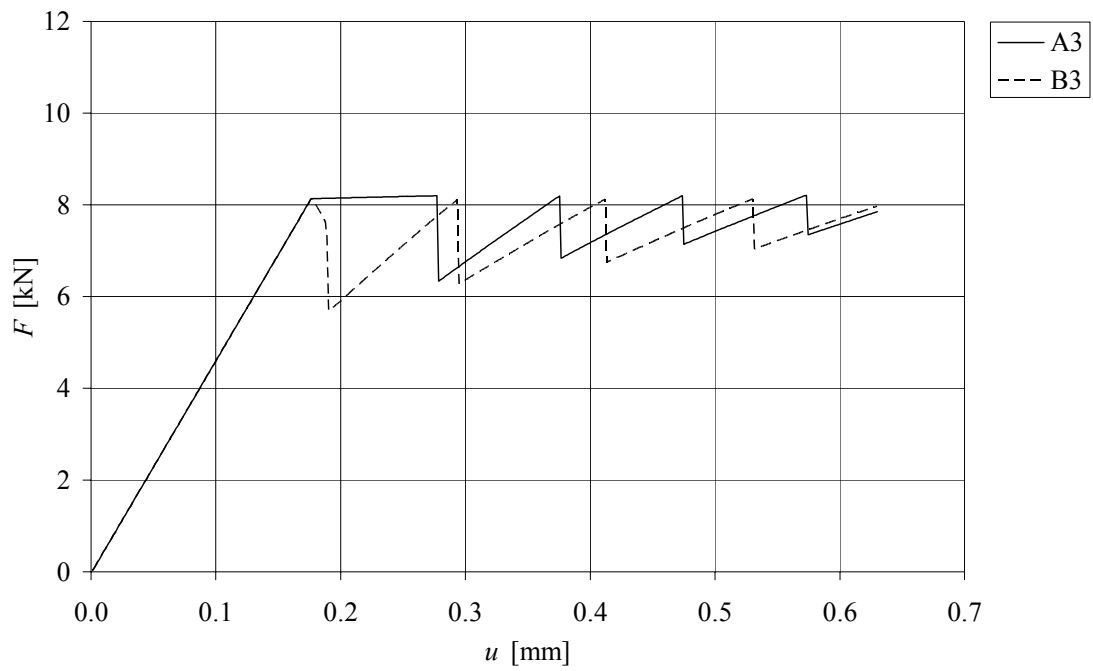


Figure F.53 Results from low (A3) and high (B3) member.

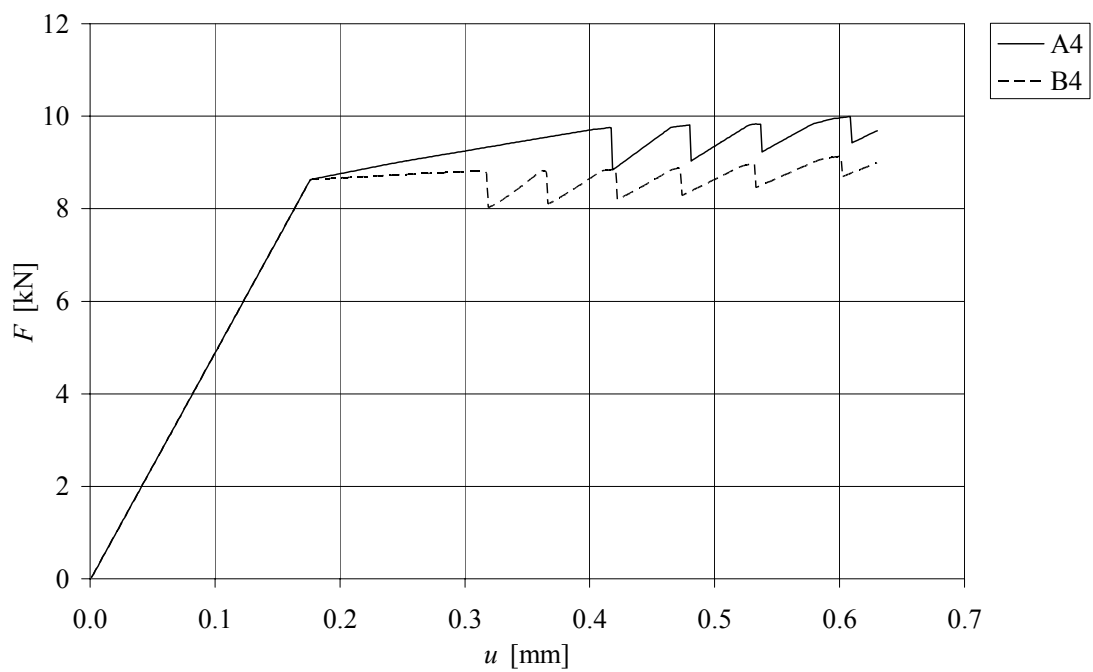


Figure F.54 Results from low (A4) and high (B4) member.

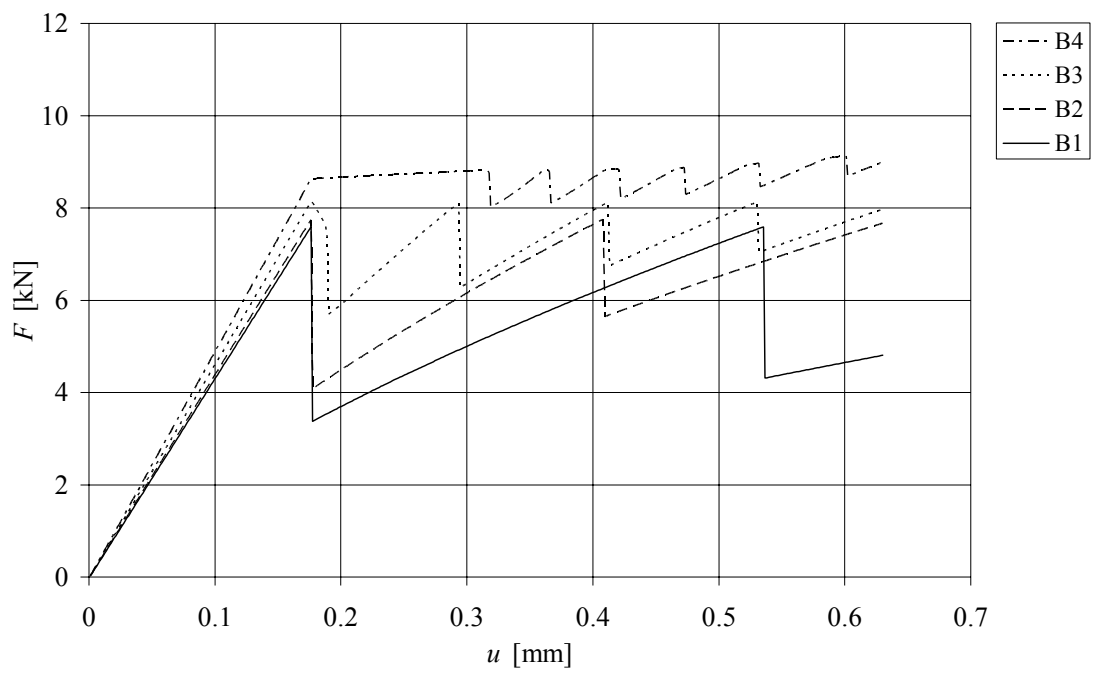
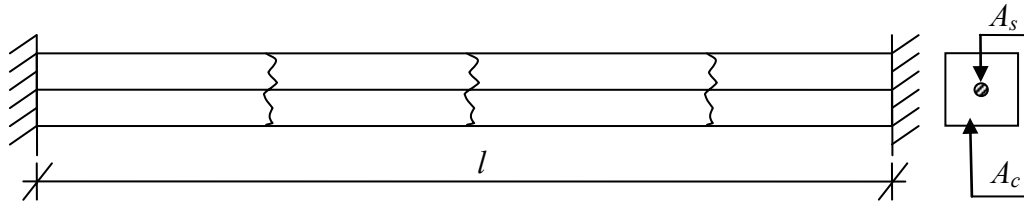


Figure F.55 Global response from analyses of high member.

APPENDIX G Calculation of concrete stresses and stiffness due to applied ΔT

By using constitutive relations it is possible to determine the total strain considering both applied temperature load and a restraint situation at the support. When using this example it is also possible to change parameters.



Geometry

$$l := 2\text{m} \quad b := 0.1\text{m} \quad h := 0.1\text{m}$$

$$n := 1 \quad \phi := 16\text{mm}$$

Materials

Concrete

$$f_{\text{ctm}} := 2.9\text{MPa}$$

$$f_{\text{ctk}0.05} := 2.0\text{MPa}$$

$$f_{\text{ctk}0.95} := 3.8\text{MPa}$$

$$E_{\text{cm}} := 33\text{GPa}$$

Steel

$$f_{\text{yk}} := 500\text{MPa}$$

$$E_{\text{sm}} := 200\text{GPa}$$

$$\alpha := \frac{E_{\text{sm}}}{E_{\text{cm}}} \quad \alpha = 6.061$$

Load

$$\Delta T := -10\text{K} \quad \alpha_{\text{cTe}} := 10.5 \cdot 10^{-6} \text{K}^{-1} \quad \varepsilon_{\text{cT}} := \alpha_{\text{cTe}} \cdot \Delta T$$

Cross section

$$A_c := b \cdot h$$

$$A_c = 0.01 \text{ m}^2$$

$$A_{si} := \frac{\pi \cdot \phi^2}{4}$$

$$A_{si} = 2.011 \times 10^{-4} \text{ m}^2$$

$$A_I := A_c + (\alpha - 1) \cdot n \cdot A_{si}$$

$$A_I = 0.011 \text{ m}^2$$

Support condition

$$n_{\text{support}} := 0.9 \text{ mm}$$

$$N_{\text{support}} := 500 \text{ kN}$$

$$S_{\text{support}} := \frac{N_{\text{support}}}{n_{\text{support}}}$$

$$S_{\text{support}} = 5.556 \times 10^5 \frac{\text{N}}{\text{m}}$$

Constitutive relationship

$$\varepsilon_{cT} = -1.05 \times 10^{-4}$$

$$\varepsilon_c := \frac{-\varepsilon_{cT}}{1 + \frac{2 \cdot E_{cm} \cdot A_I}{S_{\text{support}} \cdot l}}$$

$$\varepsilon_c = 6.347 \times 10^{-5}$$

Force due to imposed strain

$$N := \varepsilon_c \cdot E_{cm} \cdot A_I$$

$$N = 23.075 \text{ kN}$$

Restraint degree

$$R_I := \left(\frac{1}{1 + \frac{2 \cdot E_{cm} \cdot A_I}{S_{\text{support}} \cdot l}} \right)$$

$$R_I = 0.604$$

Elongation

$$\Delta l := \varepsilon_c T \cdot l$$

$$\Delta l = -2.1 \times 10^{-4} \text{ m}$$

Steel stress

$$\sigma_s := E_{sm} \cdot \varepsilon_c$$

$$\sigma_s = 12.693 \text{ MPa}$$

Concrete stress

$$\sigma_c := E_{cm} \cdot \varepsilon_c$$

$$\sigma_c = 2.094 \text{ MPa}$$

"High risk of cracking"
if $\sigma_c > f_{ctk0.95}$

$$f_{ctk0.95} = 3.8 \text{ MPa}$$

"Risk of cracking"
if $\sigma_c > f_{ctm}$

$$f_{ctm} := 2.9 \text{ MPa}$$

"Not acceptable risk of cracking"
if $\sigma_c > f_{ctk0.05}$

$$f_{ctk0.05} := 2.0 \text{ MPa}$$

Stiffness

$$A_{c.net} := A_c - A_{si}$$

Concrete stiffness

$$k_{c0} := \frac{E_{cm} \cdot A_{c.net}}{l} \qquad k_{c0} = 161.682 \frac{\text{MN}}{\text{m}}$$

Steel stiffness

$$k_{s0} := E_{sm} \cdot \frac{A_{si}}{l} \qquad k_{s0} = 20.106 \frac{\text{MN}}{\text{m}}$$

Global stiffness

$$k_{global} := \frac{1}{\frac{1}{k_{c0} + k_{s0}} + \frac{1}{S_{support}}} \qquad k_{global} = 136.97 \frac{\text{MN}}{\text{m}}$$

APPENDIX H Calculation the response using an analytical method

Material

$$\text{MN} := 1 \cdot 10^6 \text{N}$$

$$\text{GPa} := 1 \cdot 10^9 \text{Pa}$$

Concrete 30/37

$$E_{\text{cm}} := 33 \text{GPa}$$

$$f_{\text{cm}} := 38 \text{MPa}$$

$$f_{\text{ctm}} := 2.9 \text{MPa}$$

$$f_{\text{ctk}0.95} := 3.8 \text{MPa}$$

$$f_{\text{ctk}0.05} := 2.0 \text{MPa}$$

$$\phi_{\text{c}} := 0$$

$$\alpha_{\text{ef}} := \frac{E_{\text{sm}}}{E_{\text{cm}}} (1 + \phi_{\text{c}})$$

Reinforcing steel K500

$$E_{\text{sm}} := 200 \text{GPa}$$

$$f_{\text{yk}} := 500 \text{MPa}$$

$$\alpha_{\text{ef}} = 6.061$$

Evaluation of risk of cracking

Initially $\sigma_{\text{ci}} := 0 \text{MPa}$

$$\varepsilon_{\text{ci}} := 0$$

no initial stress and strain

$$\sigma_{\text{ci}} < f_{\text{ctk}0.05}$$

concrete is uncracked

Final **Restraint degree:** $R_{\text{ny}} := 1$

deformation condition for additional need for deformation

$$\Delta T := 30 \text{K}$$

$$\alpha_{\text{temp}} := 10.5 \cdot 10^{-6} \frac{1}{\text{K}}$$

$$\Delta \varepsilon_{\text{cs}} := \Delta T \cdot \alpha_{\text{temp}}$$

$$\Delta \varepsilon_{\text{cs}} = 3.15 \times 10^{-4}$$

$$\Delta\varepsilon_c := 1 \cdot 10^{-4}$$

$$l := 2\text{m}$$

$$\Delta\varepsilon_c := \text{root}\left(R_{ny} \cdot \Delta\varepsilon_{cs} \cdot l + \Delta\varepsilon_c \cdot l, \Delta\varepsilon_c\right)$$

$$\Delta\varepsilon_c = -3.15 \times 10^{-4}$$

total elastic strain

$$\Delta\varepsilon_c := \Delta\varepsilon_c \cdot -1$$

final stress

$$\sigma_c := \left(\varepsilon_{ci} + \Delta\varepsilon_c\right) \cdot \frac{E_{cm}}{1 + \phi_c}$$

$$\sigma_c = 10.395\text{MPa}$$

$$\sigma_c > f_{ctm}$$

the element will probably crack and reinforcement fc crack control is needed

Dimensions

$$t := 0.1\text{m}$$

$$n := 1$$

$$\phi := 0.016\text{m}$$

$$A_{si} := \frac{\pi \cdot \phi^2}{4}$$

$$A_{si} = 201.062\text{mm}^2$$

$$A_s := n \cdot A_{si}$$

$$A_s = 201.062\text{mm}^2$$

$$A_{I,ef} := t \cdot t + \left(\alpha_{ef} - 1\right) \cdot A_s$$

$$A_{I,ef} = 1.102 \times 10^4\text{mm}^2$$

Transformed concrete area:

$$c := 40\text{mm}$$

$$A_{ef} := \min\left[t \cdot t, \left[t \cdot 2.5 \cdot \left(c + \frac{\phi}{2}\right)\right]\right]$$

$$A_{ef} = 0.01\text{m}^2$$

New cracks can appear if the surface region cracks

$$N_1 := f_{ctm} \cdot \left[A_{ef} + \left(\alpha_{ef} - 1\right) \cdot A_s\right]$$

$$N_1 = 31.951\text{kN}$$

Response for single crack (simplified linear model)

$$f_{y2} := \frac{N_1}{A_s} \qquad f_{y2} = 158.91 \text{ MPa}$$

$$f_{yk} := 159 \text{ MPa} \qquad \text{Assuming a new } f_k \text{ for estimation of the crack width, based on } f_2 \text{ above.}$$

$$\phi := \phi \cdot \frac{1000}{m}$$

$$w_y := 0.420 \frac{\left[\frac{\phi \cdot f_{yk}^2}{0.22 \cdot f_{cm} \cdot E_{sm} \cdot \left(1 + \frac{E_{sm} A_s}{E_{cm} A_{ef}} \right)} \right]^{0.826}}{1000} + \frac{4 \cdot \phi \cdot \frac{f_{yk}}{E_{sm}}}{1000}$$

$$w_y = 1.692 \times 10^{-4}$$

$$w_y := w_y \cdot m \qquad w_y = 0.169 \text{ mm}$$

Calculating the transfer length l_t

$$w_k := 0.420 \frac{\left[\frac{\phi \cdot f_{yk}^2}{0.22 \cdot f_{cm} \cdot E_{sm} \cdot \left(1 + \frac{E_{sm} A_s}{E_{cm} A_{ef}} \right)} \right]^{0.826}}{1000} + \frac{4 \cdot \phi \cdot \frac{f_{yk}}{E_{sm}}}{1000}$$

$$w_k = 1.692 \times 10^{-4}$$

$$w_{net} := 0.420 \left[\frac{\phi \cdot f_{yk}^2}{0.22 \cdot f_{cm} \cdot E_{sm} \cdot \left(1 + \frac{E_{sm} A_s}{E_{cm} A_{ef}} \right)} \right]^{0.826}$$

$$w_{net} = 0.118$$

$$l_t := 0.443 \frac{\frac{\phi}{1000} \cdot f_{yk}}{0.22 \cdot f_{cm} \cdot w_{net} \cdot 0.21 \cdot \left(1 + \frac{E_{sm} A_s}{E_{cm} A_{ef}}\right)} + 2 \cdot \frac{\phi}{1000}$$

$$l_t = 0.22$$

$$l_t := l_t \cdot m$$

$$l_t = 0.22 \text{ m}$$

Choose length of spring from crack equal half of

Change l_t in order to find changes in stiffness

Deformation condition in case of single crack

$$n_1 := 1$$

$$\sigma_s := 300 \text{ MPa}$$

$$\sigma_s := \text{root} \left[\frac{\sigma_s \cdot A_s \cdot l}{E_{cm} \cdot A_{I,ef}} \cdot (1 + \phi_c) + n_1 \cdot \frac{\sigma_s}{f_{yk}} w_y - R_{ny} \cdot \left(\Delta \varepsilon_{cs} + \frac{\varepsilon_{ci}}{R_{ny}} \right) \cdot l, \sigma_s \right]$$

$$\sigma_s = 290.332 \text{ MPa}$$

$$N_s := \sigma_s \cdot A_s$$

$$N_s = 58.375 \text{ kN}$$

$$N_1 = 31.951 \text{ kN}$$

$$\text{cracks} := \begin{cases} 1 & \text{if } N_1 < N_s \\ 0 & \text{otherwise} \end{cases}$$

$$\text{cracks} = 1$$

number of cracks that that have occurred so far

$$w := \frac{\sigma_s}{f_{yk}} \cdot w_y \quad w = 0.309 \text{ mm}$$

$$w_k := 1.3 \cdot w \quad w_k = 0.402 \text{ mm}$$

Stiffness

$$A_{c.net} := t^2 - A_s$$

$$A_{c.net} = 9.799 \times 10^3 \text{ mm}^2$$

$$k_{c0} := \frac{E_{cm} \cdot A_{c.net}}{l}$$

$$k_{c0} = 161.682 \frac{\text{MN}}{\text{m}}$$

$$k_{s0} := \frac{E_{sm} \cdot A_s}{l}$$

$$k_{s0} = 20.106 \frac{\text{MN}}{\text{m}}$$

$$k_0 := k_{c0} + k_{s0}$$

$$k_0 = 181.789 \frac{\text{MN}}{\text{m}}$$

$$k_{c1} := \frac{E_{cm} \cdot A_{c.net}}{\frac{l-l_t}{2}}$$

$$k_{c1} = 363.359 \frac{\text{MN}}{\text{m}}$$

$$k_{s1} := \frac{E_{sm} \cdot A_s}{\frac{l-l_t}{2}}$$

$$k_{s1} = 45.186 \frac{\text{MN}}{\text{m}}$$

$$k_1 := k_{c1} + k_{s1}$$

$$k_1 = 408.544 \frac{\text{MN}}{\text{m}}$$

$$k_2 := \frac{E_{sm} \cdot A_s}{l_t}$$

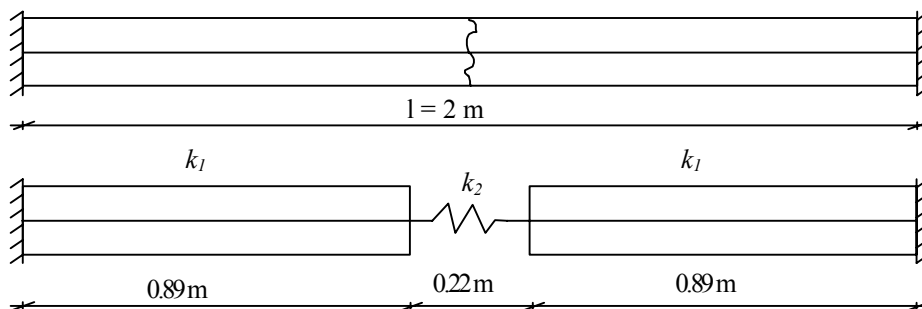
$$k_2 = 182.673 \frac{\text{MN}}{\text{m}}$$

$$k_{1.global} := \frac{1}{\frac{1}{k_1} + \frac{1}{k_2} + \frac{1}{k_1}}$$

$$k_{1.global} = 96.435 \frac{\text{MN}}{\text{m}}$$

$$\text{diff} := \frac{k_0 - k_{1.global}}{k_0}$$

$$\text{diff} = 46.952 \%$$



Assume 2 cracks

$$n_1 := 2$$

$$\sigma_s := 300 \text{ MPa}$$

$$\sigma_s := \text{root} \left[\frac{\sigma_s \cdot A_s \cdot l}{E_{cm} \cdot A_{I.ef}} \cdot (1 + \phi_c) + n_1 \cdot \frac{\sigma_s}{f_{yk}} w_y - R_{ny} \cdot \left(\Delta \varepsilon_{cs} + \frac{\varepsilon_{ci}}{R_{ny}} \right) \cdot l, \sigma_s \right]$$

$$\sigma_s = 194.814 \text{ MPa}$$

$$N_s := \sigma_s \cdot A_s$$

$$N_s = 39.17 \text{ kN}$$

$$N_1 = 31.951 \text{ kN}$$

$$\text{cracks} := \begin{cases} 2 & \text{if } N_1 < N_s \\ 1 & \text{otherwise} \end{cases}$$

$$\text{cracks} = 2$$

$$w := \frac{\sigma_s}{f_{yk}} \cdot w_y$$

$$w = 2.073 \times 10^{-4} \text{ m}$$

$$w_k := 1.3 \cdot w$$

$$w_k = 0.269 \text{ mm}$$

Stiffness

$$k_{c2} := \frac{E_{cm} \cdot A_{c.net}}{l_t}$$

$$k_{c2} = 1.469 \times 10^3 \frac{\text{MN}}{\text{m}}$$

$$k_{s2} := \frac{E_{sm} \cdot A_s}{l_t}$$

$$k_{s2} = 182.673 \frac{\text{MN}}{\text{m}}$$

$$k_3 := k_{c2} + k_{s2}$$

$$k_3 = 1.652 \times 10^3 \frac{\text{MN}}{\text{m}}$$

$$k_{c3} := \frac{E_{cm} \cdot A_{c.net}}{\frac{1-l_t}{2} - 2 \cdot l_t}$$

$$k_{c3} = 719.119 \frac{\text{MN}}{\text{m}}$$

$$k_{s3} := \frac{E_{sm} \cdot A_s}{\frac{1-l_t}{2} - 2 \cdot l_t}$$

$$k_{s3} = 89.427 \frac{\text{MN}}{\text{m}}$$

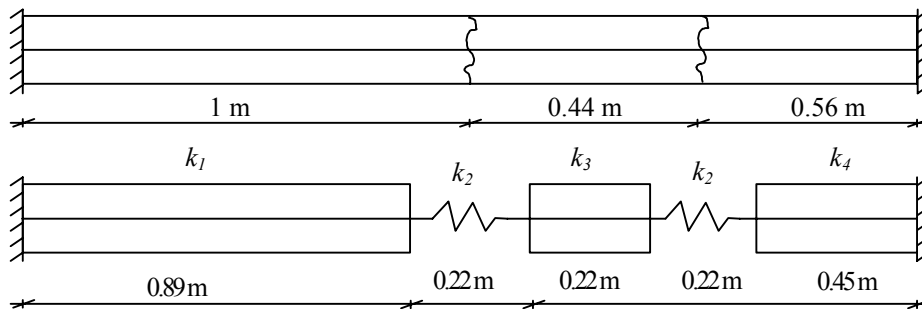
$$k_4 := k_{c3} + k_{s3}$$

$$k_4 = 808.546 \frac{\text{MN}}{\text{m}}$$

$$k_{2,global} := \frac{1}{\frac{1}{k_1} + \frac{1}{k_2} + \frac{1}{k_3} + \frac{1}{k_2} + \frac{1}{k_4}}$$

$$k_{2,global} = 65.623 \frac{\text{MN}}{\text{m}}$$

$$\text{diff} := \frac{k_0 - k_{2,global}}{k_0} \quad \text{diff} = 63.901\%$$



Assume 3 cracks

$$n_1 := 3$$

$$\sigma_s := 300 \text{ MPa}$$

$$\sigma_s := \text{root} \left[\frac{\sigma_s \cdot A_s \cdot l}{E_{cm} \cdot A_{I,ef}} \cdot (1 + \phi_c) + n_1 \cdot \frac{\sigma_s}{f_{yk}} w_y - R_{ny} \cdot \left(\Delta \varepsilon_{cs} + \frac{\varepsilon_{ci}}{R_{ny}} \right) \cdot l, \sigma_s \right]$$

$$\sigma_s = 146.588 \text{ MPa}$$

$$N_s := \sigma_s \cdot A_s$$

$$N_s = 29.473 \text{ kN}$$

$$N_1 = 31.951 \text{ kN}$$

$$\text{cracks} := \begin{cases} 3 & \text{if } N_1 < N_s \\ 2 & \text{otherwise} \end{cases}$$

$$\text{cracks} = 2$$

no new cracks will appear

$$w := \frac{\sigma_s}{f_{yk}} \cdot w_y$$

$$w = 1.56 \times 10^{-4} \text{ m}$$

$$w_k := 1.3 \cdot w$$

$$w_k = 2.027 \times 10^{-4} \text{ m}$$

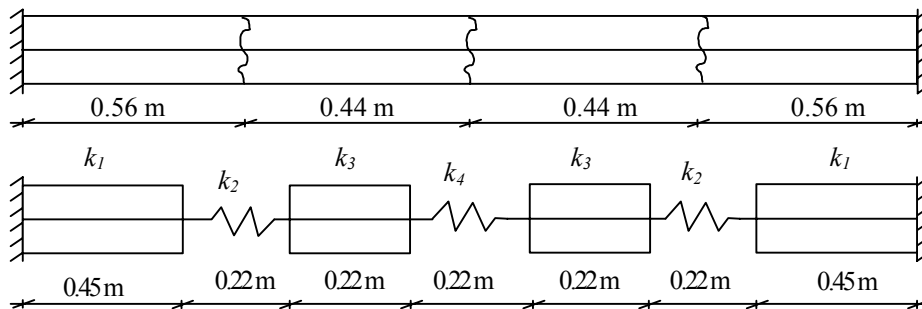
Stiffness

$$k_{2,\text{global}} := \frac{1}{\frac{1}{k_4} + \frac{1}{k_2} + \frac{1}{k_3} + \frac{1}{k_2} + \frac{1}{k_3} + \frac{1}{k_2} + \frac{1}{k_4}}$$

$$k_{2,\text{global}} = 49.733 \frac{1}{\text{m}} \text{ MN}$$

$$\text{diff} := \frac{k_0 - k_{2,\text{global}}}{k_0}$$

$$\text{diff} = 72.642 \%$$



APPENDIX I Comparison of crack width

Swedish codes

Material parameters

$$f_{yk} := 500\text{MPa}$$

$$f_{ctm} := 2.9\text{MPa}$$

$$E_s := 200\text{GPa}$$

$$E_c := 33\text{GPa}$$

$$\alpha := \frac{E_s}{E_c}$$

$$\alpha = 6.061$$

Geometry

$$\phi := 0.012\text{m}$$

$$A_s := \pi \cdot \frac{\phi^2}{4}$$

$$A_s = 113.097\text{mm}^2$$

$$b := 0.1\text{m}$$

$$t := b$$

$$A_c := b \cdot t$$

$$A_c = 0.01\text{m}^2$$

$$A_I := A_c + (\alpha - 1) \cdot A_s$$

$$A_I = 0.011\text{m}^2$$

$$\rho_r := \frac{A_s}{A_c}$$

$$\rho_r = 1.131\%$$

$$\zeta := 1.0$$

Load

$$\Delta T := -30\text{K}$$

$$\alpha_c := 10.5 \cdot 10^{-6} \cdot \frac{1}{\text{K}}$$

$$\Delta \varepsilon_{cs} := \Delta T \cdot \alpha_c$$

$$\Delta \varepsilon_{cs} = -3.15 \times 10^{-4}$$

$$\varepsilon_c := -\Delta \varepsilon_{cs}$$

$$\varepsilon_c = 3.15 \times 10^{-4}$$

$$\text{wanted_}\delta := \varepsilon_c \cdot 2\text{m}$$

$$\text{wanted_}\delta = 0.63\text{mm}$$

$$\text{wanted_}\delta_k := 1.3 \cdot \text{wanted_}\delta$$

$$\text{wanted_}\delta_k = 0.819\text{mm}$$

Assume corresponding steel stress

$$\sigma_s := 272 \text{ MPa}$$

Stress in concrete when crack will appear

$$\sigma_n := \frac{f_{ctm}}{\zeta} \quad \sigma_n = 2.9 \text{ MPa}$$

$$F_1 := \sigma_n \cdot A_I \quad F_1 = 30.66 \text{ kN}$$

Crack spacing

$$\sigma_{sr} := \frac{F_1}{A_s} \quad \sigma_{sr} = 271.092 \text{ MPa}$$

$$m_y := 1 - \left(\frac{1.0}{2.5 \cdot 0.8} \right) \cdot \frac{\sigma_{sr}}{\sigma_s}$$

$$v := \begin{cases} 0.4 & \text{if } m_y < 0.4 \\ m_y & \text{otherwise} \end{cases} \quad v = 0.502$$

$$s_{rm} := 50 \text{ mm} + 0.8 \cdot 0.25 \cdot \frac{\phi}{\rho_r} \quad s_{rm} = 0.262 \text{ m}$$

$$n := \frac{2m}{s_{rm}} + 1 \quad n = 8.628$$

Needed temperature in order to achieve 8, moving to 9 cracks is approximately 115C according to the analytical model

Crack width

$$w_m := v \cdot \frac{\sigma_s}{E_s} \cdot s_{rm} \quad w_m = 0.179 \text{ mm} \quad \text{kil} := w_m \cdot n \quad \text{kil} = 1.543 \text{ mm}$$

$$w_k := 1.7 \cdot w_m \quad w_k = 0.304 \text{ mm} \quad \text{tot}_\delta := w_k \cdot n \quad \text{tot}_\delta = 2.624 \text{ mm}$$

EUROCODE 2

$$f_{ctm} := 2.9 \text{ MPa}$$

$$\varepsilon_{diff} := \varepsilon_{sm} - \varepsilon_{cm}$$

$$\varepsilon_{diff} := \max \left[\frac{\sigma_s - 0.6 \cdot \frac{f_{ctm}}{\rho_r} \cdot (1 + \alpha \cdot \rho_r)}{E_s}, 0.6 \cdot \frac{\sigma_s}{E_s} \right]$$

$$\varepsilon_{diff} = 8.16 \times 10^{-4}$$

$$s_{rmax} := 3.4 \cdot 44 \text{ mm} + 0.8 \cdot 1.0 \cdot 0.425 \cdot \frac{\phi}{\rho_r} \quad s_{rmax} = 0.51 \text{ m}$$

$$n := \frac{2m}{s_{rmax}} + 1$$

$$n = 4.919$$

$$w_k := s_{rmax} \cdot (\varepsilon_{diff})$$

$$w_k = 0.416 \text{ mm}$$

$$\text{tot}\delta := w_k \cdot n$$

$$\text{tot}\delta = 2.048 \text{ mm}$$

APPENDIX J Determining the number of cracks

J.1 M-file

```
%%%%%%%%%%%%%%%%%%%%%%%%%%%%%%%%%%%%%%%%%%%%%%%%%%%%%%%%%%%%%%%%%%%%%%%%
%%
%%%%%%%%%%%%%%%%%%%%%%%%%%%%%%%%%%%%%%%%%%%%%%%%%%%%%%%%%%%%%%%%%%%%%%%%
%%
%% Calculating number of cracks for reinforced concrete (a prism)
%% subjected to a change in temperature.
%%
%% Göteborg 2006-10-25
%% Johan Nettet
%% Simon Skoglund
%%%%%%%%%%%%%%%%%%%%%%%%%%%%%%%%%%%%%%%%%%%%%%%%%%%%%%%%%%%%%%%%%%%%%%%%
%%
%%%%%%%%%%%%%%%%%%%%%%%%%%%%%%%%%%%%%%%%%%%%%%%%%%%%%%%%%%%%%%%%%%%%%%%%
%%

clc;
clear all;
close all;

%% Material properties
% Concrete
fctm=2.9E6;
fctk005=2.0E6;
fctk095=3.8E6;
fcm=38.0E6;
Ecm=33.0E9;
alfaTemp=10.5E-6;
phiC=0.0;
% Steel
fyk=500E6; % By calculating N1 below, maximum steel stress may be
taken as N1/As!
Esm=200E9;
alfaef=Esm/Ecm*(1+phiC);
%R=[0.25,0.5,0.75,1];
R=1.0;
rr=size(R);

%% Dimensions
%L=[2,4,6,8]; % Possible to apply various dimensions on the length
L=2; % Original value for analysis
Q=size(L); % Help for further programming

%T=[0.1,0.2,0.3,0.4]; % Possible to apply various dimensions on the
cross section
T=0.1; % Original value for analysis
P=size(T); % Help for further programming

%PHI=[0.010,0.012,0.016,0.020]; % Possible to apply various
dimensions on the reinforcement
PHI=0.016; % Original value for analysis
O=size(PHI); % Help for further programming

save=1;
```

```

for rrr=1:rr(2);
    RR=R(rrr);
    RRR=rrr*100;

    for q=1:Q(2);
        l=L(q);
        H=q*10;

        for g=1:P(2);
            t=T(g);
            b=t;

            for k=1:O(2);
                phi=PHI(k);
                Asi=(1/4)*pi*phi^2;
                As=Asi;
                rah(k)=As/(t*b);
                Aief=t*b+(alfaef-1)*As;
                c=t/2-phi/2;
                Aef=min(b*2.5*(c+phi/2),t*b);

                N1=fctm*(Aef+(alfaef-1)*As); % Maximum allowed force
in concrete
                Ac=Aef;

                wy=((0.420*(((phi*1000*fyk^2)/(0.22*fcm*Esm*(1+Esm/Ecm*As/Aef)))^0.8
                26)))+(4*phi*1000*fyk/Esm)/1000;
                deltaT=[0:0.06:30];

                [DeltaEpsilonCS,Ns,n]=numberofcracks(deltaT,alfaTemp,Ecm,phiC,N1,RR,l
                ,As,Aief,fyk,wy);

                disp(['Number of cracks that occur for deltaT =
                ',num2str(deltaT(end)),' [K] and PHI ',num2str(phi),' [m] and t=b
                ',num2str(t),' [m] and length ',num2str(l),' [m] is/are
                ',num2str(n),'!'])

                %Ns(k,:)=Ns;

                %% Calculating transfer length
                sigmaScrack=N1/As;

                wk=((0.420*(((phi*1000*sigmaScrack^2)/(0.22*fcm*Esm*(1+Esm/Ecm*As/Ae
                f)))^0.826)))+(4*phi*1000*sigmaScrack/Esm)/1000;

                wnet=((0.420*(((phi*1000*sigmaScrack^2)/(0.22*fcm*Esm*(1+Esm/Ecm*As/
                Aef)))^0.826))));

                lt=0.443*(((phi*sigmaScrack)/(0.22*fcm*(wnet^0.21)*(1+Esm/Ecm*As/Aef)
                )))+2*phi;

                % lt=lt*0.7; % The transfer length may be reduced
                Srm=2*lt;
                numcracks=l/Srm+1;

                LT(save)=lt;
                WNET(save)=wnet;
                WK(save)=wk;

```

```

        SAVEMAXNUM(save)=numcracks;
        SAVEN(save)=n;
        save=save+1;

        if n>numcracks
            disp('To many cracks for further calculation!')
            break
        end

        %% PLOTS
        figure(1)
        %figure(RRR+g+H)
        plot(deltaT,Ns)
        xlabel('?T [K]')
        ylabel('force in reinforcement [N]')
        hold on;
        N1ny=ones(size(Ns))*N1;
        %plot(deltaT,N1ny,'r--')

    end
end
end
end
end

```

J.2 Function file

```

function
[DeltaEpsilonCS,Ns,n]=numberofcracks(deltaT,alfaTemp,Ecm,phiC,N1,RR,l
,As,AIef,fyk,wy);
%%%%%%%%%%%%%%%%%%%%%%%%%%%%%%%%%%%%%%%%%%%%%%%%%%%%%%%%%%%%%%%%%%%%%%%%
%%%%%%%%%%%%%%%%%%%%%%%%%%%%%%%%%%%%%%%%%%%%%%%%%%%%%%%%%%%%%%%%%%%%%%%%
%%%%%%%%%%%%%%%%%%%%%%%%%%%%%%%%%%%%%%%%%%%%%%%%%%%%%%%%%%%%%%%%%%%%%%%%
%% Göteborg 2006-10-25
%% Johan Nasset
%% Simon Skoglund
%%%%%%%%%%%%%%%%%%%%%%%%%%%%%%%%%%%%%%%%%%%%%%%%%%%%%%%%%%%%%%%%%%%%%%%%
%%%%%%%%%%%%%%%%%%%%%%%%%%%%%%%%%%%%%%%%%%%%%%%%%%%%%%%%%%%%%%%%%%%%%%%%
%%%%%%%%%%%%%%%%%%%%%%%%%%%%%%%%%%%%%%%%%%%%%%%%%%%%%%%%%%%%%%%%%%%%%%%%
k=size(deltaT);
K=k(2);
Ns=0;
n=0;
for i=1:K;
    DeltaEpsilonCS(i)=alfaTemp*deltaT(i); %negative due to shrinking

    SigmaS=RR*DeltaEpsilonCS(i)*l/((As*l*(1+phiC)/(Ecm*AIef))+n*wy/fyk);
    Ns(i)=SigmaS*As;
    if Ns(i)>=N1;
        n=n+1;
    end
end
end
n=n;

```


APPENDIX K Input files for ADINA

K.1 Input for geometry

```
*
COORDINATES POINT SYSTEM=0
*      X      Y      Z      SYSTEM
1      0      0      0      0
2      0      0      0.05  0
3      0      0.02  0.05  0
4      0      0.04  0.05  0
5      0      0.06  0.05  0
.
.
.
203    0      1.982  0.05  0
204    0      2.002  0.05  0
205    0      0.2    0      0
206    0      1.78   0      0
207    0      1.8    0      0
*
```

K.1.1 Lines

```
*
LINE STRAIGHT NAME=      1      P1=    104      P2=    105
LINE STRAIGHT NAME=      2      P1=    105      P2=    106
LINE STRAIGHT NAME=      3      P1=    106      P2=    107
LINE STRAIGHT NAME=      4      P1=    107      P2=    108
LINE STRAIGHT NAME=      5      P1=    108      P2=    109
.
.
.
LINE STRAIGHT NAME=     96      P1=    199      P2=    200
LINE STRAIGHT NAME=     97      P1=    200      P2=    201
LINE STRAIGHT NAME=     98      P1=    201      P2=    202
LINE STRAIGHT NAME=     99      P1=    202      P2=    203
LINE STRAIGHT NAME=    100      P1=    203      P2=    204
*
```

K.1.2 Surface

```
*
SURFACE VERTEX NAME=1  P1=1      P2=2   P3=12      P4=205
SURFACE VERTEX NAME=2  P1=205 P2=12  P3=91      P4=206
SURFACE VERTEX NAME=3  P1=206 P2=91  P3=92      P4=207
SURFACE VERTEX NAME=4  P1=207 P2=92  P3=102 P4=103
*
```

K.1.3 Thickness

```
*
SFTHICKNESS
@CLEAR
1 0.0500 0.0000 0.0000,
  0.0000 0.0000
2 0.0500 0.0000 0.0000,
  0.0000 0.0000
```

3 0.0500 0.0000 0.0000,
0.0000 0.0000

4 0.0500 0.0000 0.0000,
0.0000 0.0000

@
*

K.1.4 Material

*

MATERIAL CONCRETE NAME=1 OPTION=KUPFER E0=3.300E+10,
NU=0.200 SIGMAT=2900000 SIGMATP=0 SIGMAC=-3.800E+07,
EPSC=-0.002 SIGMAU=-3.700E+07 EPSU=-0.0035 BETA=0.750,
C1=1.400 C2=-0.400 XSI=39.000 STIFAC=0.0001 SHEFAC=0.500,
ALPHA=0 TREF=0.000 INDNU=CONSTANT GF=0.0 DENSITY=2400.000,
TEMPERAT=NO MDESCRIP='Concrete'

*

MATERIAL PLASTIC-BILINEAR NAME=2 HARDENIN=ISOTROPIC,
E=2.000E+11 NU=0.200 YIELD=5.000E+08 ET=2.000E+08,
EPA=0.010 STRAINRA=0 DENSITY=7800 ALPHA=0 TREF=0.000,
DEPENDEN=NOTRANSITI=0.0001 EP-STRAI=0.000 BCURVE=0,
BVALUE=0.000 XM-INF=0.000 XM0=0.000 ETA=0.000 MDESCRIP='Steel'

*

K.1.5 Element type

*

SURF-ELEMDAT TWOSOLID

1 4 0.0000000000000000 'DEFAULT' 'DEFAULT' 0.0000000000000000,
0.0000000000000000 'NO' 0.0000000000000000

2 1 0.0000000000000000 'DEFAULT' 'DEFAULT' 0.0000000000000000,
0.0000000000000000 'NO' 0.0000000000000000

3 3 0.0000000000000000 'DEFAULT' 'DEFAULT' 0.0000000000000000,
0.0000000000000000 'NO' 0.0000000000000000

4 4 0.0000000000000000 'DEFAULT' 'DEFAULT' 0.0000000000000000,
0.0000000000000000 'NO' 0.0000000000000000

*

LINE-ELEMDAT TRUSS

@CLEAR

1 2 5.03E-05 'DEFAULT' 'DEFAULT' 0 0 0 'NO' 0

2 2 5.03E-05 'DEFAULT' 'DEFAULT' 0 0 0 'NO' 0

3 2 5.03E-05 'DEFAULT' 'DEFAULT' 0 0 0 'NO' 0

4 2 5.03E-05 'DEFAULT' 'DEFAULT' 0 0 0 'NO' 0

5 2 5.03E-05 'DEFAULT' 'DEFAULT' 0 0 0 'NO' 0

.

.

96 2 5.03E-05 'DEFAULT' 'DEFAULT' 0 0 0 'NO' 0

97 2 5.03E-05 'DEFAULT' 'DEFAULT' 0 0 0 'NO' 0

98 2 5.03E-05 'DEFAULT' 'DEFAULT' 0 0 0 'NO' 0

99 2 5.03E-05 'DEFAULT' 'DEFAULT' 0 0 0 'NO' 0

100 2 5.03E-05 'DEFAULT' 'DEFAULT' 0 0 0 'NO' 0

@
*

K.1.6 Boundary condition

```
*
FIXITY NAME=REINF
@CLEAR
'X-TRANSLATION'
'Z-TRANSLATION'
'X-ROTATION'
'Y-ROTATION'
'Z-ROTATION'
'OVALIZATION'
@
*
FIXITY NAME=NODE
@CLEAR
'X-TRANSLATION'
'Y-TRANSLATION'
'Z-TRANSLATION'
'X-ROTATION'
'Y-ROTATION'
'Z-ROTATION'
'OVALIZATION'
@
*
FIXITY NAME=WALL
@CLEAR
'X-TRANSLATION'
'Y-TRANSLATION'
'Y-ROTATION'
'Z-ROTATION'
'X-ROTATION'
'OVALIZATION'
@
*
FIXITY NAME=SURF
@CLEAR
'X-TRANSLATION'
'Y-ROTATION'
'Z-ROTATION'
'X-ROTATION'
'OVALIZATION'
@
*
FIXBOUNDARY LINES FIXITY=ALL
1      'REINF'
2      'REINF'
3      'REINF'
4      'REINF'
5      'REINF'
.
.
.
98     'REINF'
99     'REINF'
100    'REINF'
101    'WALL'
102    'REINF'
105    'REINF'
108    'REINF'
111    'REINF'
```

```

*
FIXBOUNDARY POINTS FIXITY=ALL
@CLEAR
2 'NODE'
104 'NODE'
@
*
FIXBOUNDARY SURFACES FIXITY=ALL
@CLEAR
1 'SURF'
2 'SURF'
3 'SURF'
4 'SURF'
@
*

```

K.1.7 Solution process

```

*
TIMEFUNCTION NAME=1 IFLIB=1 FPAR1=0.00000000000000,
  FPAR2=0.00000000000000 FPAR3=0.00000000000000,
  FPAR4=0.00000000000000 FPAR5=0.00000000000000,
  FPAR6=0.00000000000000
@CLEAR
0.00000000000000 0.00000000000000
1.00000000000000 1.00000000000000
@
*
TIMESTEP NAME=DEFAULT
@CLEAR
1000 0.001
@
*

```

K.1.8 Loads

```

*
LOAD DISPLACEMENT NAME=1 DX=FREE DY=6.3E-04 DZ=FREE,
  AX=FREE AY=FREE AZ=FREE
APPLY-LOAD BODY=0
@CLEAR
1 'DISPLACEMENT' 1 'LINE' 112 0 1 0 0 0 0 0 'NO',
  0 0 1 0
2 'DISPLACEMENT' 1 'POINT' 204 0 1 0 0 0 0 0 'NO',
  0 0 1 0
@
*

```

K.1.9 Elopement groups

```

*
EGROUP TWOSOLID NAME=1 SUBTYPE=STRESS2 DISPLACE=DEFAULT,
  STRAINS=DEFAULT MATERIAL=1 INT=DEFAULT RESULTS=STRESSES, DEGEN=NO
  FORMULAT=0 STRESSRE=GLOBAL INITIALS=NONE, FRACTUR=NO CMASS=DEFAULT
  STRAIN-F=0 UL-FORMU=DEFAULT, PNTGPS=0 NODGPS=0 LVUS1=0 LVUS2=0 SED=NO
  RUPTURE=ADINA, INCOMPAT=DEFAULT TIME-OFF=0.00000000000000 POROUS=NO,
  WTMC=1.00000000000000 OPTION=NONE DESCRIPT='NONE',
  THICKNES=1.00000000000000 PRINT=DEFAULT SAVE=DEFAULT,
  TBIRTH=0.00000000000000 TDEATH=0.00000000000000
*
EGROUP TRUSS NAME=2 SUBTYPE=GENERAL DISPLACE=DEFAULT,

```

MATERIAL=2 INT=DEFAULT GAPS=NO INITIALS=NONE, CMASS=DEFAULT TIME-
 OFF=0.0000000000000000 OPTION=NONE,
 RB-LINE=1 DESCRIPT='NONE' AREA=1.00000000000000, PRINT=DEFAULT
 SAVE=DEFAULT TBIRTH=0.00000000000000, TDEATH=0.00000000000000

*

K.1.10 Meshing

*

SUBDIVIDE SURFACE NAME=1 MODE=LENGTH SIZE=0.020
 SUBDIVIDE SURFACE NAME=2 MODE=LENGTH SIZE=0.020
 SUBDIVIDE SURFACE NAME=3 MODE=LENGTH SIZE=0.020
 SUBDIVIDE SURFACE NAME=4 MODE=LENGTH SIZE=0.020

*

SUBDIVIDE LINE NAME=1 MODE=LENGTH SIZE=0.020

@CLEAR

1

2

3

4

5

.

.

96

97

98

99

100

@

*

GSURFACE NODES=4 PATTERN=AUTOMATIC NCOINCID=BOUNDARIES,
 NCEDGE=1234 NCVERTEX=1234 NCTOLERA=1.000E-08 SUBSTRUC=0, GROUP=4
 PREFSHAP=AUTOMATIC MESHING=MAPPED, SMOOTHIN=NO DEGENERA=NO
 COLLAPSE=NO MIDNODES=CURVED, METHOD=ADVFRONT FLIP=NO

@CLEAR

1

4

@

*

GSURFACE NODES=4 PATTERN=AUTOMATIC NCOINCID=ALL,
 NCEDGE=1234 NCVERTEX=1234 NCTOLERA=1.000E-08 SUBSTRUC=0, GROUP=3
 PREFSHAP=AUTOMATIC MESHING=MAPPED, SMOOTHIN=NO DEGENERA=NO
 COLLAPSE=NO MIDNODES=CURVED, METHOD=ADVFRONT FLIP=NO

@CLEAR

3

@

*

GSURFACE NODES=4 PATTERN=AUTOMATIC NCOINCID=ALL,
 NCEDGE=1234 NCVERTEX=1234 NCTOLERA=1.000E-08 SUBSTRUC=0, GROUP=1
 PREFSHAP=AUTOMATIC MESHING=MAPPED, SMOOTHIN=NO DEGENERA=NO
 COLLAPSE=NO MIDNODES=CURVED, METHOD=ADVFRONT FLIP=NO

@CLEAR

2

@

*

GLINE NODES=2 NCOINCID=ENDS NCENDS=12 NCTOLERA=1.000E-08,
 SUBSTRUC=0 GROUP=2 MIDNODES=CURVED

@CLEAR

1

2

3
4
5
.
.
.
96
97
98
99
100
@
*

K.1.11 Non-linear springs

```

*
PROPERTY NONLINEAR-K NAME=1 RUPTURE=NO
-0.100000      -1050.5485834
-0.0070000    -1050.5485834
-0.0030000    -2101.0971667
-0.0010000    -2101.0971667
-0.0009950    -2098.8866445
-0.0009900    -2096.6673293
-0.0009850    -2094.4391416
-0.0009800    -2092.2020005
.
.
.
-0.0000200    -923.9797137
-0.0000150    -869.8118129
-0.0000100    -798.8148634
-0.0000050    -690.6051904
0.0000000     0.0000000
0.0000050     690.6051904
0.0000100     798.8148634
0.0000150     869.8118129
0.0000200     923.9797137
.
.
.
0.0009800     2092.2020005
0.0009850     2094.4391416
0.0009900     2096.6673293
0.0009950     2098.8866445
0.0010000     2101.0971667
0.0030000     2101.0971667
0.0070000     1050.5485834
0.100000      1050.5485834
*
PROPERTYSET NAME=1 K=0.000 M=0.000,
C=0.000 NONLINEA=YES NK=1 NM=0 NC=0
*
EGROUP SPRING NAME=5 PROPERTY=1 RESULTS=FORCES
NONLINEA=MNO SKEWSYST=YES OPTION=NONE DESCRIPT='NONE'
PRINT=DEFAULT SAVE=DEFAULT TBIRTH=0.000 TDEATH=0.000
*
*el n1 id1 n2
SPRING POINTS
1      104    2      2      2      1      'DEFAULT' 'DEFAULT' 0 0
2      105    2      3      2      1      'DEFAULT' 'DEFAULT' 0 0

```

```

3      106    2      4      2      1      'DEFAULT' 'DEFAULT' 0 0
4      107    2      5      2      1      'DEFAULT' 'DEFAULT' 0 0
5      108    2      6      2      1      'DEFAULT' 'DEFAULT' 0 0
.
.
.
97     200    2      98     2      1      'DEFAULT' 'DEFAULT' 0 0
98     201    2      99     2      1      'DEFAULT' 'DEFAULT' 0 0
99     202    2      100    2      1      'DEFAULT' 'DEFAULT' 0 0
100    203    2      101    2      1      'DEFAULT' 'DEFAULT' 0 0
101    204    2      102    2      1      'DEFAULT' 'DEFAULT' 0 0
*

```

```

KINEMATICS DISPLACE=SMALL STRAINS=SMALL UL-FORMU=DEFAULT,
PRESSURE=NO INCOMPAT=NO
*

```

```

ITERATION METHOD=BFGS LINE-SEA=YES MAX-ITER=500,
PRINTOUT=ALL
*

```

```

****

```

For dynamic analysis, following data must be considered.

```

****

```

```

*MASTER ANALYSIS=DYNAMIC-DIRECT-INTEGRATION,
*   MODEX=EXECUTE TSTART=0 IDOF=0 OVALIZAT=NONE,
*   FLUIDPOT=AUTOMATIC CYCLICPA=1 IPOSIT=CONTINUE,
*   REACTION=YES INITIALS=NO FSINTERA=NO IRINT=DEFAULT,
*   CMASS=NO SHELLNDO=AUTOMATIC AUTOMATI=ATS,
*   SOLVER=SPARSE CONTACT-=CONSTRAINT-FUNCTION,
*   TRELEASE=0 RESTART-=NO FRACTURE=NO LOAD-CAS=NO,
*   LOAD-PEN=NO MAXSOLME=0 MTOTM=2 RECL=3000 SINGULAR=YES,
*   STIFNES=1E-09 MAP-OUTP=NONE MAP-FORM=NO,
*   NODAL-DE=" POROUS-C=NO ADAPTIVE=0 ZOOM-LAB=1 AXIS-CYC=0,
*   PERIODIC=NO VECTOR-S=GEOMETRY EPSI-FIR=NO STABILIZ=NO,
*   STABFACT=1E-12 RESULTS=PORTHOLE FEFCORR=NO,
*   BOLTSTEP=1
*

```

```

***

```

```

*TOLERANCES ITERATION CONVERGE=ED ETOL=1E-04,
*   DTOL=1E-06 DNORM=1E-04,
*   DMNORM=1E-04 STOL=5E-04,
*   ENLSTH=1E-04,
*   LSLOWER=1E-02 LSUPPER=1,
*   RCTOL=0.05 RCONSM=0.01
*

```

```

*RAYLEIGH-DAM ALPHA=0.0000000000000000 BETA=0.0000000000000000

```

```

*1      1.255E-01      3.180E-06
*2      1.255E-01      3.180E-06
*3      1.255E-01      3.180E-06
*4      1.255E-01      3.180E-06
*5      1.255E-01      3.180E-06
*

```

K.1.12 Saving blocks

```

*
*NODESAVE-STE
1 1 1000 2
*
*ELEMSAVE-STE
1 1 1000 2
*

```

APPENDIX L Notation and details for analyses

Note1: AM is a shortening for Analytical Method and IAM for Improved Analytical Method.

Note2: Some of the analyses have the same input data but with different notations. This is to clarify that a comparison has been made with similar input data.

notation	ϕ [mm]	A_c [mm ²]	$\varphi(\infty, t_0)$	ρ_r [%]	Software	Solution category
A1	10	100x100	0	0.79	ADINA	Static
A2	12	100x100	0	1.13	ADINA	Static
A3	16	100x100	0	2.01	ADINA	Static
A4	20	100x100	0	3.14	ADINA	Static
B1	10	50x200	0	0.79	ADINA	Static
B2	12	50x200	0	1.13	ADINA	Static
B3	16	50x200	0	2.01	ADINA	Static
B4	20	50x200	0	3.14	ADINA	Static
C1	10	69x100	0	1.13	ADINA	Static
C2	12	100x100	0	1.13	ADINA	Static
C3	16	178x100	0	1.13	ADINA	Static
C4	20	278x100	0	1.13	ADINA	Static
M1	10	100x100	0	0.79	MATLAB	AM
M2	12	100x100	0	1.13	MATLAB	AM
M3	16	100x100	0	2.01	MATLAB	AM
M4	20	100x100	0	3.14	MATLAB	AM
M3-creep1	16	100x100	1	2.01	MATLAB	AM
M3-creep2	16	100x100	2	2.01	MATLAB	AM
M3-creep3	16	100x100	3	2.01	MATLAB	AM
M1-I	10	100x100	0	0.79	MATLAB	IAM
M2-I	12	100x100	0	1.13	MATLAB	IAM
M3-I	16	100x100	0	2.01	MATLAB	IAM
M4-I	20	100x100	0	3.14	MATLAB	IAM